Dividing Flow in Closed Conduits With Ninety Degree Branches

Mariampillai Stanislaus Perinpanathan

A Thesis

in

The Department
of
Civil Engineering

Presented in Partial Fulfillment of the Requirements
for the Degree of Master of Applied Science at
Concordia University
Montreal, Quebec, Canada

April, 1992

ISBN 0-315-90873-4

Canada

ABSTRACT

Dividing Flow in Closed Conduits With Ninety Degree Branches

M.S.Perinpanathan

Dividing flow in general and particularly in closed conduits has been studied in the past both experimentally and theoretically. Most of the experimental studies were carried out with circular pipes to obtain flow parameters such as loss coefficients and pressure coefficients. The discrepancy between different experimental investigations and the theoretical derivations made it impossible to generalize the flow parameters for differing applications. The earlier studies were not comprehensive and lacked details related to the study of pressure variations at the junction of conduits.

The present study of closed rectangular conduits set at 90° has attempted to overcome some of the existing deficiencies like pressure measurements at and around the junction. These measurements are very tedious but nevertheless are needed to determine the minimum pressures, and thereby to evaluate the free stream velocity of the separating stream line and the contraction coefficient of the jet entering the branch conduit. The rectangular conduit system chosen for the present tests was meant to represent two dimensional flow and the test results therefore could be compared with the available two dimensional theoretical results [McNown's1950].

Mainly, the present study has considered in detail the pressure recovery factor concept proposed by Bajura[1970]. This parameter is useful in the design of manifold

systems. A consolidated presentation of all the previous approximate formulae for the pressure recovery factor has been provided in this study. The proposed pressure recovery factor is validated by using experimental data based on measurement of net forces on the lateral walls. Also a new model based on velocity triangles is proposed. This correlates the pressure recovery factor (R_d), the contraction coefficient (C_c) and velocity parameter(η).

Detailed discussions related to the dependence of pressure coefficient (C_{p21}) on discharge ratio and area ratio (though small), m, are included by making use of some of the previous test results. By this means, the pressure recovery factor (R_d) and energy loss coefficient (E_{12}) based on the previous tests are also verified.

The present experimental study reveals that the location of the stagnation point near the junction depended on the discharge ratio (q) and does not occur at the junction corner as it is assumed normally. This particular value of q, denoted as q_{cr}, is derived theoretically and compared with experimental values and its effect on the behavior of some of the main parameters is pointed out in this study.

Finally the present study formulated equations for contraction coefficients and velocity parameters for lateral flows and compared contraction coefficients of both lateral and lateral orifices with the view to aid the design engineer.

ACKNOWLEDGEMENT

The author thanks Dr. A. S. Ramamurthy for suggesting and supervising the present research project. He also thanks Dr. R Balachandar for being of great assistance in the setting up the equipment and in the subsequent stages of the research project. Thanks are due to Mr. Weimin Zhu for verifying some of the straight through flow test results.

This tedious and time consuming project could not have been accomplished without the skill and cooperation of Messrs Ernest Haefeli and Paul Scheiwiller of the machine shop and the assistance of Messrs. N.Lang Vo and A.Chociwski of the Water Resources Laboratory. My sincere thanks are due to them.

Finally, my ever gratitude to my family Joyce, Shirani, Nishanthan, Niranjan, Sharmila and the grand parents for the understanding, encouragement and their financial support throughout this long period of my studies.

I dedicate this work to my parents who strove to educate me and to make me a useful member of the society. They will not be disappointed in this continuing educational process.

TABLE OF CONTENTS

List of Notations ---------- xi
List of Figures ---------- xvi
List of Tables ---------- xx

Chapter I Thesis Outline ---------- 1
1.1 Introduction
1.2 The Present Study 2
1.2.1 Multiports 3

Chapter II Review of Literature ---------- 4
2.1 General Remarks
2.2 Previous Studies
2.2.1 Theoretical Investigations 5
2.2.1.1 Free Streamline Theory and Conformal Mapping
2.2.2 Experimental Studies 6
2.2.2.1 Momentum Equations and Pressure Recovery factor
2.2.2.3 Pressure Coefficient in the Main 7
2.2.2.3 Other Major Studies
2.2.3 Correlated Equations for Energy Losses From Existing Data 9
2.2.3.1 Vazsonyi
2.2.3.2 Ito & Imai 10

2.2.3.3 Gardel

2.2.3.4 Losses for m=1 11

2.2.3.5 Energy Loss Coefficient Under Laminar Flow Conditions

Chapter III Experimental Set-Up & Procedure ---------- 13

3.1 General Remarks

3.2 Experimental Set-Up 14

Chapter IV Characteristics of Dividing Closed Conduit Flows---- 16

4.1 General Remarks

4.2 Theoretical Considerations

4.3 Flow in The Main Conduit 17

4.3.1 Momentum and Energy Equations 18

4.3.2 Pressure Recovery Factor R_d 22

4.3.2.1 Unbalanced Pressure Force on Lateral Walls 23

4.3.3 Expanding Through Flow in The Main Conduit

4.3.3.1 Flow Models 26

4.3.3.1.1 Linear Pressure variation model

4.3.3.1.2 A parabolic pressure variation model

4.3.3.1.3 General Flow Model 28

4.4 Flow Through The Lateral

4.4.1 Momentum and Energy Equations 29

4.4.2 Contraction Coefficient 31

4.4.3 Pressure Coefficient (Cp_{13}) in The Lateral 32

4.4.4 Contraction Coefficient From Irrotational Theory (C_d) 33

4.4.5 The Velocity Parameter (η) 37

4.4.6 Other Pressure Characteristics 38

Chapter V Experimental Results and Analysis ---------- 40

5.1 General Remarks

5.2 Pressure Diagrams 41

5.2.1 Stagnation Pressure P_s 42

5.2.2 Pressure Coefficient C_{p21} 44

5.3 Energy Loss Coefficient E_{12} 47

5.4 Pressure Recovery Factor 49

5.5 Contraction Coefficient C_c 50

5.6 Contraction Coefficient C_d 53

5.7 Pressure Coefficient C_{p13}

5.8 Energy Loss Coefficient E_{13} 55

5.9 Velocity Parameter η 57

5.10 The Velocity Triangle Model 58

5.11 Dependence of C_c on η and q/m 61

5.12 Manifold Designs 63

Chapter VI Conclusions ---------- 65

6.1 The Pressure Coefficients

6.2 The Contraction Coefficient

6.3 Wall Pressure Measurements

6.3.1 Minimum Pressures 66

6.3.2 Stagnation Points

6.4 Pressure Recovery Factor

6.5 The Effect of C_{p3J}

6.6 The Velocity Triangle Model 67

6.7 Design of Multiports

6.8 Scope for Further Study

Appendix I Straight Through Flow Tests 68

AI.1 Straight Through Flows

AI.1 Straight Through Flow Tests

AI.2 Friction Factor 69

AI.3 Energy and Momentum Coefficients 70

AI.3.1 Wall Law 71

AI.3.2 Power Law

AI.3.3 Empirical Relations With ε 73

AI3.4 Experimental Values 74

AI.4 Pressure Gradients

AI.5 Conclusion 75

Appendix II Experimental Uncertainties---------- 76

A2.1 Uncertainty in the Measurements

A2.2 Uncertainty in Computed Results 77

Appendix III References ---------- 78

Appendix IV Sample Calculation Sheet ---------- 82

A4.1(b) Calculation Sheet of Sample Test 1/18

Lateral 1 (q=0.93) 82 to 85

Appendix V Figures 86 to 152

Appendix VI Tables 153 to 190

LIST OF NOTATIONS

ABCD	control volume in the main
AB_1T_2CD	control volume in the main above the dividing stream line
A_r	cross sectional area
a	mapping position of A_∞ in the t-plane
b	mapping position of B_∞ in the t-plane
B_1BT_2S	control volume for the parabolic model
b_x	breadth of conduit
C	contraction coefficient
C_c	contraction coefficient from minimum pressure
C_d	contraction coefficient from free vortex model
C_{p21}	pressure (gain) coefficient in the main conduit across the lateral opening
C_{p13}	pressure (loss) coefficient in the lateral conduit
D	diameter
d	hydraulic diameter
Ex	total energy head
E_{12}	energy loss coefficient due to dividing flow in the main conduit
E_{13}	energy loss coefficient due to dividing flow in the lateral conduit
e_{12}	energy loss coefficient in the main conduit across the control volume

e_{13}	energy loss coefficient in the lateral conduit across the control volume
F	net force on walls
f	friction factor
H	ratio of the square of jet velocity (V_j) to the square of incoming main conduit velocity (V_1) - Jet head
H_x	straight through flow tests (x=3 to 5) for Plexiglas
h	pressure head (ft. or in cms)
h_x	straight through flow tests (x=1 to 5) for Aluminium
h_{fx}	pressure head due to friction
K_1	constant in the average velocity across the lateral opening (K_1 V_j)
k	multiplying factor to define the inner radius for free vortex theory
Lx	projected horizontal length from the control section to the centerline-axis of the pressure diagram
l_3	length over which the lateral wall pressures vary
m	area ratio
N	factor in the power law of velocity distribution
n	factor in power of y in the general flow model
P_x	pressure at reference axis
P'	pressure at control sections
P_{AV}	average pressure variation along dividing stream line
P_e	wetted perimeter
P_f	pressure loss due to friction
P_u	sum of pressures on the upstream wall of lateral conduit

P_D	sum of pressure on the downstream wall of lateral conduit
P_S	stagnation pressure
Q_x	discharge in cusec.
q	ratio of lateral discharge to main discharge
q_d	incremental discharge
Rd	pressure recovery factor after accounting for friction terms
Re	Reynolds number
Rf	pressure recovery factor from the force difference on the lateral walls
Rm	pressure recovery factor across the control section ABCD in the main conduit
R_x	separated regions 1,2 etc.
r_i	inner radius in free vortex theory
r_o	outer radius in free vortex theory
Sn	stagnation point
S_x	slopes of pressure heads along conduits
T_1	upstream corner of lateral / main junction
T_1T_2MN	control volume in the lateral conduit
T2	downstream corner of lateral / main junction
t	t-plane in conformal mapping
U_x	velocity in potential flow theory
V_x	average velocity in conduits
V_i	inner velocity for free vortex theory
V_j	jet velocity due to minimum pressure
V_{max}	maximum velocity in conduits

V_o	outer velocity in conduits for free vortex theory
w	velocity plane in conformal mapping
w_x	width of conduits
y	vertical offset in analysis of parabolic model
Y	ratio of the square of lateral velocity $(V_3)^2$ to the square of main conduit velocity $(V_1)^2$
Z_x	datum height
z	physical plane in conformal mapping
α'	kinetic energy flux correction coefficient at the control section
α	junction angle
β'	momentum flux correction coefficient at the control section
ΔM	momentum difference in the main across control volume ABCD
ΔP	radial pressure difference across vena contracta in the lateral
ε	velocity deformity coefficient
ϕ	equivalent angle in Vazsonyi's formula
γ	specific weight of water
η	velocity parameter (V_1/V_j)
η^2	ratio of the square of main conduit velocity (V_1) to the square of jet velocity (V_j)
λ	coefficient in Vazsonyi's formula
μ	dynamic viscosity
ν	kinematic viscosity

θ	angle in velocity triangle
ρ	density of water
τ	shear stress
ζ	ζ– plane in conformal mapping

Subscripts (x) where not defined:

1	limb 1 - main conduit u/s of the lateral junction
2	limb 2 - main conduit d/s of the lateral junction
3	limb 3 - lateral conduit

Abbreviations:

u/s	upstream
d/s	downstream

LIST OF FIGURES

Figures.		Page
1.1:	Hydrodynamic Parameters in Dividing Flow in Closed Conduits & Conduit Geometry	86
2.1:	Conformal Mapping for Free Efflux (McNown 1950)	87
2.2:	Division of Flows By Vazsonyi[1944]	87
2.3:	Lateral Loss Coefficient By Previous Researchers for m=0.77 and m=0.225	88
2.4:	Loss Coefficient E12 and E13 from Smith[1980] for m=1	89
3.1:	Dividing Flow- Rectangular Closed Conduits	90
3.2:	General Arrangement of Pressure Tappings -Lat 3 (off centered)	91
3.3:	General Arrangement of Pressure Tappings -Lat 3 Centered	92
3.4:	Test Set-Up	93
4.1:	General Flow Characteristics- Dividing Flow	94
4.2:	Control Volumes ABCD & T_1T_2NM	94
4.3 (a) to(c):	Pressures At The Junction in The Main Conduit and After the Junction in The Lateral Conduit	95
4.4 (a) &(b):	Control Volume AB_1T_2CD and The Parabolic Model	96
4.5(a) & (b):	General Description of Lateral Flow and Measurement of Lateral Wall Pressures.	97
4.6(a) & (b):	Contraction Coefficient Cd By Free Vortex Model and Measurement of ΔP	98

5.1(a) to (e):	Pressure Diagrams of the Representative Tests- Lateral 1 (m=1)	99 to 103
5.2 (a) to (e):	Pressure Diagrams of the Representative Tests- Lateral 2 (m=0.77)	104 to 108
5.3 (a) to (c):	Pressure Diagrams of the Representative Tests- Lateral 3 (m=0.225)	109 to 113
5.4 (a) & (b):	Pressure Diagram- Stagnation in the Main and Stagnation in the Lateral.	114
5.5:	Dividing Flow- Adapted from O'Neill [1986]	115
5.6 (a) &(b):	Stagnation in t plane and Stagnation in Z plane	116
5.7 (a),(b)&(c):	Pressure Coefficient C_{p21} Vs q for the three laterals	117
5.7 (d)&(e):	Pressure Coefficient C_{p21} Vs q -Previous Studies	118
5.8 (a),(b) & (c):	Loss Coefficient E_{12} Vs q for the three laterals	119
5.9(a),(b) & (c):	Pressure Recovery Factors R_m ,R_f for the three laterals	120
5.9 (d):	Pressure Recovery Factor By Previous Studies	121
5.9 (e):	Pressure Recovery Factor By Eqns. 5.18 to 5.21	121
5.10A:	Secondary Separation Due to Stagnation	122
5.10 (a), (b) & (c):	Contraction Coefficient C_c Vs q and Cc vs η^2 For the Three Laterals	123
5.11 (a),(b) & (c):	C_c and $1/C_c$ Vs (q/m)2, (q/m) etc.	124
5.12 (a), (b) & (c):	Contraction Coefficient Cd Vs q (Free Vortex)	125
5.13 (a), (b) & (c):	Pressure Coefficient Cp13 Vs q For the Three Laterals	126
5.13(d) & (e):	Pressure Coefficient Cp13 Vs $(q/m)^2$ &(q/m)	127
5.14 (a), (b) & (c):	Loss Coefficient E_{13} Vs q For the Three Laterals	128
5.14(d), (e) & (f):	Loss Coefficient E_{13} Vs (q/m), $(q/m)^2$	129
5.14(g),(h) &(i):	E13^0.5 vs q/m For the Three Laterals	130
5.15 (a):	η Vs q For the Three Laterals	131

5.15 (b) & (c) : $1/\eta^2$ and η Vs q for Laterals 1&2 131

5.15 (d),(e) & (f): $1/\eta^2$ Vs $(q/m)^2$ and (q/m) For the Three Laterals 132

5.16.(a), (b) & (c): C_{p3j}/H Vs q For the Three Laterals 133

5.16 (d) & (e) : C_{p3j}/H Vs q and q/m For the Three Laterals 134

5.17: The Velocity Triangle Model 135

5.18 (a) ,(b) & (c): $C_c/(1-\eta^2)$ and K_1 vs q For the Three Laterals 136

5.18 (d) & (e): $C_c/(1-\eta^2)$ and K_1 Vs $(q/m)^2$ For the Three Laterals 137

5.19 (a), (b) & (c): $T\eta^2$ Vs η^2 For the Three Laterals 138

5.20 (a), (b) & (c): Comparison of Contraction Coefficient From Eq.5.37, Eqs.5.41 to 5.43 and Minimum Pressures 139

5.21 (a), (b) & (c): Comparison of Contraction Coefficient From Eqns. 5.47 and 5.40 140

5.22 (a), (b) & (c): Comparison of Contraction Coefficients of Slots (Eq.5.40) and Laterals (Eq.5.41) 141

A1.1 (a) to (c): Pressure Head, h cm, Vs Distance cm. For the Through Flow Tests h1 to h3 for Aluminium Conduit. 142

A1.1 (d) & (e): Pressure Head, h cm, Vs Distance cm.For the Through Flow Tests h4 to h5 for Aluminium Conduit 143

A1.2 (a) & (b): Pressure Head, h cm Vs Distance cm. For the Through Flow Tests, H3 to H4, for Plexiglas Conduit. 144

A1.2 (c) & (d): Pressure Head, h cm ,Vs Distance, cm For the Through Flow Tests H5 to H6 For Plexiglas Conduit 145

A1.3 (a) & (b): Friction coefficient f Vs Re for Plexiglas and Aluminium conduits 146

A1.4: N and (V/V_{max}) Vs ln (Re) -from Schlichting H. 147

A1.5: Q^2f Vs S For the Through Flow Tests 148

A1.6: f Vs Re For Lateral 1 (m=1) Experiments 149

A1.7:	f Vs Re For Lateral 3 (m=0.225) Experiments	150
A1.8:	f Vs Re For Lateral 2 (0.77) Experiments	151
A1.9:	Q^2f Vs S For Lateral 1 Experiments	152
A1.10:	Q^2f Vs S For Lateral 3 Experiments	152

LIST OF TABLES

Tables		Page
2.1	Typical Studies Based on Free Streamline Theory	153
2.2:	Typical Studies on Pressure Recovery Factor	154
2.3:	Major Experimental Studies in The Past	155
3.1	Selected Conduit Geometries	90
5.1	List of Experiments Carried Out	156
5.2	Manometric Table of Test Results for Lateral 1- Representative Table For Test 1/18	157
5.3	Manometric Table of Test Results for Lateral 3- Representative Table For Test 3/7	158
5.4	Manometric Tables of Test Results for Lateral 2 - Representative Table For Test 2/19	159
5.5 :	Representative Test Numbers For the Three Laterals.	160
5.6 (a) to (d):	Main Parameters For Lateral 1 (m=1)	161 to 164
5.7 (a) to (c):	Main Parameters For Lateral 2 (m=0.77)	165 to 167
5.8 (a) to (c):	Main Parameters For Lateral 3 (m=0.225)	168 to 170
5.9 (a) to (c):	Summary of More Parameters Lateral 1	171 to 173
5.10 (a) to (c):	Summary of more Parameters Lateral 2	174 to 176
5.11 (a) to (c):	Summary of more Parameters Lateral 3	177 to 179
5.12:	Observed Stagnation Points	180
5.13:	Critical Discharge Ratio q_{cr} by Potential Flow Theory	180
5.14:	Contraction Coefficient C_d from Free Vortex Theory	181

A1.1: Straight Through Flow Tests-Aluminium Duct 182

A1.2: Straight Through Flow Tests- Plexiglas Duct 183

A1.3: Friction Coefficients by Different Methods For the Two Types of Conduits 184

A1.4: The Energy and Momentum Coefficients (α, β) by the Wall Formula For the Through Flow Tests. 185

A1.5: Evaluation of N and ε in Power Law for the Straight Through Flow Tests. 186

A1.6: The Energy and Momentum Coefficients (α,β) by the Power Law For the Through Flow Tests. 187

A1.7: The Energy and Momentum Coefficients (α,β) by Empirical Equations For the Through Flow Tests 188

A1.8: Summary of α,β Coefficients by the Three Methods For the Through Flow Tests. 188

A1.9: Summary of Friction Coefficients and Reynolds Numbers For All Lateral Flow Tests. 189 - 190

CHAPTER I

THESIS OUTLINE

DIVIDING FLOW IN CLOSED CONDUITS

WITH NINETY DEGREE BRANCHES

CHAPTER I

THESIS OUTLINE

1.1 Introduction

Division of flow occurs in both open channel systems and in closed conduit systems and covers a vast area of engineering applications. In open channels, division of flow occur in branch channels, side weirs and floor outlets while in closed conduits, it is commonly encountered in systems dealing with sewage disposal, sprinklers, drip irrigation, water treatment plant appurtenances, water supply networks, thermal diffusers, air conditioning systems and gas burners. Such a variation of applications associated with vastly differing sizes, shapes, branch orientations and roughness of conduits required to transport varying volumes of fluid discouraged previous researchers from attempting a general solution to the dividing flow problem. In the past,this resulted in studies which were carried out to obtain reliable data only for specific applications. Thus, there is a need for a comprehensive study of the dividing flow problem and the present experimental study is pertaining to two closed conduits set at 90^{o} to each other. This has its special application in manifold flows and water supply networks.

1.2 The Present Study -Lateral Flow

The present study with the two sharp edged conduits set at right angles to each other (Fig.1.1) has the objective of establishing the main functional relationship between the principal geometrical and hydrodynamic parameters. The two dimensional test model was selected so that the experimental data could be verified with the theoretical predictions available for two dimensional conduit models. Moreover, from the two dimensional flow results, qualitative predictions of flow characteristics can be made for some three dimensional flows (which have practical applications as in circular pipe networks). The present study specifically deals with the determination of the following relationship for lateral conduit flows branching at 90° to the main conduit (Fig.1.1):

(1) Location of the stagnation pressure point in the branching region as a function of the discharge ratio Q_3/Q_1 (q) where Q_3 and Q_1 are the respective discharges in the lateral and the main conduit.

(2) Measurement of the minimum wall pressure in the lateral conduit and the subsequent evaluation of the contraction coefficient (Cc) and the velocity parameter (η) defined as the ratio of V_1/V_j where V1 is the main conduit velocity and Vj is the jet velocity corresponding to the minimum pressure.

(3) Determination of the functional relationship between the discharge ratio (q) and the following hydrodynamic parameters:

(a) Contraction coefficient (Cc),

(b) Pressure Coefficients in the main and lateral conduits (Cp_{21},Cp_{13}),

(c) Loss Coefficients in the main and lateral conduits (E_{12},E_{13}) and

(d) Pressure recovery factor (R_d),

where suffixes 1,2,3 indicated above are the limbs of the main (1,2) and lateral (3) conduits (Fig.1.1).

(4) Determination of the effects of the conduit area ratio (m) on the above parameters. The variable introduced is the ratio q/m which represents the velocity ratio V_3/V_1 where V_3, V_1 are the velocities in the lateral and main conduits respectively.

(5) Developing equations for the key parameters to aid the design of conduit systems with 90^o branching.

1.2.1 Multiports

In the final discussion, the aspect of interference in the design of multiports and manifolds is discussed. Also the discharge coefficients in lateral conduits are compared with those of lateral orifices, the latter being a limiting case of a lateral conduit having zero length. This comparison is essential to compare or to derive the contraction coefficient for one type of flow knowing the other as was theoretically evaluated in the past studies [McNown 1950].

The next chapter deals with the review of literature on dividing flows.

CHAPTER II

REVIEW OF LITERATURE

CHAPTER II

REVIEW OF LITERATURE

2.1 General Remarks

Dividing flow has drawn the attention of several investigators in the past [Smith 1980, Miller 1971] including the possibility of the first recorded sketch by Leonardo da Vinci [Carusi 1923]. Its application is many fold in both open channel and closed conduit systems. Detailed study of dividing flows in an open channel were carried out by Taylor[1944], Joy and Townsend[1981]. More recently, Duc Tran [1988] reported on the division of flows in open channels and related the momentum recovery factor to the discharge ratio and the Froude number. The concept of momentum recovery factor R_d was also verified by Tran [1988] and by Satish [1986] by direct measurements of the pressure forces on the branch channel walls. As stated earlier, the present study deals with dividing flow in closed conduits set at 90^0 to each other. The study is based on the momentum recovery factor approach and more significantly, the study attempts to relate all the main nondimensional parameters associated with dividing flows in closed conduits.

2.2 Previous Studies.

Dividing closed conduit flow problems have been studied very extensively in the past and many studies have been conducted on different aspects of the flow. The majority of the studies dealt with energy head losses associated with many types of dividing flows, namely, 90^o tees,branches set at other angles, lateral orifices and plenum outlets. These

extensive studies lead to a review of literature on the division and the combination of flow in closed conduits by Crow and Wharton [1968] comprising sixty studies dating back to 1925. This review was meant as an introduction to future experimental work with suggestions to standardize definitions and to rationalise terminology. However, it failed to compare or correlate existing data. This review mentions that 'many experimenters published their results without attempting to analyze the problem or relate their results to any theory' and that many scale models of civil engineering works were carried out due to the lack of dependable design data.

Literature survey presented in this chapter gives additional information related to the main results obtained in the previous studies. The survey also lists details of some of the major theoretical and experimental investigations, formulas presented for energy loss coefficients and other parameters studied.

2.2.1 Theoretical Investigations

One of the important parameters studied previously by theoretical means is the contraction coefficient using free stream line theory [McNown 1950] and an outline of this study is given below.

2.2.1.1 Free Streamline Theory And Conformal Mapping.

The complexity of the problem of dividing flow led to the mathematical analysis of an idealized flow pattern using conformal transformations. In this approach, the bounding streamlines are composed of either fixed straight lines along which streamline direction is constant or free streamlines along which the velocity magnitude is constant. During the course of this analysis, the transformation of the physical (z) plane (Fig.2.1) on to the velocity planes (w &U) gives a simpler representation of the flow pattern. The velocity

plane is then transformed into one half of an auxiliary plane (ζ) by a direct complex function. By the method of conformal mapping and transformations stated above, equations for contraction coefficients for differing sizes of laterals and flow ratios have been derived. Some of the studies related to dividing flows for both separating free streamline and non separating lateral flows can be traced to McNown [1950], Tsakonas [1957], Modi [1981] and Ramamurthy [1979] and described in Table[2.1]. Chorlton [1986] has analyzed the dividing flow problem without flow separation in a similar manner and used the Schwarz - Christoffel transformation to obtain equations for the stagnation points of dividing flows in two dimensional channels. His equations (Fig.5.2) are used as a starting point to obtain the theoretical stagnation points in the present study in Chapter 5 Section (5.2.1).

2.2.2 Experimental Studies.

The experimental studies in the past dealt mainly with the energy loss coefficients, the pressure recovery factor and the pressure coefficient in the main conduit. A brief description of the studies pertaining to the last two parameters are given below and that of the energy loss coefficient is given in section 2.2.3.

2.2.2.1 Momentum Equations And Pressure Recovery Factor.

The momentum equation for a control volume in the main conduit spanning the lateral (Fig.4.1) correlated the pressure (gain) coefficient to the unbalanced momentum in the direction of the main pipe. The unbalanced momentum is also referred to as momentum loss due to the presence of the lateral. Relating the momentum loss to the initial momentum in the main conduit, a coefficient called the pressure recovery factor was introduced by Bajura [1971]. He used the data of McNown [1954] in his studies and obtained the

pressure recovery factor (R_d) for dividing flows in closed circular conduits. This coefficient is an important parameter in manifold flow analysis and a brief summary of its study is given in Table 2.2.

2.2.2.2 Pressure Coefficient In The Main (C_{p21}).

Ward Smith[1980] has summarized the study of flows in branching conduits and presents the accepted concept of projecting the pressure head lines in the three limbs (Fig.4.3a) for analyzing the behavior of dividing flows. The difference between the pressure heads in the upstream and downstream sections of the main conduit (P_1P_2) is the pressure rise $\Delta P/\gamma$ due to the division of flows. The pressure coefficient based on $\Delta P/\gamma$ is due to the effects of branching only excluding friction losses. Hudson [1979] has summarized the pressure coefficient data taken from McNown [1954], Thoma [1929] and the British Hydromechanics Research Association [BHRA 1971] studies for different area ratios of conduits. The variation of the pressure coefficient with the area ratio of lateral to the main conduit though small is definitely a function of the area ratio of the conduits (m).

2.2.2.3 Other Major Studies

Besides the experimental studies of McNown [1954], BHRA [1971] and Bajura [1971] mentioned above, other studies have also contributed significantly to the solution of the dividing flow problem. Some of the major studies in the field of dividing flow are given in Table.2.3

Miller [1971] has published extensive design data including test results for square sections (12 inch.) at the British Hydromechanics Research Association [BHRA]. He mentions that on comparing non circular and circular conduits, friction coefficients appear to be independent of the aspect ratio although the losses in the ducts of the same area are

not. From the experiments of Gunn [1963], it was found that the ratio of friction coefficients vary with Reynolds number (Re) and depend on the ratio of P_e/A^3 where P_e is the perimeter and A is the area of the section. The ratio of friction coefficients, f , approach unity at high Reynolds numbers (R_e) and at lower values of R_e it becomes 0.77 (i.e. $f_{noncircular} / f_{circular} = 0.77$). Miller [1971] also comments on the discrepancies between Vogel's [1929] results and those of other studies especially on the pressure gradients. Popp et al [1983] studied a Tee junction of rectangular section and measured pressure variations and velocity profiles at the junction by Laser Doppler anemometer [LDA]. This study of velocity distributions at the junction gave the following results ,

(a) the initial flow development length of 21 widths was insufficient in the main duct. In fact it resulted in a skewed development of velocity profiles depthwise (z direction).

(b) the velocity profiles presented in the direction of the main conduit (x) show that there are no major effects due to the junction for small discharge ratios. The study also identified the flow separation which occurs in the main conduit immediately after the junction for a discharge ratio of 0.81. The main conduit wall pressures across the junction (Fig.4.1) show pressure drops for all q ratios.

(c) the velocity profiles in the direction of the lateral conduit (y), very clearly identify the flow separation in the inner wall for two discharge ratios of 0.38 and 0.81.

(d) the flow was found to become highly turbulent in the downstream section of the main conduit beyond the junction for very high discharge ratios and large eddies were observed to penetrate the entire length of the main conduit.

However their studies did not provide the pressure variation on the inner wall T_1N of the lateral conduit (Fig.4.1).

2.2.3 Correlated Equations for Energy Losses From Existing Data

Three investigators Vazsonyi [1944], Ito [1973] and Gardel[1957] have correlated energy losses due to branching in closed conduit pipes and their equations are discussed in this section.

2.2.3.1 Vazsonyi

Vazsonyi [1944] correlated all the results of previous experiments. His equation for losses (Fig.2.2) in Tees ($K_{0,1}$) at any angle α is,

$$(K_{0,1})\ \text{tee} = \lambda_1 + (2\lambda_2 - \lambda_1)(V_1/V_0)^2 - 2\lambda_2(V_1/V_0)\cos\phi \qquad (2.1)$$

where, $\phi = 1.41\,\alpha - 0.00594\,\alpha^2$ in which α= Tee angle.

When $\alpha < 22.5^o$

$$\lambda_1 = 0.0712\,\alpha^{0.7041} + 0.37$$

$$\lambda_2 = 0.0592\,\alpha^{0.7029} + 0.37$$

and when $\alpha > 22.5^o$

$$\lambda_1 = 1.0$$

$$\lambda_2 = 0.9$$

The loss coefficients for the branch at 90^o ($\alpha = 90^\circ$) and for the main ($\alpha = 0^\circ$) are derived as below.

When $\alpha = 90^o$, $\lambda_1 = 1.0$, $\lambda_2 = 0.9$, $\phi = 78.786^o$, $\cos\phi = 0.19447$

$$K_{0,1} = E_{13} = 1 + 0.8\,(V_1/V_0)^2 - 0.35\,(V_1/V_0) \qquad (2.2)$$

and when $\alpha = 0^o$, $\lambda_1 = 0.37$, $\lambda_2 = 0.37$ and $\phi = 0^o$

$$K_{0,1} = E_{12} = 0.37\,(V_1/V_0)^2 = 0.37\,q^2 \qquad (2.3)$$

where, $q = Q_{branch}/Q_{main}$.

It is noted that negative losses in the main conduit for small discharge ratios are not evident in the above formula.

2.2.3.2 Ito and Imai

Ito and Imai [1973] tested circular smooth drawn copper tubings of diameter 35 mm with 90° branching and correlated equations for energy losses in terms of flow ratios ($q = Q_{branch}/Q_{main}$) and radius of curvature of the joining edge (r/d). For sharp edged conduits loss coefficient in the main (E_{12}) is given by two formulas.

For the main conduit,

$$E_{12} = 1.55(0.22-q)^2 - 0.03 \qquad \text{when } 0 < q < 0.22 \qquad (2.4)$$

$$\text{and } E_{12} = 0.65\,(q-0.22)^2 - 0.03 \qquad \text{when } 0.22 < q < 1, \qquad (2.5)$$

and for the lateral as

$$E_{13} = 0.99 - 0.82\,q + 1.02\,q^2 \qquad (2.6)$$

Eq.(2.4) and (2.5) for the main conduit account for the existence of negative losses. However the significance of the discharge ratio q=0.22 where the crossover from negative to positive values take place is not discussed well.

2.2.3.3 Gardel

Gardel's [1957] equations for sharp edged entrances from his experiments for area ratio 1 are as below. For main conduit losses,

$$E_{12} = K_{32} = 0.3\,(1-q)2 + 0.35q2 - 0.2q\,(1-q) \qquad (2.7)$$

and for branch losses.

$$E_{13} = K_{31} = 0.95(1-q)2 +0.8\ q\ (1-q) +1.3\ q2 \qquad (2.8)$$

where $q=Q_{branch}/Q_{main}$

The above equations when expressed in terms of velocity parameter q/m ($=V_3/V_1$) instead of discharge ratio (q) enables one to obtain head losses for any area ratios (A_3/A_1). The loss coefficients (E_{13}) by such modification are presented in Fig.2.3 for the area ratios used in the present experiment (m= 0.77 and 0.225). However, such an extension of their formulas have not been verified by earlier investigators. The comparisons for loss coefficient E_{13} in Fig.2.3 show that Gardel's equation tend to give higher values than the other formulas for small area ratios. Hence, Gardels' formulae [1957] are not used to compare the present experimental results in Chapter 5. McNown's values of E_{13} for m=0.25 are also shown in the same figure.

2.2.3.4 Losses for m=1

The energy loss coefficient obtained in the different studies for area ratio of one are presented in Ward Smith [1980] which indicate the variation between the results of various studies (Fig.2.4). The empirical formulas discussed in this section are referred to in Chapter 5 related to data analysis of the present study.

2.2.3.5 Energy Loss Coefficient Under Laminar Flow Conditions.

Jamaison et al [1971] studied the Division and Combination of flows in the laminar (or viscous) and transition regimes (10<Re< 10000) and correlated the loss coefficients to Reynolds numbers. The loss coefficients were related to an envelope of linear graphs

varying from 2000/Re to 6000/Re for increasing discharge ratios (q). In the present set of experiments, 95% of the tests and studies were limited to the turbulent stage and no attempt was made to study the laminar range. However when q ratios were very small ($q<0.07$ for $m=1$) flow regime in the present set of experiments were either in the transitional or laminar regime in the lateral conduit.

CHAPTER III

EXPERIMENTAL SET-UP AND PROCEDURE

CHAPTER III

EXPERIMENTAL SET UP & PROCEDURE

3.1 General Remarks

Fig. 3.4 indicates the experimental set-up used for the tests. The test sections of both main and laterals were chosen as rectangular so that the dividing flow behavior will be nearly two dimensional least affected by cross flows while turning into the lateral. The main and one of the lateral ducts (Lateral 1) was made from Aluminium sections and the other two laterals were made from plexiglas. The lateral duct was aligned and assembled carefully at right angles to the main by means of guide pins provided in the main duct flange and sealed with flexible rubber in the matching grooves provided in the two flanges of the conduits to avoid leakages and discontinuity in the boundary. The sizes of the conduits tested are given below and the general arrangement is shown in Fig.3.1.

Main conduit	4.125 cm x 9.15 cm	m= Area of lateral/Area of main
Lateral 1	4.125 cm x 9.15 cm	m=1
Lateral 2	4.125 cm x 7.04 cm	m=0.77
Lateral 3	4.125 cm x 2.08 cm	m=0.225

The length of the approach conduit to the main conduit was about 15 ft (L>40d) to ensure that a fully developed flow occurred in the test sections and the length of laterals were about

1.8 ft in length to ensure complete pressure recovery. Sharp edged wall taps of 1.0 mm size were provided at approximately 6 inches spacing in the main conduit except near the junction where the intervals were much closer. These closer spacings of the pressure taps near the junction were found to be necessary to record the sudden or sharp pressure changes. These wall tappings are shown in Figs.3.2 and 3.3 which show different details at the head of the lateral conduit 3. The off - centered piece was added to observe pressures near the stagnation region and these pressure tappings were 0.5mm in diameter. These tappings were sand papered and made flush with the wall to avoid burrs which result in erroneous pressure readings.

3.2 Experimental Set Up

The main conduit in three lengths were cleaned, wire brushed and the pressure tappings cleaned regularly to ensure that the deposits in the water did not form deposits,burrs or block the tappings. To this effect the sump was also periodically cleaned throughout the period of the experiment.

The test sections of main and lateral were assembled and supported rigidly after ensuring a straight alignment and levelling. The battery of pressure taps were connected through four manifolds on to four manometric glass tubes to facilitate quick reading of the large number of pressure taps. The fluctuations in the pressures near the junction were noted and presented a problem for the pressure measurement. Measurement of pressures by transducers of different sensitivity for different sections were attempted but proved to be less efficient than the direct manometric method which was read to an accuracy of 0.5 mm. The manifolds provided some form of damping and near steady stages were noticeable.

To control further the pressure fluctuations a constant head tank was provided to eliminate variations of pressure by pump performance. This tank supplied the piping system

(Fig.3.4) through 6 inch P.V.C. pipe reducing to 3 inch at the entry of the main conduit. Special circular to rectangular transition fittings were incorporated at the entry and at the exit ends to smoothen out the flows. In an extension piece before the main test section honeycombs were provided to dampen any fluctuations caused by bends,valves etc and to facilitate the growth of fully developed flow. A bypass arrangement on the piping system facilitated control of discharges into the main and also eliminated entry of air into the system of manifolds at the commencement of the experiment. The flow exited through the main (limb 2) and the lateral (limb 3) into two 60° V notch tanks which were sufficiently long and had screens and baffles to prevent the formation of waves. The V notches were designed to ASME standards and could read up to a minimum head of 0.1 mm and for smaller discharge rates the gravimetric method was resorted to.

In spite of all the precautions there was always the possibility of pressures changing after a period of time due to air accumulation near the control valves. Any changes by the entry of air was avoided by opening the overflow valves on the top of manifolds to drive out any air entry into the system before taking each manometric reading. While testing the smallest lateral, maintaining positive pressures close to the junction was also found to be very necessary to prevent reverse flows from the manifold into the minimum pressure region of the lateral. To achieve this the initial pressure and flows in the main conduit were adjusted at the commencement of each experiment in relation to taps on the inner wall of the lateral near the junction where minimum pressures were likely to occur. Throughout the tests some of the pressure head readings on the main conduit and the V notch readings were repeated to ensure that the main flow system of pressure and discharge remained unchanged.

In the last part of the experiment the main conduit was also made from plexiglas with the view to visualize the flow and the pressure taps were numbered differently from Figs. 3.2 as shown in the tables of pressure readings. The laterals were tested both in the horizontal and vertical modes.

CHAPTER IV

CHARACTERISTICS OF DIVIDING CLOSED CONDUIT FLOWS

CHAPTER IV

CHARACTERISTICS OF DIVIDING CLOSED CONDUIT FLOWS.

4.1. General Remarks

The study of the characteristics of single closed conduit laterals (Fig.1.1) branching at 90° is essential to understand the flow behavior at T junctions and multi-ports encountered in field installations. The study involves the following aspects of the flow characteristics:

(1) Relating the momentum loss and energy loss with the other hydrodynamic parameters such as discharge ratio, pressure recovery factor, pressure coefficient and energy loss coefficient for the main and lateral conduits,

(2) Relating the momentum loss in the main conduit with the unbalanced force on the walls of the lateral conduit,

(3) Evaluation of the coefficient of lateral discharge, determination of the minimum pressure and comparing the various parameters with the results of previous studies.

4.2 Theoretical Considerations.

Consider a steady, tw › dimensional, incompressible fluid flowing at a rate Q_1 in a main conduit of uniform cross sectional area A_{r1} (Fig.4.1). As the flow traverses the junction, a part of the fluid Q_3 leaves the main conduit and flows through the lateral conduit of uniform cross sectional area A_{r3} and the remainder of the discharge ,Q_2, continues to flow along the main conduit.

The flow field is characterized by two separated regions R_1 and R_2 (Fig.4.1) in the vicinity of the junction. These regions have been identified in many of the previous studies (Hager [1984], Popp [1983]) and are a consequence of the boundary discontinuity and adverse pressure gradients respectively . The boundary discontinuity on the main conduit arises due to the upstream (u/s) corner T_1 (Fig.4.1) of the lateral opening. An adverse pressure gradient occurs in the region of the main conduit near the branch caused by the deceleration of the flow as Q_2 negotiates the junction.

The location of the stagnation point S_n varies with the discharge ratio q ($=Q_3/Q_1$) and three typical types of dividing stream lines and stagnation points are possible (Fig.4.1). For purposes of theoretical analysis, the dividing stream line is assumed to meet the junction at the downstream (d/s) corner (T_2) of the branch which is the specific stagnation point S_o corresponding to the critical discharge ratio q_{cr}.

4.3 Flow In The Main Conduit

Dividing flow through the lateral conduit causes deceleration of the flow in the main conduit. This results in momentum and energy losses and gives rise to pressure recovery in the main conduit. To analyze these characteristics, a control volume ABCD (Fig.4.2.) is chosen such that the sections AB and CD are outside the influence of the disturbance caused by the lateral. The two upstream and downstream sections of the main conduit, the lateral conduit, and the corresponding cross sectional areas are referred to as limb 1, limb 2, limb 3 and A_{r1}, A_{r2} ($=A_{r1}$) & A_{r3} respectively. The widths of the sections of the two conduits are denoted as b_1,b_2 ($=b_1$) & b_3 respectively.

4.3.1 Momentum And Energy Equations

Applying a momentum balance to the control volume ABCD (Fig.4.2) in the direction of the flow, from limb1 to limb 2, the following equation is obtained.

$$P'_1 A_{r1} + \beta'_1 Q_1 V_1 \rho = P'_2 A_{r2} + \beta'_2 Q_2 V_2 \rho + \Delta M \qquad (4.1)$$

where, P' is the pressure at the control sections AB and CD

A_r cross sectional areas

V average velocity at the control sections

β' momentum coefficient at control sections

ΔM the unbalanced momentum in the main conduit due to the flow in the lateral ,

and suffixes 1and 2 indicate the main conduit limbs.

The unbalanced component of the momentum in the main conduit is defined as,

$$\Delta M = R_m Q_3 V_1 \rho \qquad (4.2)$$

where, R_m is the pressure recovery factor or the static pressure gain component as defined by Bajura [1971]. Referring to Fig.4.2 and Fig.4.3a one can rewrite Eq.(4.1) as follows:

$$(P_1 + P_{f_1}) A_{r1} + \beta'_1 A_{r1} V_1^2 \rho = (P_2 - P_{f_2}) A_{r1} + \beta'_2 A_{r1} V_2^2 \rho + R_m Q_3 V_1 \rho \qquad (4.3)$$

where, P_1, P_2 are the pressures on the lateral centerline obtained by extending the pressure lines (Fig.4.3a), P_f denotes the pressure loss due to friction based on average velocity along sections BB_2 and AA_2 (Fig.4.2). Further P_f is related to friction factor as follows:

$$P_f = \frac{f L}{d} \frac{\rho V^2}{2} \tag{4.3a}$$

where f = friction factor,

d= Hydraulic diameter= $4A_f/P_e$

P_e= wetted perimeter of flow

and L = length of conduit.

From the pressure gain between limbs 1 and 2 (Fig.4.3a) a pressure coefficient, C_{P21}, is defined as

$$C_{P_{21}} = \frac{P_2 - P_1}{\frac{1}{2} V_1^2 \rho}$$

Eq.(4.3) therefore can be rewritten as

$$Cp_{21} = 2\beta_1' - 2\beta_2' (1 - q)^2 - 2 R_m q + \frac{f_1 L_1}{d_1} + \frac{f_2 L_2}{d_1} (1 - q)^2 \tag{4.4}$$

where, $q = Q_3/Q_1$ and L_1, L_2 are the extrapolated lengths (Fig.4.3a) from the control volume sections to the reference axis. The pressure coefficient C_{P21} is also related to the energy loss coefficient e_{12} based on Bernoullis equation. Thus for the control volume ABCD,

$$(Z_1 + \frac{P_1'}{\gamma}) + \alpha_1' \frac{V_1^2}{2g} = (Z_1 + \frac{P_2'}{\gamma}) + \alpha_2' \frac{V_2^2}{2g} + e_{12} \frac{V_1^2}{2g} \tag{4.5}$$

where, Z_1 is the height from the datum, α' the energy coefficient at the control sections and γ the specific weight of water.

Rewriting Eq. (4.5) in terms of the extrapolated pressures (P_1 and P_2) at the reference axis (Fig.4.3a) and rearranging one obtains,

$$C_{P\,21} = \alpha_1' - \alpha_2' (1 - q)^2 - e_{12} + \frac{f_1 L_1}{d_1} + \frac{f_2 L_2}{d_1} (1 - q)^2 \qquad (4.6)$$

since, $P_1' = P_1 + P_{f1}$ and $P_2' = P_2 - P_{f2}$.

Equating Eqns.(4.4) and (4.6), the relationship for the main conduit energy loss coefficient across the control volume,between limbs 1 and 2, (Fig.4.3a) is obtained as,

$$e_{12} = (\alpha_1' - 2 \beta_1') + (1 - q)^2 (2 \beta_2' - \alpha_2') + 2 R_m q \qquad (4.7)$$

The energy loss in the main conduit consists of the boundary friction loss, dependent on the Reynolds number, and the loss due to branching in the lateral conduit. The former is discussed in Appendix A.1, while the latter is discussed in this chapter.

The energy loss due to branching flow is depicted as $e_{12}.V_1^2/2g$ in equation (4.5). By extending the uniformly decreasing pressure lines on to the reference axis (Fig.4.3a) also accounts for the average friction losses within the control volume. This is shown as E_{12} $V_1^2/2g$ in Fig.4.3a and these two coefficients, e_{12} and E_{12}, are related by Eq. (4.8) below.

$$e_{12} = E_{12} + \frac{f_1 L_1}{d_1} + \frac{f_2 L_2}{d_1} (1 - q)^2 \qquad (4.8)$$

Eq. (4.6) can be recast in terms of E_{12} as,

$$C_{P_{21}} = \alpha_1' - \alpha_2' (1 - q)^2 - E_{12} \qquad (4.9)$$

In most of the previous studies [Smith 1980], the loss coefficient E_{12} was evaluated from Eq.(4.9) assuming uniform velocity distributions ($\alpha' = 1$) as in equation (4.10).

$$E_{12} = 2\,q - q^2 - C_{P_{21}} \tag{4.10}$$

Since the pressure coefficient C_{p21} is related to the momentum relation (4.4) the loss coefficient E_{12} can also be written as,

$$E_{12} = (\alpha_1' - 2\,\beta_1') + (1 - q)^2 (2\,\beta_2' - \alpha_2') + 2\,R_d\,q \tag{4.11}$$

where, the term R_d represents the pressure recovery factor after accounting for the frictional terms given by,

$$2\,R_d\,q = 2R_m\,q - \frac{f_1\,L_1}{d_1} - \frac{f_2\,L_2}{d_1}(1 - q)^2 \tag{4.12}$$

For uniform velocity distribution (α', β' =1), the above equation reduces to the following form.

$$E_{12} = q\,(q - 2 + 2\,R_d) \tag{4.13}$$

From these equations it can be inferred that to solve the four main variables Cp_{21}, q, E_{12} and R_d a correlation on test data between Cp_{21} and q is needed. The simplified Eq. (4.13) for E_{12} suggests that it becomes zero for two values of q, namely at q=0 and at q=2-2R_d. Also it becomes negative when q < 2-2R_d. For the through flow condition (q=0), the value of C_{P21} =0 (as P_1=P_2) and therefore E_{12} (and e_{12}) is approximately zero. At the other extreme condition when q=1 (no through flow), the energy loss in the main is a maximum [Smith 1980].

Having established a C_{p21}, q relationship experimentally, the solution to the dividing flow problem is achieved.

4.3.2 Pressure Recovery Factor, R_d

Eq.4.2 of section 4.3.1, denotes the pressure recovery factor relation to the unbalanced momentum component ΔM and repeated below as,

$$\Delta M = R_m Q_3 V_1 \rho$$

Omitting the frictional terms within the control volume ABCD (Fig.4.3a) and replacing R_m with R_d in Eq.(4.4) as in Eq.(4.12) one gets,

$$C_{P_{21}} = 2 \beta_1' - 2\beta_2' (1 - q)^2 - 2 R_d q \qquad (4.14)$$

For uniform velocity distribution at the sections ABand CD the coefficients α' and $\beta' = 1$ and hence the above equation becomes,

$$C_{P21} = 2 q \{ 2 - R_d . q \} \qquad (4.15)$$

i.e., R_d can be evaluated using Eq.(4.15)

4.3.2.1 Unbalanced Pressure Force on Lateral Walls.

The momentum loss in the main duct due to the lateral flow can also be verified experimentally by determining the net force on the lateral walls. Thus, by recording the pressures on both the upstream and downstream walls of the lateral, from the junction onwards up to the point where the two pressures become equal, and assuming the flow as two dimensional, the net force in the same direction as the main conduit axis can be evaluated. Considering the control volume T_1T_2NM (Fig.4.3b) and applying the momentum equation in the direction normal to the lateral conduit axis, the net wall force (F) is given by,

$$F = (P_U - P_D)w_3 = \Delta M = R_d Q_3 V_1 \rho, \qquad (4.16)$$

where, $(P_U - P_D)$ = sum of differential pressures between upstream and and downstream walls over a length l_3,

= area between the pressure diagrams of the two walls

w_3 = width of lateral wall,

and l_3 = length over which the two pressures vary.

Thus R_d can be evaluated independent of the momentum balance considerations in section 4.3.2.

4.3.3 Expanding Through Flow (Q2) in The Main Conduit.

Hager [1984] has analyzed the main conduit through flow component, Q_2, as a diverging flow across the lateral junction. The parameter P_{AV}, shown in Fig.4.4(a) across section T_2E, is the average of the pressure variation along the dividing streamline between

P_S (stagnation pressure) and P_1. Considering the control volume AB_1CD (Fig.4.4a) and applying the momentum equation,

$$P_1' (1 - q) A_{r1} + \beta_1' Q_2 V_1 \rho + P_{AV} q A_{r1} = P_2' A_{r1} + \beta_2' Q_2 V_2 \rho \qquad (4.17)$$

Replacing pressure terms P_1' and P_2' with the reference axis pressure terms,

$$\begin{aligned} &(P_1 + P_{f1}) (1 - q) A_{r1} + \beta_1' (Q_1 - Q_3) V_1 \rho + P_{Av} q A_{r1} \\ &= (P_2 - P_{f2}) A_{r1} + \beta_2' \frac{(Q_1 - Q_3)^2}{A_{r1}} \rho \end{aligned} \qquad (4.18)$$

Replacing Q_3/Q_1 with q and rearranging, the pressure coefficient Cp_{21} in terms of P_{AV} - P_1 and P_{AV} - P_2 is obtained as follows

$$C_{P_{21}} = \frac{(P_{AV} - P_1) q}{V_1^2 \rho / 2} + 2 \beta_1' (1 - q) - 2 \beta_2' (1 - q)^2 + \frac{f_1 L_1}{d_1} (1 - q) + \frac{f_2 L_2}{d_1} (1 - q)^2 \qquad (4.19)$$

$$C_{P_{21}} = \frac{P_{AV} - P_2}{V_1^2 \rho / 2} \frac{q}{1 - q} + 2 \beta_1' - 2 \beta_2' (1 - q) + \frac{f_1 L_1}{d_1} + \frac{f_2 L_2}{d_1} (1 - q) \qquad (4.20)$$

Equating (4.19) to Eq. (4.6) and omitting the last two frictional terms ,

$$\frac{P_{AV} - P_1}{V_1^2 \rho / 2} q = (\alpha_1' - 2 \beta_1') + 2 \beta_1' q + (1 - q)^2 (2\beta_2' - \alpha_2') - e_{12} \qquad (4.21)$$

Equating (4.19) to Eq.(4.4),

$$\frac{P_{AV} - P_1}{V_1^2 \rho / 2} = 2 (\dot{\beta_1} - R_m) + \frac{f_1 L_1}{d_1} \qquad (4.22)$$

Similarly the terms of P_{AV} and P_2 are related through equations (4.20) and (4.4) as,

$$\frac{P_{Av} - P_2}{V^2_1 \rho / 2} \frac{q}{(1 - q)} = 2\dot{\beta_2} q (1 - q) - 2 R_m q - q (1 - q) \frac{f_2 L_2}{d_1} \qquad (4.23)$$

In Eq.(4.22) by omitting the small frictional term one gets,

$$P_{AV} = 2 (\dot{\beta_1} - R_m) \frac{V_1^2 \rho}{2} + P_1 \qquad (4.24)$$

For all practical purposes the stagnation pressure, P_S, is given by,

$$P_S = P_1 + \dot{\alpha_1} \frac{V_1^2 \rho}{2} \qquad (4.25)$$

From the above relationship Eq.(4.25) is transformed to a form which relates the pressure terms as,

$$P_{AV} = 2 \frac{(\dot{\beta_1} - R_d)}{\dot{\alpha_1}} P_S + (1 - \frac{2(\dot{\beta_1} - R_d)}{\dot{\alpha_1}}) P_1 \qquad (4.26)$$

Here the term R_d is the replaced R_m by omitting the friction terms.

For $\alpha, \beta = 1$ conditions the above equation becomes,

$$P_{AV} = 2 (1 - R_d) P_s + \{1 - 2(1 - R_d)\} P_1 \qquad (4.27)$$

Similar relations can be drawn relating P_{AV} and P_2 through Eq.(4.23).

4.3.3.1. Flow Models

Flow models have been proposed for the determination of P_{AV} by several investigators and some of these are discussed in this section.

4.3.3.1.1. Linear pressure variation model

A model proposed by Hager [1984] assumes a linear variation of pressure along the dividing stream line in which the pressure is P_1 at B_1 and the stagnation pressure P_s at S_n. The average pressure is hence $P_{AV}=(P_1+P_S)/2$ and substituting this in Eq(4.25),

$$P_{AV} = P_1+V_1^2 \rho /4$$

Using Eq.(4.27),the pressure recovery factor becomes,

$R_d = 0.75$, a constant value for all discharge ratios.

4.3.3.1.2 Parabolic Pressure Variation Model.

This model is similar to Duc Tran [1988] and explained below.

Here the pressure p at any distance x is assumed to vary parabolically with the offset distance y as shown in Fig. 4.4 b. Thus

$$p=A\, y^2 + B\, y +C \qquad (4.27a)$$

With limiting conditions dP/dy =0 at y=0; B=0. , at y=o , $p=P_1$: $C= P_1$ and at y=q. b_1, $p=P_S$. resulting in

$$A = \frac{(P_s - P_1)}{(q\, b_1)^2}.$$

The flow model relation becomes,

$$p = \frac{(P_s - P_1)}{(q\, b_1)^2} y^2 + P_1 \qquad (4.28)$$

Neglecting boundary friction in the short distance considered and applying momentum equation to the control volume B_1BS (enclosing Q_3)

$$P_1\ q\ b_1\ w_1 + \beta_1\ q\ Q_1\ V_1\ \rho - w_1 \int_0^{q\, b_1} p\, dy\ =\ \Delta M \qquad (4.29)$$

where, dx = incremental horizontal distance

w_1 = width of duct

and dy = incremental vertical distance.

Using Eq.(4.27a) in Eq.(4.29) the pressure variation term reduces to the following form,

$$\int_0^{qb_1} p\, dy\ = q.b_1\ (\frac{P_s + 2\ P_1}{3}) \qquad (4.29a)$$

Thus, $P_{AV} = (P_s+2P_1)/3$ and substituting in Eq. (4.27), $R_d=5/6=0.83$, a constant value for all q ratios. Substituting for P_s from Eqn.(4.25) for this model,

$$P_{AV} = P_1 + V_1^2\rho/6 \qquad (4.29b)$$

4.3.3.1.3 General Flow Model

A general flow model can be written by replacing the quadratic term in Eq.4.28 by y^n. Then the average pressure P_{AV} can be evaluated as,

$$P_{AV} = \frac{P_s + nP_1}{(n+1)} = P_1 + \frac{V_1^2 \rho}{2(n+1)} \tag{4.30}$$

and the pressure recovery factor is related as,

$$R_d = 1 - \frac{1}{2(n+1)} \tag{4.31}$$

The value of R_d has been generalized with n and as an example,

for n =3,

$$P_{AV} = (3P1+Ps)/4$$
$$= P1+V1^2\rho/8 \tag{4.31a}$$

and $R_d = 7/8.$

All the models discussed above are approximate and have limitations. The average pressure term P_{AV} can have a maximum value close to the stagnation pressure, P_s, for reservoir conditions (m - 0) or attain the value of P_2 when q=1. Rd appears to be not sensitive to high values of the exponent n.

4.4 Flow Through the Lateral.

As seen from Fig.4.5(a) the flow into the lateral initially contracts up to GH and then expands until section MN. This results in a loss of total energy ($P_1/\gamma+\alpha_1 V_1^2/2g$).

The flow continues beyond MN with a constant friction loss per length. Due to the nature of the flow, the pressures along the two lateral walls differ, accounting for the momentum loss in the main duct (ΔM) as discused in section 4.3.2.1 and illustrated in Fig.4.5b.

From the entrance of the lateral to the vena contracta the two wall pressures fall rapidly to minimum values and then rise to merge together to a value P_3' at a section MN of this conduit. Beyond MN the pressures continue to drop with a constant pressure gradient. From the entrance of the lateral there is flow separation on the inner wall of the lateral due to discontinuity of the main duct and the separating streamline is well defined up to the vena contracta with a speed of Vj along the free streamline T_1T_3 (Fig.4.5a) determined by the minimum inner wall pressure at the corner T_1.

4.4 .1 Momentum and Energy Equations

Considering the control volume GHMN (Fig.4.5a) and applying the momentum balance equation between sections GH and MN where the pressures and velocities are P_4,V_4 and P_3', V_3 respectively.

$$P_4 A_{r3} + \beta_4 Q_3 V_4 \rho = P_3' A_{r3} + \beta_3' Q_3 V_3 \rho \qquad (4.32)$$

Here, β_4,β_3' denote the respective momentum coefficients. Extending the straight line pressure gradient from MN on to the junction point T_1,T_2 and replacing P_3' by P_3 -Pf_3 (Fig.4.3 c) and assuming that the average coefficient of contraction at GH as C_c equation (4.32) is transformed into,

$$P_3 - P_4 = V_3^2 \rho \left(\frac{\beta_4}{C_c} - \beta_3' \right) + \frac{f_3 L_3}{d_3} \frac{V_3^2 \rho}{2} \qquad (4.33)$$

Applying Bernoulllis equation between sections GH and MN,

$$\frac{P_4}{\gamma} + Z_1 + \alpha_4 \frac{V_4^2}{2g} = \frac{P_3'}{\gamma} + Z_1 + \alpha_3' \frac{V_3^2}{2g} + e_{43} \frac{V_1^2}{2g} \tag{4.34}$$

where e_{43}. $v_1^2/2g$ is the total energy loss between the two sections. .

In a similar manner, by the replacement of P_3' with P_3-P_{f3} and V_4 with V_3/C_c the above equation is transformed to Eq.(4.35),

$$P_3 - P_4 = \alpha_4 \frac{V_3^2}{C_c^2} \frac{\rho}{2} \alpha_3' \frac{V_3^2}{2} \rho - e_{13} \frac{V_1^2}{2} \rho + \frac{f_3 l_3}{d_3} \frac{V_3^2}{2} \rho \tag{4.35}$$

Since there is negligible loss in the contracting section up to GH, $e_{43}=e_{13}$.

Equating Eqs.(4.33) and (4.35) and substituting for V_3/V_1 as q/m where m is the area ratio of the lateral and the main conduits (A_{r3}/A_{r1}),

$$e_{43} = e_{13} = \left(\frac{q}{m}\right)^2 \{ \frac{\alpha_4}{C_c^2} - 2 \frac{\beta_4}{C_c} + 1) \tag{4.36}$$

At the contracted section GH, (Fig.4.5a) the coefficients α_4,β_4 are essentially one and therefore Eq.(4.36) reduces to,

$$e_{13} = \left(\frac{q}{m}\right)^2 \{ \left(\frac{1}{C_c} - 1\right)^2 \} \tag{4.37}$$

To evaluate the coefficient of contraction and the nearly uniform velocity at the vena contracta a knowledge of the pressure of the separating stream line T_1G_1, (the inner stream) at G is necessary.

4.4.2 Contraction Coefficient C

When the lateral opening is very small ($A_{r3} << A_{r1}$) reservoir condition occurs and the coefficient of contraction C approaches a value derived from potential flow solution [Kirchoff 1869] given as,

$$C_{co} = \frac{\pi}{\pi + 2}$$
$$= 0.611$$

The term $(1/C_{co} - 1)^2$ in Eo (4.37) becomes 0.406 which is also the energy loss term e_{13} in terms of $V_3^2/2g$. McNown [1950] has shown from experimental results for dividing flows that this loss coefficient is reached for m=1/16 (circular pipes) at q=1. It is to be noted that this loss coefficient in terms of $V_1^2/2g$ is 104 due to the effect of the area ratio and is more useful for design purposes rather than being related to $V_3^2/2g$.
For the flow assumptions made in the development of the model the factor $(q/m)^2$ can be expressed in terms of the contraction coefficient C_c and velocity parameter η ($=V_1/V_j$).

$$(q/m)^2 = (Cc * 1/\eta)^2$$

Therefore, the energy loss term for $C_{co} = 0.611$ can also be written as,

$$e_{13} = 0.152(1/\eta)2 = 0.152\ H$$

where, $H = (E_1 - P_j)/V_1^2/2g$, P_j being the pressure at the vena contracta and dealt in section 4.4.5.

For sharp edged small circular orifices (1/4 " and 1/2 " diameter orifices in a 4 " diameter pipe) Rawn et al [1961] obtained an empirical relationship between C_c and E for dividing flow situation as,

$$C = 0.63 - 0.58 \frac{V_1^2}{2g\,E}$$

$$= 0.63 - 0.58\ \eta^2 \qquad (4.37a)$$

where, E is the total energy head inside the pipe given by $E = V_1^2/2g + h$ and h is the static pressure head difference $(P_1-P_j)/\gamma$ between the inside and outside of the pipe.

4.4.3 Pressure Coefficient Cp_{13} In The Lateral

The pressure and energy loss coefficients in the lateral are obtained by applying Bernoullis extended equation between sections AB in the main and MN in the lateral,where the α,β coefficients as well as the magnitudes of the average pressures and velocities are known.

$$\frac{P_1'}{\gamma} + Z_1 + \alpha_1' \frac{V_1^2}{2g} = \frac{P_3'}{\gamma} + Z_1 + \alpha_3' \frac{V_3^2}{2.g} + e_{13} \frac{V_1^2}{2g} \qquad (4.38)$$

Replacing P_1' , P_3' with P_1,P_3 etc, as in the previous section ,

$$C_{P13} = \alpha_3' \left(\frac{q}{m}\right)^2 - \alpha_1' + E_{13} \qquad (4.39)$$

where,

$$E_{13}\frac{V_1^2\rho}{2} = e_{13}\frac{V_1^2\rho}{2} - \frac{f_3 L_3}{d_3}\frac{V_3^2\rho}{2} - \frac{f_1 L_1}{d_1}\frac{V_1^2\rho}{2} \qquad (4.40)$$

Thus, obtaining the value of C_{p13} from experimental results, the term E_{13} can be calculated. Since the flow is contracting up to section GH in the lateral the loss due to turning flow is totally in the expanding region beyond GH. As mentioned before $e_{43} = e_{13}$.

Neglecting the frictional terms in Eq.(4.40), Eq. (4.37) becomes

$$E_{13} = \left(\frac{q}{m}\right)^2 \left\{ \left(\frac{1}{C_c} - 1\right)^2 \right\} \qquad (4.41)$$

Thus, by comparing the values of E_{13} obtained from Eq. (4.38) with the direct measurements of pressures and velocities, the validity of the assumptions made to derive Eq.(4.41) could be verified.

4.4.4 Contraction Coefficient From Irrotational Flow Theory, Cd.

The curvilinear nature of the flow is analyzed using the free vortex flow model based on irrotational flow theory. Fig.4.6 shows the inner and outer velocities and the radii at section GH as V_i, V_o, r_i and r_o respectively.

The inner velocity V_i is normal to section GH and is derived as before from the total energy (E_1) and the known inner pressure P_i on the inner wall at section GH. It was not possible to obtain the corner pressure due to the absence of pressure taps at the corners. Therefore as an approximation the minimum pressure on the wall P_i was used in its place. Thus,

$$V_i = \left\{ (E_1 - P_i)\frac{2}{\rho} \right\}^{\frac{1}{2}} \qquad (4.42)$$

Alternatively one could have used the extrapolated value of wall pressure at the entrance (P_e) to calculate the stream speed V_j.

The cavity flow is somewhat similar to a free vortex flow. An infinitesimal section of width dr in the contracted jet (Fig.4.6a) at a distance r from the center, O , is considered and its velocity v is given by,

$$v\, r = V_i\, r_i = V_o\, r_o \tag{4.43}$$

The resulting pressure difference across the inner and outer stream lines is given by ,

$$dp = \frac{v^2}{r}\rho\ dr = V_i^2\, r_i^2\, \rho\, \frac{1}{r^3}\ dr \tag{4.44}$$

Integrating between limits r_o & r_i, the total radial pressure difference ΔP of the bounding streamlines at section GH is given by,

$$\Delta P = \frac{V_i^2\, \rho}{2}\{\ 1\ -\ (\frac{r_i}{r_o})^2\ \} \tag{4.45}$$

Setting $r_i = k\, b_3$ and $r_o = (k + C_d)\, b_3$ where C_d is the coefficient of contraction and substituting these values in (4.45),

$$\frac{\Delta P}{V_i^2\, \rho\, /2} = \frac{\frac{2k}{C_d} + 1}{(\frac{k}{C_d} + 1)^2} \tag{4.46}$$

A further rearrangement of terms give,

$$\frac{k}{C_d} = \frac{Z}{1-Z} \tag{4.47}$$

where

$$Z = \sqrt{1 - \left(\frac{2\,\Delta P}{V_i^2\,\rho}\right)}$$

From the experimental results and the evaluation of ΔP and V_i, the ratio k/C_d can be found. The volumetric flow, q_d, ($=v.w_3.dr$) through the incremental area $w_3.dr$ (w_3 = lateral width) when integrated between limits r_o & r_i gives,

$$Q_3 = w_3\, V_i\, k\, b_3 \ln\left(\frac{k + C_d}{k}\right) \tag{4.48}$$

Rearranging the above equation,

$$\frac{V_3}{V_i} = k \ln\left(\frac{\frac{k}{C_d} + 1}{\frac{k}{C_d}}\right) \tag{4.49}$$

From Eqs. (4.47) & (4.49) k and Cd can be found. The mean velocity of the flow across GH by continuity equation is ,

$$V_{av} = \frac{V_3}{C_d}$$

The momentum and energy coefficients α,β at section GH, considering the jet flow, is given by,

$$\beta = \int_{r_i}^{r_o} \frac{v^2\, dr}{q_w^2 / (b_3\ C_d)} \qquad \alpha = \int_{r_i}^{r_0} \frac{v^3\, dr}{q_w^3 / (b_3^2 C_d^2)}$$

where

$$q_w = \frac{Q_3}{w_3} = \frac{1}{w_3}\int_{r_i}^{r_o} q_d\ dr$$

Substituting for r_i, r_o etc,

$$\beta = \left(\frac{V_i}{V_3}\right)^2 \frac{k C_d^2}{(k + C_d)}$$

$$= \left(\frac{V_i}{V_{av}}\right)^2 \frac{k}{k + C_d} \qquad (4.50)$$

$$\alpha = \frac{1}{2}\left(\frac{V_i}{V_3}\right)^3 \frac{k C_d^3 (2k + C_d)}{(k + C_d)^2}$$

$$= \frac{1}{2}\left(\frac{V_i}{V_{AV}}\right)^3 \frac{k (2k + C_d)}{(k + C_d)^2} \qquad (4.51)$$

The above relations take into account only the effects of streamline curvature. The C_d values thus obtained are compared with C_c values described in the previous sections (C_c by assuming a constant velocity V_i at the vena contracta with $\alpha_4, \beta_4 = 1$, and C_c obtained from the lateral energy loss coefficient E_{13}).

4.4.5 The Velocity Parameter η

By definition, the velocity parameter $\eta = (V_1/V_i) = (V_1/V_j)$ relating the incoming velocity in the main duct (V_1) and the inner jet velocity (V_J) at the vena contracta in the lateral conduit which, as explained in the previous paragraphs, determine the coefficient of contraction (C_c &C_d). If P_J is the inner wall pressure (=P_i) corresponding to V_J ,then

$$\eta^2 = \frac{\frac{V_1^2 \rho}{2}}{(E_1 - P_j)} = \frac{\frac{V_1^2 \rho}{2}}{h_{1J} + \alpha_1 \frac{V_1^2 \rho}{2}} \tag{4.52}$$

where E_1, (=$P_1 + \alpha_1 V_1^2 \rho/2$) , is the incoming total energy at the U/S corner T_1 of the junction, and h_{1j} (= $P_1 - P_J$), is the difference in pressure head between the junction and the minimum pressure point G in the lateral. Thus η^2 is a measure of the ratio of the kinetic to the total energy at G. Since η is also related to Cc through the continuity equation ($\eta = V_1/V_j = V_1 V_3/V_3 V_j$) it becomes,

$$\eta = \frac{m}{q} C_c \tag{4.53}$$

The minimum pressure at G could be predicted for known E_1,C_c and q values based on Eq.(4.53) and (4.52). Alternatively, by defining the ratio of pressure head at the jet to the kinetic energy in the main as,

$$\frac{P_1 - P_J}{\frac{V_1^2 \rho}{2}} = C_{P\,min}$$

it is related to η^2 from equation (49) as,

$$C_{P\,min} = \frac{1}{\eta^2} - 1 = \frac{q^2}{(m\,C_c)^2} - 1 \qquad (4.54)$$

Thus negative pressures could be avoided if the relationship of η & C_c are known for various discharge ratios (q) as they have cavitation potential.

4.4.6 Other Pressure Characteristics

The pressure variations inside the lateral is similar to that in orifice plates, step flows and side channel weirs. The pressure recovery from the vena contracta has similar curve patterns and in order to study this behavior some of the pressure coefficients relating to the minimum pressure P_j are related to each other with η^2 ,Cp_{21} and Cp_{13} as below.

As shown earlier, $1+Cp_{1J} = 1/\eta^2 \cdot = H$

and the other pressure coefficients C_{P2J} and $C\,P_{3\,J}$ are given by

$$\frac{C_{P21} + C_{P1J1}}{1 + C_{P1J1}} = \eta_1^{\,2}\, C_{P2J1} = 1 - \eta_1^2\,(1 - C_{P21}) \qquad (4.55)$$

and

$$\frac{C_{P1J1} - C_{P13}}{1 + C_{P1J1}} = \eta_1^2 C_{P3J1} = 1 - \eta_1^2 (1 + C_{P13}) \tag{4.56}$$

From Eq.(4.56), the minimum pressure in terms of C_{p13} and η^2 is,

$$C_{P3j} = \frac{1}{\eta^2} - 1 - C_{P13} \tag{4.57}$$

Eq.(4.33) also defines CP_{3J} ($P_4=P_j$) in terms of q and C_c with the assumption of constant jet velocity Vj at the vena contracta. By omitting the friction term in the above momentum equation between sections GH and MN (Fig.4.5a) and assuming $\beta'=1$, it reduces to,

$$C_{P3j} = 2 \left(\frac{q}{m}\right)^2 \left(\frac{1}{C_c} - 1\right) \tag{4.58}$$

The energy loss coefficient e_{13} in equation (4.37) can be also written in terms of C_{p3j} by replacing the terms inside the bracket in Eq.(4.58). Thus,

$$E_{13} = (m/q)2\ C_{p3j}^2 / 4 \tag{4.59}$$

By equating (4.57) and (4.58), a relation between C_c and C_{p13} can be obtained.

$$\frac{1}{C_c} = \{ (1 + C_{p13}) \left(\frac{m}{q}\right)^2 - 1 \}^{0.5} + 1 \tag{4.60}$$

The next Chapter deals with the experimental results and analysis based on the theoretical study in this Chapter.

CHAPTER V

EXPERIMENTAL RESULTS AND ANALYSIS

CHAPTER V

EXPERIMENTAL RESULTS AND ANALYSIS

5.1 General Remarks

The experimental set-up and the three rectangular ducts tested are described in Chapter 3. The experiments carried out with each laterals are listed in Table 5.1. Test results and analysis representative of each lateral are included in Table 5.2, 5.3 and 5.4 with suffix (b) denoting the test number in Table 5.5. Pressure diagrams for the laterals are shown in Figs.5.1, 5.2 and 5.3 with suffixes (a), (b), (c), (d) and (e) denoting different test numbers. Representative calculation sheets are given in Appendix IV and the representative test numbers are as underlined in Table 5.1 and also given in Table 5.5. Test observations and computations of some of the main parameters for each experiment are summarized in Table 5.6 (a,b,c,d) for lateral 1, Table 5.7 (a,b,c) for lateral 2, and Table 5.8 (a,b,c) for lateral 3 in which R, indicates the Reynolds number, a indicates the energy coefficient, B indicates the momentum coefficient and N indicates the factor in the power law of velocity variation in the conduit. The other parameters discussed in Chapter 4 are summarized in Tables 5.9 (a,b,c) to 5.11 (a,b,c) for the three laterals. In this Chapter the various parameters are evaluated, analyzed and compared with previous results wherever possible.

5.2 Pressure Diagrams (Figs.5.1 to 5.3)

The laterals were tested in both the vertical and horizontal configurations. The water columns of the manometric heads were observed to the nearest 0.5 mm and the pressure heads were plotted for both limbs of the main conduit and the lateral conduit. By extending the uniform straight line pressure gradients of the two limbs of the main conduit on to the center line of the lateral, the pressure head P_1 and P_2 (Fig. 4.3a) were obtained. Similarly, the lateral uniform pressure gradient was extended back to the entrance point and P_3 was obtained (Fig.4.3c). From the flow measurements of Q_2 and Q_3, the average velocities, frictional terms and α,β values in the main and branch sections were determined (Appendix A.1.1). The same Appendix A.1.1 also includes straight through flow tests to derive the correct straight line pressure gradients and friction characteristics for varying Reynolds numbers. These gradients were used as the reference to verify the pressure gradients and also to assist minor corrections of gradients in cases of very low discharges and very low pressures. For these reasons the tests referred to as straight through flow tests (in Appendix A.1.1) were called calibration tests by Barton [1946]. Some of the main features of the lateral flow test pressure diagram can be seen in Fig.5.4 (a) & (b) which include:

(1) Stagnation or near stagnation pressures occur at point a_1 either in the main or in the lateral conduits (Fig.5.4) discussed in section 5.2.2

(2) Steep pressure drop ab along the wall of the main just ahead of the upstream (u/s) corner T_1. A minimum pressure point c or a region on the u/s (or the inner) lateral wall. A pressure recovery ,cm_2, followed by a uniform pressure gradient m_2m_3 on the u/s wall of the lateral,

(3) Pressure drop a_1b_1 near the downstream (d/s) corner of the lateral, T_2, from the stagnation point a_1 very steeply to a minimum value b_1 followed

immediately by a steep rise b_1c_1. From c_1 the pressure drops gradually to a second minimum point m_1, merges with the inner wall pressure diagram, rises to m_2 and continues along m_2m_3 with a uniform pressure gradient.

The first part of the pressure diagram mentioned in (3) to minimum point b_1 was not recorded clearly for lateral 1 due to lack of sufficient pressure taps close to the junction.

5.2.1 Stagnation Pressure P_S

Following the physical description of the stagnation pressure in section 4.2 (Chapter 4), it was observed that the experimental results show a peak pressure reading close to the d/s corner T_2 either in the main or in the lateral, depending on the discharge ratio (q). For larger q ratios the stagnation point was in the main, and as q was reduced it moved to the corner and then for much smaller q ratios it occurred in the d/s wall of the lateral conduit (Fig.4.1). It was not always possible to obtain the stagnation point at the exact location due to the absence of pressure taps and on the presence of pressure pulsations. The peak pressure observed was checked for its accuracy by comparing it with the total theoretical head of $P_1 + V_1^2/2g$ and in some circumstances were extrapolated to the total theoretical head value. This procedure in turn enabled the establishment of the stagnation point. Some of the observed results are summarized in Table 5.12.

The particular critical discharge ratio that corresponds to the stagnation at the d/s corner T_2 (Fig.4.1) is denoted as q_{cr}. Its determination will justify the q range of application for the control volume selected in Fig.4.2. Since experimental results did not yield this critical ratio q_{cr} exactly, potential flow analysis was adapted from O'Neill & Chorlton [1986] to determine it. The Schwarz -Christoffell transformation was used to obtain dz/dt in the t plane where z denotes the physical plane (z=x+iy). The differentiation of the complex potential yielded dw/dt (refer Fig.5.5 for the main equations). From these two equations

the complex velocity, dw/dz, was obtained. At the stagnation point dw/dz was made equal to zero. For the particular stagnation at the corner point in the z plane, following O'Neill [1986], the corresponding point in the t plane was chosen as t = 0 (Fig.5.5). The application of the corresponding velocity potential at each corner of the Schwarz - Christoffel polygon (t =- a, t = - b, and t = d) in Fig.5.5 and making use of the continuity equation, the following equation for the particular q ratio (q_{cr}) in terms of the ratio of the width of lateral (b_3) to the width of main conduit (b_1) was obtained;

$$q_{cr} = -\frac{1}{2}\left(\frac{b_3}{b_1}\right)^2 + \frac{b_3}{2\,b_1}\sqrt{\left(\frac{b_3}{b_1}\right)^2 + 4} \qquad (5.1)$$

The above width ratios also represent area ratios and the values of discharge ratio q_{cr} corresponding to the location of the stagnation point at the downstream corner, calculated for the three laterals tested and for some sizes tested previously are given in Table 5.13.

On plotting a graph and fitting a curve a much simpler equation follows:

$$q_{cr} = 0.93\,\frac{b_3}{b_1} - 0.32\left(\frac{b_3}{b_1}\right)^2 \qquad (5.2)$$

From this equation, it is inferred that the maximum value of q_{cr} is o.67 for a width ratio of 1.45 and the maximum value of the width ratio of lateral to main is 2.9. This equation also indicates that when b_3 is very small (b_3 --> 0), q_{cr} value also tends to zero.

In the case of potential flows, it is relevant to mention that Modi [1981] obtained stagnation points for combining flows in two dimensional channels with q_{cr} values of o.618 and 0.390 for diameter ratios of 1 and 0.5 respectively (area ratio = 0.25). This agrees with the values shown above in the table, as dividing flows could be obtained by reversing flow directions in combined flow models. It is achieved by changing the two sources into two

sinks, interchanging the positive and the negative sides of the real axis etc, the solution of other stagnation points also could be obtained from his combined flow solutions. It is also noted, that the values in the real axis of the ζ plane for dividing flow is a mirror image of the values about its origin of coordinates, which is the junction corner point T_2 in the z plane, and this is illustrated in Fig.5.6(a). Physical interpretation of Fig.5.6a in the z plane for dividing flow is shown in Fig.5.6(b) which identifies the location of the stagnation points and the cross over point (q_{cr}) from the main into the lateral conduit. The experimental points are plotted to illustrate the similarity especially for the cross over of the stagnation point location from the main to the lateral.

5 .2.2 Pressure Coefficient C_{p21}

The variation of pressure coefficient Cp_{21} obtained from the extrapolated pressures P_1 and P_2 in the test pressure diagram (Figs.5.1 to 5.3 and Tables 5.2 to 5.4) with the discharge ratio (q) for the three lateral sizes tested are shown in Fig.5.7.(a),(b) and (c). Some of the previous test results for similar area ratios, as cited in McNown [1954] and Hudson [1979], are also shown in the same figures showing that they are in close agreement with the present experimental results. In Fig.5.7(b), the graph for area ratio of 0.67 from the previous studies should be compared qualitatively.

As discussed in section 4.3.1 a correlation between C_{p21} and q is necessary to solve the variables E_{12} and R_d in the main conduit. A comprehensive correlation between the pressure coefficient and discharge ratio q from the previous studies (Hudson 1979) are used to achieve this goal. For an area ratio m=1, the C_{p21} values are depicted in Fig.5.7(d) and the equations fitted with correlation coefficients of 0.97 and 0.99 are given below:

$$C_{p21}(\text{McNown}) = 0.08 + 2.28q - 1.69\, q^2 \qquad (5.3)$$

$$C_{p21}(\text{Vogel}) = 0.09 + 2.17q - 1.62\ q^2 \qquad (5.4)$$

Vogel's [1928] values, referred to also as Munich experiments, were found to disagree slightly with the results of other studies [Miller 1971]. Nevertheless these data are also taken into consideration in the present study to obtain an overall pattern of all existing experimental results. Thus the mean values of the two equations above gave the following equation for an area ratio $A_3/A_1=1$,

$$C_{p21}\ (\text{mean}) = 0.05 + 2.39q - 1.77\ q^2 \qquad (5.5)$$

Similarly, previous test results for area ratios of 0.336, 0.25 and 0.0625 are shown in Fig:5.7(e) and the resulting equations fitted with correlation coefficients in the range of 0.97 to 0.99 are,

for m=0.25 $$C_{p21}(\text{McNown}) = 0.02 + 2.16q - 1.54\ q^2 \qquad (5.6)$$

for m=0.0625 $$C_{p21}(\text{McNown}) = 0.003 + 2.06q - 1.44\ q^2 \qquad (5.7)$$

and for m=0.336 $$C_{p21}(\text{Vogel}) = 0.015 + 2.20q - 1.58\ q^2 \qquad (5.8)$$

To obtain a much representative correlation in terms of area ratios, the equation from the present test results for lateral 2 (m=0.77) is also utilized.

$$C_{p21}(\text{present}) = 0.04 + 2.33q - 1.71q^2 \qquad (5.9)$$

These graphs indicate that the variation of C_{p21} with q is parabolic and the correlation appears to be of the form

$$Cp_{21} = Aq - B\,q^2 + C \qquad (5.10)$$

where A,B and C are assumed to vary with the area ratio m as follows;

$$A = A_1 + A_2\,m + A_3\,m^2 + A_4\,m^3$$

$$B = B_1 + B_2\,m + B_3\,m^2 + B_4\,m^3$$

$$C = C_1\,m$$

Using equations (5.5), (5.6), (5.7) and (5.9) the parameters A,B and C are related as,

$$A = 2.02 + 0.68\,m - 0.52\,m^2 + 0.21\,m^3$$

$$B = 1.4 + 0.68\,m - 0.52\,m^2 + 0.21\,m^3$$

$$C = 0.05\,m$$

From the above relations, Cp_{21} for the three lateral sizes tested in terms of q are;

(1) For (m=1) $Cp_{21} = 2.39\,q - 1.77\,q^2 + 0.05$ (5.11)

(2) For (m= 0.77) $Cp_{21} = 2.33\,q - 1.71\,q^2 + 0.04$ (5.12)

(3) For (m=0.225) $Cp_{21} = 2.15\,q - 1.52\,q^2 + 0.01$ (5.13)

The variations of C_{p21} with q between each laterals are very small. As stated earlier the present test results for area ratio m =1 agree very closely with McNown's results (Fig.5.7a) which is claimed to agree with the Stanford tests,Vennard [1954]. These previous tests were carried out with circular pipes and hence rectangular conduits appears to have little effect on the dependency of C_{p21} on q. It may also be mentioned that by combining both the studies at Iowa (McNown 1954) and Munich (Vogel 1929) with the present studies to correlate C_{p21} with q, the resulting equations in the subsequent determination of the other parameters like R_d and E_{12} in terms of q will show only a mean trend reflecting the results of the the present and previous studies.

5.3 Energy Loss Coefficient E_{12}.

The energy loss coefficient E_{12} denotes the loss coefficient between the upstream and downstream lengths of the main conduit (Fig.4.3a) and the present experimental values are shown in Fig.5.8. It is seen that the effect of the lateral sizes is very little although the negative energy loss region reduces with the decreasing sizes. The maximum value of E_{12} for q=1 varies from 0.36 to 0.45, the highest value occurring with the smallest lateral in place. Using the equations (5.11) to (5.13) for C_{p21}, following correlated equations for E_{12} from Eq.(4.9) are obtained.

(1) m=1 (Lateral 1)

$$E_{12} = 0.77\, q^2 - 0.39\, q - 0.05 \qquad (5.14)$$

(2) m=0.77 (Lateral 2)

$$E_{12} = 0.71\, q^2 - 0.33q - 0.04 \qquad (5.15)$$

(3) m=0.225 (Lateral 3)

$$E_{12} = 0.53\, q^2 - 0.15\, q - 0.01 \qquad (5.16)$$

Using equation (5.7), the loss coefficient for the smallest lateral size (m=1/16) tested by McNown is,

$$E_{12} = - 0.06\, q + 0.44\, q^2 \qquad (5.17)$$

and this relation will be made use of in the determination of R_d in the next section.

E_{12} from the above equations (5.14 to 5.16) along with equations proposed by Ito & Imai [1973] and Vazsonyi [1944] (section 2.2.3) are also shown in Fig.5.8. Their equations are independent of m and the correlation by Vazsonyi for a straight branch is $E_{12} = 0.37\, q^2$. Considering only the constant terms A_1 in A and B_1 in B in the correlation of Cp_{21} in the previous section, Eq.5.10 becomes $Cp_{12} = 2q - 1.4\, q^2$ and $E_{12} = 0.4\, q^2$ which is similar to Vazsonyi's equation (section 2.2.3.1). Ito`s equation plotted for the two ranges of q in his formula (q< 0.22.and q> o.22) reduces to a combined equation as follows:

$$E_{12} = 0.74\, q^2 - 0.39q - 0.03. \qquad (5.17a)$$

Eq.5.17a is similar to Eq. (5.14) and (5.15) and the present test results of laterals 1 (m=1) and 2 (m=0.77) appear to agree with the results of Ito (section 2.2.3.2). However the mean trend relationship based on all existing tests for m=1 given in Eq.5.14 do not agree with Ito's results very well. The mean trend curves in Fig. 5.8 a,b,c also appear to cross over from negative to positive values at about the critical discharge ratios (q_{cr}) pertaining to stagnation point at the d/s corner of each lateral, the values of which are presented in Table 5.13. This significant factor should be noted.

5.4 Pressure Recovery Factor R_d

The pressure recovery factor obtained indirectly from the momentum balance in the main, Rm (Eq.4.14), and that obtained directly from the net wall pressure forces on the lateral walls, Rf (Eq.4.16), are shown in Fig.5.9. These results indicate that both the indirect and direct methods generally yield nearly identical values for the range $q > 0.25$ where the change of momentum is significant. For q=0, as expected, the Rf value is also zero since the pressures on the two branch walls and the extrapolated pressures P_1,P_2 and P_3 are identical. The values of Rd reported by Bajura [1970] and Sivarudrappa [1977] are also shown in Fig.5.9 for purposes of comparisons. Since the mean trend relationships of Cp_{21} and E_{12} have been established, it is now possible to derive a relationship for the variation of R_d with q through Eqn.(4.14). Thus equations (5.11) to (5.13) become,

(1) For m=1 (lateral 1)

$$R_d = 0.81 - 0.12\,q - 0.03/q, \qquad q \neq 0 \qquad (5.18)$$

and $R_d = 0$ at $q=0.037$

(2) For m=0.77 (lateral 2)

$$R_d = 0.83 - 0.14q - 0.02/q, \qquad q \neq 0 \qquad (5.19)$$

and $R_d = 0$ at $q=0.024$

(3) For m=0.225 (lateral 3)

$$R_d = 0.93 - 0.24q - 0.005/q, \qquad q \neq 0 \qquad (5.20)$$

and $R_d = 0$ at $q=0.0054$.

(4) Similarly for a very small lateral size m=1/16 Eq.(5.7) gives

$$R_d = 0.97 - 0.28\, q - 0.0015/q \qquad (5.21)$$

and $R_d = 0$ at $q = 0.00155$

which indicates that as the ratio m tends towards zero the recovery factor approaches a maximum value of unity for q values near to zero. However it approaches a value of 0.68 at q=1. For very small laterals the average value of R_d over the full range of q values can be taken as 0.85 (Fig.5.9d). For the laterals tested the average values of R_d are o.83, 0.77 and o.75 for laterals 3, 2 and 1 respectively. The value from wall pressure measurements for the smallest lateral is close to 0.90. One recalls that the theoretical models based on different variations of pressure along the dividing streamline B_1S (Fig.4.4b) give R_d values varying from 0.75 to 0.88 which are of the same order of magnitude as the data shown in Fig.5.9.

The Eqs.(5.18) to (5.20) relating R_d and q indicate that the maximum value occurs in the vicinity of the corresponding q_{cr} (Table 4.13) values for the different m values (Fig.5.9e). These graphs also show that R_d is approximately equal to 0.67 at q=1 for all the three laterals tested presently. At this flow ratio of q=1, E_{12} =0.34 according to Eq.4.13 (agreeing with Gardel's findings Table 2.3) and Cp_{21}=0.66 according to Eq.4.15.

5.5 Contraction Coefficient C_c

The theoretical analysis to calculate the energy loss term e_{43} is explained in section 4.4.1. Here P_4 and V_4 shown in Fig.4.5(a) depict the average pressure and velocity at section GH. The speed V_j along the free streamline T_1T_3 (Fig.4.5a) is the same as the flow speed along the streamline separating at T_1. Assuming α=1,β =1 across section GH, the resulting uniform velocity of the jet entering the branch at this contracted section becomes V_j. To evaluate V_j it is further assumed that the wall pressure P_i is the average pressure at this section.

From the wall pressure diagrams (Fig.4.5 b) it is seen that a minimum pressure (P_i) occurs on the inner wall at the vena contracta. The contraction coefficient Cc of the jet flow is totally dependent on the separating streamline velocity Vj. It can be obtained from potential flow models of McNown [1950] related to a lateral outlet fitted with an infinitely long barrier (Fig.5.10 A-3). The stagnation streamline branches off at S_M and separates at the corner of the downstream branch wall forming a secondary separation bubble (Fig5.10.A-1) on the downstream lateral wall. Similarly when $q < q_{cr}$, the stagnation of the dividing streamline occurs at S_L on the downstream branch wall and a secondary bubble occurs on the d/s wall of the main conduit (Fig.5.10.A-2).

Reservoir conditions are reached as the area ratio becomes small and the contraction coefficient C_c approaches o.64 for sharp edged square holes. This value of C_c is close to the value of 0.61 [Kirchoff 1869].

Using the observed minimum pressures P_i, the jet velocity at the vena contracta was obtained from Eq.(4.42). The contraction coefficient C_c was obtained through continuity equation (5.23). The contraction coefficients were evaluated for the three laterals and shown in Figs.5.10(a),to (c) as experimental results. The corresponding theoretical relationship between C_c and q [McNown 1950] is shown in solid line. The continuity equation used is,

$$qQ_1 = q\ A_{r1}\ V_1 = Cc\ \ A_{r3}\ V_{j1} = A_{r3}\ V_3\ = Q_3 \qquad (5.22)$$

from which,

$$C_c\ = (V_3/V_j)\ = (q/m)\ \eta \quad \text{where } \eta = (V_1/V_j) \qquad (5.23)$$

The contraction coefficient C_c is also evaluated from the energy losses E_{13} (=e_{43}) in the lateral as in Eq.(4.41). These values and the values obtained from minimum pressures at the vena contracta for the three laterals are also shown together in Figs.5.10 (a),(b) and (c). The results of the C_c values by the two methods (E13 & minimum pressures) are very

close showing that the energy loss coefficient (E_{13}) could be used to evaluate C_c. The slight differences between the present results and McNown`s [1950] theoretical results are noticeable for the larger two laterals in Figs.5.10 (a) and (b). McNown too has noticed the differences between test data and theoretical predictions for larger q ratios ($q > 0.4$). The relationship of C_c vs η^2 shown in the same Fig.5.10 will be discussed subsequently.

The experimental results of Cc for all the three lateral area ratios are summarized very approximately by a linear correlation between 1/Cc and m/q (= V_1/V_3) ratio in Fig. 5.11(a) culminating in an equation dominated by the results of the two larger laterals. Theoretically 1/Cc and m/q are related through E_{13} in equation (4.37) as below,

$$1/C_c=(E_{13})^{0.5}\,(m/q)+1 \qquad (5.24)$$

The above equation is essentially the same form as the equation shown in Fig.5.11(a).

The plot of C_c vs $(q/m)^2$ of the experimental results are shown Fig.5.11(b) indicating that all the results fall on a single curve and the bounds of the velocity ratio (V_3/V_1) for each lateral size are shown. This graph is useful as a first design to compare or to select C_c values for known q/m ratios . The plot of $1/C_c$ Vs $(m/q)^2$ in Fig.5.11(c) show that for C_c >0.15 the variation is linear. The theoretical equivalent to this curve is Eq.(4.58) repeated below and possibly Eq.(4.60) relating C_{p13} and it is an alternative presentation involving the pressure coefficients where, $Cp3j = (P_3-P_j)/V_1^2/2g$

$$1/C_c = (1/2)C_{p3j}\,(m/q)^{\wedge 2} + 1 \qquad (5.24\ a)$$

These variations with (q/m), (q/m)^2 etc. will be analyzed further in section 5.2.10 pertaining to this pressure coefficient (C_{p3j}).

5.6. Contraction Coefficient C_d

The analysis of ideal flow through a lateral outlet located in a two dimensional channel provides a contraction coefficient C_d as a function of discharge ratio q (section 4.4.4). In this analysis as an approximation the velocity V_i (Fig.4.6a) of the inner streamline across the contracted section GH is assumed to be the same as the velocity V_j corresponding to the minimum recorded wall pressure at N. The values of C_d and k are summarized in Table 5.14 and the variation of C_d with discharge ratio q is shown in Fig.5.12. On comparing with McNown`s [1950] values in the same Figs, shown as solid lines, it is seen that the results of the present free vortex model and the theoretical model of McNown(1950) give identical results for laterals 1 (m=1)& 2 (m=0.77). However for lateral 3 (m=0.225) the experimental results are slightly higher than the theoretical predictions with C_d as 0.64 instead of McNown`s 0.611. It may be added that the value of contraction coefficient has also been assumed as 0.63 by Rawn et al [1961] and others for sharp edged orifices.

The α,β coefficients calculated at this section are close to 1 (Table.5.14).

5.7 Pressure Coefficient Cp_{13}

The pressure coefficient C_{P13} relating the pressures P_1 in the main conduit at the center line of the lateral and that of P_3 in the lateral conduit at the corner T_1 or T_2, Figs.(4.3a,4.3b), is a test parameter like Cp_{21} and its relationship to the energy losses in the lateral conduit is given in Eq.4.39. The experimental values of C_{P13} plotted against q for the three laterals are shown in Fig.5.13. The resulting curves fitted to the data have the following relations.

(1) For m=1 (Lateral 1)

$$C_{P13} = -037q + 1.56\ q^2 \qquad (5.25)$$

(2) For m=0.77 (Lateral 2)

$$C_{P13} = -0.21q + 2.60\ q^2 \qquad (5.26)$$

(3) For m=0.225 (Lateral 3)

$$C_{P13} = 1.86\ q + 28.5\ q^2 \qquad (5.27)$$

The experimental values of C_{p13} for the three laterals are also plotted against q/m ($=V_3/V_1$) and $(q/m)^2$ ratios in Fig5.13 (e) and (d) respectively. The Cp13 values have the following relationship with $(q/m)^2$,

$$C_{p13} = -0.11 + 1.55\ (q/m)^2 \qquad (5.28)$$

The linear variation of C_{p13} with (q/m)^2 (= (V_3/V_1)^2) in Fig.5.13d is very useful in practice for predicting C_{p13} knowing V_3, V_1 values. However the above equation is applicable for m values less than 0.77. For m=1, the equation (5.25) with the q term has to be applied and for area ratios in between (o.77 < m < 1) this q term of 0.37 can be linearly varied with the area ratio (Fig.5.13d). These formulae indicate that the loss coefficient E_{13} and therefore $1/C_c$ could also be related to (q/m) ratios. Comparing C_{p13} with C_{P21} values it is observed that C_{P13} is the domineering pressure term for large q ratios and C_{p21} becomes almost negligible for the smallest lateral size. This is further explained by studying the total pressure variation term C_{p23}. The total pressure coefficient C_{P23} between the main and the lateral conduits is the sum of C_{P21} and C_{P13} and its variation with q is obtained from Eqs. (4.9) and (4.39) as below.

$$C_{P23} = (q/m)^2 - (1-q)^2 + E13 - E12 \qquad (5.29)$$

For m=1 (lateral 1) the coefficient C_{p23} obtained experimentally has a linear variation with q (Cp23 = 0.11+ 1.76 q) having very little influence by the q^2 term. For m=0.225 (lateral 3) the $(q/m)^2$ term is dominant and $C_{P23} \approx C_{P13}$ for all q`s and the variation of C_{P13} with q is parabolic..

The only reported C_{p13} values of Kinne [1931] for a Tee junction with 43mm circular pipes is much different at low q ratios than the present values for an area ratio of one (m =1). Kinnes equation is approximately ,

$$C_{p13} = -0.82q + 2.21\ q^2 \qquad (5.29a)$$

Since there was no other data available the difference is difficult to explain.

5.8 Energy Loss Coefficient E_{13}

The energy loss coefficient E_{13} for the three laterals are shown in Fig 5.14. The influence of α is shown for the two larger laterals and the experimental values are compared with the empirical formulas of Ito [1973] and Vazsonyi [1944] presented in section 2.2.3.1 and 2.2.3.2 respectively. Ito`s formula has been modified by replacing the discharge ratios with velocity ratios as the area ratio was unity in his experiment.

It is noticed that in Figs.5.14 a,b and c the present data is in between the trends established by Vazsonyi [1944] and Ito [1973] except for very low q values (q < 0.25). Also the loss coefficient for the smallest lateral is similar to McNown's [1950]. The scatter of the data in Figs.5.14 makes it difficult to suggest any reliable relationship between E_{13} and q and therefore for design purposes the more reliable C_{P13} relations with q should be used to derive E_{13} and other design parameters like C_c etc.

The loss coefficient E_{13} is plotted against q/m and $(q/m)^2$ ratios in Fig.5.14 (d) and (e) and the approximated linear fit of the data from Fig.5.14(e) for all the laterals are given by the equation,

$$E_{13} = 0.93 + 0.51\ (V_3/V_1)^2 \qquad (5.30)$$

This relation is very similar to the dependence of E_{13} on $(q/m)^2$ proposed by Hudson [1979]. However his loss coefficient was in terms of $V_3^2/2g$ and dependent on the flow development length in the lateral. For long laterals, which were defined by him as greater than three diameters, the constants were 0.90 and 0.4.and for short laterals, defined as less than three diameters long, the constants were 1.67 and 0.7. Some of the results in Hudson when plotted as E_{13} vs $(q/m)^2$ (Fig.5.14f) give a single line graph as below,

$$E_{13} = 0.83 + 0.45\ (q/m)^2 \qquad (5.31)$$

From the experimental results of Syamala Rao et al [1968], for m=1 at 90° branching, the loss coefficient was found to behave fairly close to the present results and given as,

$$E_{13} = 0.96 + 0.6\ (V_3/V_1)^2 \qquad (5.32)$$

The differences between the present and previous experimental results [Hudson 1979] could be explained by the fact that E_{13} present is inclusive of the energy coefficient α, and that the rectangular conduit used is two dimensional than the circular pipes used before. However all the above equations based on $(q/m)^2$ (or on q/m) are not applicable to the two larger laterals as they tend to give higher losses. Therefore as mentioned before the equation for C_{p13}, Eq.(5.25) for m=1, should be used to derive E_{13} values for the range m >0.7.

Thus for m=1,

$$E13 = 1 - 0.37\ q + 0.55\ q^2 \qquad (5.33)$$

and similarly, the loss coefficients for other m ratios > 0.7 could be derived using the respective Cp13 relations.

The evaluation of contraction coefficient C_c from the loss coefficient E_{13} has been already dealt with in section 5.2.5 and the close agreement with Cc obtained from the minimum inner wall pressures justifies the present jet flow flow model and therefore the study of the jet velocity parameter is important and described in the section below.

5.9. Velocity Parameter η

The jet velocity parameter η is described in section 4.4.5.and its direct relationship to the contraction coefficient Cc (jet flow) from (Eq.5.23) is $\eta=(m/q)\ C_c$.

η is evaluated from the experimental values of V_1 and V_j (Eq.4.42) and shown in Fig.5.15(a) having $\eta \longrightarrow 1$ when q=0. The graphs attain limiting values of 0.5,0.4 and 0.12 for m=1,m=0.77 and m=0.225 (laterals 1,2 and 3) respectively at q=1. In the case of m=0.225 (lateral 3) the maximum value of $1/\eta^2$ (or H) is about 57 (Fig.5.15d) indicating that negative gauge pressures could occur very easily if not anticipated in advance. This is explained in the experimental procedure in Chapter 3.

In general H and $1/\eta$ has a linear and parabolic variations with $(q/m)^2$ and q/m ratios and these are shown in Figs.5.15(e) and (f) respectively.

As seen earlier in the previous sections the dominant pressure coefficients for the dividing flow are C_{P13} and C_{P23} and these could be related to the jet total head $1/\eta^2$. In addition the pressure coefficient C_{p3_j} (Fig.4.6b) is also an important parameter and is evaluated next. The difference between the lateral pressure P_3 and the jet pressure P_j ,referred to as P_{3j}, is determined from the Eq. (4.57) as,

$$\frac{C_{p3j}}{H} = 1 - \eta^2 - \frac{C_{p13}}{H} \qquad (5.34)$$

where, $H=1/\eta^2$ and is a useful parameter when pressure (P'_3) at the section MN (Fig.4.5b) of the lateral conduit is prescribed. On plotting Cp3j/H vs q in (Fig.5.16) for the three laterals (m=1, 0.77 and 0.225) it is noticed that it reaches asymptotical values of 0.45, 0.44 and 0.43 for q ratios > q_{cr}. Taking this value as an average of 0.44 (Fig.5.16d & e) the total head ratio at the jet $1/\eta^2$ or H can be expressed as follows,

$$1/\eta^2 = (1/0.56)\,(1 + C_{p13}) \qquad (5.34a)$$

In a simplified form,within the limitation of $q>q_{cr}$

$$1/\eta^2 = 1.80\,(1+Cp13) \qquad (5.35)$$

By also knowing the velocity ratios q/m (= V_3/V_1) as well, the other parameters like 1/Cc and E13 could be easily evaluated from equations (4.60) and (4.59) as,

$$\left(\frac{1}{C_c} - 1\right)^2 = \frac{1 + C_{p13}}{Y} - 1 \qquad (5.36)$$

where $Y = (q/m)^2$

5.10 The Velocity Triangle Model

Having analyzed the experimental results parameter wise and made comparisons with previous studies there is still no interconnection between all the main conduit variants and the lateral parameters except through the energy and continuity relations. Therefore a velocity triangle model as shown in Fig.5.17 is proposed.

In this model the average velocity of the dividing flow at the entrance of the junction is assumed as $K_1 V_j$ at an angle θ to the direction of main conduit axis. Here V_j is the jet velocity at the contracted section as discussed in the previous sections. For q ratios > q_{cr}, the average vertical component of $K_1 V_j$ at entrance in the direction of the lateral axis is V_3 and its average velocity component in the direction of the main conduit axis s $R_d V_1$. The velocity component in the direction of the main conduit axis causes the momentum loss across the lateral conduit as net force on the walls which in turn is equal to the ΔM (Eq.4.1) in the main through flow.

From the velocity triangle (Fig.5.17A),

$$K_1^2 = C_c^2 + R_d^2 \eta^2 \qquad (5.37)$$

The value of K_1 obtained from the experimental values of C_c, η based on wall pressures and R_d for the three laterals tested presently are plotted in Figs.5.18, and its value is seen to be a constant for all the three laterals over a wide range of discharge ratios, from q=0.25 upwards. These constant values are :

K_1 = 0.62 for Lateral 1 (Fig.5.18a)

= 0.62 for Lateral 2 (Fig.5.18b)

= 0.60 for Lateral 3 (Fig.5.18c)

Selecting an average value of o.61 for K_1, the contraction coefficient C_c in terms of η^2 from Eq. (5.37) is,

$$C_c = 0.61 \left(1 - T \eta^2 \right)^{0.5} \qquad (5.38)$$

where, $T = (R_d/0.61)^2$

The variation of the second term ($T \eta^2$) inside the bracket for the three laterals in terms of $\eta 2$ is shown in Fig.5.19 and for the larger laterals 1 and 2 the variation is parabolic and almost linear in the range of $\eta^2 = 0.24$ to 0.5 and $\eta^2 = 0.18$ to 0.6 for laterals 1 and 2 respectively. These ranges of η^2 values correspond to discharge ratios higher than o.5 and 0.3 for these two laterals (Fig.5.10) indicating that the parabolic variation is due to the η^2 values of small discharge ratios. In the case of lateral 3 this variation shown in Fig.5.19(c) is linear for almost all discharge ratios(for q>0.12) and gives the following relationship,

$$T = 2.25$$

which corresponds to an average R_d value of 0.91. Incidentally this value of R_d is close to the experimental values from the wall pressures in Fig.5.9(c).

Substituting in Eq.(5.38) and expanding, the contraction coefficient C_c in terms of η^2 for lateral 3 (m=0.225) reduces to the general form,

$$C_c = 0.61 - 0.69 \eta^2 + 0.38 \eta^4 - 0.43 \eta^6 \qquad (5.39)$$

Note that $C_c = 0.61$ for $\eta \longrightarrow 0$, reservoir condition.

The above derivation shows that the coefficients of $\eta 2$, $\eta 4$ etc. as in Fig.5.10(c) can be related very closely to the pressure recovery coefficient Rd.

In general, for all the laterals, using Eq.5.37, taking the average value of K_1 as 0.61 and relating η in terms of (C_c m/q), a useful relationship for C_c in terms of R_d m/q is obtained,

$$C_c = \frac{0.61}{\{\, 1 + (\frac{R_d\, m}{q})^{2} \,\}^{0.5}} \qquad (5.40)$$

Cc from this equation is compared with Cc values obtained by other methods and described under in section 5.3.1.

5.11 Dependence of Cc on η and q/m

Tables 5.9 to 5.11 give the experimental data used to plot Figs.5.10 and 5.15 which show the variation of Cc with q, η and η^2. The variation of Cc with η^2 shown in Fig.5.10 and the curves fitted to the experimental values indicate that η^2 attains limiting values and approaches zero (reservoir condition) for lateral 3 (m=0.225). For the two larger laterals η^2 attain limiting values of 0.25 (lateral 1) and 0.16 (for lateral 2). These graphs take the general form $Cc = A - B\eta^2 + C\eta^4 - D\eta^6$ having coefficient A varying from o.68 to 0.60 for laterals 1 to 3 (Fig.5.10) and the sum of the other coefficients B+C+D approaching to the value of A ($\eta^2 = 1$ condition). However C_c and η^2 can also be expressed in a simpler manner with very high regression coefficients as follows:

(1) Lateral 1(m=1) $\quad C_c = 0.63 - 0.63\eta^2 \quad$ for $\eta^2 > 0.25 \qquad (5.41)$

(2) Lateral 2 (m=0.77) $\quad C_c = 0.63 - 0.62\eta^2 \quad$ for $\eta^2 > o.16 \qquad (5.42)$

(3) Lateral 3 (m=0.225) $\quad C_c = 0.60 - 0.61\eta^2 \quad$ for $\eta^2 > 0.01 \qquad (5.43)$

The contraction coefficients by the three main methods, one from minimum wall pressures as in Fig.5.10, the second from Eq.5.37 and the third from the above equations 5.41 to 5.43 are plotted for each lateral size in Fig.5.20 as a summary and verification. The other method by which Cc obtained from energy loss coefficient E13 has been already compared in Fig.5.10.

The equations 5.41 to 5.43 are somewhat similar to the equation by Rawn [1961] for an area ratio of 1/16 as given below:

$$C_c = 0.63 - 0.58\eta 2 \tag{5.44}$$

Fig.5.18(a) to (c) show the dependency of the ratio $C_c / (1-\eta^2)$ on q for all the laterals and for $q > 0.25$ this ratio is essentially a constant. Hence the equations 5.41 to 5.43 can be replaced by a general equation as given below:

$$C_c = 0.61\ (1-\eta^2) \tag{5.45}$$

One notes that the term $(1-\eta^2)$ is also the pressure coefficient C_{p1j} or $\Delta P_{1J} / (V12/2g)$. Another form of the above equation in terms of $(V_3/V_1)^2$ is obtained by substituting for η from Eq.5.23 { $\eta = (m/q)C_c$ } and generalized as:

$$Cc^2 + \left(\frac{q}{m}\right)^2 \frac{1}{0.61} Cc - \left(\frac{q}{m}\right)^2 = 0 \tag{5.46}$$

Replacing $(q/m)^2$ as Y,

$$C_c = -\frac{Y}{1.22} + \sqrt{\frac{Y^2}{(1.22)^2} + Y} \tag{5.47}$$

The comparison of C_c by the two equations (5.47) and (5.40) are shown in Fig.5.21(a),(b) and (c) respectively. It is to be noted that the R_d values for evaluating C_c in Eq.5.40 are obtained from the Cp_{21} mean trend equations, which also include experimental results reported by others. It is found that the C_c obtained from this equation (5.39) is higher than by the other equation (5.47). Part of the discrepancy can be traced to the reported inaccuracy in interpreting the Munich results [Miller 1980]. Having determined C_c from Eq.(5.47), the pressure recovery factor (Eq.5.40),the energy loss coefficient E_{13} (Eq.5.24), pressure coefficient Cp_{13} (Eq.4.39), the minimum pressure head $1/\eta^2$ etc.can be evaluated and also checked from the experimentally derived equations (5.30) and (5.28) in terms of $(q/m)^2$ ratio. The velocity parameter η can be derived similar to equation (5.47) as,

$$\eta = \frac{\sqrt{Y}}{1.22} + \frac{1}{1.22}\sqrt{Y + (1.22)^2} \qquad (5.48)$$

and the other parameters could be evaluated as before. In these formulas the limiting values for each area ratio m has to be taken care of when q=1, i.e. when $V_1 = m.V_3$.

5.12 Manifold Design

The present study finds application in the design of laterals for sprinklers and in manifolds discharging effluents into a body of water. The spacing of the laterals to avoid interference effects is an important factor in these designs (Table 2.2). The present study indicates that the length required for recovery at the downstream of the main conduit varies from a maximum of 12d to an average of 6d where d is the hydraulic diameter of the main conduit. The upstream of the main conduit needs a maximum of 6d and the lateral recovery length for lateral 1 conduit is also about 6d. Thus the total length of main conduit in

between junctions should be about 20d for almost a total recovery and the lateral conduit should be at least 6d for large laterals and about 3d for the smallest size for the same reason. It may be noted that the minimum pressures occur at a length of 1 to 1.5d from the entrance for lateral 1, m =1, and 0.5 to 1d for the smallest lateral size. At the extreme, when laterals are of zero length the flow behavior is that of a slot and McNown [1950] has shown that the contraction coefficients for slots are higher than those of the laterals for large lateral openings and in the case of small lateral opening area ratios the contraction coefficients for both lateral and slot are nearly the same. The present study relates the contraction coefficient for the lateral in terms of η^2 (Eq.5.45) and it is found that a similar equation for slots though approximate , proposed by Subramanya [1970] and given as,

$$C_c = C_{co} (1-\eta 2)^{0.5}$$

where, C_{co} is the contraction coefficient under reservoir conditions, will be very useful for the design engineer. The comparisons of the two formulae are shown in Fig.5.22.

CHAPTER VI

CONCLUSIONS

CHAPTER VI

CONCLUSIONS

Based on the present study the following conclusions can be drawn:

6.1 The Pressure Coefficients: The pressure coefficients C_{p21} and C_{p13} are more dependable after correcting or checking for the straight through flow gradients and the energy loss coefficients could then be derived from Eq.5.28 for $m < 0.7$ and for larger laterals from Eq.5.25 (for m=1) and for area ratios in between as described in Section 5.7.

6.2.The Contraction Coefficient: The variation of contraction coefficient with the area ratio, m, obtained from (a) the free vortex theory (Fig.4.6a) and (b) the free stream velocity Vj (Fig.4.5a) are quite similar. The free vortex theory is strictly applicable when the streamlines are concentric. It is concluded that the relationship between, Cc, and the area ratio, m, based on the free stream line theory is the more appropriate since the assumptions made in its derivation are not far fetched as verified by comparison with the energy loss coefficient E_{13}.

Simplified formulae for the contraction coefficient (Eq.5.47) and velocity parameter (Eq.5.48) are proposed in terms of $(V_3/V_1)^2$ or $(q/m)^2$ so that energy loss coefficient (E_{13}) and jet head (H) can be evaluated.

6.3 Wall Pressure Measurements: Wall pressure data directly provided an expression for the momentum term transfer ΔM and found to agree well with the value obtained indirectly from the traditional application of the momentum balance for the main conduit flow.

6.3.1 Minimum Pressures: The measurement of the minimum wall pressures and its upstream location on the lateral wall enabled the evaluation of the contraction coefficients (Cd & Cc) and the velocity parameter (η). These parameters are useful to the design engineer as mentioned earlier.

6.3.2 Stagnation Points: The locations of the stagnation points change with the discharge ratio q and move from the lateral wall to the main wall as the discharge ratio, q, is increased. The theoretical values of the critical discharge ratio, q_{cr}, for differing area ratio,m, at which the stagnation point meets the corner of the branch and the main are found from potential flow theory (Table 5.13). A qualitative verification of the theoretical predictions of q_{cr} were verified by the data. This critical discharge ratio seem to have definite effect on the behavior of many parameters discussed in the thesis. Further it is inferred from the pressure diagram that when the stagnation occurs on the main, a secondary separation bubble occurs on the down stream wall of the branch (Fig.5.10A) and vice versa when the stagnation occurs in the lateral..

6.4. Pressure Recovery Factor: Equations have been derived for pressure recovery factor from experimental results and its range extended to cover almost all q ratios. The significant result of the maximum value of Rd occurring at $q=q_{cr}$ is noted. For large lateral / main area ratios (m) the maximum pressure recovery factor is close to 0.70 and this should be included in the design of supports or anchor blocks.

The pressure recovery factor data from past investigations also has been reviewed and a general flow model is proposed(Chapter 4, section 4.3.3.1.3).

6.5 The Effect of C_{p3j}: The pressure coefficient C_{p3j} is found to behave asymptotically to reach a constant value in the range of 0.45 to 0.43 as m varies from 1 to

0.225 for q ratios > q cr. For very small laterals, C_{p13} can be related to the jet head ($1/\eta^2$) through Eq.5.35 and is very useful to check for negative pressures when pressures in the lateral dictate the overall designs as in the design of sprinkler heads. The negative pressures are indicative of the cavitation potential of the system.

6.6 Velocity Triangle Model: A model relating pressure recovery to the contraction coefficient is also proposed. This explains that Rd is a useful factor in designing of multi ports which in turn affects the pressure coefficient Cp21 in the main conduit. This model gives rise to the constant factor K1 (close to 0.61) in defining the average velocity at the junction.

6.7 Design of Multi-ports: The design of multi ports spaced sufficiently far apart (>20d) to avoid interference can be undertaken using the results presented. The new parameter η^2 should be used to check for cavitation potential when large velocities and large pressures of the incoming flow are expected in the junction. Further, it is noted that when using laterals of small area ratios the energy losses in the laterals are very high and limits the smallest m ratio that could be economically or practically justified.

The present experimental results enables one to design multiports as the experimental data is now available for area ratios varying from 1/16 (McNown 1950) to 1.

6.8 Scope for Further Study: It is recommended that a similar detailed study with velocity measurements at the junction be undertaken for:

(a) Lateral orifice and,

(b) Combining lateral conduit flow.

APPENDIX I

STRAIGHT THROUGH FLOW TESTS

APPENDIX I.

STRAIGHT THROUGH FLOW TESTS FOR CALIBRATION

A.I Straight Through- Flows

Straight through- flow tests were carried out to establish pressure gradients and to evaluate friction, momentum and energy coefficients. Different methods were used to analyze these results to obtain and compare these coefficients and are explained in this Chapter. The resulting method or equations formed the basis to evaluate similar gradients and coefficients in the "dividing flow tests". For this reason the straight through flow tests are sometimes referred to as Standard Tests and referred to in Section 5.2.1 (Chapter 5).

A.I.1 Straight Through Flow Tests

These tests were carried out with the same cross sections of main conduit and adapting similar procedures and precautions as in the dividing flow tests. The main conduits tested were made of Aluminium and Plexiglas having rectangular sections of 4.125 cm X 9.15 cm.. Care was taken to minimize flow turbulence by providing honeycombs well ahead of the test section and fully developed flow conditions were ensured by an adequate approach length (>>40d). Manometer readings were taken after steady states were established and test results h1 to h5 for Aluminium conduit and H3 to H6 for the Plexiglas conduit are given in Tables A.1.1., A.1.2 and the pressure heads along the conduits shown in Figs.A.1.1 and A.1.2.

A.I.2 Friction Factor f

The pressure gradients $\frac{dh}{dx}$ (=S) and Reynolds number $Re\ (=\frac{Vd}{\nu})$, based on average velocity, were the basis to evaluate the friction factor by three different methods.

A.I.2.1 In Darcy - Weisbach [1858] equation, $f = f_{Darcy}$ defined as,

$$\frac{\Delta h}{\Delta L} = S = \frac{f}{d}\frac{V^2}{2.g} \qquad (A.1.1)$$

where d= hydraulic diameter

$= \frac{4\,Ar}{Pc}$ for rectangular sections

A.I.2.2 In Wall Formula, $f = f_{Wall}$ is given by the smooth pipe velocity profile (Prandtle and Von Karman) as,

$$\frac{1}{\sqrt{f}} = 2\log_{10}(Re\sqrt{f}) - 0.8 \qquad (A.1.2)$$

An explicit formula by Colebrook [1939] was used to evaluate f,

$$f = \left[1.56 \ln\left(\frac{Re}{7}\right)\right]^{-2} \qquad (A.1.3)$$

which represents the previous equation to within 1% in the range $10^4 \angle Re \angle 10^7$ [Ward Smith 1980].

A.I.2.3 Blasius Formula, $f = f_{Blasius}$

Blasius formula is given by

$$f = 0.3164 Re^{-0.25} \qquad (A.1.4)$$

and applicable for smooth pipes in the turbulent range $Re < 10^5$

A.I.2.4 Experimental Values

The friction factor f by the above three methods (2.1,2.2 and 2.3) for the straight through flow tests are given in Table A.I.3 and plotted against Reynold number (Re) in Fig A.I.3. which show very close agreement between f_{wall} and $f_{Blasius}$. The f_{Darcy} values are also close but are consistently higher than the other two values accounting for additional friction losses around the corners of the rectangular test sections in comparison to circular sections. Thus f_{Darcy} based on perimeter averaged wall shear stress is chosen to represent f in evaluating other flow coefficients like momentum, energy etc.

Table A.I.3 also shows the smoothness parameter to be < 5 assuming roughness heights of 0.000013 ft. for Al and 0.000005 ft. for Plexiglas as given in Hwang[1986].

A.I.3 Energy and Momentum Coefficients

The energy coefficient (α) and momentum coefficient (β) were calculated using both the wall and power law.

A.I.3.1 Wall Law

From the log law formula for smooth pipes in Smith [1980] and in Benedict [1980] the energy coefficient (α) is given by,

$$\alpha_{\log\ law} = 1 + \frac{15}{32} A^2 f - \frac{9}{64\sqrt{2}} A^3 f^{3/2} \qquad \text{(A.1.5)}$$

where A=2.5. On simplification the above equation becomes.

$$\alpha_{log} = 1 + 2.9296875\ f - 1.5537014\ f^{3/2} \qquad \text{(A.1.6)}$$

The momentum coefficient is given by,

$$\beta_{\log\ law} = 1 + \frac{5}{32} A^2 f \qquad \text{(A.1.7)}$$

and with A=2.5 ,

$$\beta_{log} = 1 + 0.9765625\ f \qquad \text{(A.1.8)}$$

As mentioned earlier $f=f_{Darcy}$ is adapted in the above equations and the resulting coefficients are shown in Table A.1.4.

A.I.3.2 Power Law

In the power law, the factor N and the ratio of average velocity (V) to maximum velocity (V_{max}) was evaluated with respect to Reynolds number (Re) in the range

$4 \times 10^3 < Re < 3.2 \times 10^6$. To achieve this, the co-relation given in Schlichting [1979] and Weighardt [Smith 1980] for both N vs. Re and (V/V_{max}) vs Re were plotted in Figs.A.1.4 and the following fit obtained.

$$N = 12.72 - 1.57 \ln Re + 0.09 (\ln Re)^2 \qquad \text{(A.1.9)}$$

in the range N=6 to 10 and

$$\frac{V}{V_{max}} = 0.82 - 0.012 \text{ Ln } Re + 0.001 (\ln Re)^2 \qquad \text{(A.1.10)}$$

Values of N and the velocity deformity coefficient ε defined as $\varepsilon = (V_{max}/V - 1)$ are evaluated from the above equations and tabulated in Table A.1.5

Knowing the value of N and the velocity ratios (V/V_{max}), the energy and momentum coefficients were evaluated (Table A.1.6) using the following relationships:

$$\frac{V}{V_{max}} = \frac{2.\ N^2}{(N+1)(2\ N+1)} \qquad \text{(A.1.11)}$$

$$\alpha_{Power} = \frac{(N+1)^3 (2N+1)^3}{4\ (3+N)(3+2N)\ N^4} \qquad \text{(A.1.12)}$$

$$\beta_{Power} = \frac{(N+1)^2\ (2N+1)^2}{4\ .N^2\ (2+N)\ (1+N)} \qquad \text{(A.1.13)}$$

In particular when N=7 called the 1/7th power law consistent with $R_d = 10^5$ and f=0.01799, Benedict [1980] shows α,β values as follows:

α(log) =1.049 α(power)=1.058

β (log) =1.018 β(power) =1.02

A.1.3.3 Empirical Relation For α and β With ε

An empirical relation by Rehbock [Chow 1959] using the velocity deformity coefficient ε ($=V_{max}/V - 1$) was used to evaluate α&β. These coefficients were defined as,

$$\alpha = 1 + \varepsilon^2 \qquad \text{(A.1.14)}$$

$$\beta = 1 + \frac{\varepsilon^2}{3} \qquad \text{(A.1.15)}$$

and tabulated in Table A1.7.

When N=7, ε=0.224 and from the above equations,

α=1.05

β=1.017

which are very close to the values obtained from the power and the wall formulae given in the previous paragraph.

A.1.3.4 Experimental Values

The α,β coefficients for the straight through flow tests by the methods described above are tabulated in Table A.1.8 and show close agreement in the Reynolds number

range tested. Hence a simple method like in the previous section (A.1.3.3) was favoured to evaluate α,β coefficients in the dividing flow tests and explained further in section A.1.5.

A.1.4. Pressure Gradients

In the straight through flow tests manometric drops were measured and pressure gradients were calculated as explained in para A.1.1.and shown in Figs.A.1.1 and A.1.2. From the Darcy formula, Eq.A.1.1,

$$\frac{\Delta h}{\Delta L} = S = \frac{f}{d}\frac{V^2}{2.g}$$

$$= \frac{f Q^2}{2.g.A_r^2\, d} \qquad \text{(A.1.16)}$$

where Q= discharge in cusec

A_r = Area of section in sq. ft.

d= hydraulic diameter ft

To ensure a check on the test measurements and on the calculations, the term (Q^2 . f) was plotted against S for the two types of conduits and shown in Fig.A.1.5. The slope of the graphs for the test results shown is a constant value of 0.0198 and agrees with the value of $2g\, A_r^2\, d$ for the two conduits tested. Thus for any sections of conduits similar slopes can be predicted knowing the geometrical properties. Knowing Q and f (from Reynolds no.) the hydraulic gradient S can thus be predicted.

A.1.5. Summary

The straight through flow tests results explained in this Chapter were used as a guide to compare and select methods to evaluate the friction and the energy ,momentum flow coefficients for the dividing flow tests, where unsteadiness of manometric heads were a major difficulty encountered. The procedure adapted in the dividing flow tests to evaluate α,β was to determine the value of N and (V/V_{max}) from a known Re value from equations A.I.9 and A.I.10 and then applied the empirical equations A.I.14 and A.I.15 in section A.I.3.3. To ensure that these conclusions are valid for Reynolds numbers outside the values tested in the straight through flow tests, the calculations by the different methods were repeated for all dividing flow tests and shown in Table A.I.9 and in Figs.A.I.6 to A.I.8 for the three laterals. These figures show the smoothness of the conduits tested.
The slopes of graphs of Q^2.f vs S (Eq.A1.16) are also similarly checked and shown in Figs.A.I.9 and A.I.10.

APPENDIX II

EXPERIMENTAL UNCERTAINTY

APPENDIX 11

EXPERIMENTAL UNCERTAINTIES

A.2.1 Uncertainty in the Measurements:

1.Conduit dimensions	Length = $L_x \pm 0.02$mm
	Breadth = $b_x \pm 0.02$mm
	Width = $w_x \pm 0.02$mm
2. V notch readings	Vernier least count = 0.1 mm
	Notch height = h± 0.1 mm
3.Pressure measurements	Manometric board-
	Minimum division = 1mm
	Pressure head = $P/\gamma \pm 0.05$ mm
4. Pressure taps	Tap size = 1mm
(Refer Robert [1980] pg.469)	Pressure head = $P/\gamma \pm 0.03$ mm
5.Pressure fluctuation	major fluctuation = ± 3mm
	average fluctuation =± 1mm
	Pressure head = $P/\gamma \pm 1$ mm
6. Temperature	T ± 0.25° F

A.2.2 Uncertainty in Computed Results:

The uncertainties in the computed results were obtained by the method described in Fox(1985) at an odds of 20:1. The following are some of the maximum uncertainties in the computed results of some main parameters:

7.Discharge $Q=0.673(h+0.0072)^{2.5}$,

Uncertainty in $Q=U_Q=(h/Q)(dQ/dh)U_h$, Uncertainty in V notch measurement,

U_h =0.01cm

Uncertainty in Q =2.5*0.01/100=2.5% Say Q ± 3 %

8.Mean velocity V ± 3 %

9. Viscosity due to temperature μ ± 1.5 %

(Temperature Variation 68°F to 74° F)

10.Reynolds number Re ± 2.5 %

(As in Appendix E ,Fox[1985])

11.Pressure Head P/γ ± 1.5 %

(Minimum pressure head 450mm.).

11.Pressure Coefficient Cp ± 2.0 %

APPENDIX III

REFERENCES

APPENDIX III

REFERENCES

1. Bajura, R. A., "A Model for Flow Distribution in Manifolds", paper presented at the ASME Joint Power Generation Conference (Pittsburg), Sept.1970, 27-30.
2. Bajura, R. A., and Jones, E. H., " Flow Distribution Manifolds", ASME, t976, pp. 654-666.
3. Barton, J. R., " A Study of Diverging Flow in Pipe Lines", M.Sc. Thesis, State University of Iowa, Iowa City, Iowa, 1946.
4. Chow, V. T., " Open Channel Hydraulics", McGraw Hill, New York, 1959, p.37.
5. Colebrooke,C. F., "Turbulent flow in pipes with particular reference to the transition region between the smooth and rough pipe laws", J. Institution of Civil Engineers, 11, 1939, pp.133-156.
6. Crow, D. A., and Wharton, R., " A Review of Literature On the Division and Combination of Flow in Closed Conduits", The British Hydromechanics Research Association, 1968.
7. Duc Tran, M., " Junction Flow In Open Channels", Ph.D. Thesis, Concordia University, Montreal, Canada, 1988.
8. Fox, R.W. and McDonald, A. T., "Introduction to Fluid Mechanics", 3Rd Edition, John Wiley & Sons Ltd., 1985.
9. Gardel, A., " Pressure drops in flows through T-shaped pipe fittings ", Bull. Techn. Suisse Rom. 83, 9, Apr.1957 pp.123-30, and 10, May 1957, pp.143-8, (In French). Translation by Blaisdell,F.W., Agricultural Research Service, St.

Anthony Falls Hydraulic Laboratory, Minneapolis. Minn. 1960.

10. Gunn,D.J. and Darling, C. W. W., " Fluid flow and energy losses in non-circular conduits". Trans. Inst. Chem. Engrs., 41, 4, 1963, pp. 163-173.

11. Hager, W. H., " An Approximate Treatment of Flow in Branches and Bends", Proc. Instn. Mech. Engrs., Vol. 198 C, No.4, Nov. 1983.

12. Hudson, H. E., Jr., Uhler, R. B., and Bailey,R. W.,"Dividing-Flow Manifolds With Square-edged Laterals", Journal of The Environmental Engineering Division, ASCE, Vol.105, 1979, pp.745-755.

13. Ito, H. and Imai, K., " Energy Losses at 90° Pipe Junctions", J. Hydraulics Div. ASCE, Vol.99 , No-HY9, Sept. 1973, pp. 1353-1367.

14. Jamison, D. K. and Villemonte, J. R., " Junction Losses in Laminar and Transitional flow", Journal of the Hydraulics Division, ASCE, July 1971, pp. 1045 to 1063.

15. Joy, D. M. and Townsend, R. D., " Improved flow characteristics at a 90° channel confluence" , 5th Canadian Hydrotechnical Conference, May 1981, Fredericton, New Brunswick.

16. Kinne, E., " Contribution to the knowledge of hydraulic losses in branches ", Hydr. Instit. Techn. Hoschl. Munchen, No.4, 1931, pp.70-93 (In German). Translation by Bureau of Reclamation, U.S. Dept. of the Interior, Washington, D.C.1955.

17. Kirchoff, G.,"Zur Theorie freier Flussigkeitsstrahlen", Crelles J., Vol. 70, 1869,p. 289. Translated as " On the theory of free fluid jets".

18. Leonardo da Vinci: " Del moto e misura dell' aqua", edited by E.Carusi and A.Favoro, Bologna, 1923, A158 and quoted in Ref.25.

19. McNown, J. S., " Mechanics of manifold flow ", Trans. ASCE, Vol.119, Paper No.2714 , 1954, pp.1103-1142.

20. McNown, J. S. and Hsu, E. Y., "Application of conformal mapping to divided flow " , Proceedings of The Midwestern Conference on Fluid Mechanics, First Conference, State University of Iowa, Reprint No.96, 1950, pp.143-155.

21. Miller,D. S., " Internal Flow, A guide to losses in pipe and duct systems ", BHRA , Cranfield, Bedford,England, 1971.

22. Modi, P. N., Ariel. P. D. and Dandekar, M.M., " Conformal mapping for channel junction flow ", J. Hydraulics Div. ASCE, Vol 107, No HY12, Dec. 1981, pp. 1713-33.

23. O'Neill, M. E. and Chorlton, F., "Ideal and Incompressible Fluid Dynamics", Ellis Harwood Limited, Sussex,England, 1986.

24. Petermann,F.," Loss in oblique-angled pipe branches". Trans. Hydraulic Inst. Technical Univ., Munich, Bulletin 3, 1929. Translation published by ASME, Bulletin 3, pp.65-77,1935.

25. Popp, M. and Sallet, D. W.,' Experimental Investigation of One and Two Phase Flow Through A Tee Junction", Int. conference on the Physical Modelling of Multi-Phase Flow, BHRA Fluid Engineering, Coventry, England 1983, pp. 67 to 90.

26. Rawn, A.M., Bowerman, F.R., and Brooks, N. H., " Diffusers for Disposal of Sewage in Sea Water", Transactions, ASCE, Vol. 126 Part 111. 1961, pp.344-388.

27. Robert P. Benedict, " Fundamentals of Pipe Flow", John Wiley & Sons, 1980.

28. Ramamurthy, A.S. and Carballada B.L., " Two Dimensional Lateral Flow Past a Barrier", Journal of Fluids Engineering, vol. 101, Dec. 1979, Pp.449-452.

29. Satish, M., Ph.D. thesis, Concordia University, Montreal, Canada, 1986.

30. Schlichting, H.," Boundary Layer Theory ", Mc Graw-Hill, New York.

31. Sivarudrappa, K. B., Sargunar, E. V. M. and Sakthivadivel, R., " An Experimental Investigation of Pressure Recovery Factor in Discharging Manifolds ", Austral-Asian Conference, Adelaide, Australia ,Dec. 1977, pp 209-212.

32. Subramanya, K., Discussion on " Internal Hydraulics Of Thermal Discharge Diffusers", by Vigander et al [ref.2] , J.of the Hydraulic Division, HY 12, Dec.1970.

33. Syamala Rao, B. C., Lakshmana Rao, N. S. and Shivaswamy S. M., "Distribution

of energy losses at conduit trifurcations", Journal of the Hydraulics Division, Proceedings of the ASCE, Vol.94, No. HY6, Nov. 1968.pp.1363 to 1374

34. Taylor, E.H., " Flow characteristics at rectangular open channel junctions ", Transactions, ASCE, Vol.109, 1944, pp.893-912.

35. Thoma, D., " The Hydraulic Loss In Pipes", World Power Conference, Tokyo, Vol.2, 1929, pp.446-72 (In German).

36. Tsakonas, S., " Divided Flow Through A Divergence Inlet Conduit", Journal of the Hydraulic Division. ASCE, Vol.83, No.HY 6, Dec.1957, pp 1492-1 to 25.

37. Vazsonyi, A., " Pressure loss in elbows and duct branches ", Trans. A.S.M.E., 66, April 1944, pp. 177-83.

38. Vigander, S., Elder, R.A. and Brooks, N.H, " Internal Hydraulics of Thermal Discharge Diffusers ", Journal of the Hydraulics Division, ASCE,vol 96,No. HY1, Feb.1970, pp. 509 to 527.

39. Vogel, G., " Investigation of the loss in right angled pipe branches", Mitt. d. Hydr. Instututs d. Techn. Hoschl. Munchen, No. 1, 1926, pp. 75-90 and No.2, 1928, pp.61-4 (In German).

40. Ward Smith, A. J., " Internal Fluid Flow ", Oxford University Press, Oxford, 1980.

APPENDIX IV

SAMPLE CALCULATIONS

A4.1 (b): Sample Calculation Sheet for Test No. Lat 1/18 (q=0.93)

		LAT 1/18h		Date	Nov-25-89
DISCHARGE RATIO Q3/Q1=q=		0.9257493		q	=0.9257493
		LATERAL		MAIN	
		Flexi-glas		Aluminium	
Length	cm	9.15		9.15	
Breadth	cm	4.125		4.125	
Area	ft^2	0.040627		0.040627	
perim	ft	0.871063		0.871063	
Hydr.Diam	ft	0.186563		0.186563	
Area ratio(m)		1		1	m=1
Temperature		Air	F	75.8	
		Water	F	69.5	
Specific Wt			lb/ft^3	62.31	
Density				1.9350932	
Kinematic viscosity			ft^2/sec	1.067E-05	

V-NOTCH READINGS	Reading	Zero-Read	Height	Height
	cms	cms	cms	ft
Main2	20.03	14.56	5.47	0.1794619
Lateral	20.67	5.28	15.39	0.5049213

(1) DISCHARGE:Q, VELOCITY HEAD:V^2/2g

	Ht. H_1	Q	V	V^2	V^2/2g
	ft	cusecs	ft/sec	ft^2/s^2	ft
Main2	0.1794619	0.0101311	0.2493672	0.062184	0.0009656
Lateral	0.5049213	0.1263127	3.1090804	9.6663811	0.1500991
Main1	----	0.1364438	3.3789938	11.417599	0.1772919

(2)REYNOLD NUMBER:R

	Rey.No Re	N From Std N&Re value	2*N^2	(N+1)(2N+1	U/V
Main2	4360.1409	5.88	69.1488	87.7888	1.2695636
Lateral	54361.707	6.3	79.38	99.28	1.2506929
Main1	59081.093	6.34	80.3912	100.4112	1.2490322

(3) β, α, COEFFICIENTS

	e=U/V-1	e^2	e^2/3	β	α
Main 2	0.2695636	0.0726645	0.0242215	1.0242215	1.0726645
Lateral	0.2506929	0.0628469	0.020949	1.020949	1.0628469

Main 1	0.2490322	0.0620171	0.0206724	1.0206724	1.0620171

(4)PRESSURE RECOVERY COEFF: Cp21

	(P/y+Z200) P2(Z) ft	P/y+Z200 P1(Z) ft	V1^2/2g ft	P2-P1 ft	Cp21
Main	10.97	10.84	0.1772919	0.13	0.733254

(5)MOMENTUM LOSS COEFF. IN THE MAIN: Rm

	β1V1^2*d lbs/sq ft	β2V2^2*d lbs/sqft	d*(β1V1^2-β2V2^2)	dP21 lbs/sq ft	dM
Main	22.550855	0.1232465	22.427609	8.1003	0.5820761

M=Q3*V1*Y	q=Q3/Q1	Rm=dM/M
0.8259169	0.9257493	0.7047635

(6)MOMENTUM LOSS COEFF. FROM FORCE DIAGRAM IN THE LATERAL: Rf

Area Sq. Divisions	Scale of Diagram	lateral cm	Force=F lbs	Rf=F/M
0.39	0.2	4.125	0.6577507	0.7963885

(7)FRICTIONAL LOSS COEFF: f

	Slope ft/ft	f value	f Blasius	Friction Velo.= Ut	U/Ut
Main 1	0.02	0.0210459	0.0202943	0.3466217	9.7483628
Main 2	0.0002	0.0386423	0.0389369	0.0346622	7.1942195
Lateral	0.018	0.0223728	0.0207211	0.3288342	9.4548576

(8)STAGNATION PRESSURE Pstg

	Pstg	Distance Main ft	Distance Lateral ft	q
Observed high readin	11.04	0.145	----	0.9257493
Calculated	11.028287			

(9)ENERGY LOSS COEFF: E12,E13

	P1+ a*V1^2/2g	P2+ a*V2^2/2g	Loss ft	E12
Main	11.028287	10.971036	0.0572513	0.322921

Lateral	P3	P3+ aV3^2/2g	Loss ft	E13

	10.66	10.819532	0.2087547	1.1774631

Loss Coefficient without α

Main	P1+V1^2/2g	P2+V2^2/2g	Loss ft	E12
	11.017292	10.970966	0.0463263	0.2612997

Lateral	P3+V3^2/2g	LOSS ft	E13
	10.810099	0.2071928	1.1686536

(10)LATERAL PRESSURES & Cp13

P3	P1-P3	Cp13	P5	Pj=Pmin	Cp3j
10.66	0.18	1.0152748	10.64	10.33	1.8613371
		Distance	1.25	0.22	

(11)CONTRACTION COEFF: Cc

Pj (1)Pentry (2)Pmin	P1 +aV1^2/2g	Vj	C_c = V3/Vj	Loss ft	E13 from C_a
10.5	11.028287	5.8328111	0.5330329	0.1151973	0.6497608
10.33		6.705944	0.4636305	0.2008917	1.1331128

(12)COEFFICIENT n

P1+ aV1^2/2g	(1)Pmin (2)Pentry	Jet Ener. Ea	hm=P1-Pmin	η^2	η
11.028287	10.33	0.698287	0.51	0.2538955	0.5038804
11.028287	10.5	0.528287	0.34	0.3355977	0.5793079

Ca and n

	$1-\eta^2$	$C_a/(1-\eta^2)$	$m*Cc/q=\eta$
Pj=Pmin	0.7461045	0.6214016	0.5008165
Pj=Pentry	0.6644023	0.8022744	0.5757854

(13)PRESSURE HEAD RATIOS AND CHECKING n^2

dP21/hm	dP13/hm	E12/hm	E13/hm	hm/Ea	(1-hm/Ea)/a
0.254902	0.3529412	0.6331784	2.3087512	0.7303587	0.2538955
0.3823529	0.5294118	0.7685285	3.4631268	0.6435895	0.3355977

(14)MOMENTUM FACTOR AND CONTRACTION COEFF. FROM VELOCITY TRIANGLE

Vh=Rm V1

$$Rm^2 \eta^2 + Ca^2 = K1^2$$

	Rm^2	ß^2	Ca^2	K1^2	K1
Pi=Pmin	0.1261077	0.2149533	0.341061	0.5840043	
Pj=Pentry	0.1666885	0.2841241	0.4508127	0.6714258	

(15)COEFFICIENT OF DISCHARGE Cd FROM FREE VORTEX MODEL

dh ft (Pmin,Pen)	dP/d=dh*g	dP/(d*Vi^2)=X/2	1-X	(1-X)^.5
0.33	10.626	0.2362925	0.527415	0.7262334
0.45	14.49	0.4259048	0.1481903	0.384955

	k/Cd	V3/Vi=Cc (Vi cons.)	(1+k/Cd)/(k/Cd)	k	Cd
Pc=Pmin	3.6527467	0.4636305	1.2737666	1.9160002	0.5245369
Pc=Pe	1.6258972	0.5330329	1.615045	1.1119613	0.6839063

(k+Cd)/Cd	VikLn(co1) V mean	Vi/Vmean-1 =e(Vi,Pmi, e(Vi,Pen)	a=1+e^2	B=1+e^2/3
1.2737666	5.9272869	0.1313682	1.0172576	1.0057525
1.615045	4.546062	0.283047	1.0801156	1.0267052

(16) Loss from free vortex model e13=α/Cd^2 -2β/Cd +(2β3-α3) E13=e13*q^2

	α/Cd^2	2*β/Cd	2β3-α3	E13=e13*q^2
Pj=Pmin	3.697251	3.8348213	0.979051	0.7211588
Pj=Pentry	2.3092823	3.0024733	0.979051	0.2449854

APPENDIX V

FIGURES

Note: Some additional notations used in the tables are defined near the tabulations.

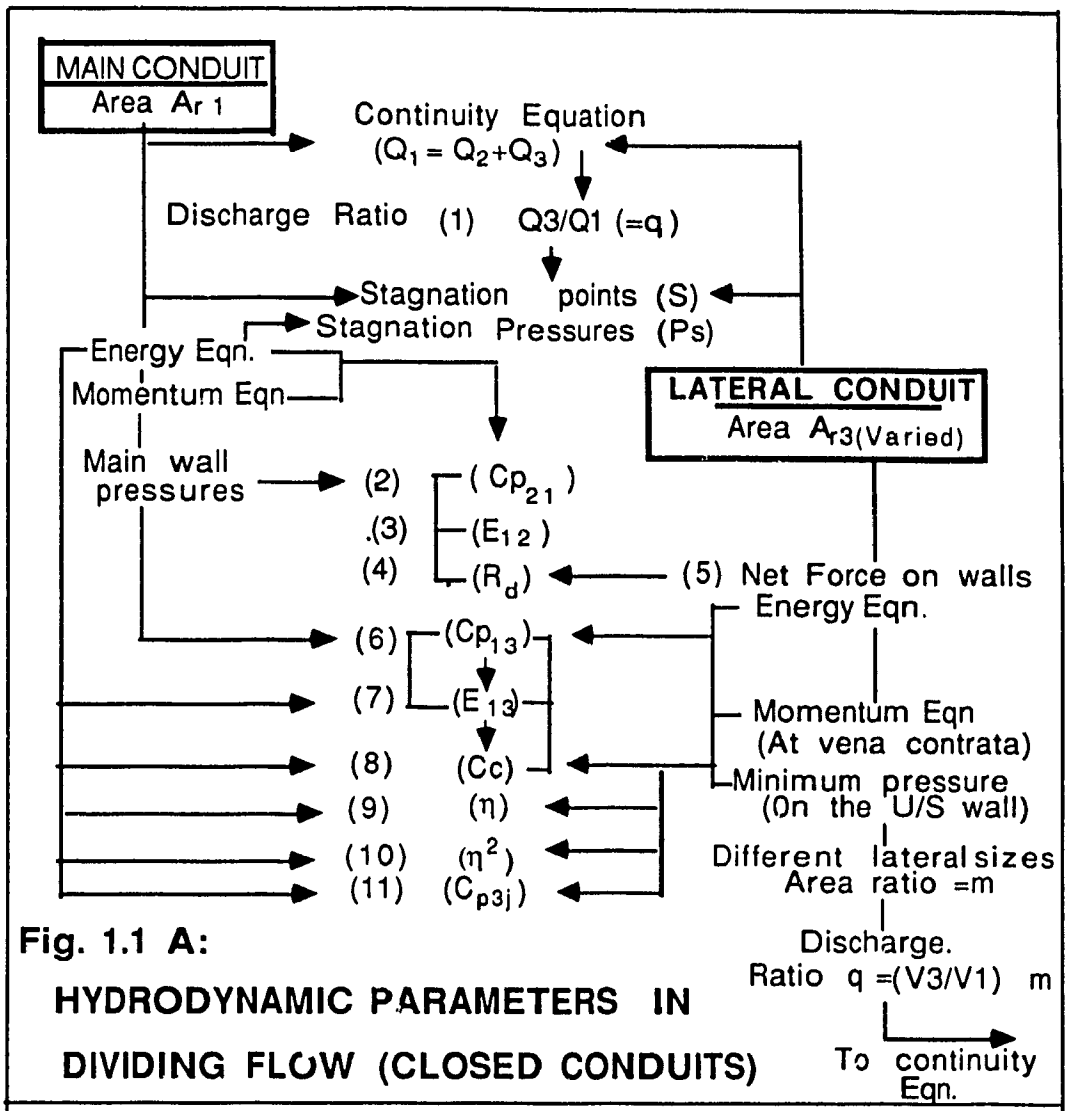

Fig. 1.1 A:

HYDRODYNAMIC PARAMETERS IN DIVIDING FLOW (CLOSED CONDUITS)

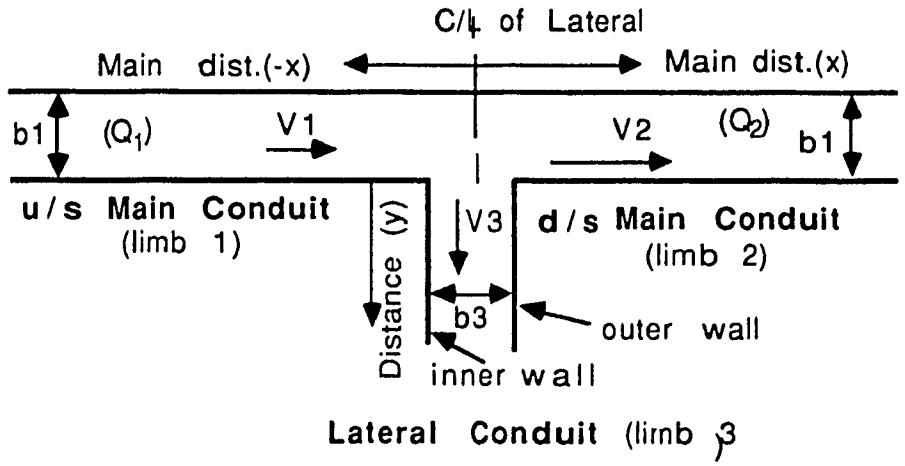

Fig.1.1B: CONDUIT GEOMETRY (90° BRANCH)

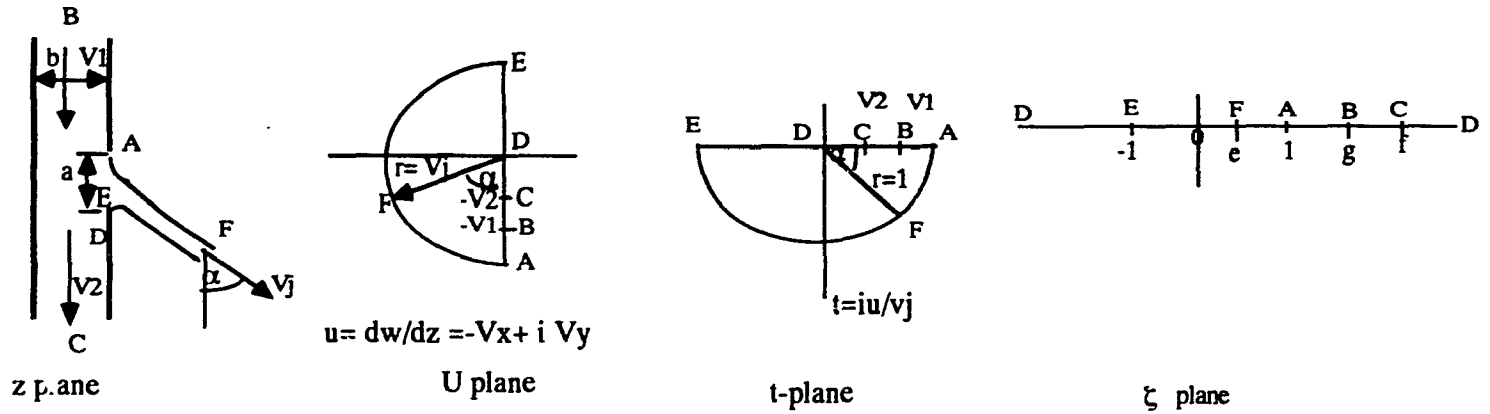

Fig.2.1 Conformal mapping for free efflux by McNown [1950]

N.B. Efflux with a barrier from E represents lateral flows [McNown] using different conformal mapping

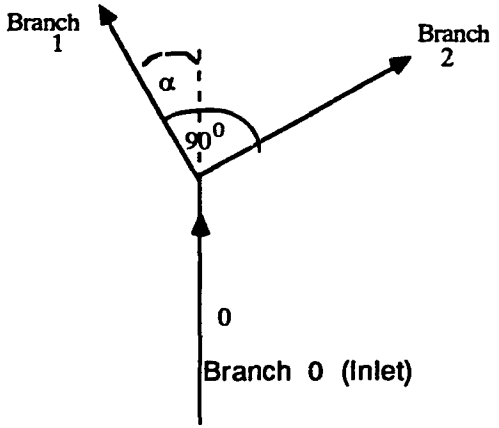

Fig.2.2 Division Of Flows By Vaszonyi [1944]:
Physical Configuration

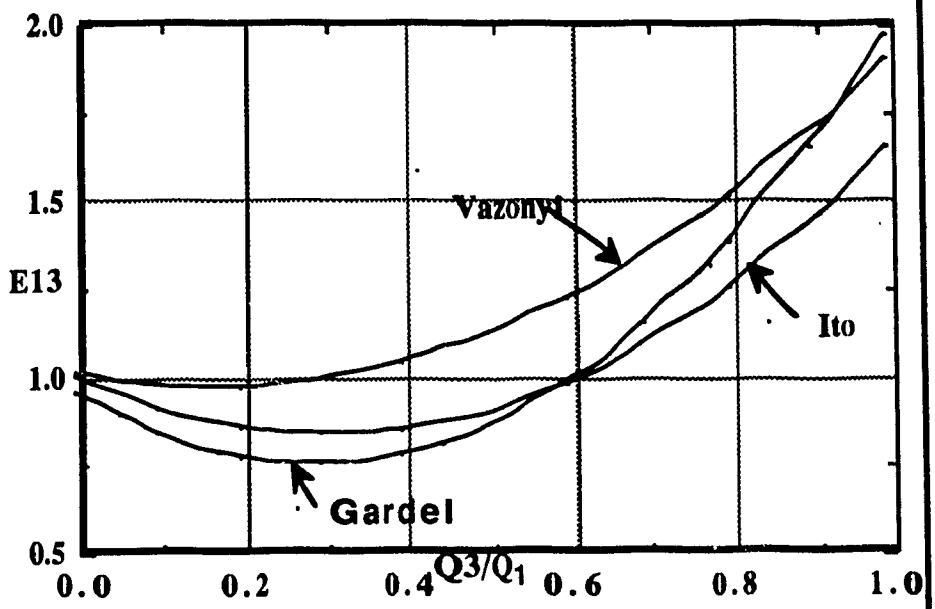

Fig.2.3(b): Lateral Loss Coefficient E13 Vs q
by previous researchers for m=0.77

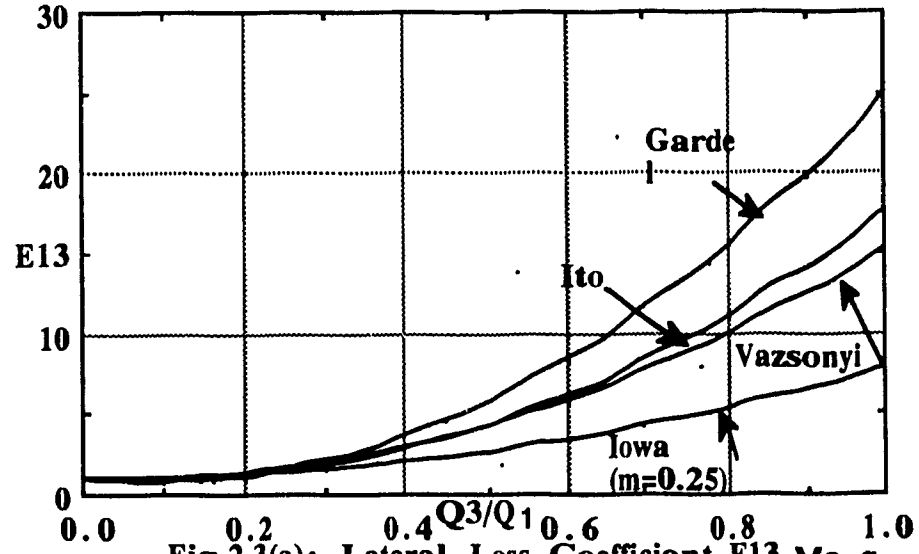

Fig.2.3(a): Lateral Loss Coefficient E13 Vs q
by previous researchers for
m=o.225

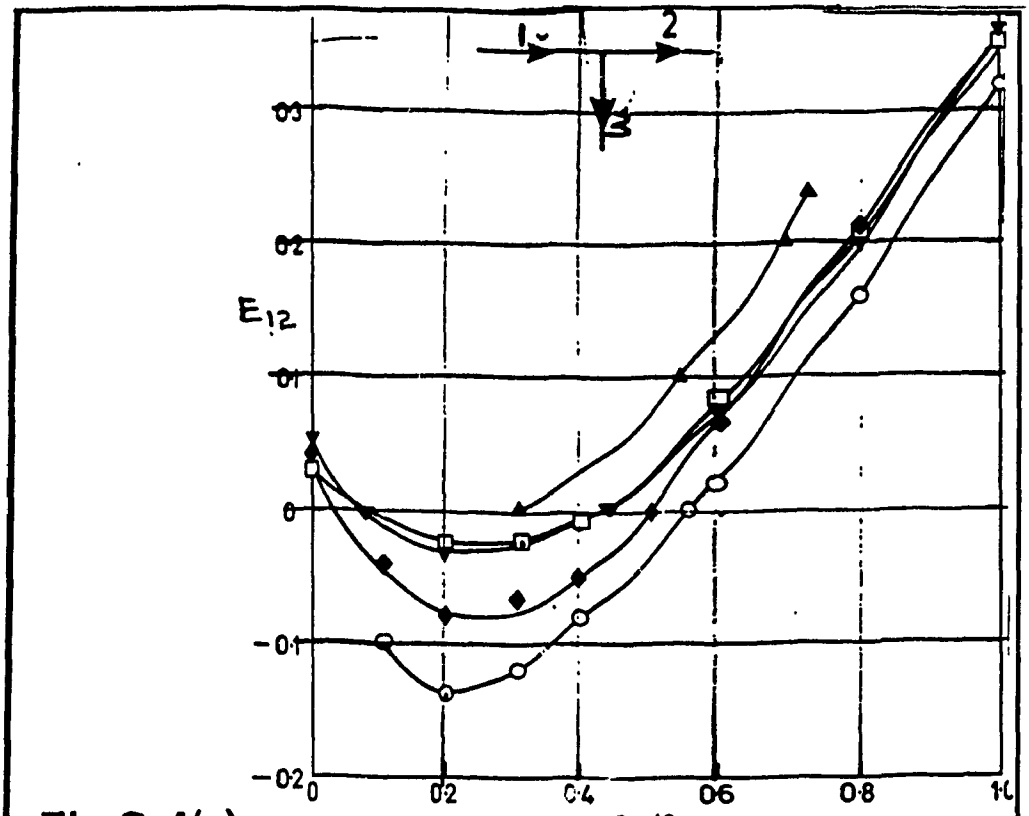

Fig.2.4(a):
Loss Coefficient E12 Vs q (Smith 1980)

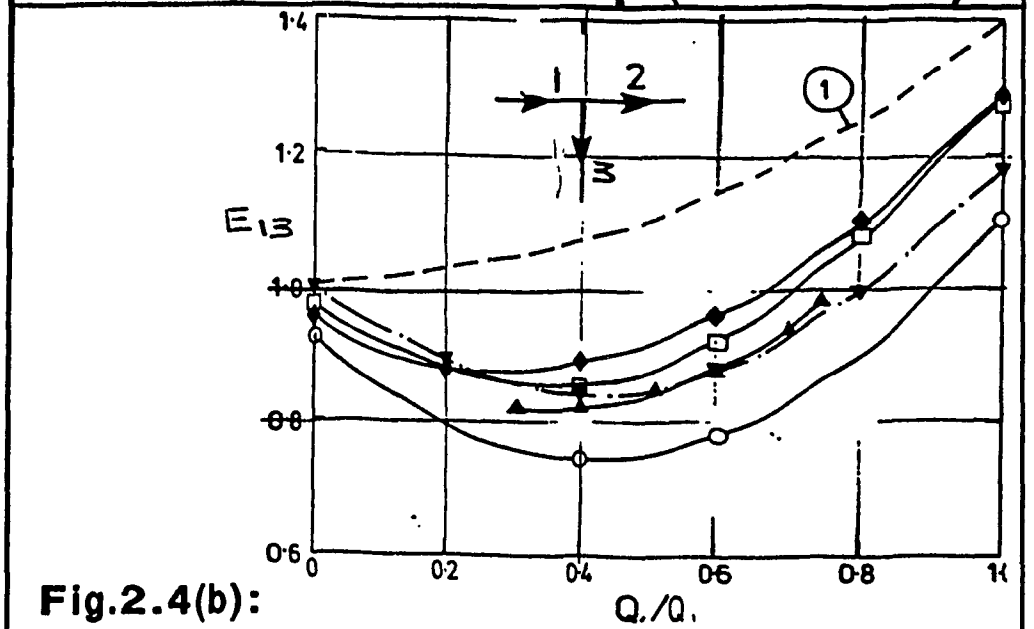

Fig.2.4(b):
Loss Coefficients E13 Vs q for m=1.(Smith 1980): (◆) Vogel(1929): (□) Kinne (1932): (○) McNown (1954): (▲) Miller (1971): (▼) Ito and Imai (1973): (1) Rhone(1973)

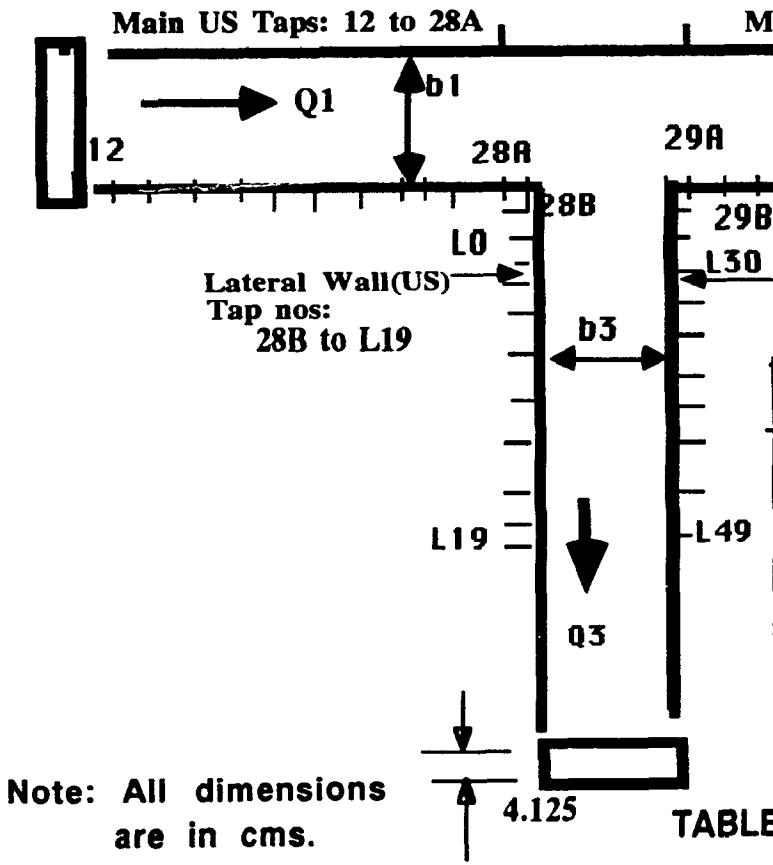

LATERAL	b3	b3/b1 = m	wall thickness
①	9.15	1.00	0.5
②	7.040	0.77	1.2
③	2.06	0.225	1.2
MAIN	b1 = 9.15	width= 4.125	0.5

TABLE3.1: SELECTED CONDUIT GEOMETRIES

TEST SECTIONS (vertical set up)

Main and Lateral Ducts

Fig. 3.1 DIVIDING FLOW IN RECTANGULAR CLOSED CONDUITS

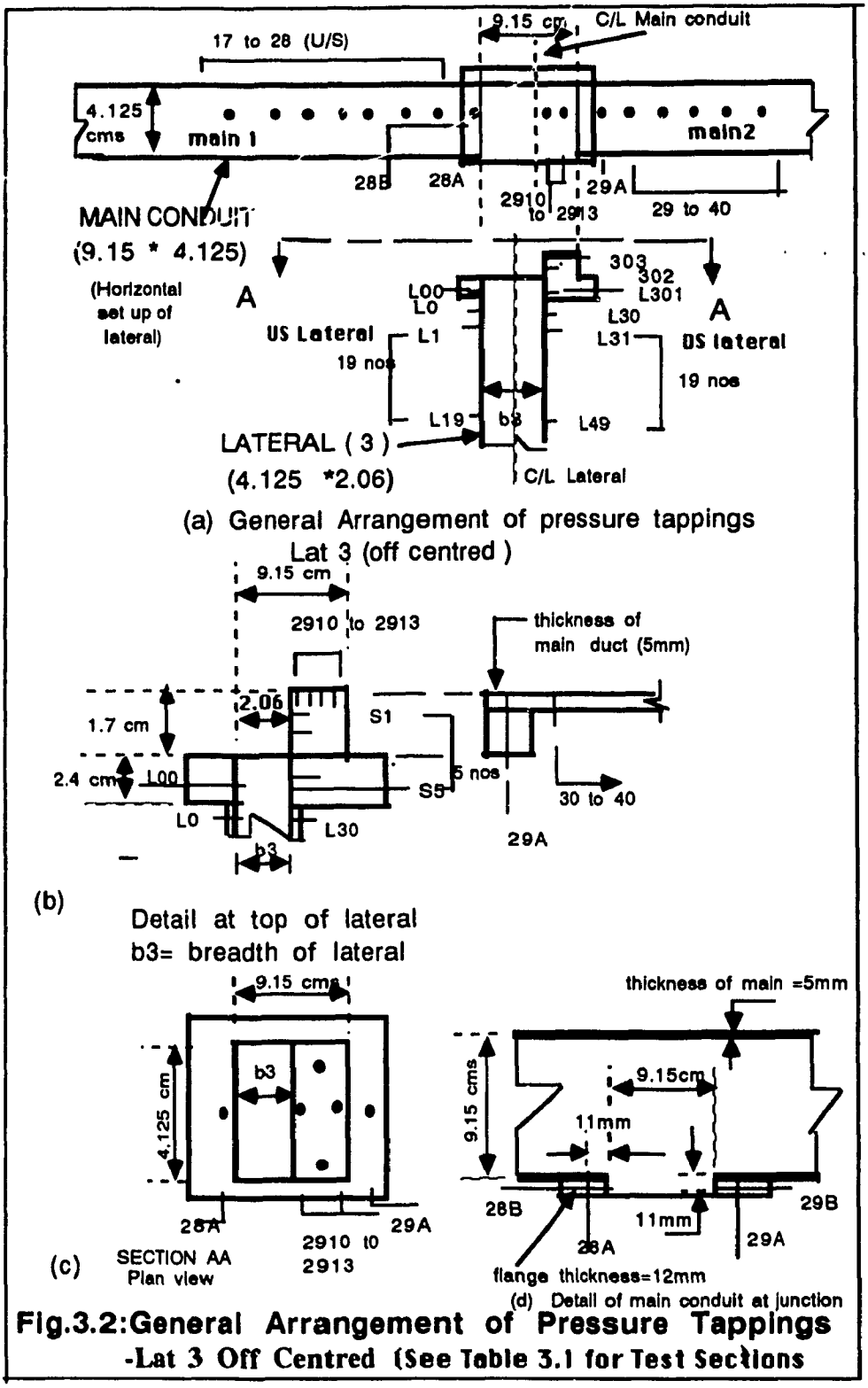

Fig.3.2:General Arrangement of Pressure Tappings -Lat 3 Off Centred (See Table 3.1 for Test Sections

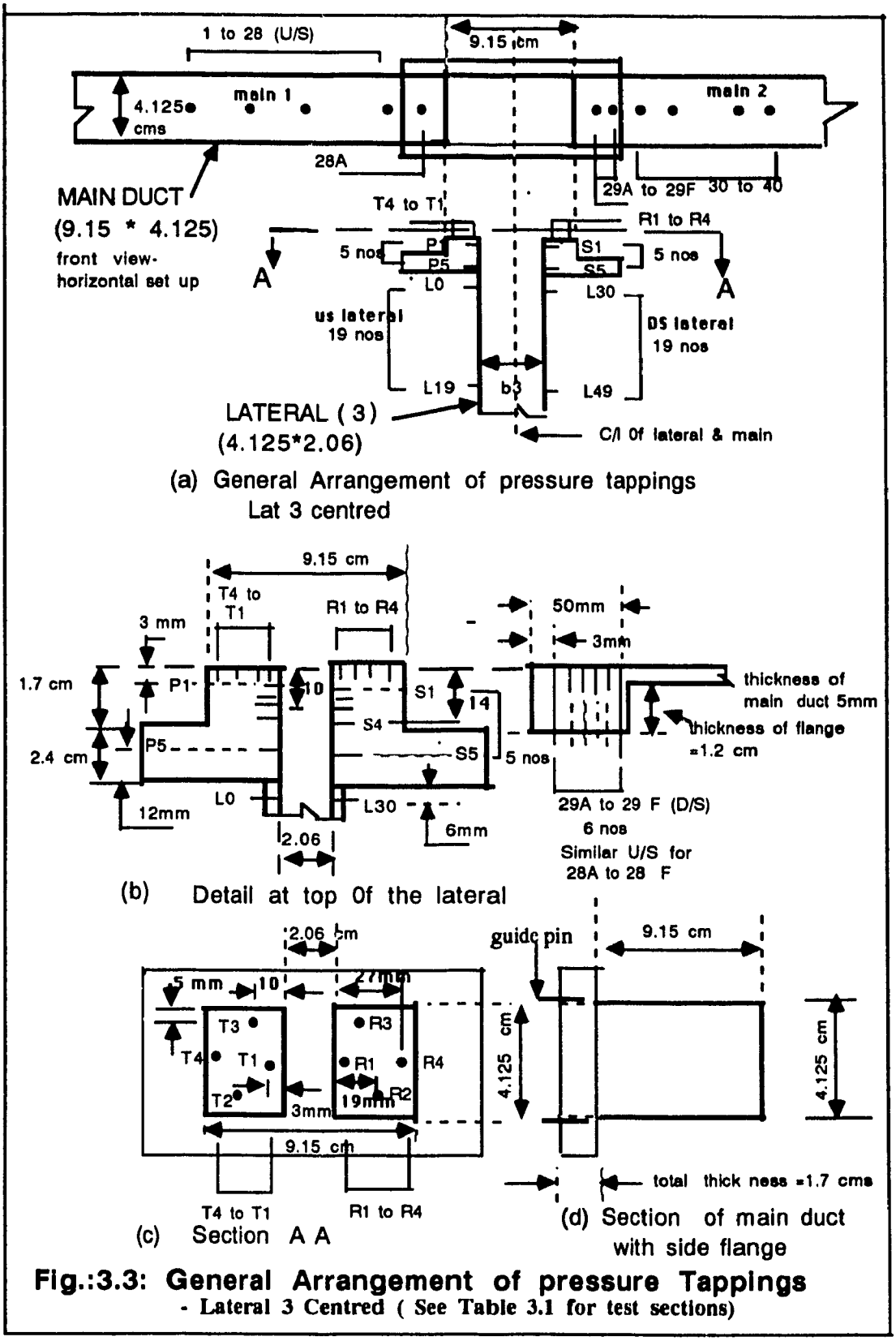

Fig.:3.3: General Arrangement of pressure Tappings
- Lateral 3 Centred (See Table 3.1 for test sections)

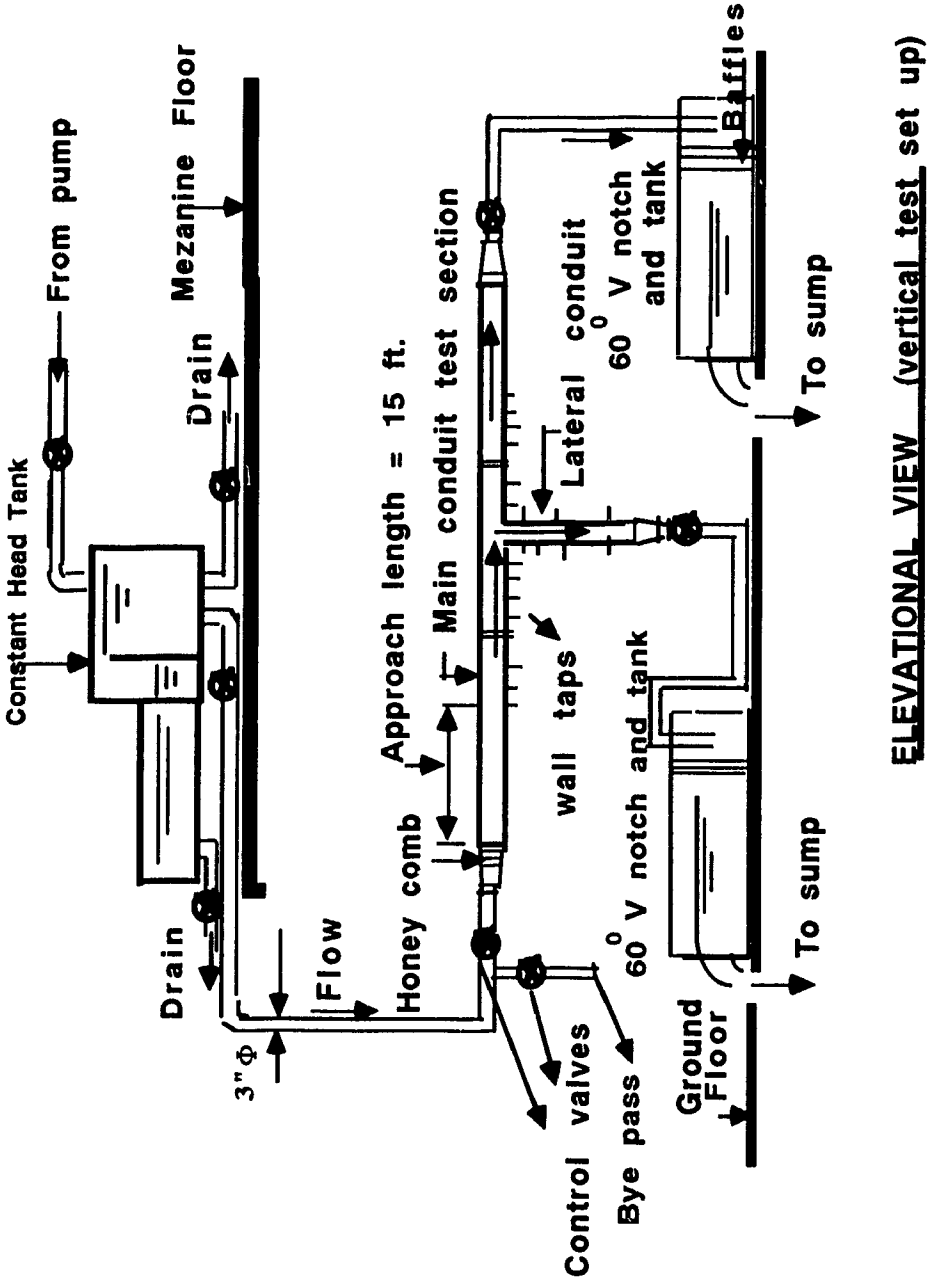

Fig. 3.4 Test Set-Up

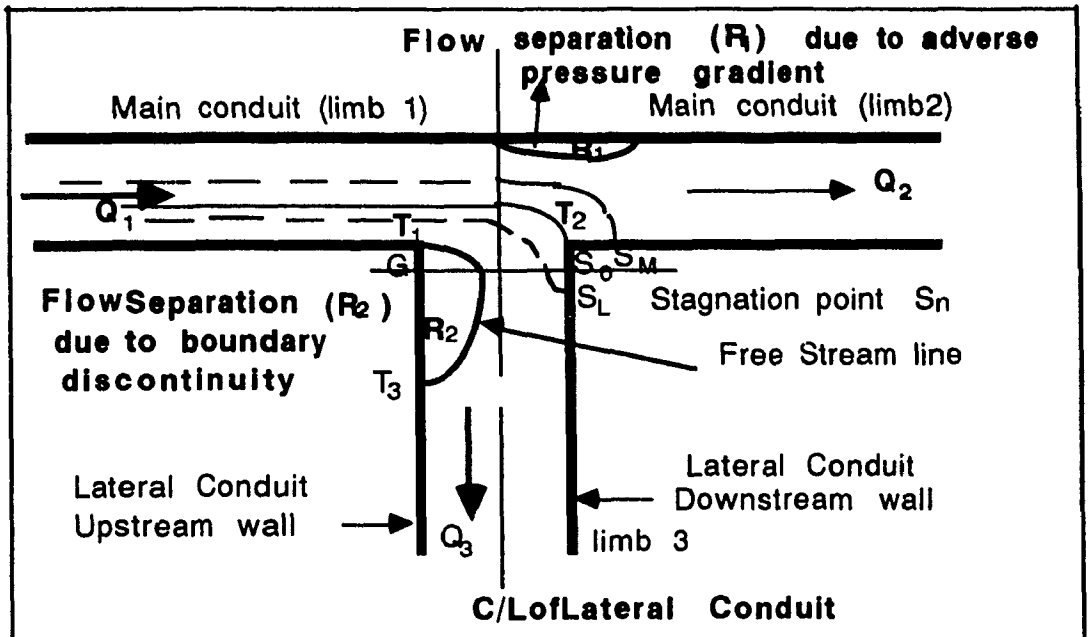

Fig. 4.1: GENERAL FLOW CHARACTERISTICS

Dividing flow in closed conduits

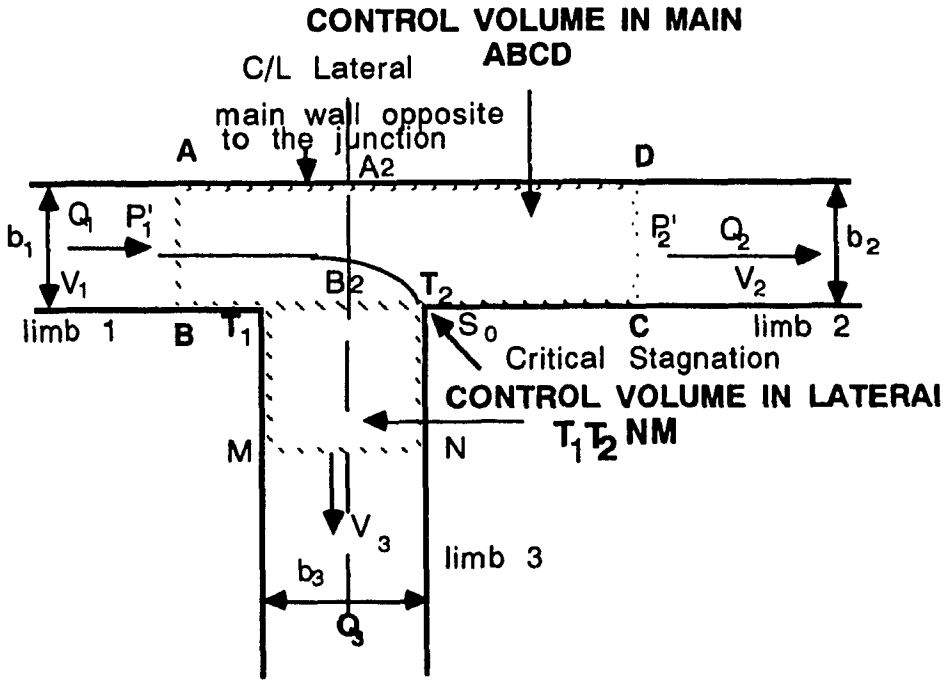

Fig. 4.2: CONTROL VOLUMES ABCD & T_1T_2 NM

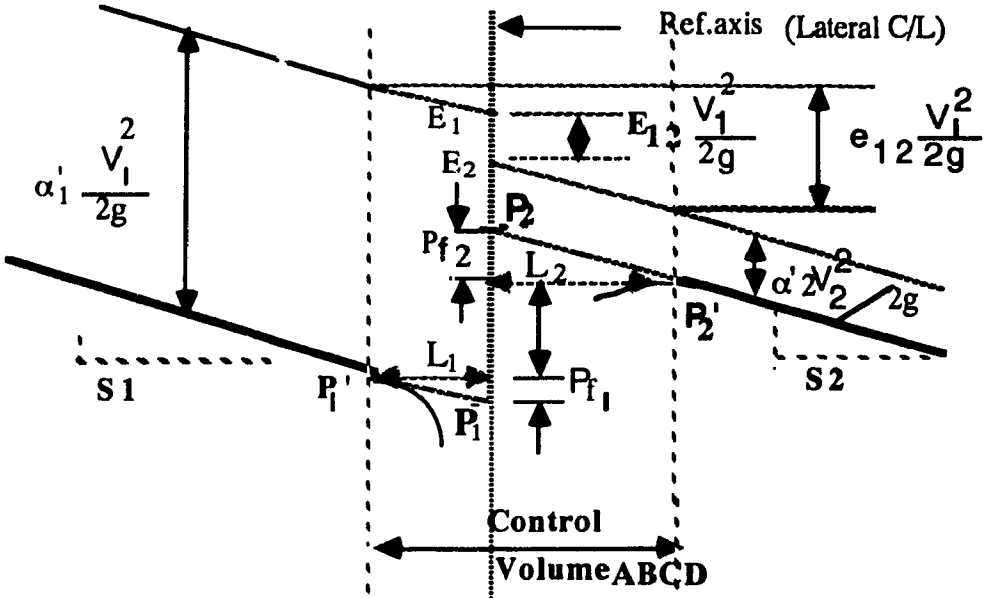

Fig 4.3 (a) MAIN CONDUIT PRESSURES AT LATERAL JUNCTION

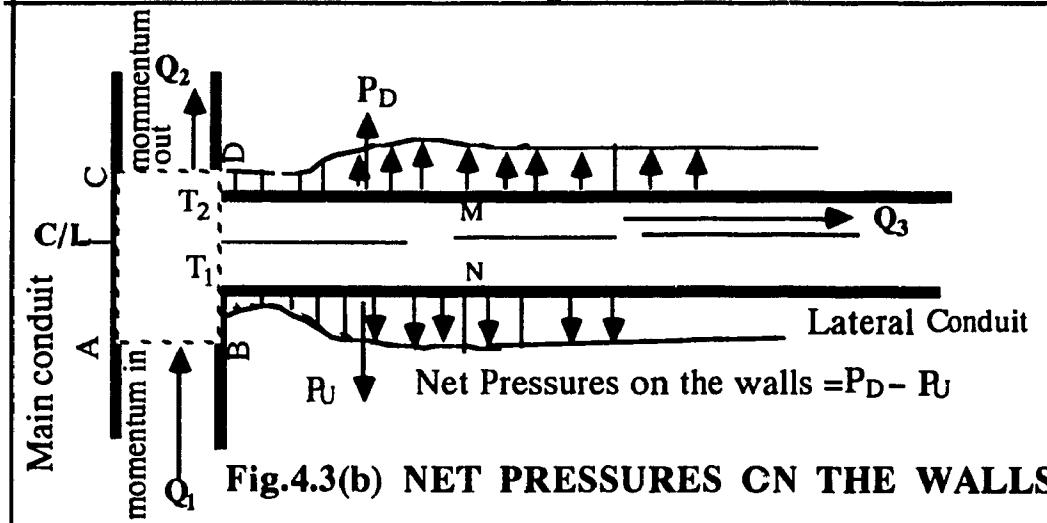

Fig.4.3(b) NET PRESSURES ON THE WALLS

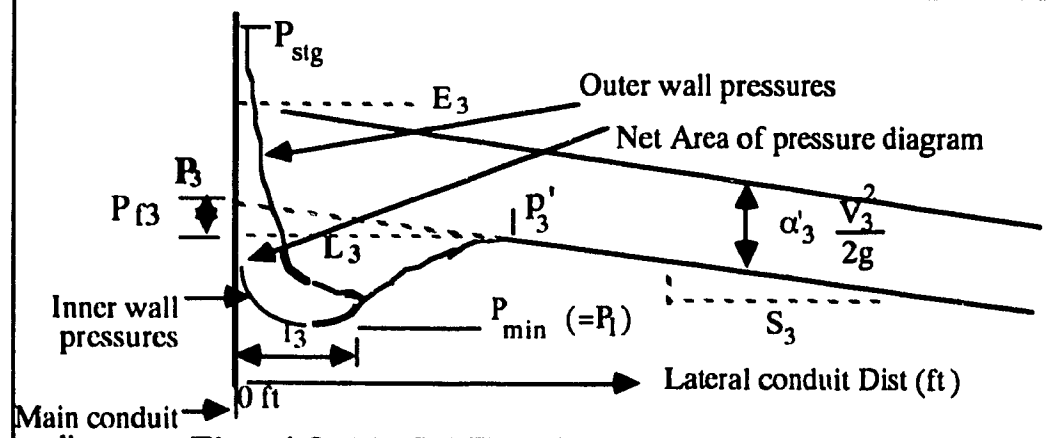

Fig: 4.3 (c) LATERAL CONDUIT PRESSURES

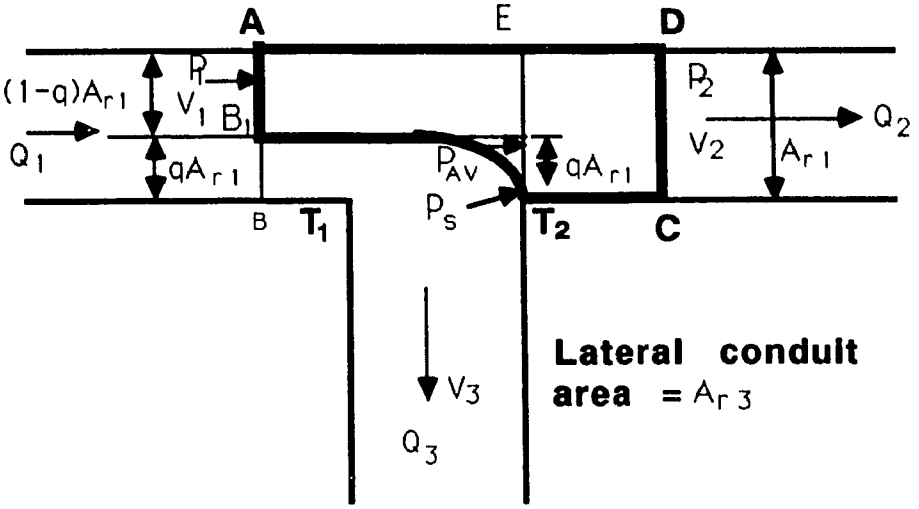

Fig. 4.4 (a): CONTROL VOLUME AB_1T_2CD (Enclosing Q_2)

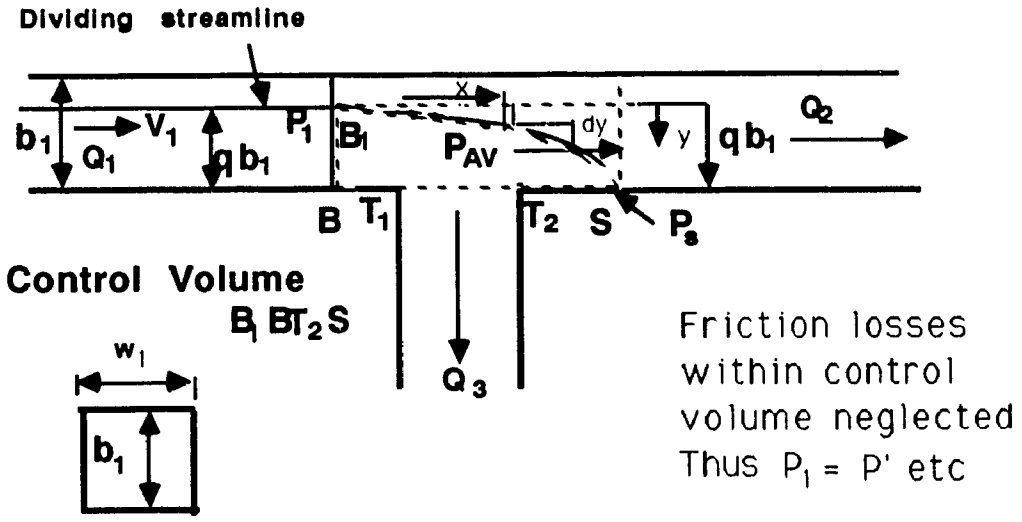

Fig. 4.4(b): PARABOLIC MODEL

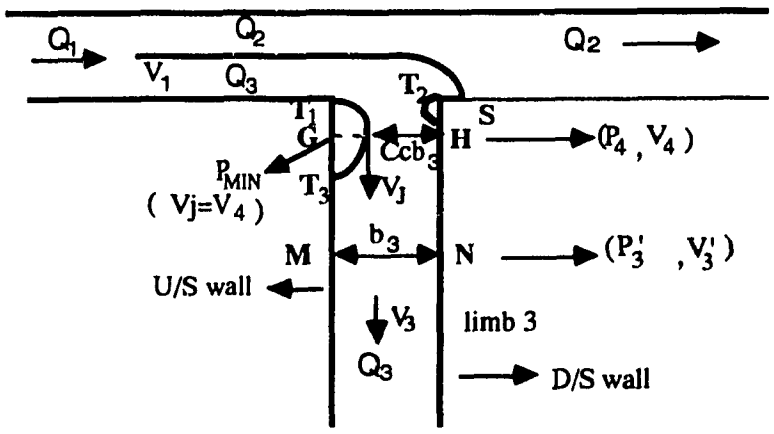

Fig: 4.5 (a).

GENERAL DESCRIPTION OF LATERAL FLOW

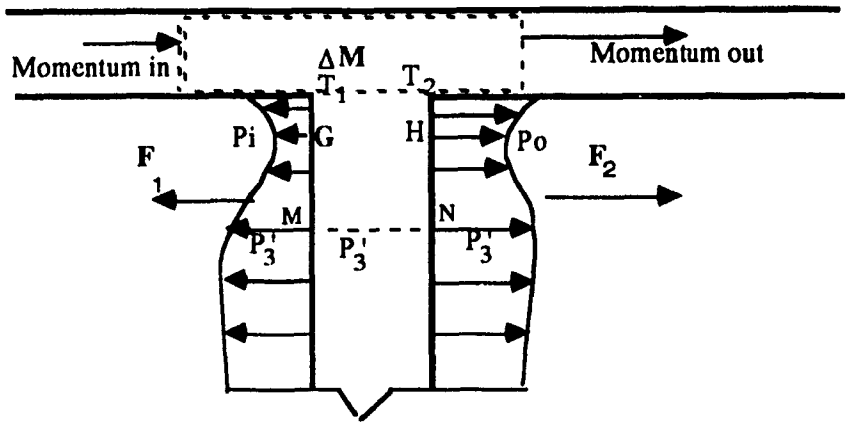

Loss of momentum in the main across lateral $\Delta M = F_2 - F_1$

Fig.4.5 (b)

MEASUREMENT OF LATERALWALL PRESSURES TO DETERMINE MOMENTUM LOSS IN THE MAIN

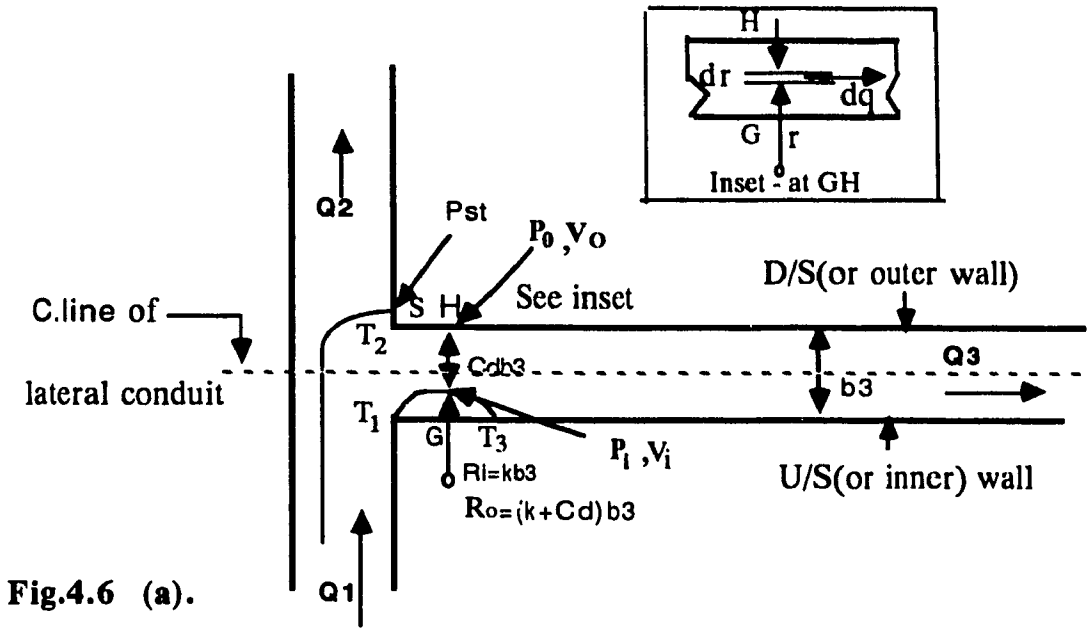

Fig.4.6 (a).

CONTRACTION COEFFICIENT Cd By FREE VORTEX MODEL

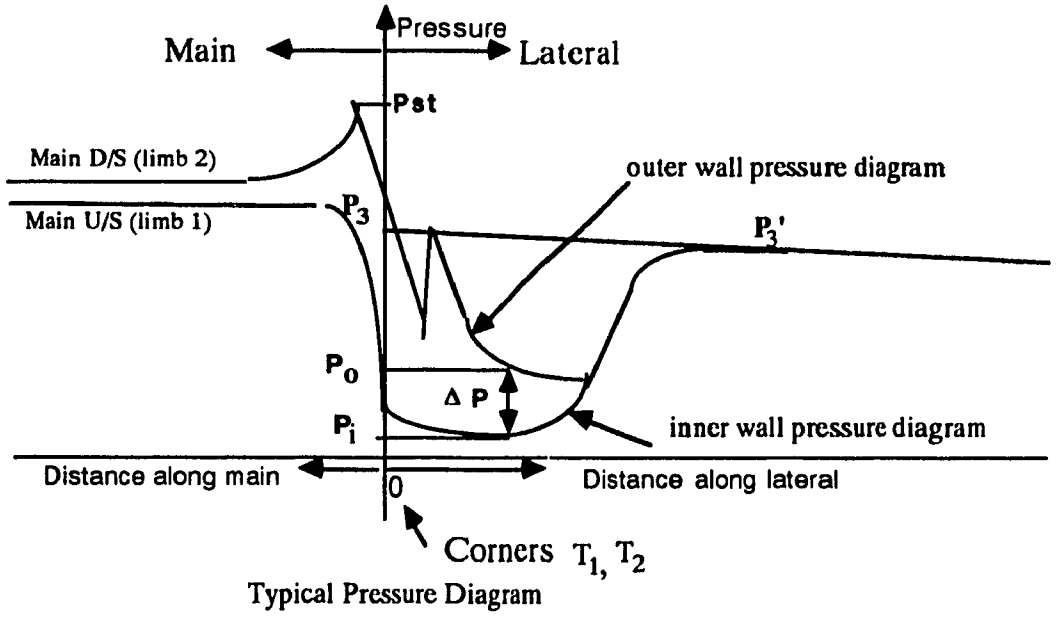

Typical Pressure Diagram

Fig. 4.6(b) MEASUREMENT OF ΔP IN FREE VORTEX MODEL

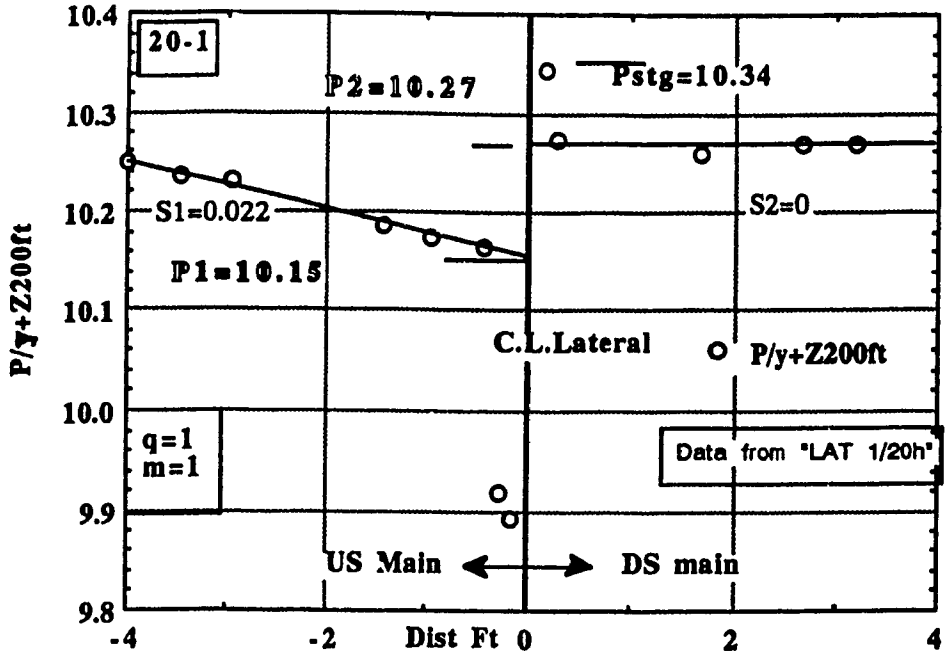

Pressure diagram on the main

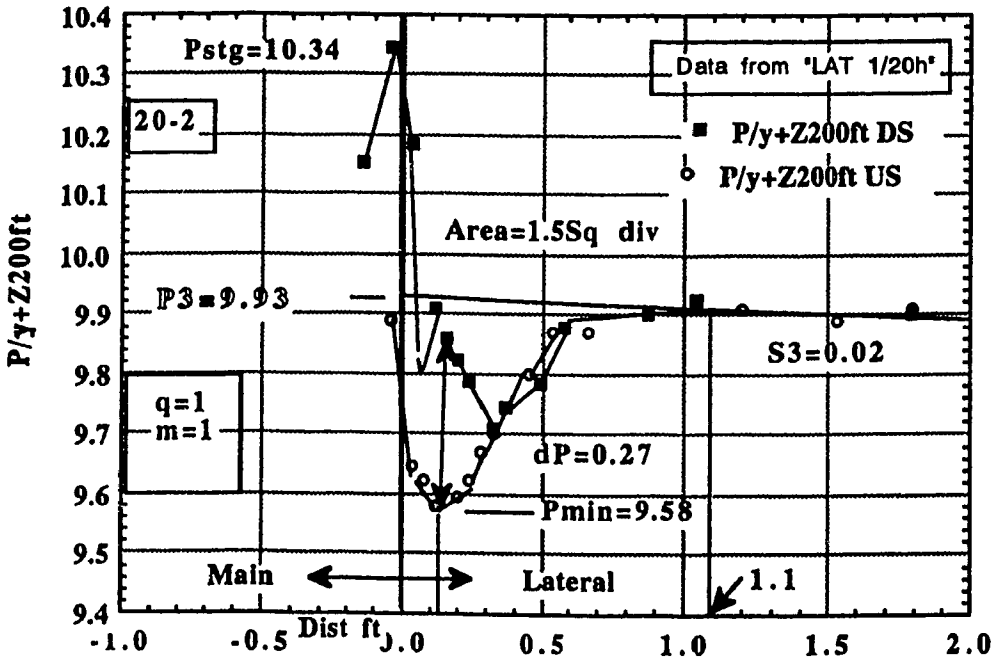

Pressure diagram on the walls

Fig.5.1(a): Pressure Diagrams on the Main and Lateral Conduits

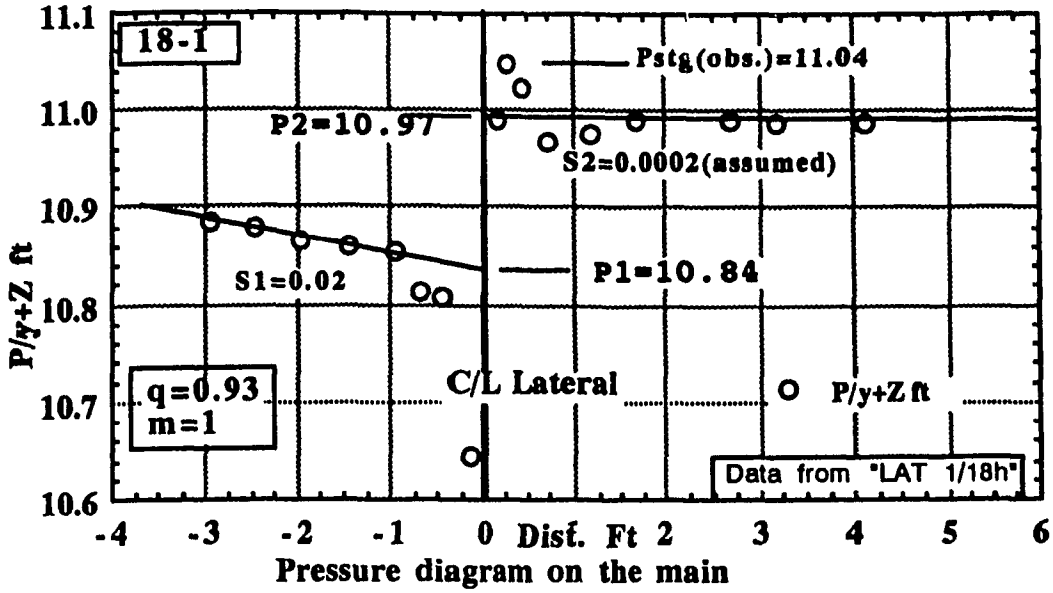

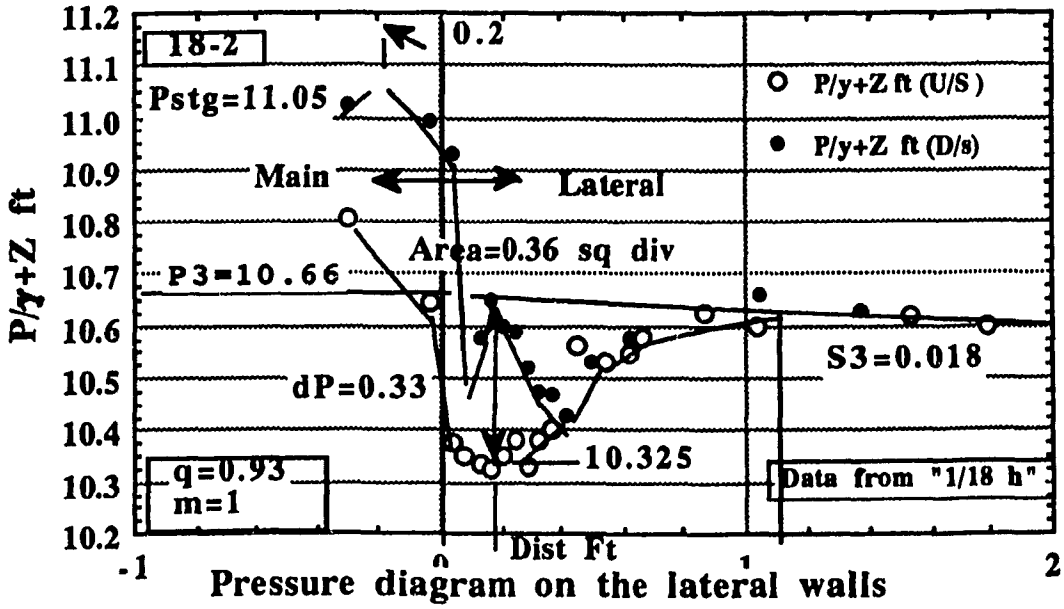

Fig.5.1(b): Pressure Diagrams on the Main and Lateral Conduits

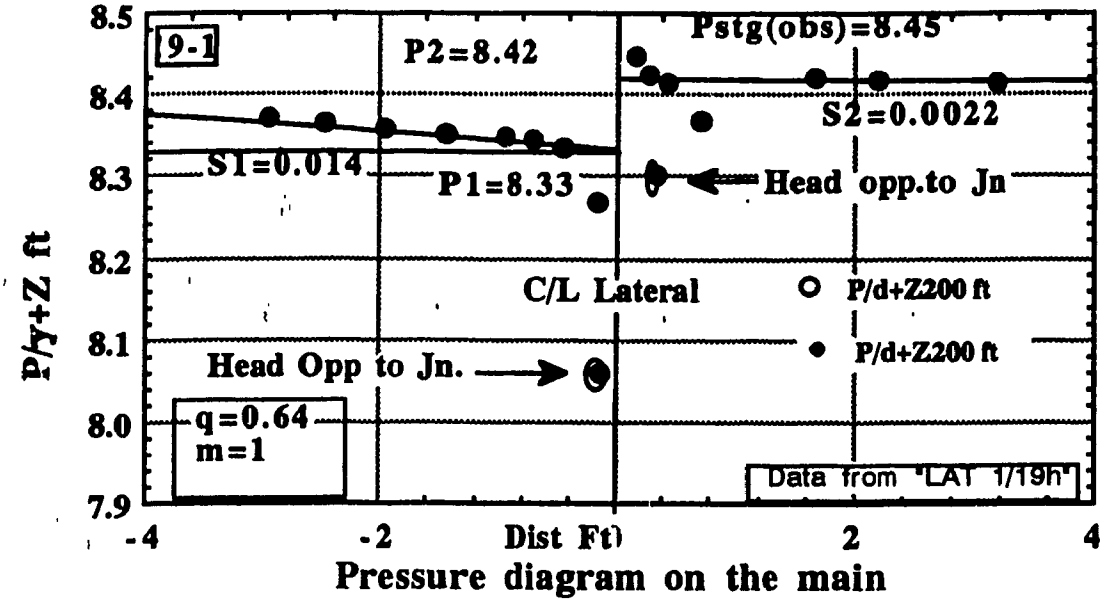

Pressure diagram on the main

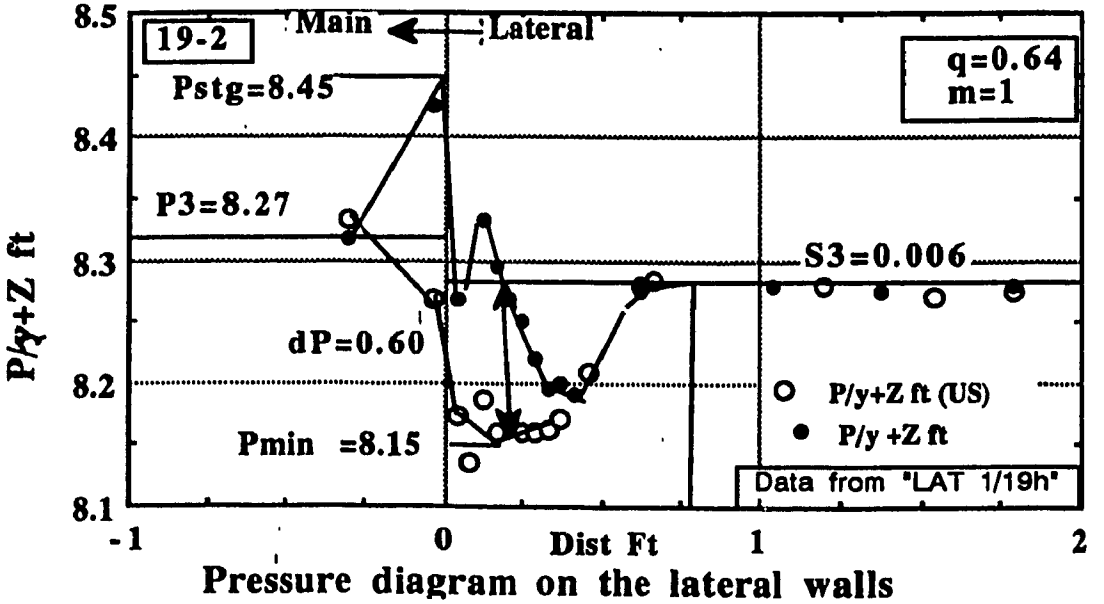

Pressure diagram on the lateral walls

Fig.5.1(c): Pressure Diagrams on the Main and Lateral Conduits

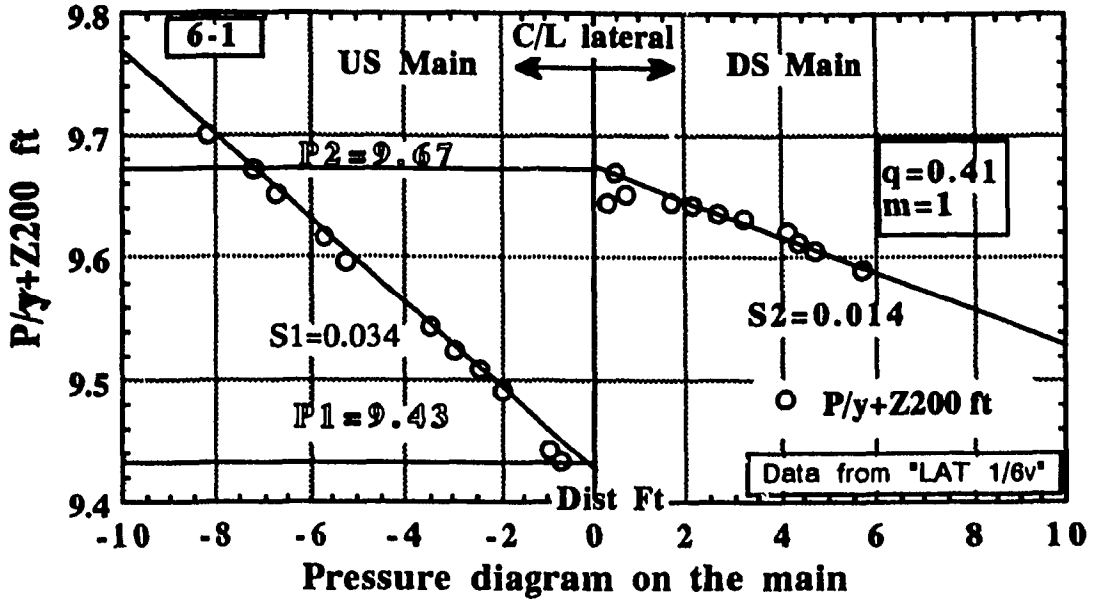

Pressure diagram on the main

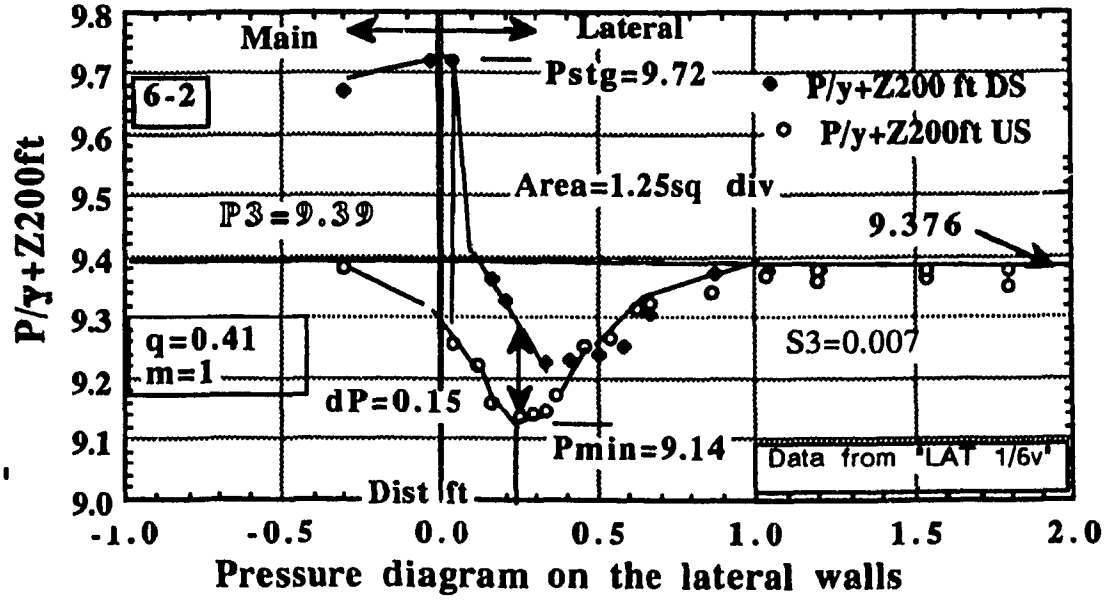

Pressure diagram on the lateral walls

Fig.5.1(d): Pressure Diagrams on the Main and Lateral Conduits

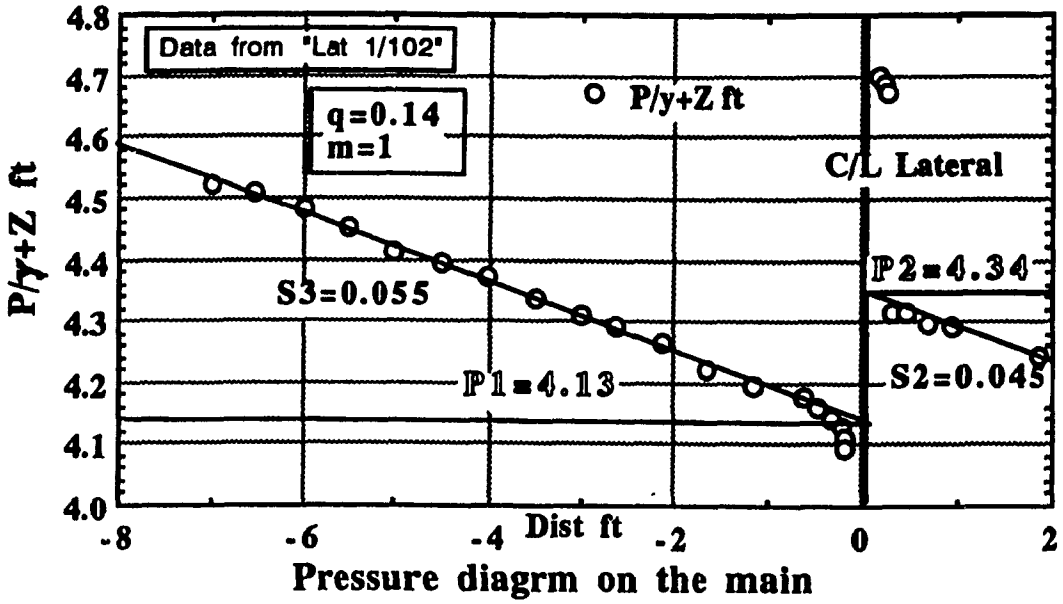

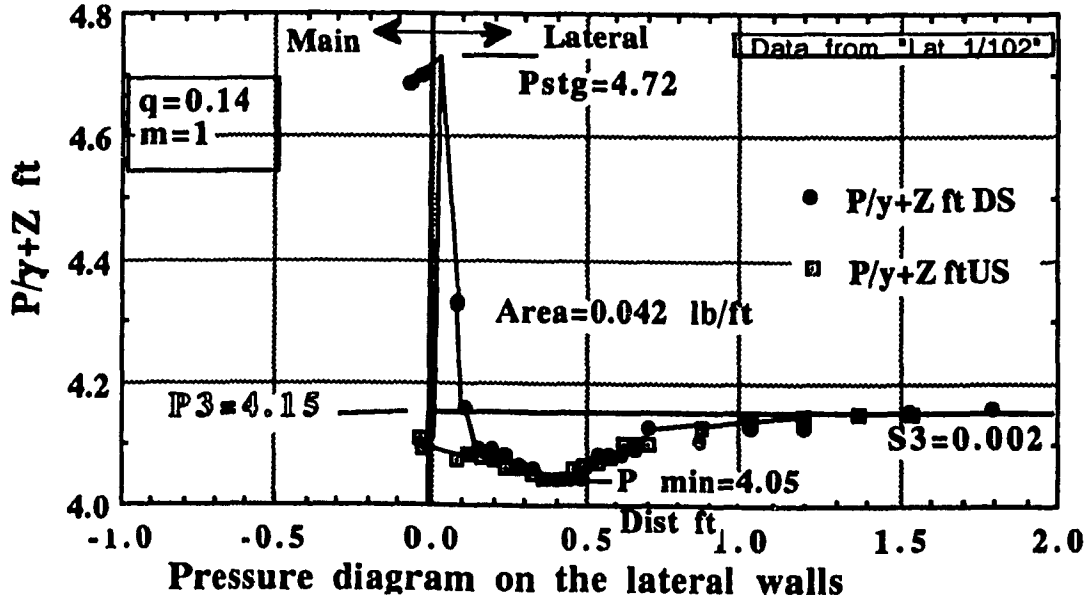

Fig.5.1(e): Pressure Diagrams on the Main and Lateral Conduits

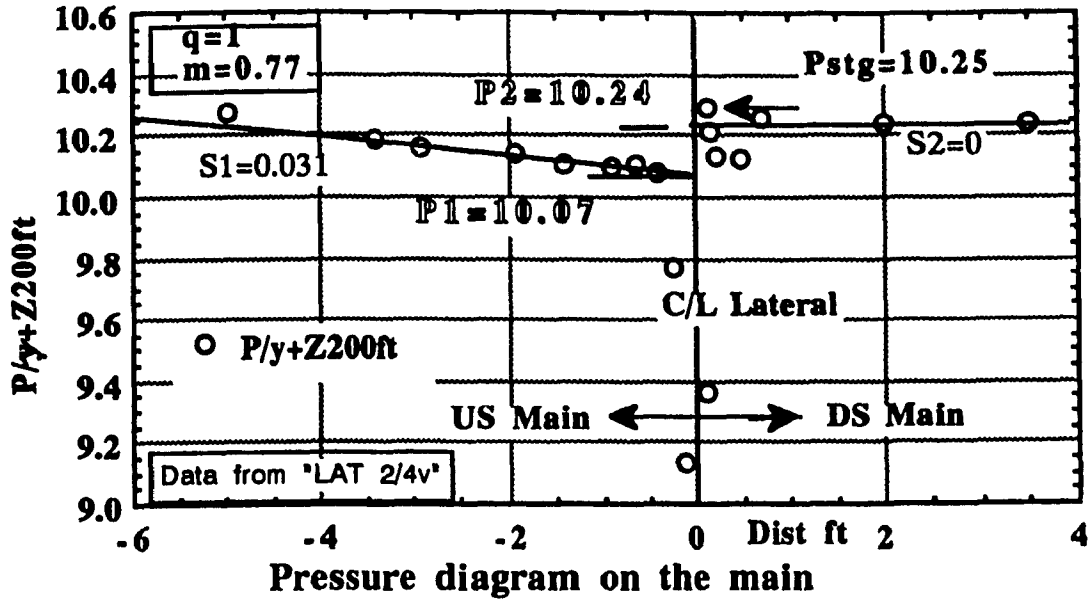

Pressure diagram on the main

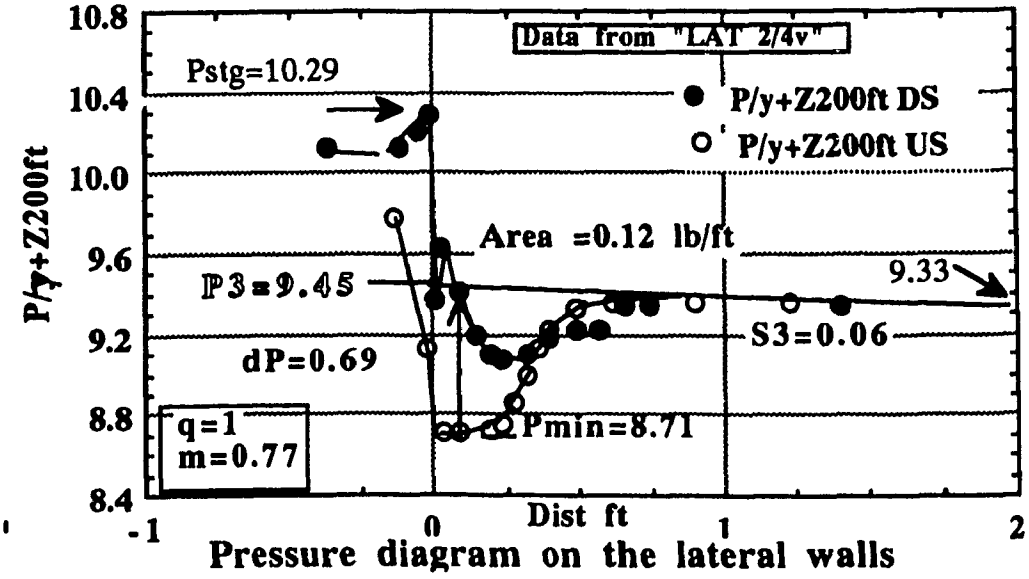

Pressure diagram on the lateral walls

Fig.5.2(a): Pressure Diagrams on the Main and Lateral Conduits

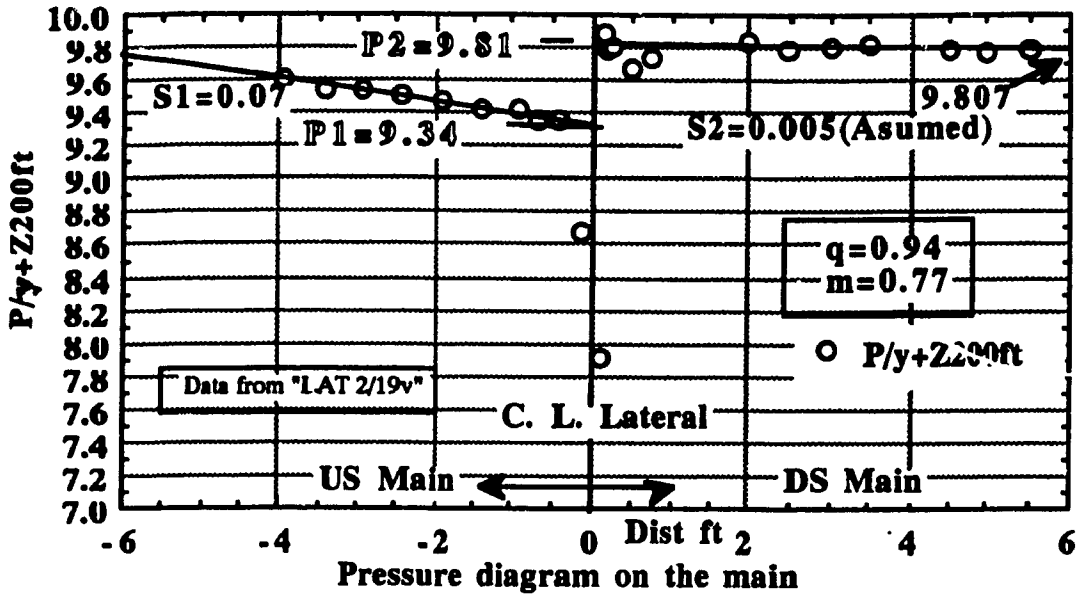

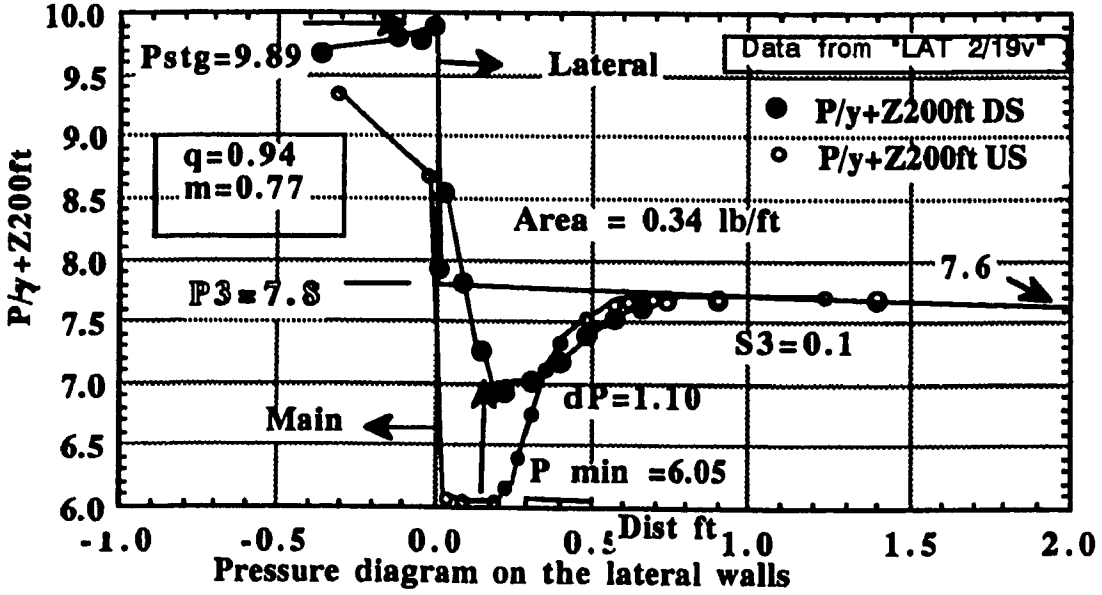

Fig.5.2(b): Pressure Diagrams on the Main and Lateral Conduits

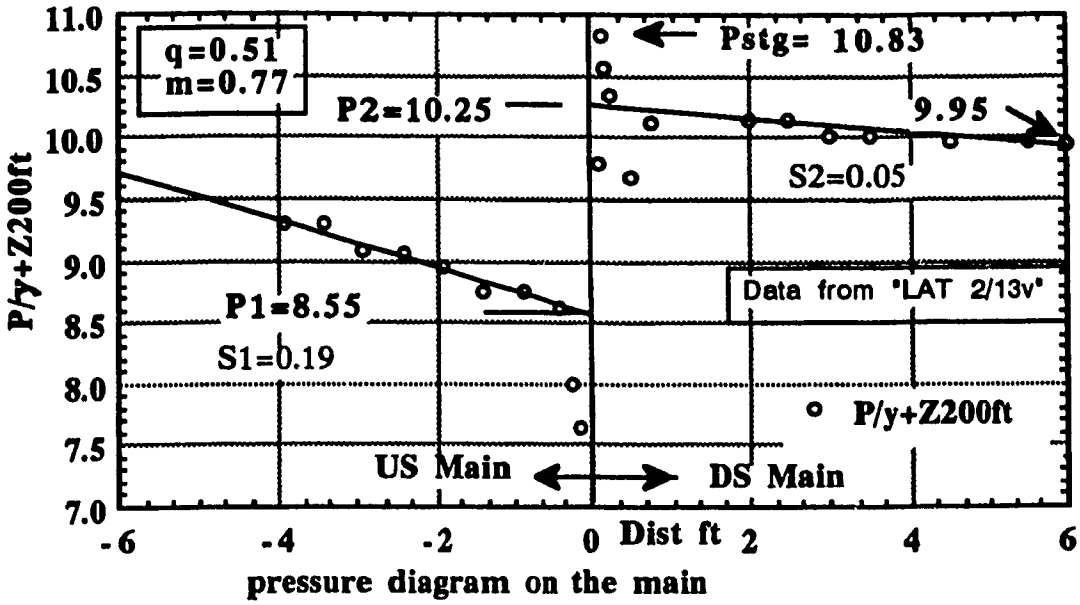

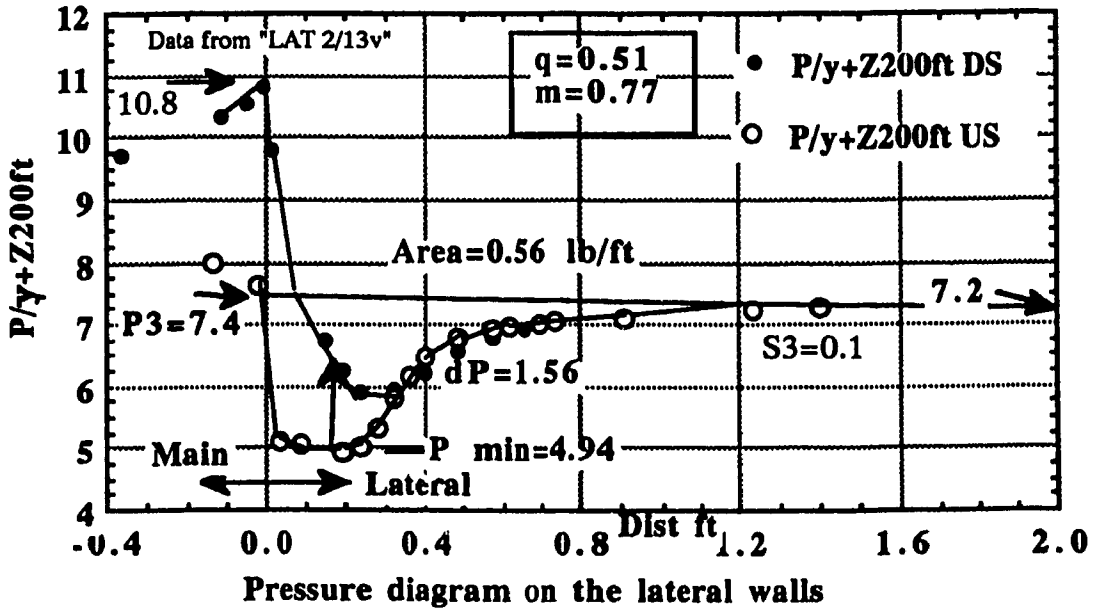

Fig.5.2(c): Pressure Diagrams on the Main and Lateral Conduits

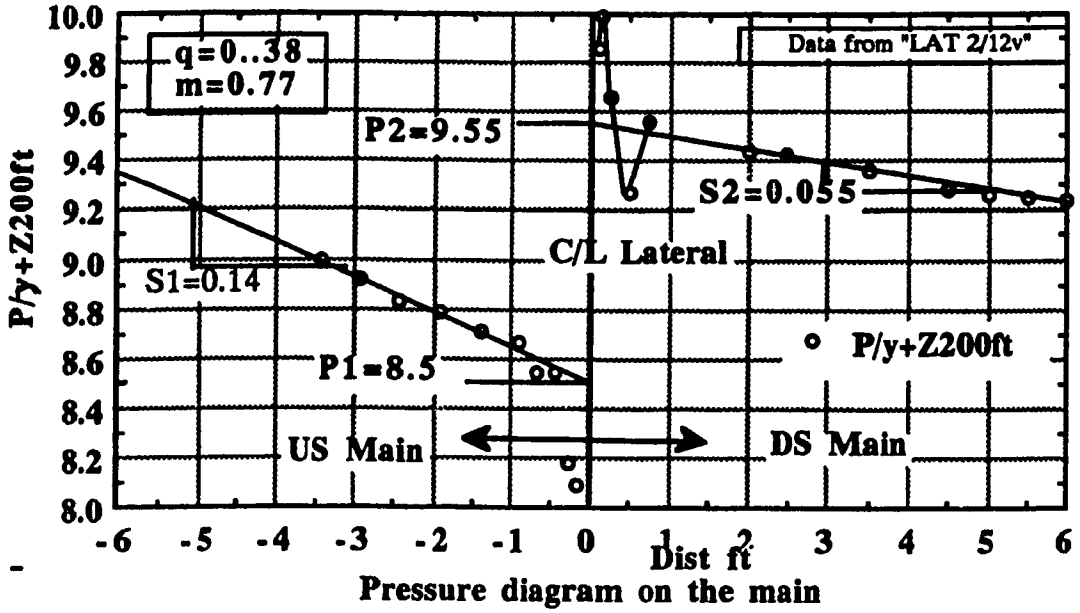

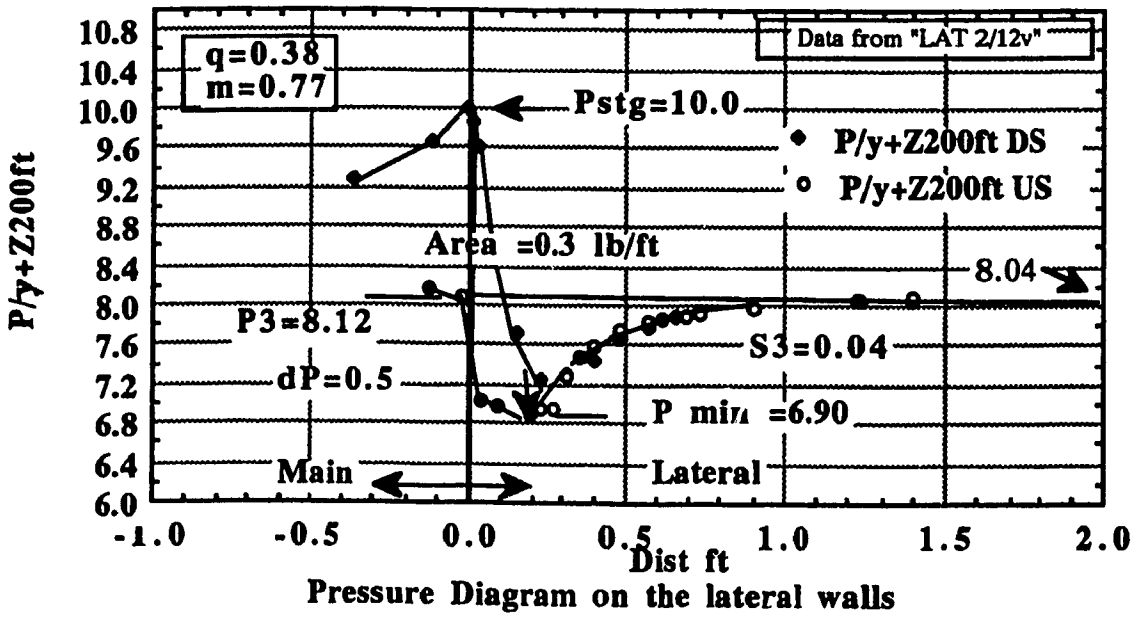

Fig.5.2(d): Pressure Diagrams on the Main and Lateral Conduits

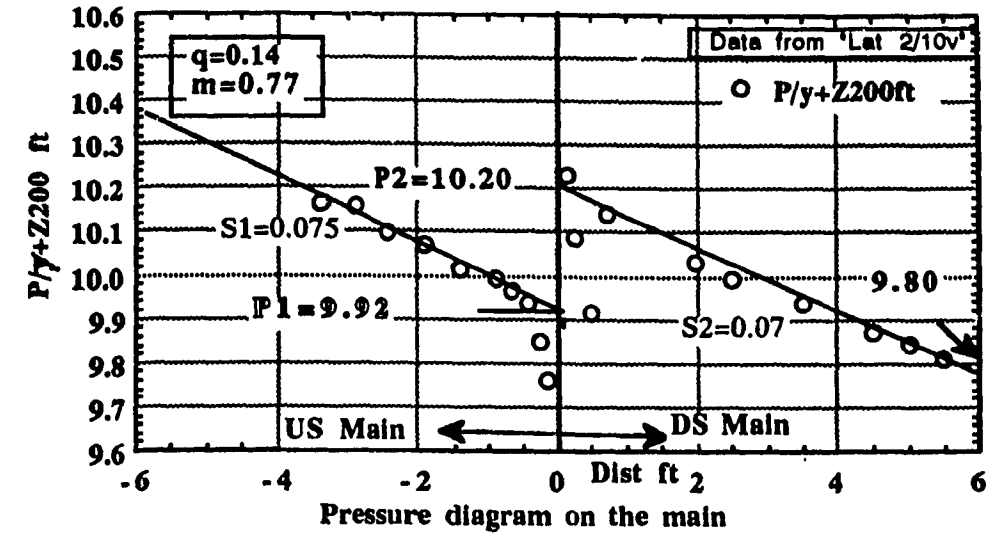

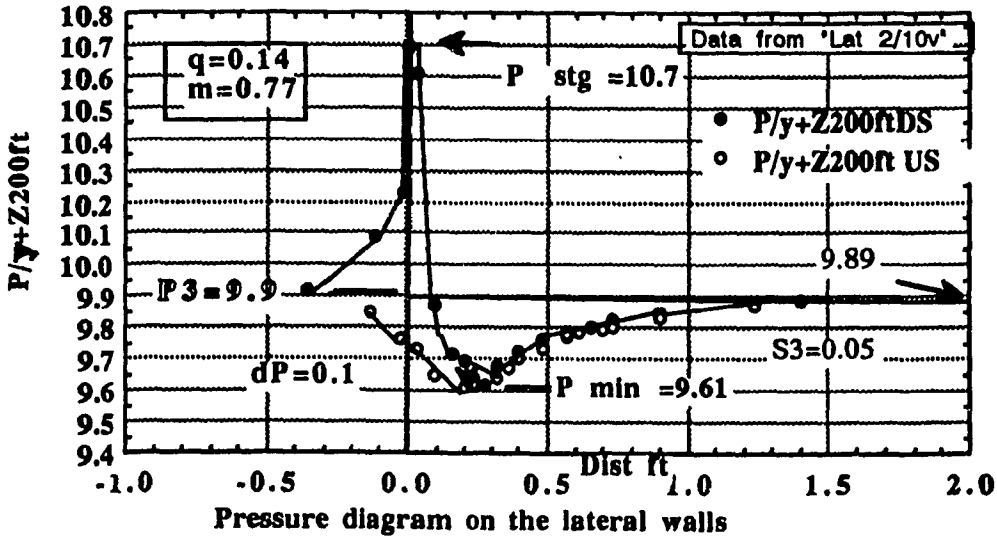

Fig.5.2(e): Pressure Diagrams on the Main and Lateral Conduits

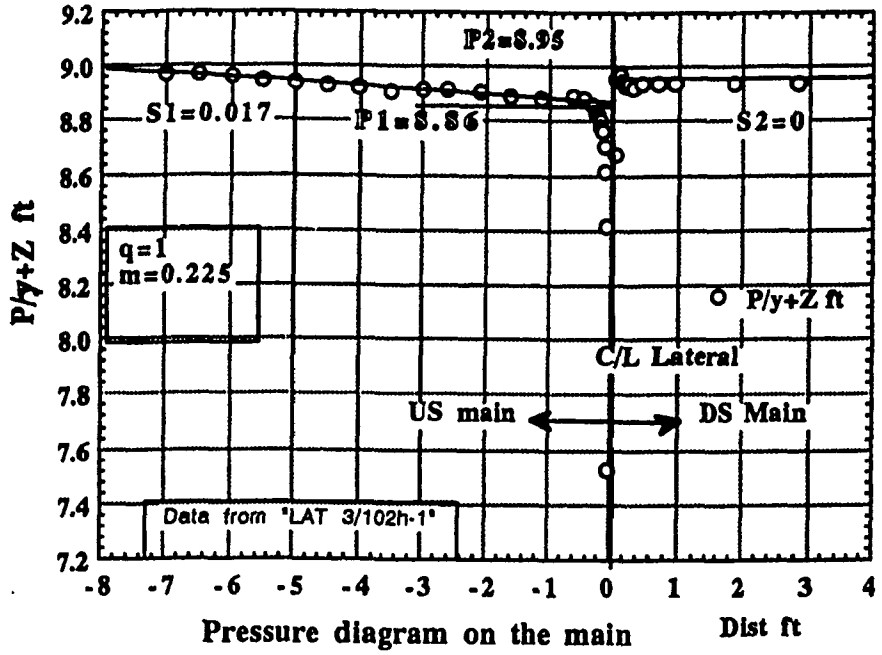

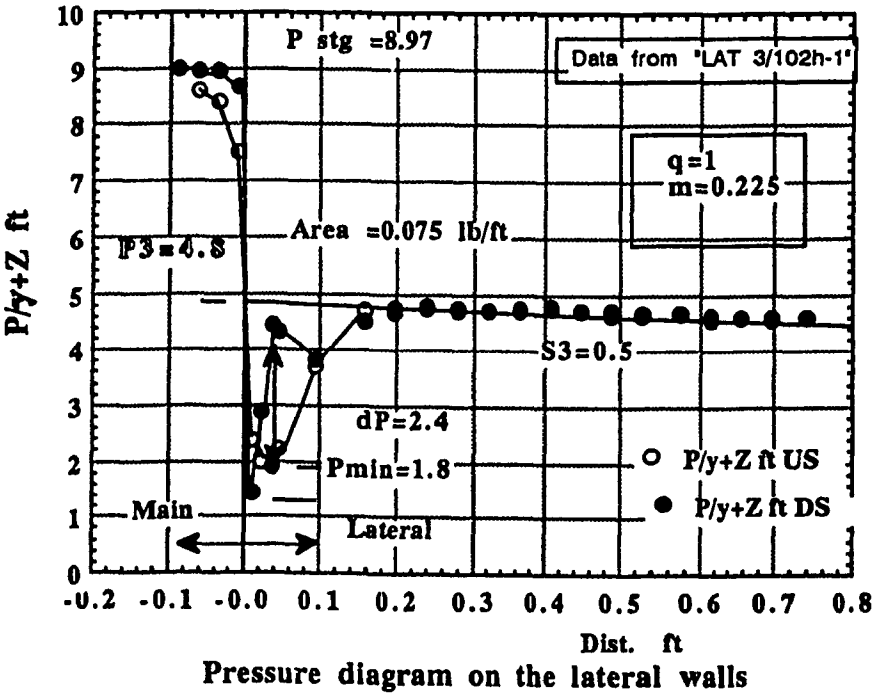

Fig.5.3(a): Pressure Diagrams on the Main and Lateral Conduits

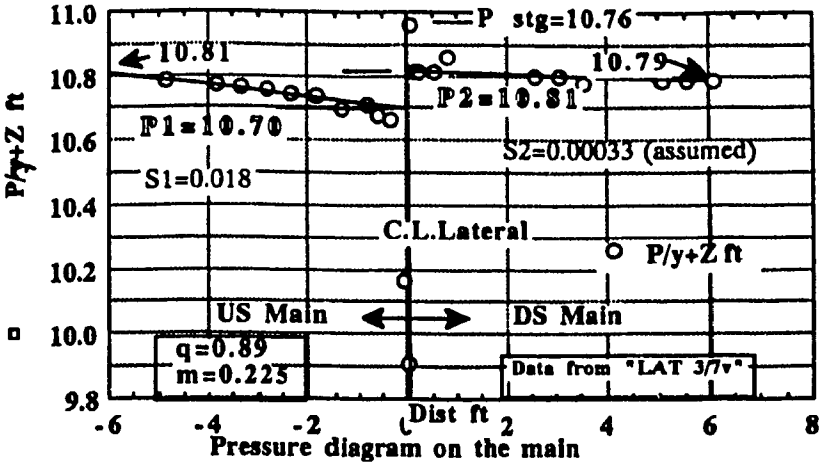

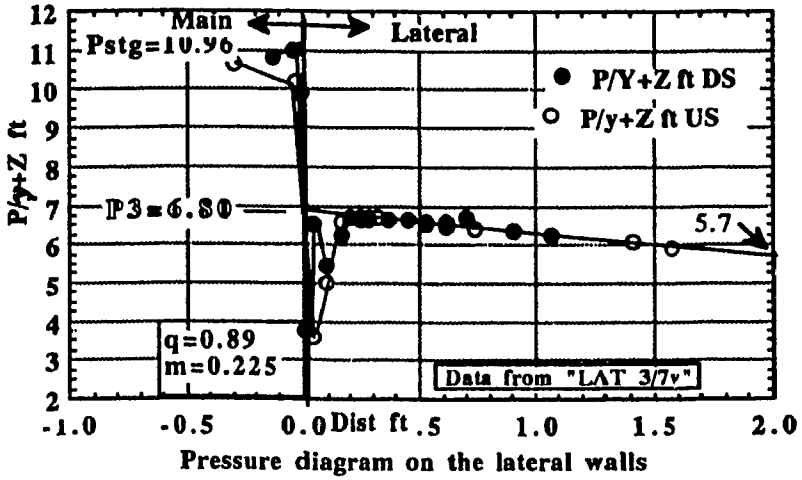

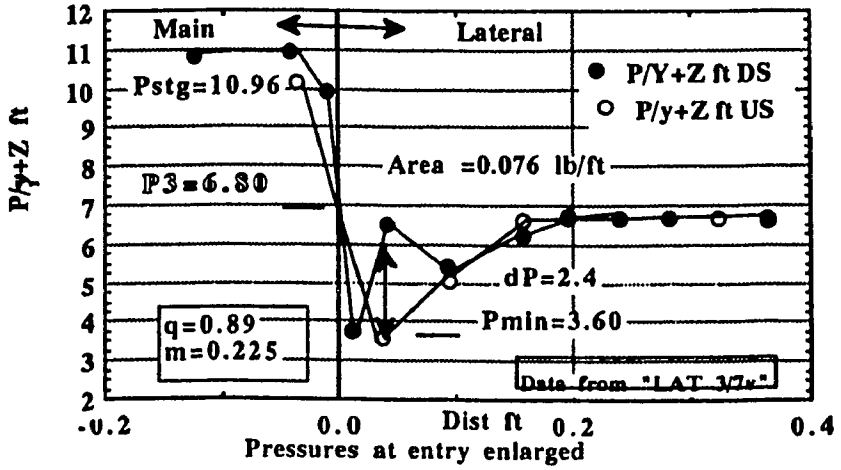

Fig.5.3(b): Pressure Diagrams on the Main and Lateral Conduits

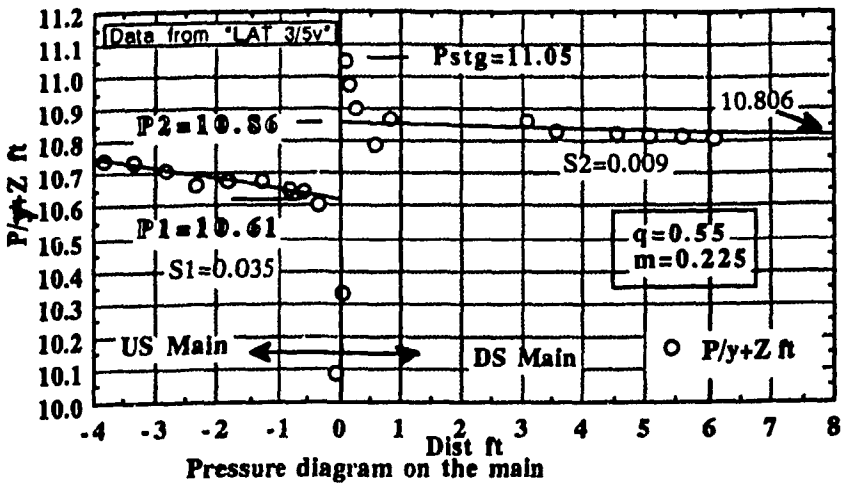

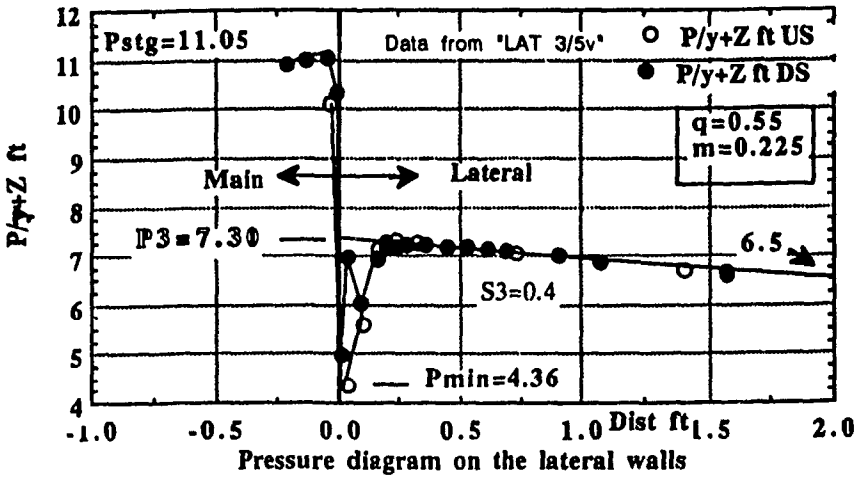

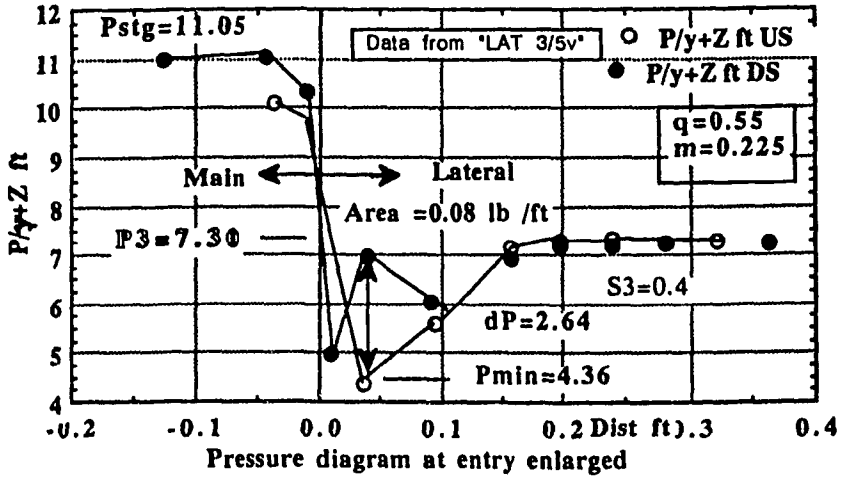

Fig.5.3(c): Pressure Diagrams on the Main and Lateral Conduits

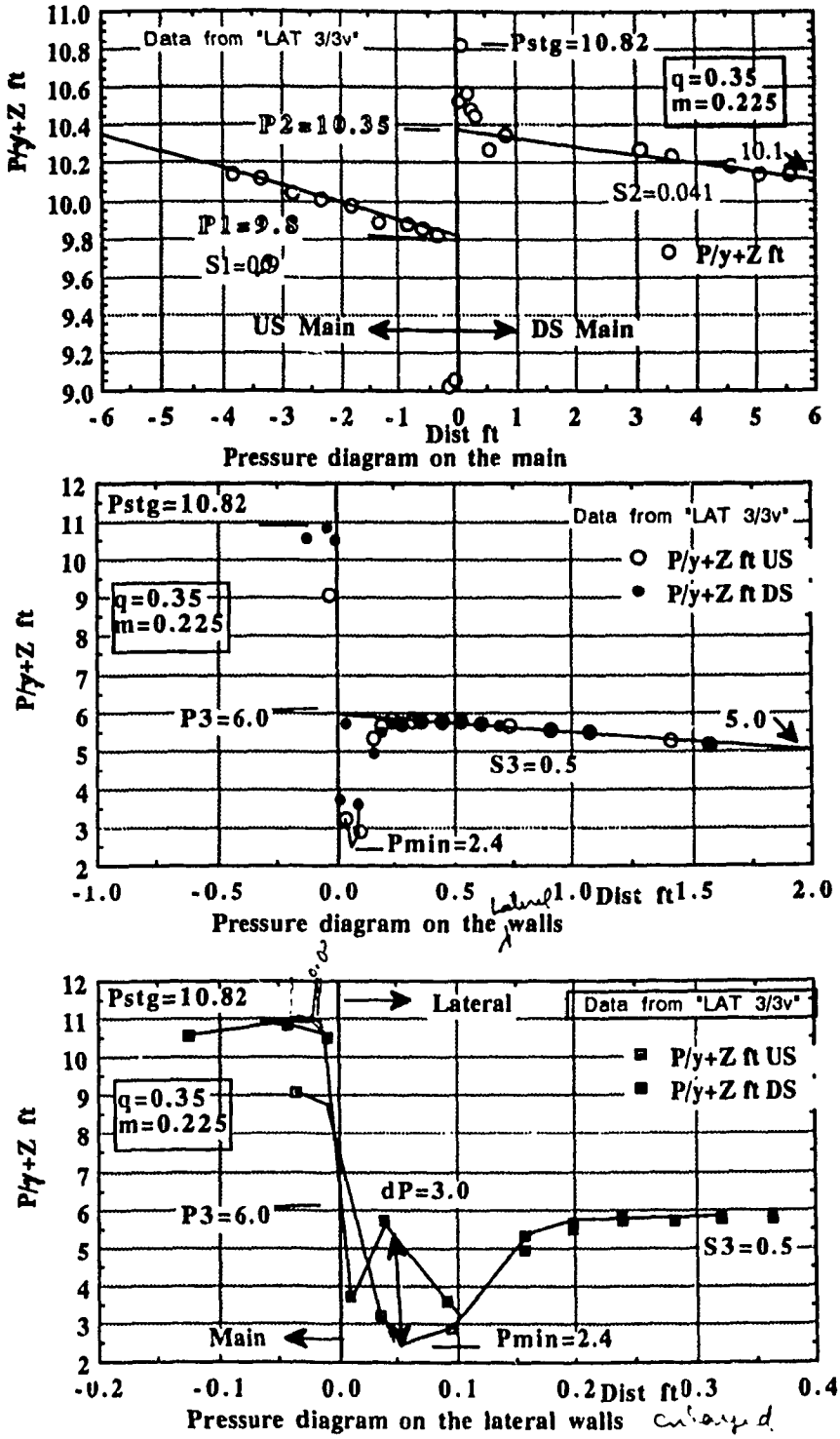

Fig.5.3(d): Pressure Diagrams on the Main and Lateral Conduits

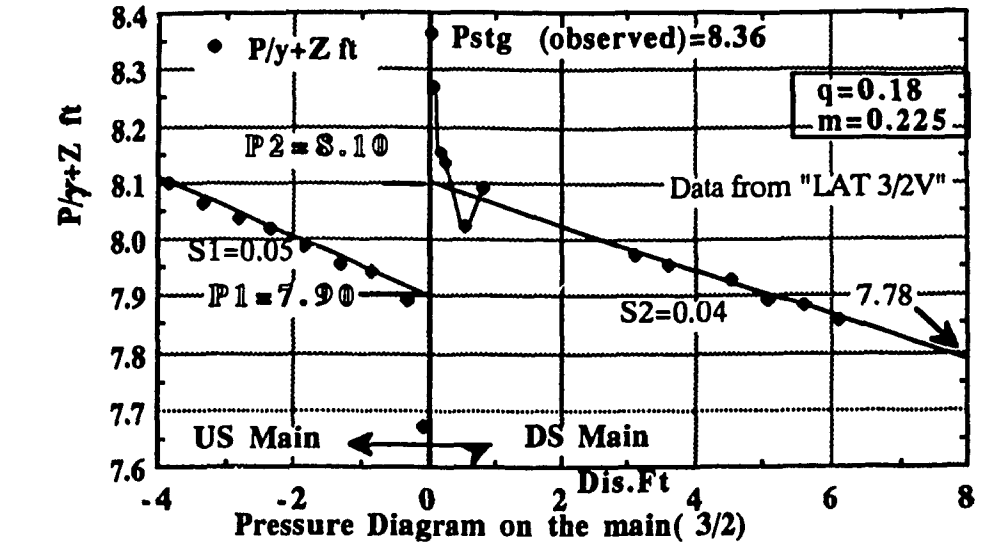

Pressure Diagram on the main(3/2)

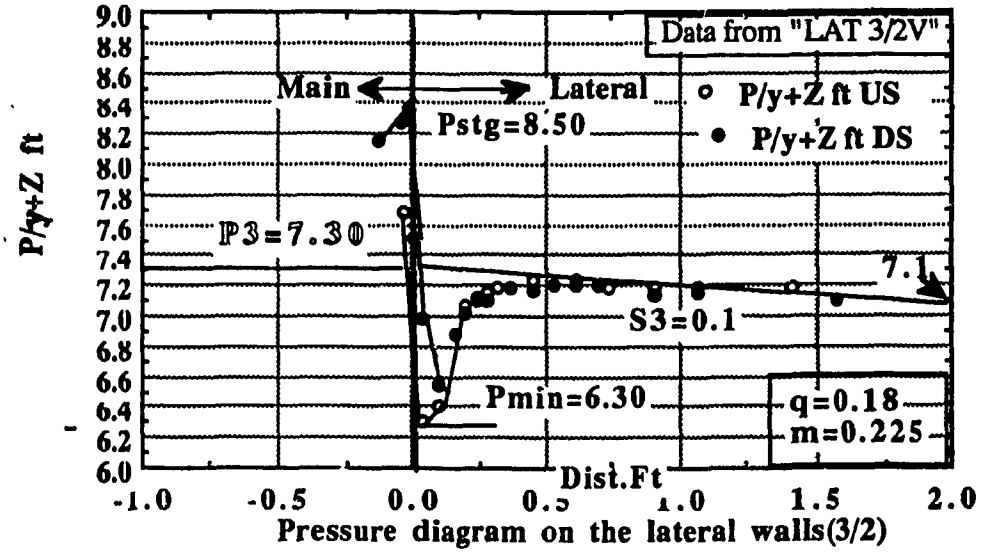

Pressure diagram on the lateral walls(3/2)

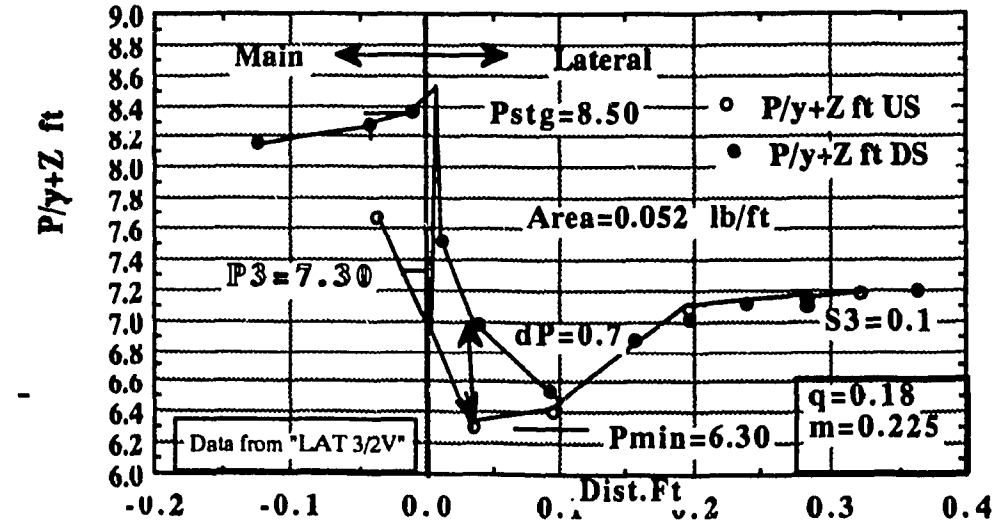

Fig.5.3(e): Pressure Diagrams on the Main and Lateral Conduits

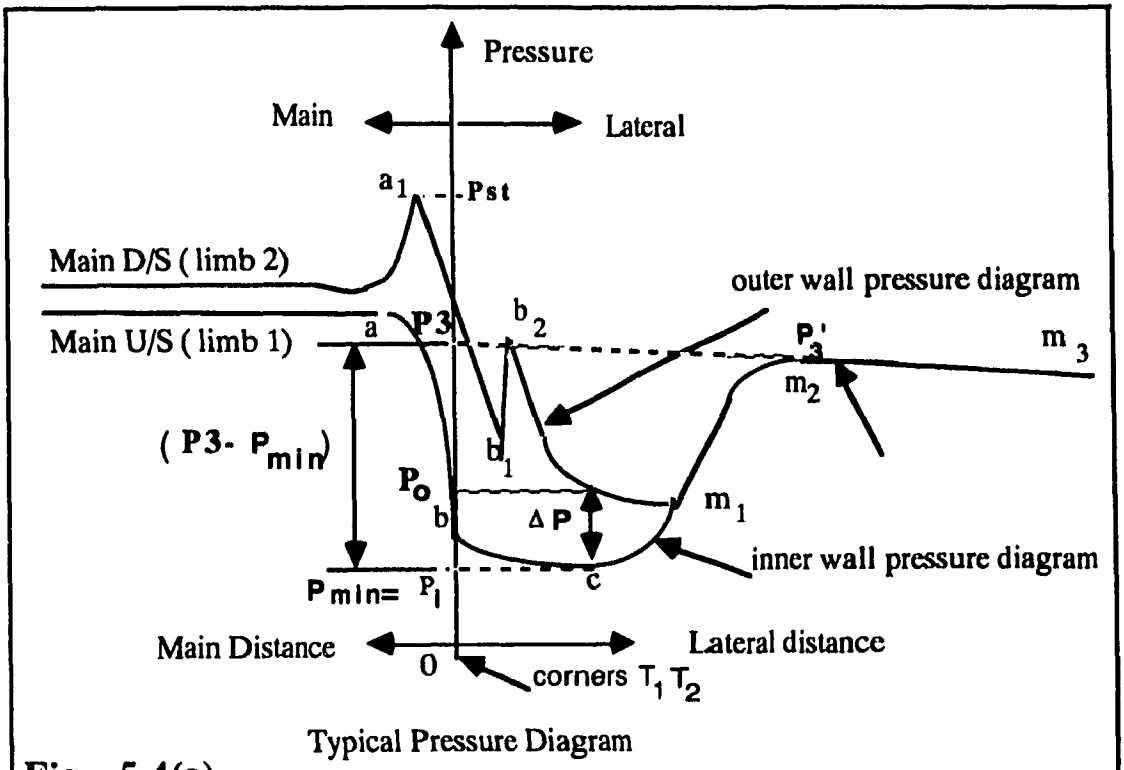

Typical Pressure Diagram

Fig. 5.4(a)

PRESSURE DIAGRAM (STAGNATION IN THE MAIN)

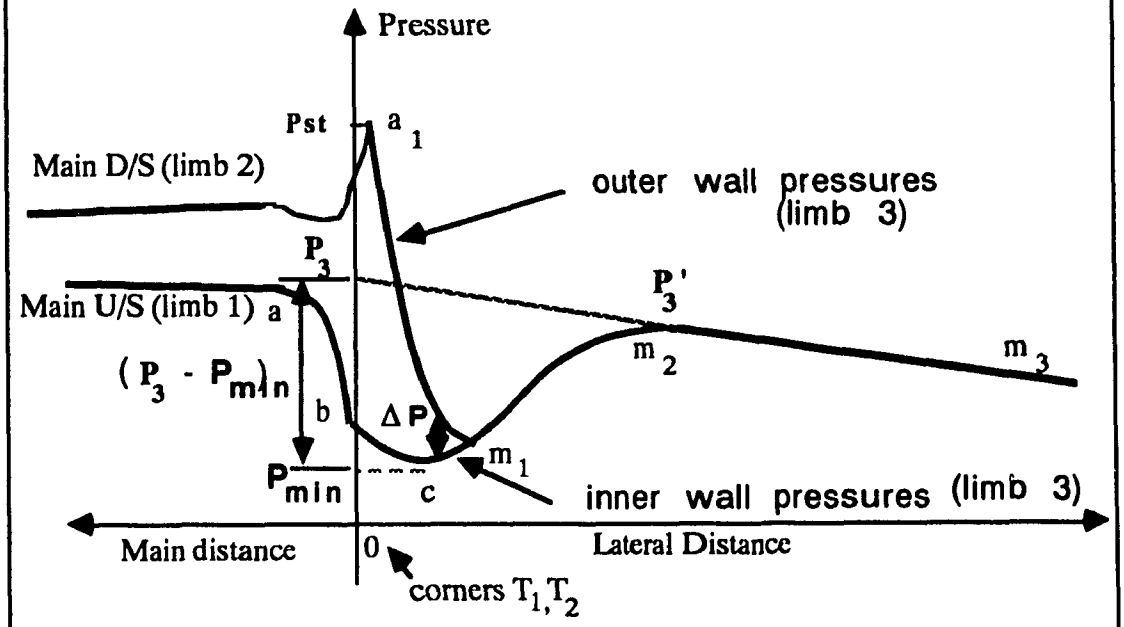

Fig:5.4(b)

PRESSURE DIAGRAM (STAGNATION IN THE LATERAL)

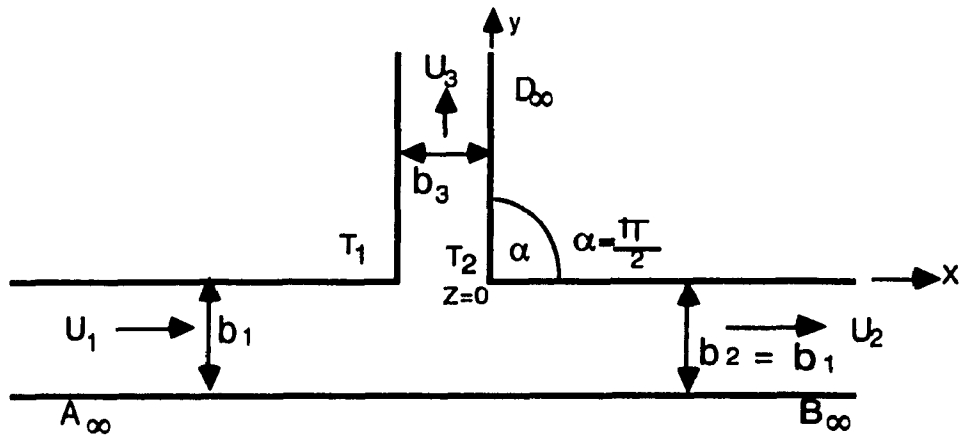

Physical Plane (z). (continuity eqn., $U_1 b_1 = U_2 b_2 + U_3 b_3$)

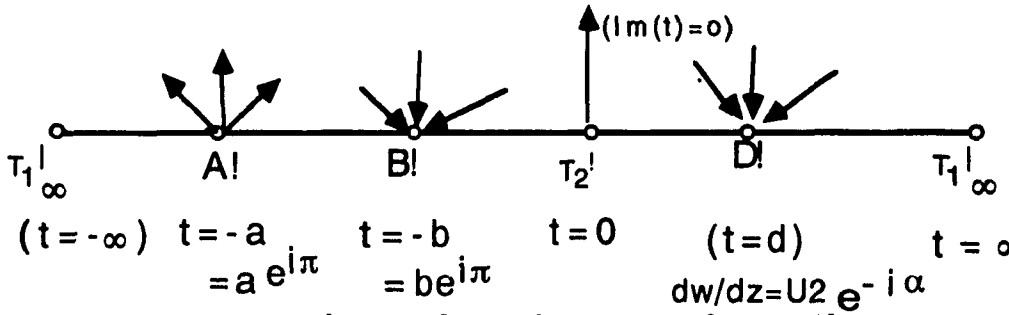

t plane for the transformation

For stagnation at t=0, $U_1 b_1 / a = U_2 b_2 / b - U_3 b_3 / d$

FIG.5.5

Dividing Flow (adapted from O'Neill &Chorlton 1986)

THE MAIN EQUATIONS FOR THE TRANSFORMATIONS.

(1) The complex potential (w) of the line source and line sinks is given by,

$$w = \{U_1 b_1 \ln(t+a) - U_2 b_2 \ln(t+b) - U_3 b_3 \ln(t-d)\}/\pi \qquad (1)$$

Differentiating with respect to t

$$\frac{dw}{dt} = \{U_1 b_1 (t+a)^{-1} - U_2 b_2 (t+b)^{-1} - U_3 b_3 (t-d)^{-1}\}/\pi \qquad (2)$$

(2) The Schwarz-Christoffell transformation, mapping the polygon $A_\infty B_\infty T_2 D_\infty T_1$ on to the real axis of the t-plane

$$\frac{dz}{dt} = k(t+a)^{-1}(t+b)^{-1}(t-0)^{1-(\alpha/\pi)}(t-d)^{-1} \qquad (3)$$

(Angles of the pentagon are, 0 at A_∞, 0 at B_∞, 0at D_∞, $2\pi - \alpha$ at T_2 and $\pi + \alpha$ at T_1)

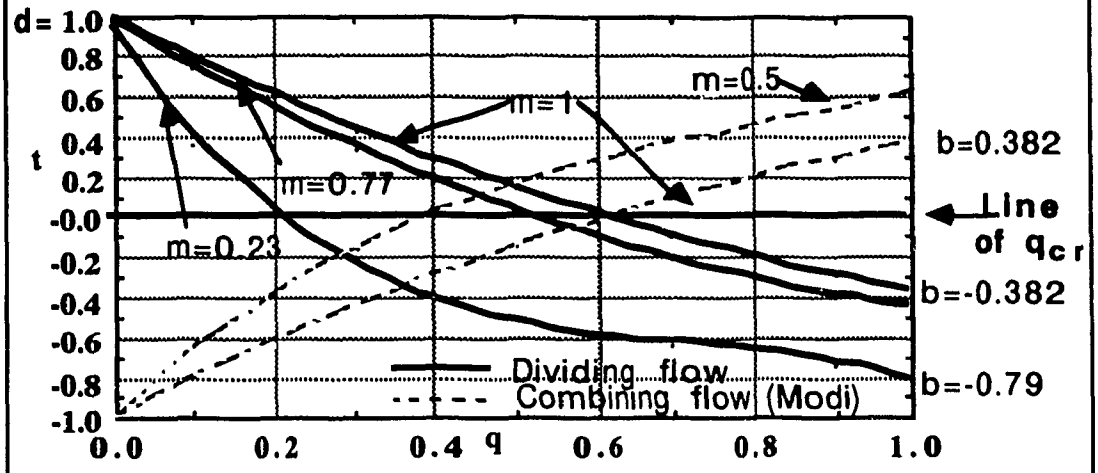

Fig: 5. 6(a): Stagnation t(in t plane) Vs Discharge ratio q for different m ratios (=b3/b1)

(Adapted from Ref.O'Neill &Chorlton)

See also Fig.5.6b for corresponding physical plane. representation.

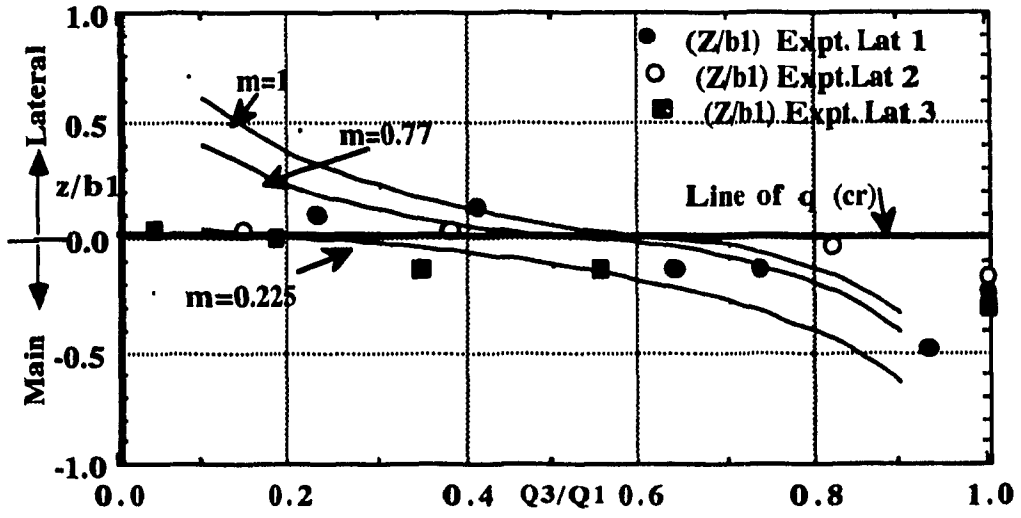

Fig.5.6(b): Stagnation dist. ratio Z/b1 Vs Discharge ratio Q3/Q1

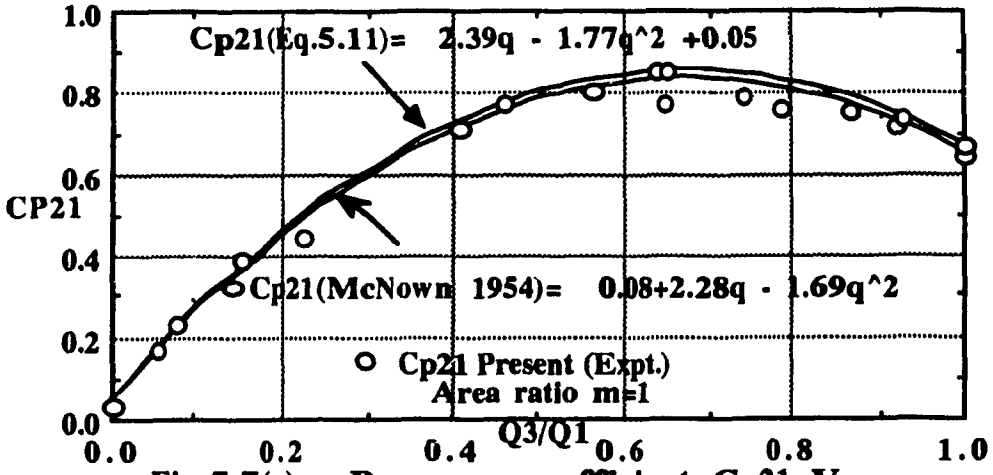

Fig.5.7(a): Pressure coefficient Cp21 Vs q for m=1 (Lateral 1)

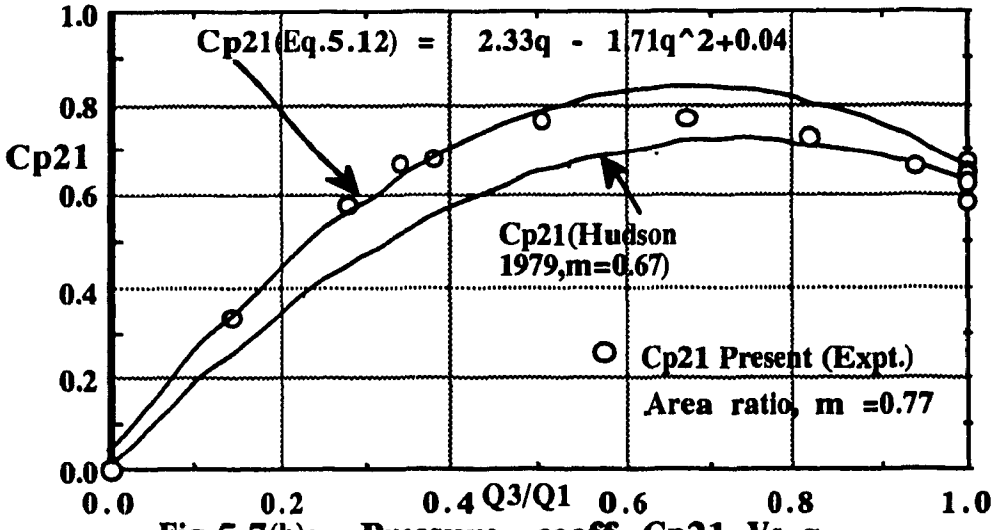

Fig.5.7(b): Pressure coeff. Cp21 Vs q for m=0.77 (Lateral 2)

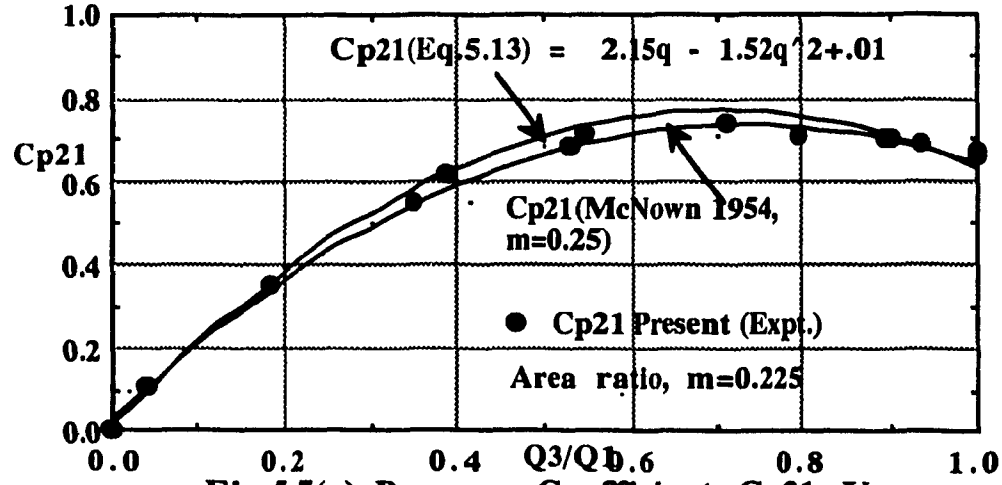

Fig.5.7(c):Pressure Coefficient Cp21 Vs q for m=0.225 (Lateral 3)

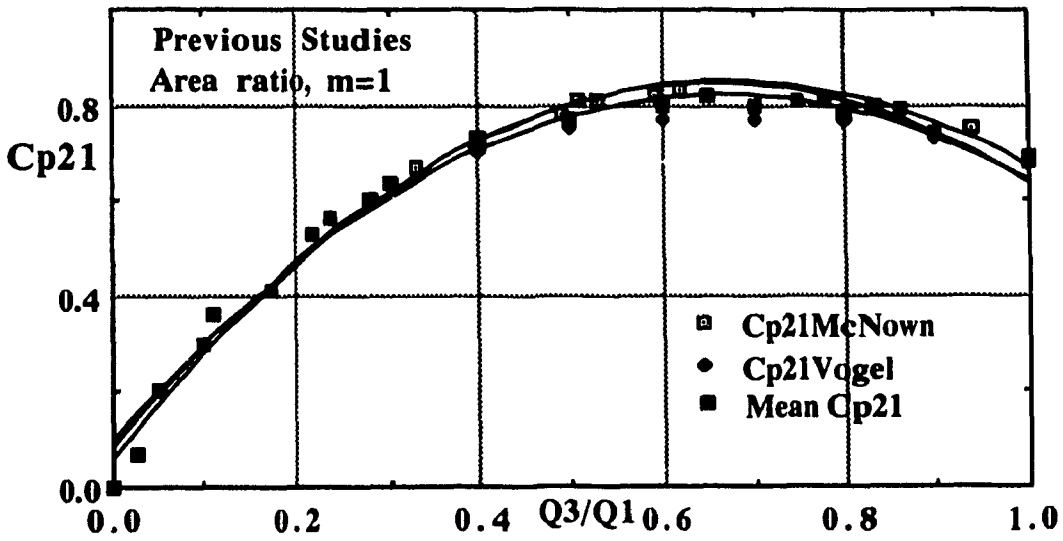

Fig.5.7(d): Cp21 Vs q for m=1 (Previous studies)

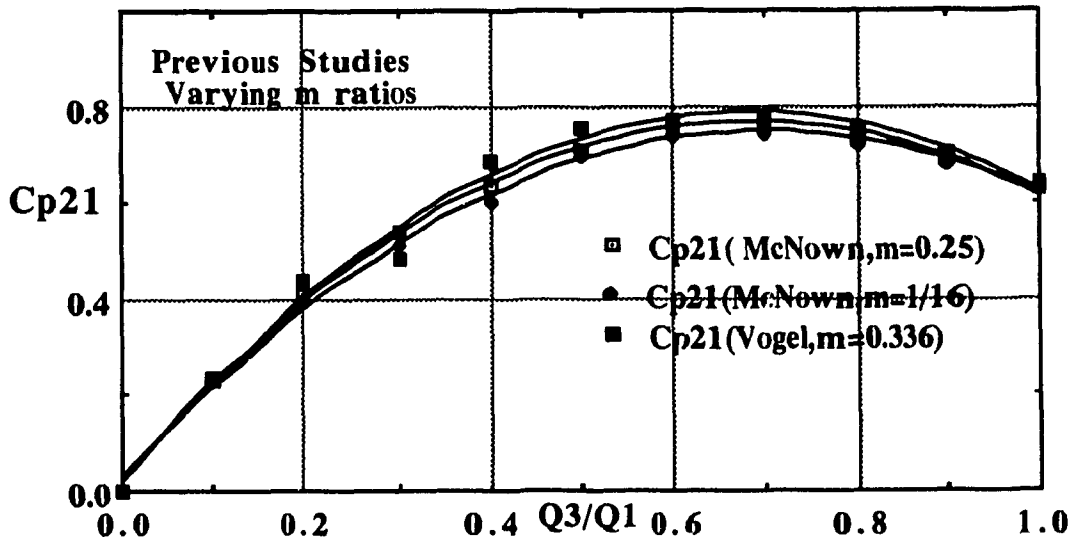

Fig.5.7(e): Cp21 vs q for different m ratios (Previous Studies)

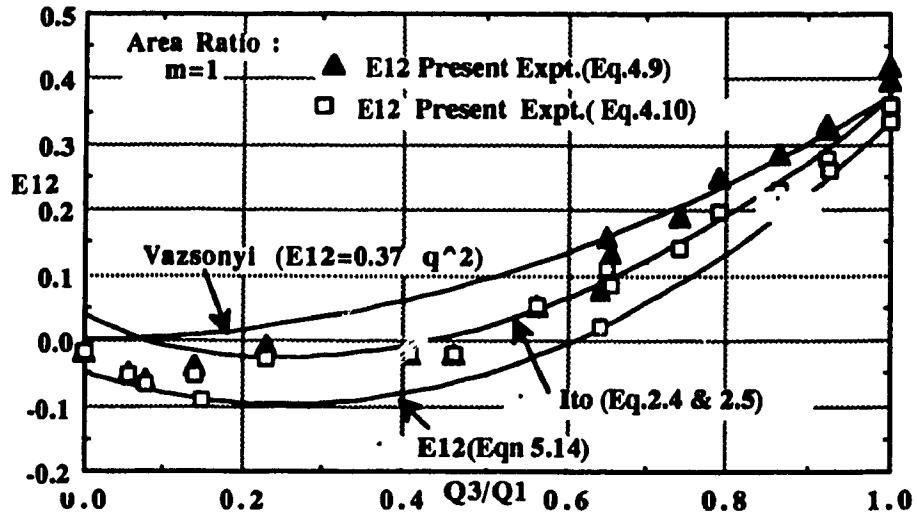

Fig.5.8(a):Loss coefficient E12 Vs q for m=1 (Lateral 1)

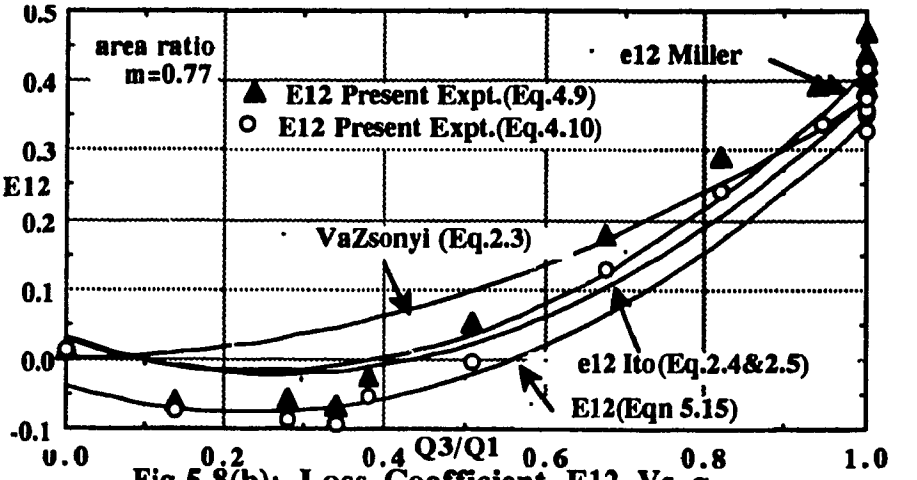

Fig.5.8(b): Loss Coefficient E12 Vs q for m=0.77 (Lateral 2)

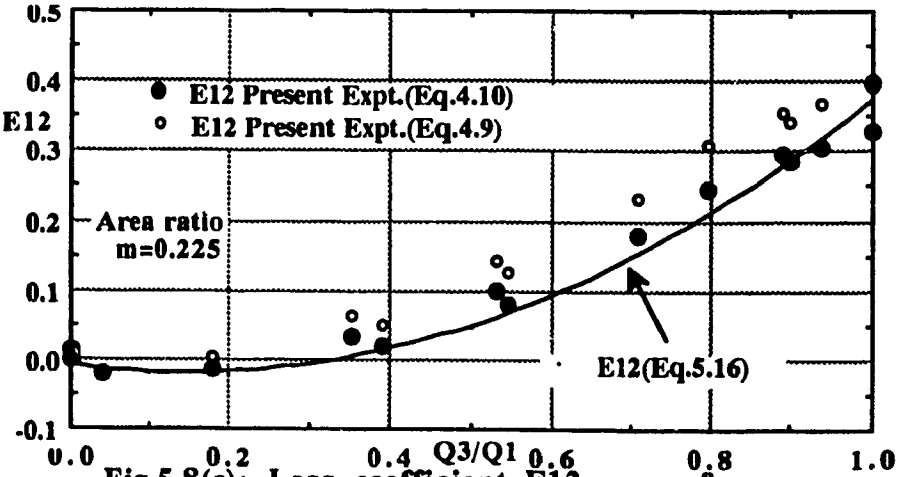

Fig.5.8(c): Loss coefficient E12 vs q for m=0.225 (Lateral 3)

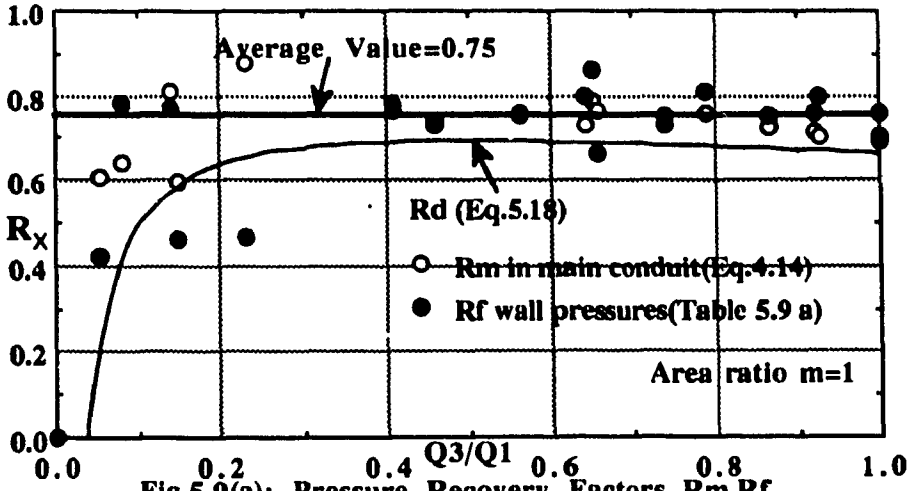

Fig.5.9(a): Pressure Recovery Factors Rm,Rf Vs Discharge ratio q for m=1

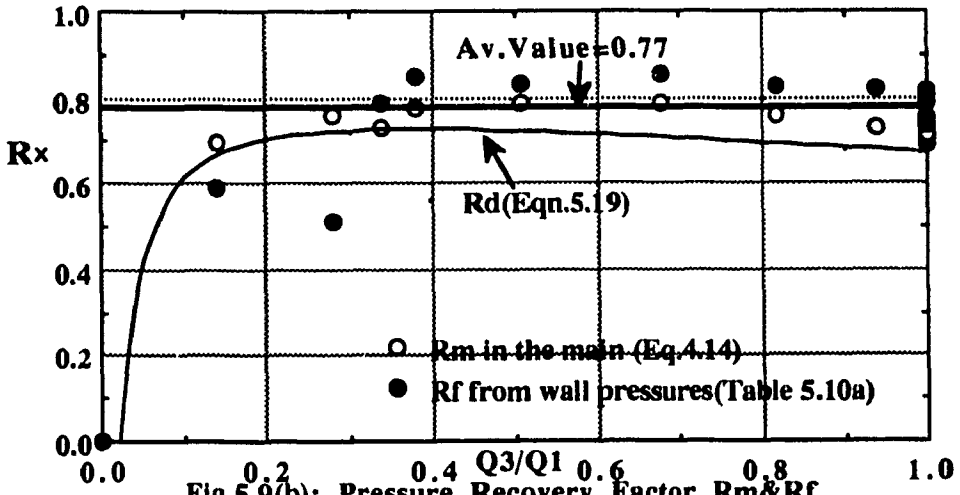

Fig.5.9(b): Pressure Recovery Factor Rm&Rf Vs Discharge ratio q for m=0.77

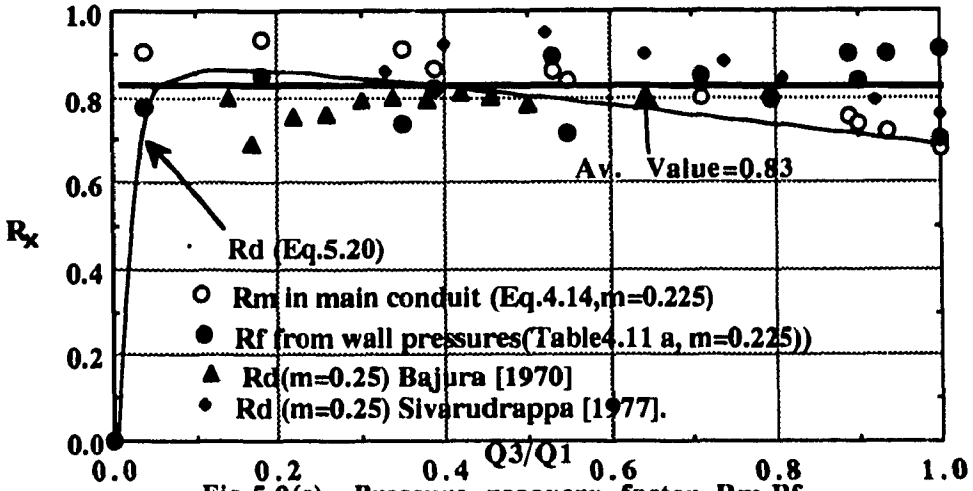

Fig.5.9(c): Pressure recovery factor Rm,Rf Vs Discharge ratio q for m=0.225

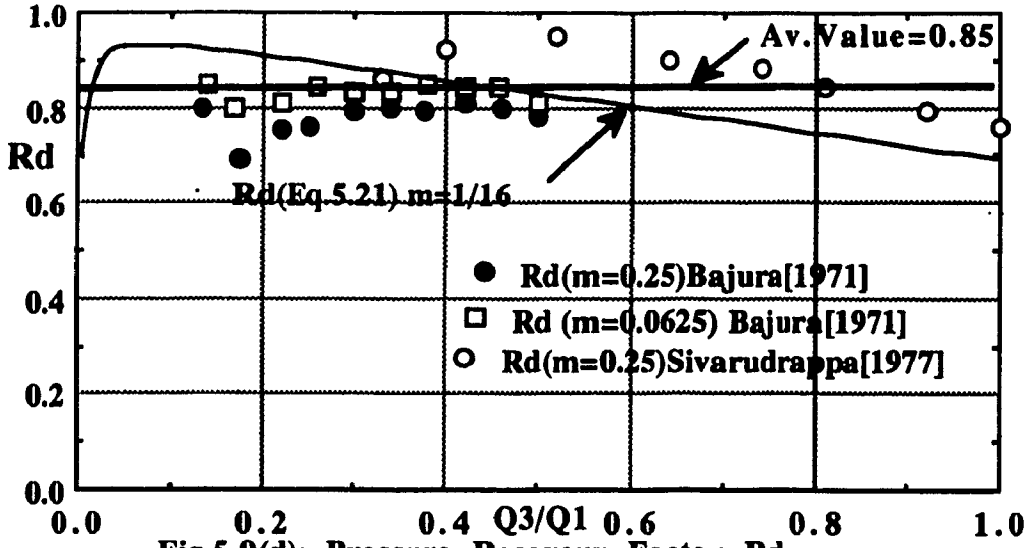

Fig.5.9(d): Pressure Recovery Factor Rd vs Discharge ratio q by previous tests.

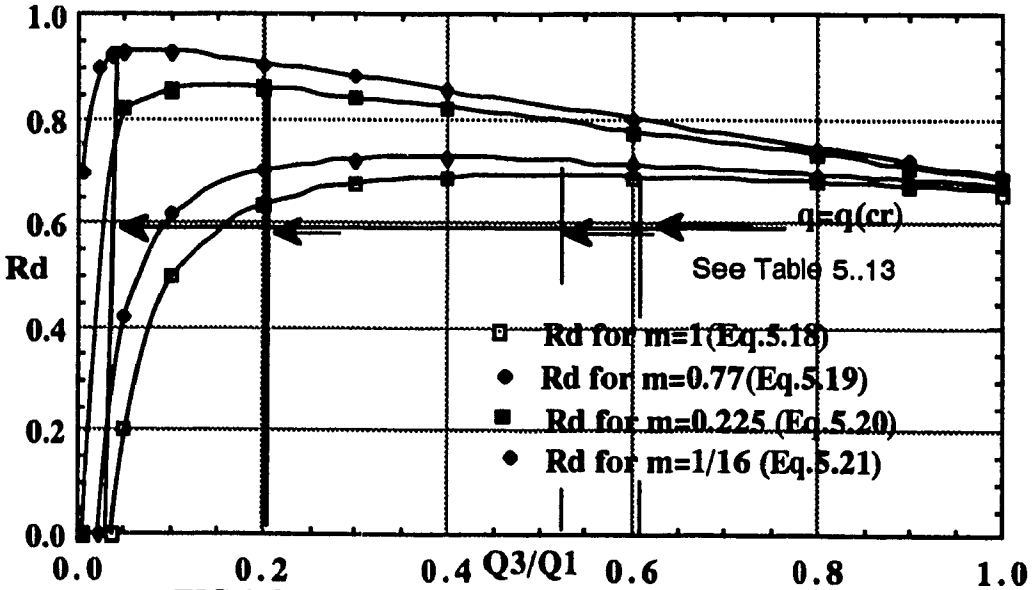

FIG.5.9(e): Pressure Recovery Factor Rd vs Discharge ratio q from Eq.(5.18 to5.21)

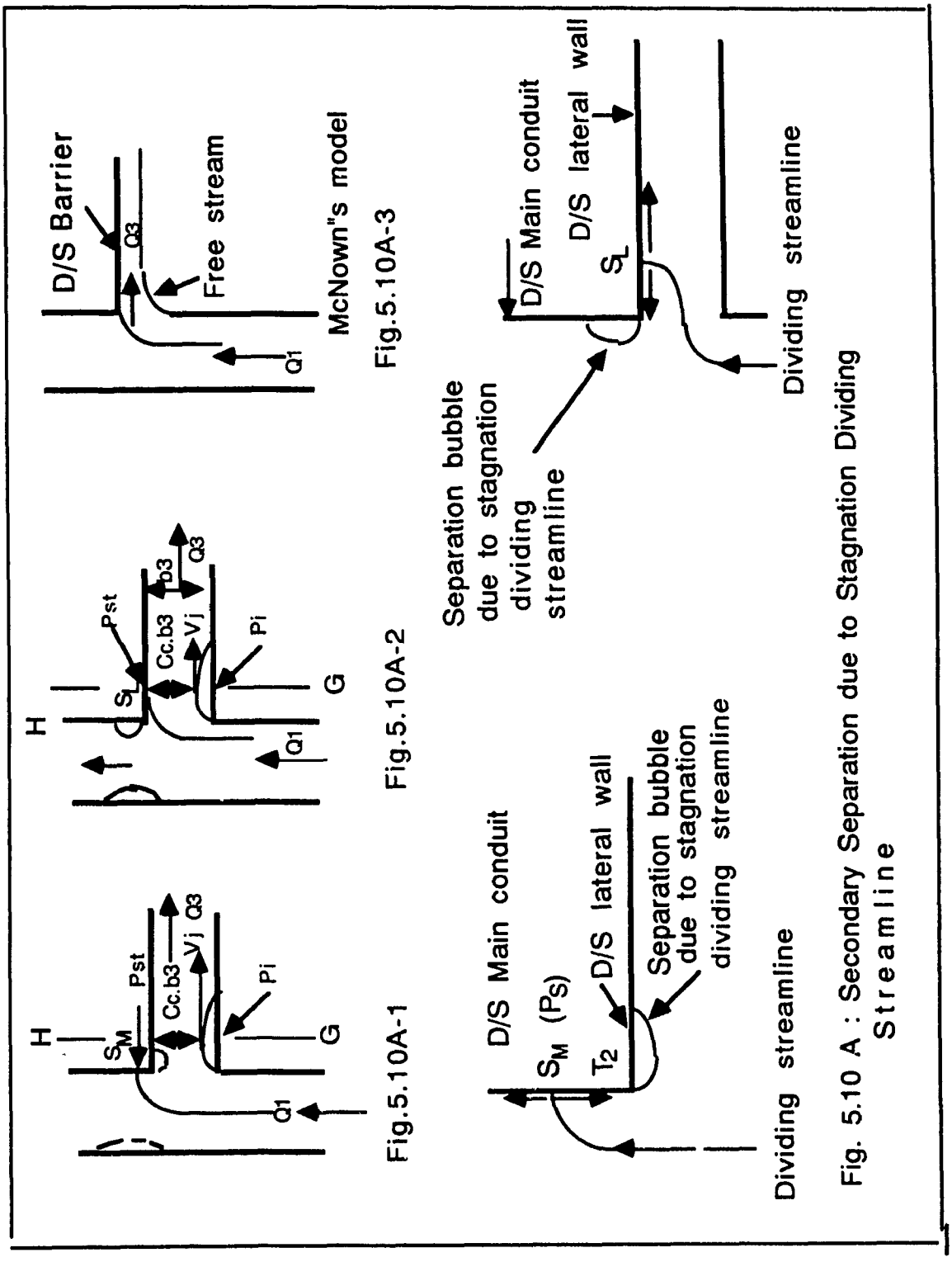

Fig. 5.10 A : Secondary Separation due to Stagnation Dividing Streamline

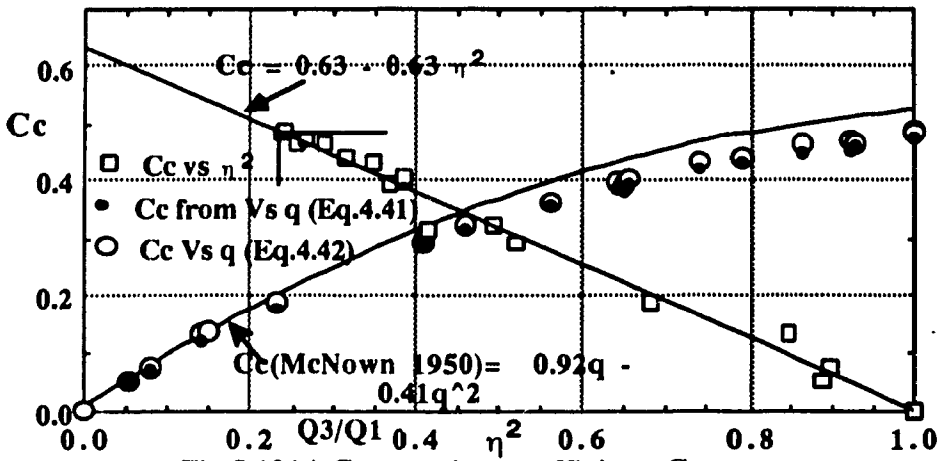

Fig.5.10(a):Contraction coefficient Cc vs q and Cc vsη^2 for m=1(Lateral 1)

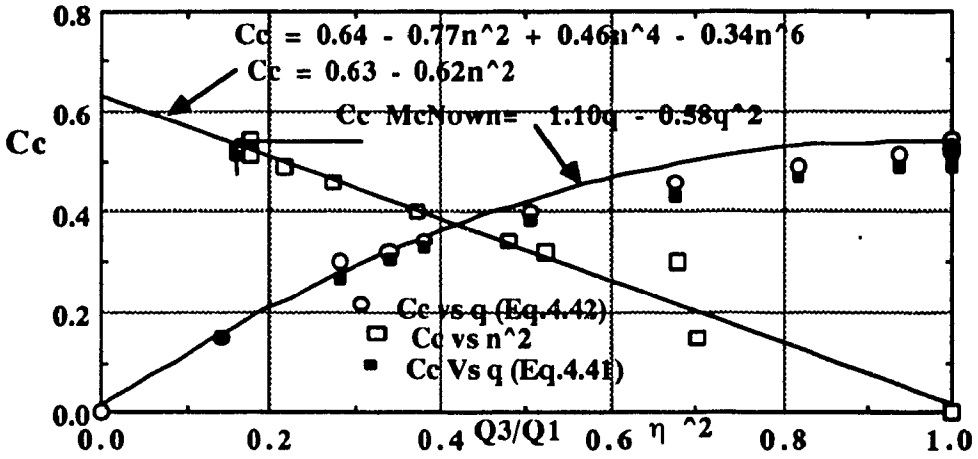

Fig.5.10(b):Contraction Coefficient Cc vs q and Cc Vs n^2 for m=0.77 (Lateral 2)

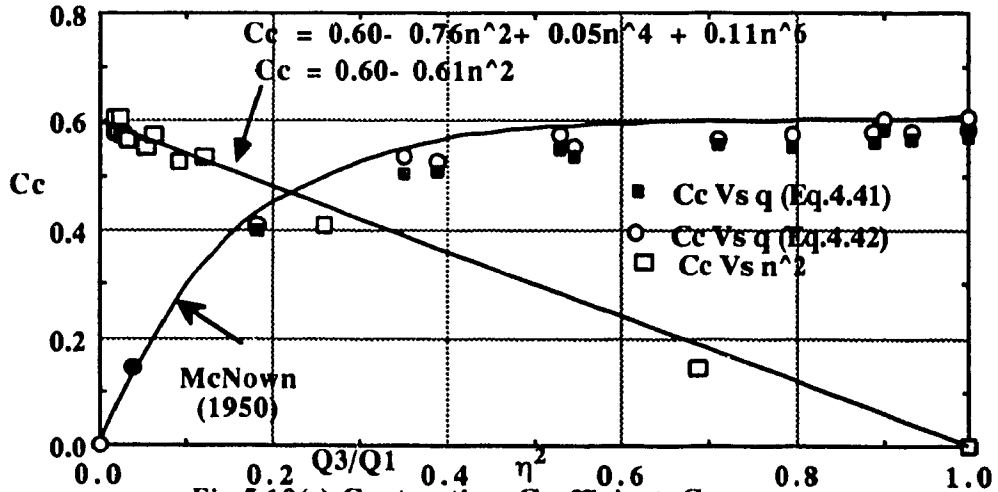

Fig.5.10(c):Contraction Coefficient Cc vs q and Cc Vsη^2 for m=0.225 (Lateral3)

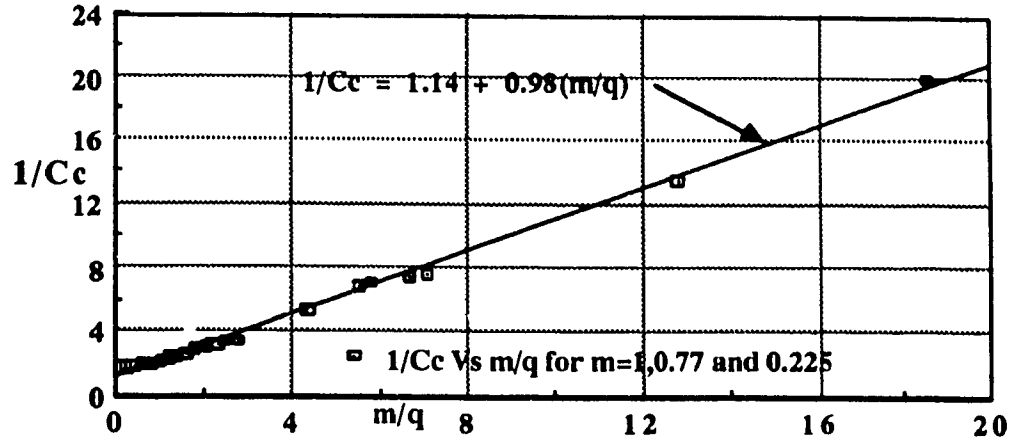

Fig.5.11.(a): 1/Cc Vs (q/m) for all laterals

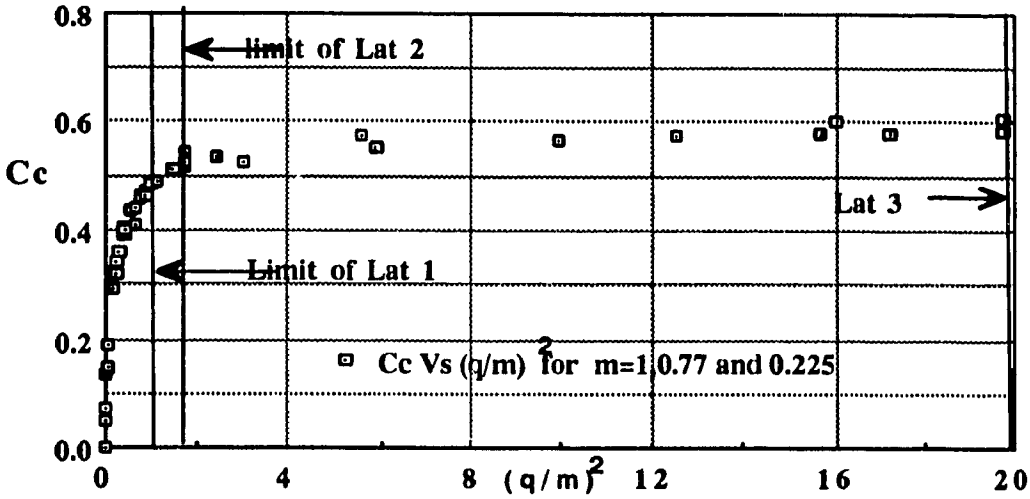

Fig.5.11(b): Cc vs $(q/m)^2$ for all laterals

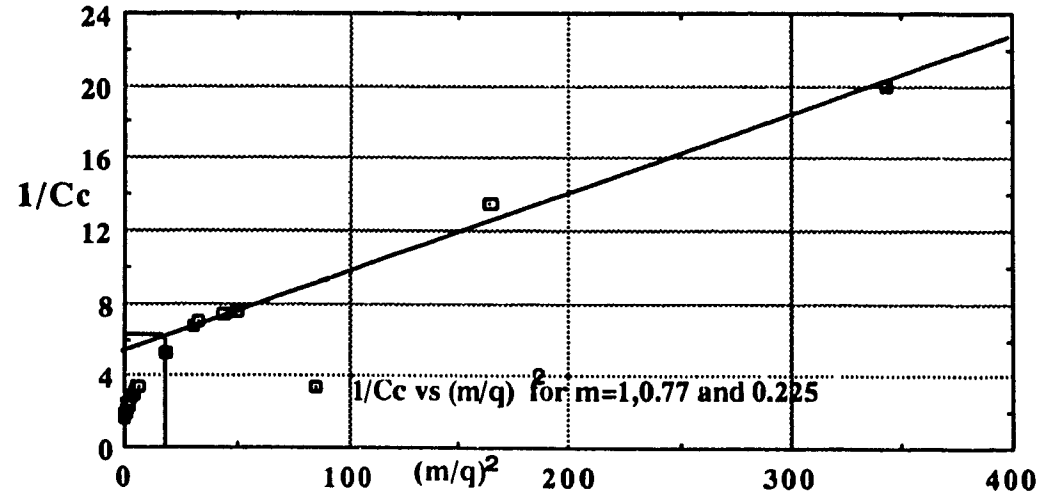

Fig.5.11(c): 1/Cc Vs $(m/q)^2$ For All Laterals

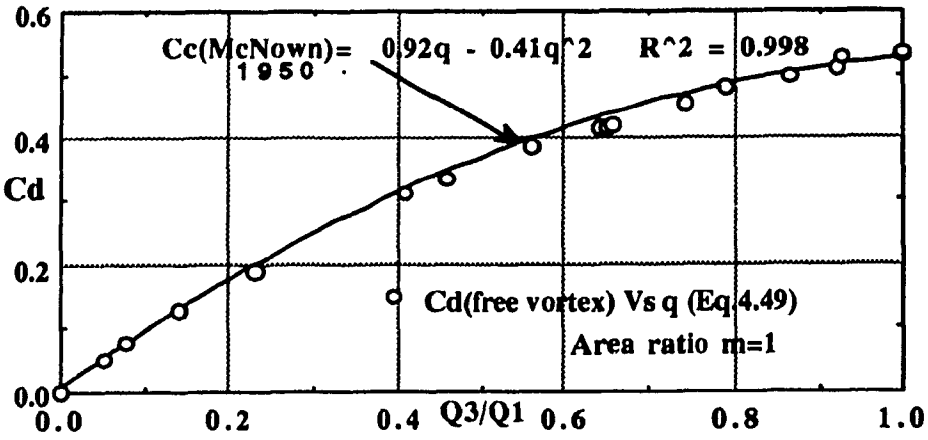

Fig.5.12(a): Contraction Coeff. Cd Vs q by free vortex theory for m=1 (Lat 1)

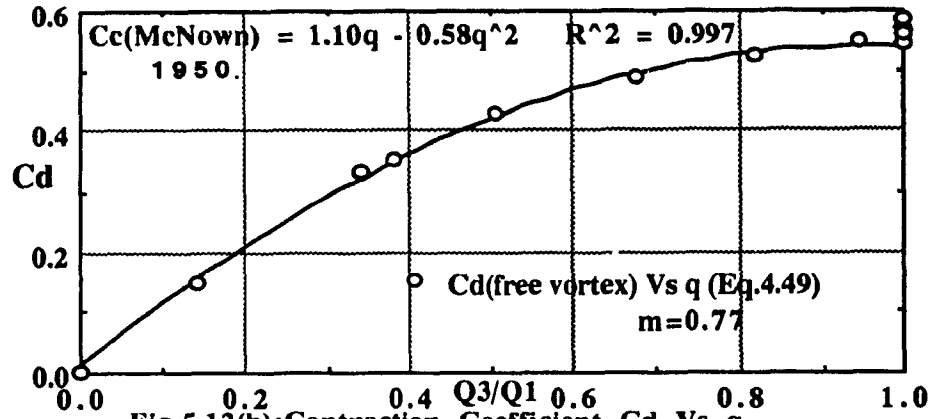

Fig.5.12(b):Contraction Coefficient Cd Vs q by free vortex for m=0.77 (Lateral 2)

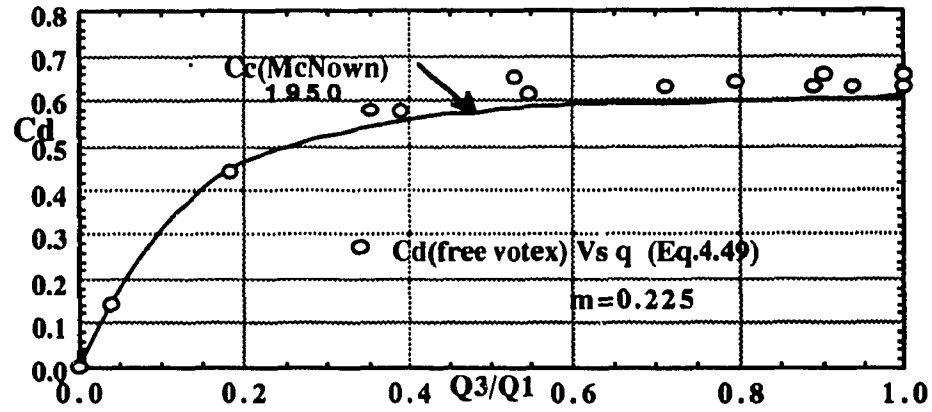

Fig.5.12(c):Contraction Coefficient Cd Vs q by free vortex theory for m=0.225

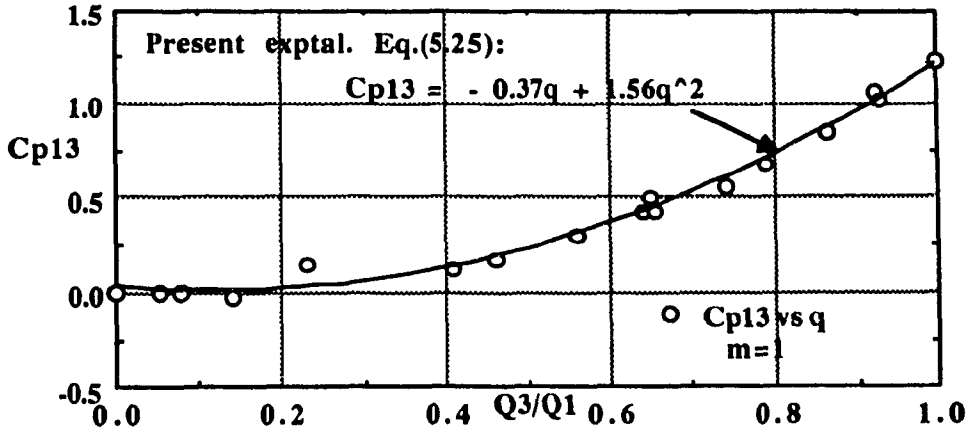

Fig.5.13(a): Pressure Coefficient Cp13 Vs Discharge ratio q for m=1(Lateral 1)

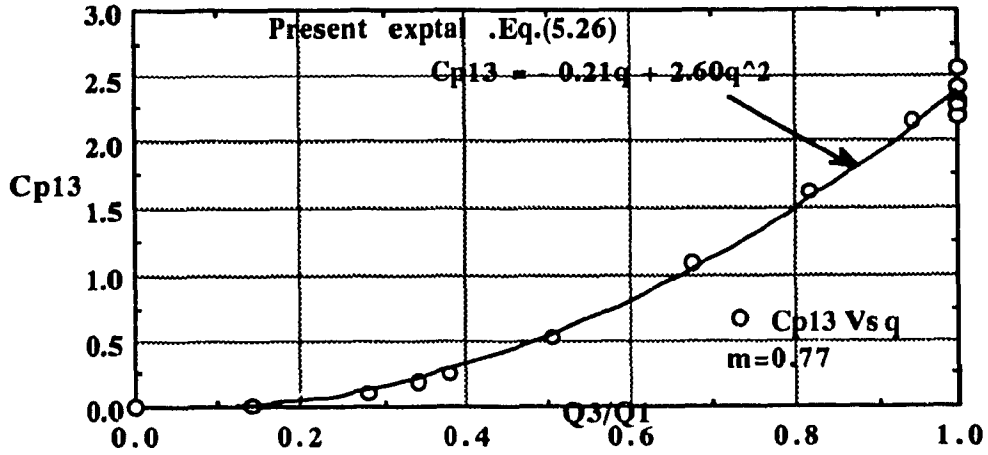

Fig.5.13(b): Pressure Coefficient Cp13 Vs Discharge ratio q for m=0.77(Lateral 2)

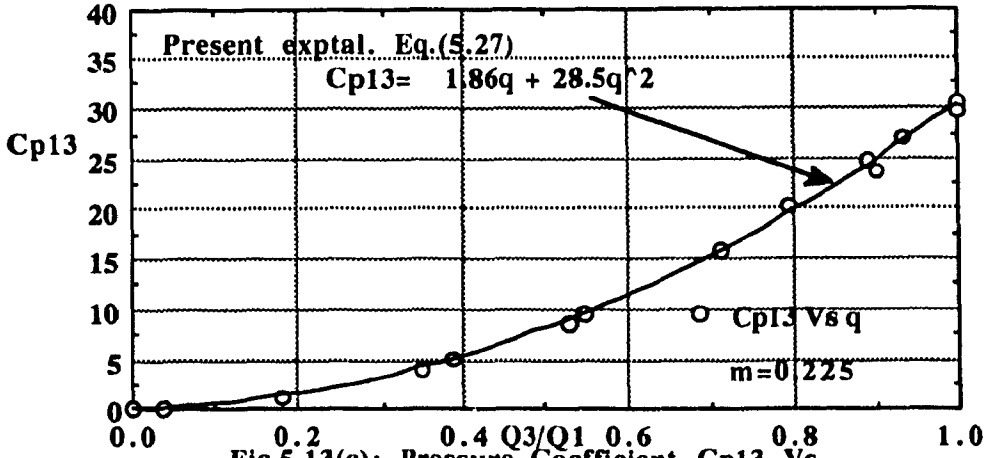

Fig.5.13(c): Pressure Coefficient Cp13 Vs Discharge ratio q for m=0.225 Lateral 3

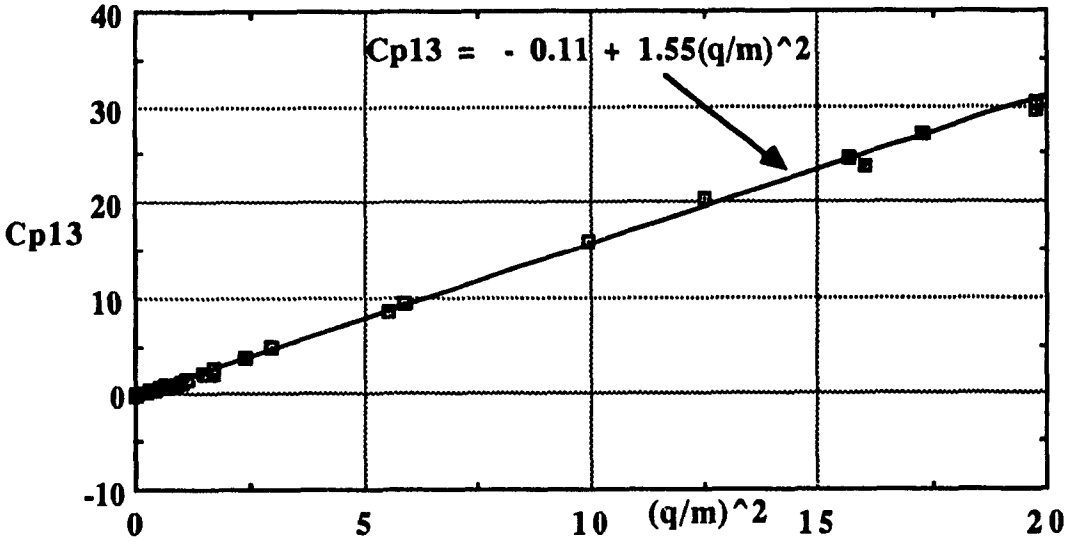

Fig.5.13(d): Pressure Coefficient Cp13 Vs (q/m)^2 for the threeLaterals.

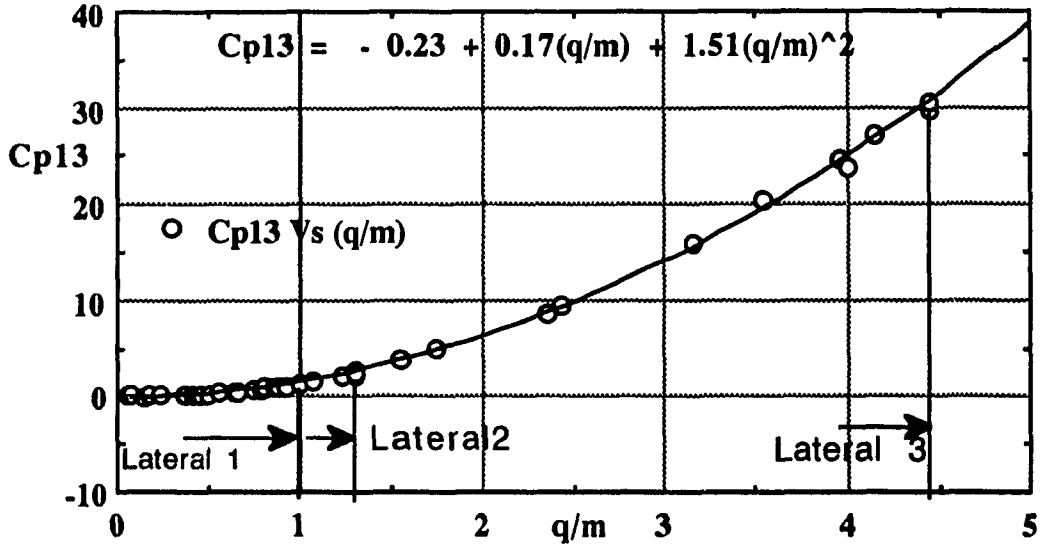

Fig.5.13(e): Pressure Coefficient Cp13 Vs (q/m) for the three laterals

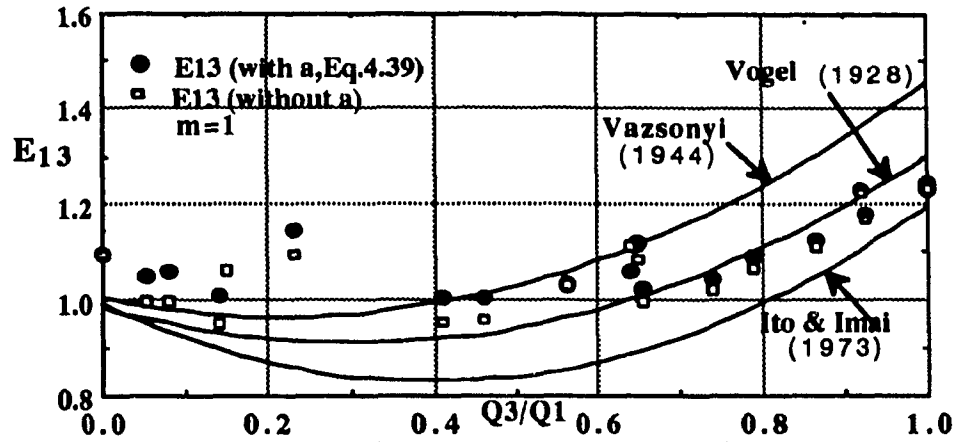

Fig. 5.14(a): Loss coeff. E13 vs discharge ratios q for m=1 (lateral 1)

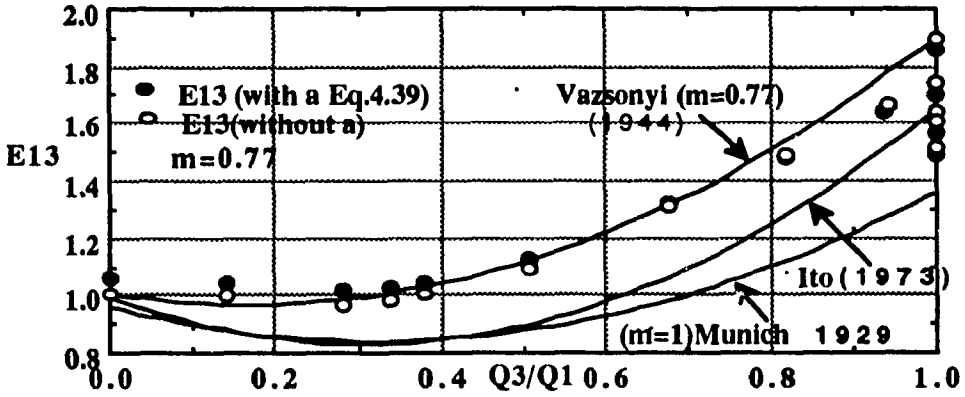

Fig.514(b): Loss coeff. E13 vs Discharge ratio q for m=0.77 (lateral 2)

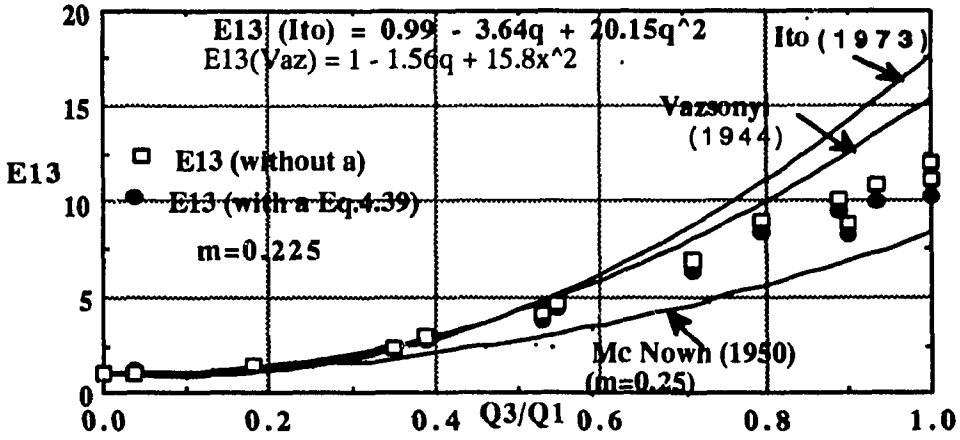

Fig.5.14(c): Loss coeff. E13 vs Discharge ratio q for m=0.225 (lateral 3)

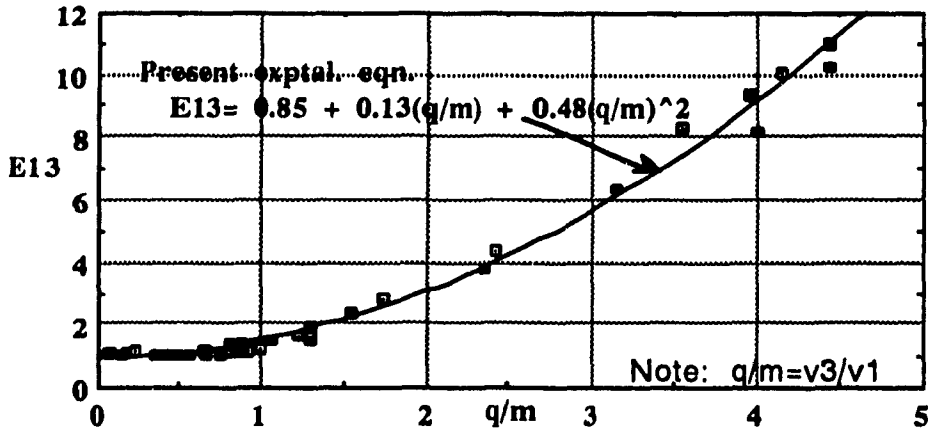

Fig.5.14(d): Loss Coefficient E13 Vs Velocity ratio q/m for the three laterals.

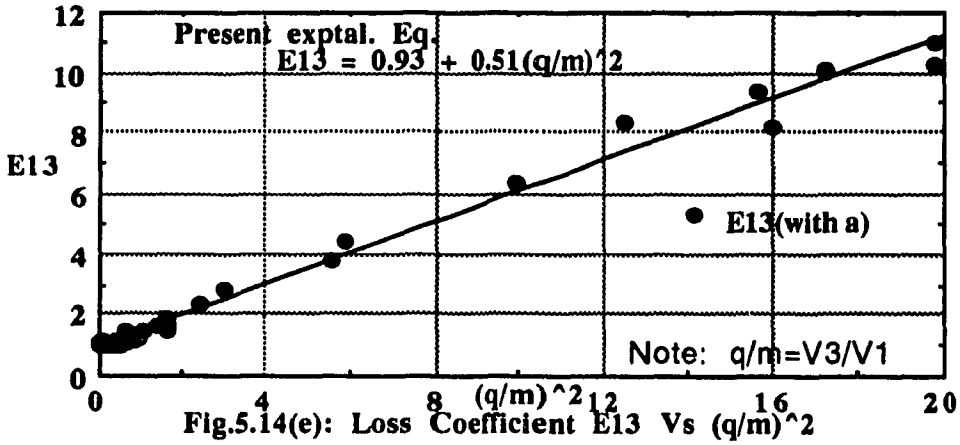

Fig.5.14(e): Loss Coefficient E13 Vs (q/m)^2 for the three laterals

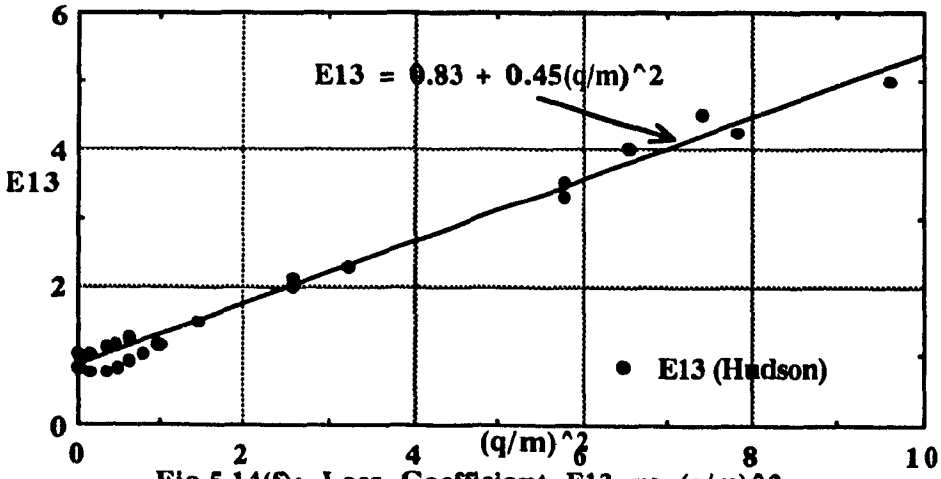

Fig.5.14(f): Loss Coefficient E13 vs (q/m)^2 From Hudson[1979]

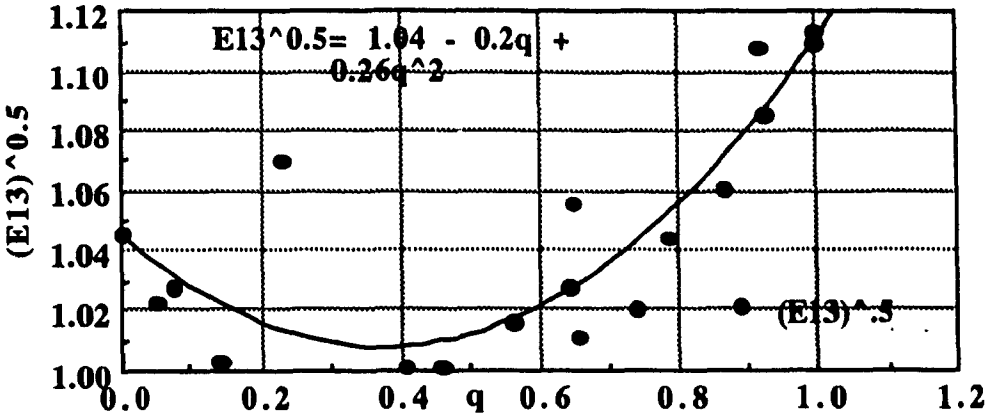

Fig.5.14g: E13^0.5 Vs q/m for Lateral 1 (m=1)

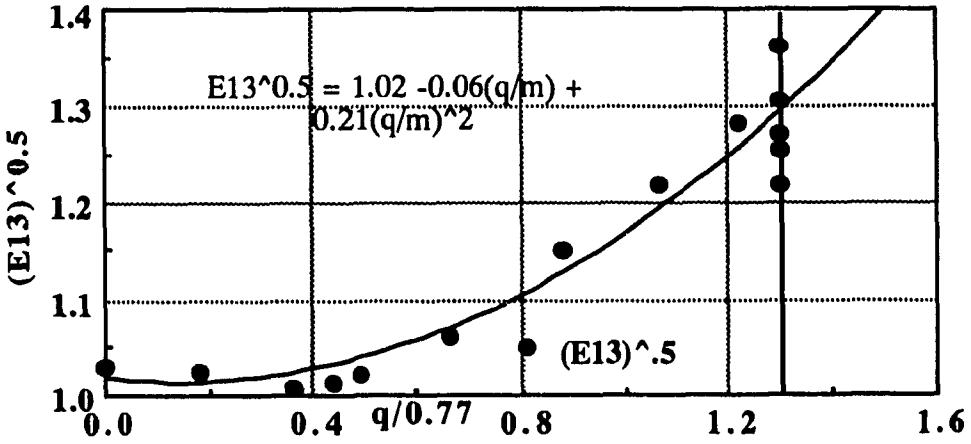

Fig.5.14h: E13^0.5 Vs q/m for lateral 2 (m=0.77)

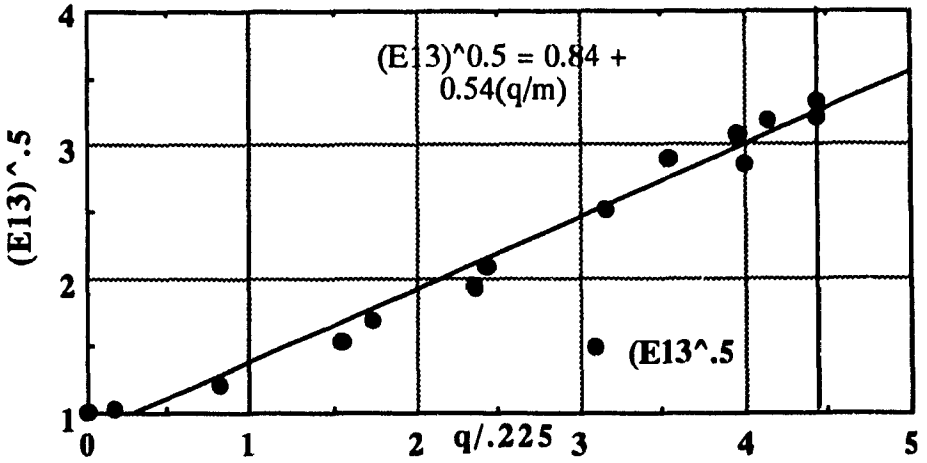

Fig.5.14(i): E13^0.5 Vs q/m for Lateral 3 (m=0.225)

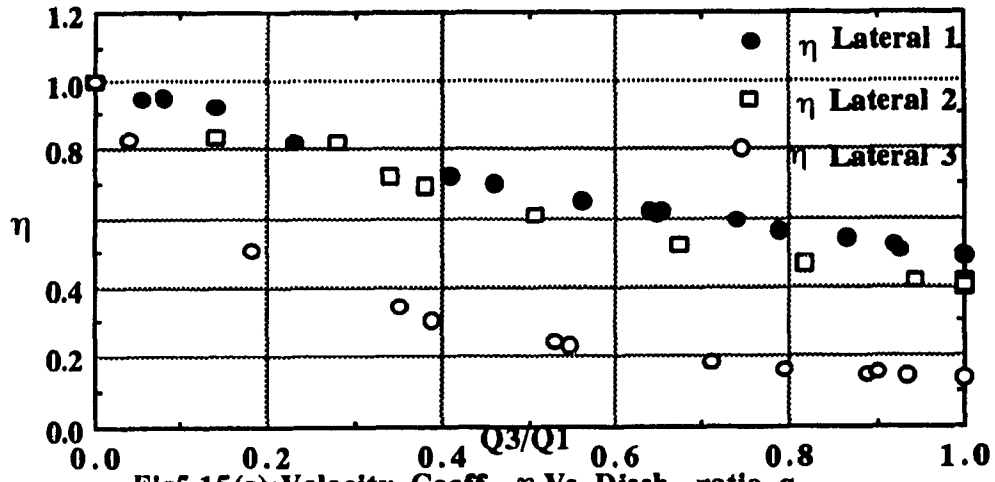

Fig5.15(a):Velocity Coeff. η Vs Disch. ratio q for the three Laterals

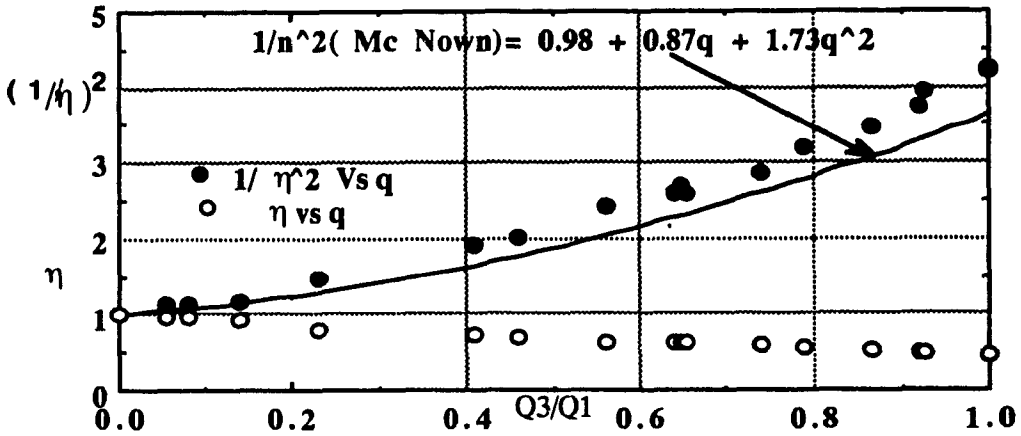

Fig.5.15(b):Velocity Coeff. η and 1/ η ^2 Vs Discharge ratio q for m=1(lateral 1)

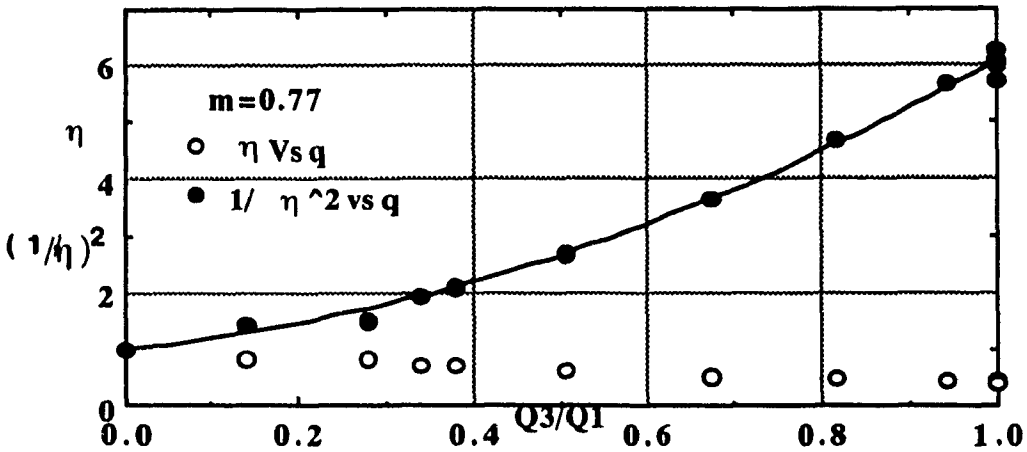

Fig. 5.15(c): (1/η)2 and η Vs q for m=0.77 (Lateral 2)

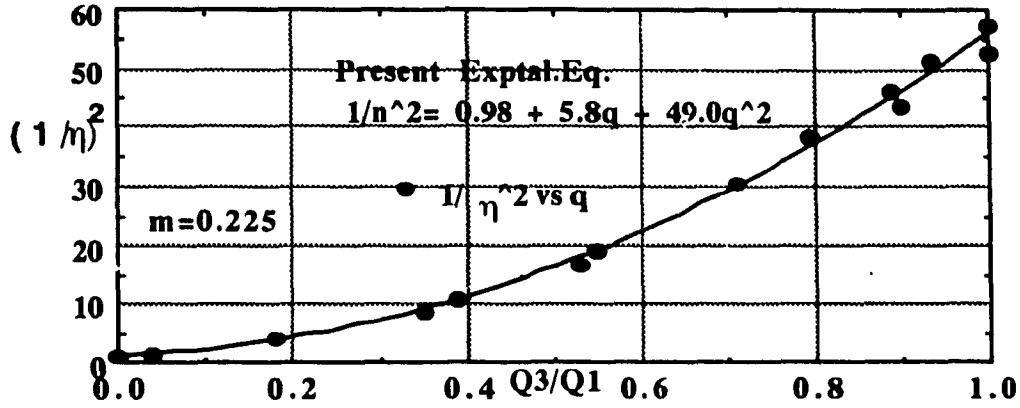

Fig. 5.15(d): 1/ η ^2 Vs q for m=0.225 (Lateral 3)

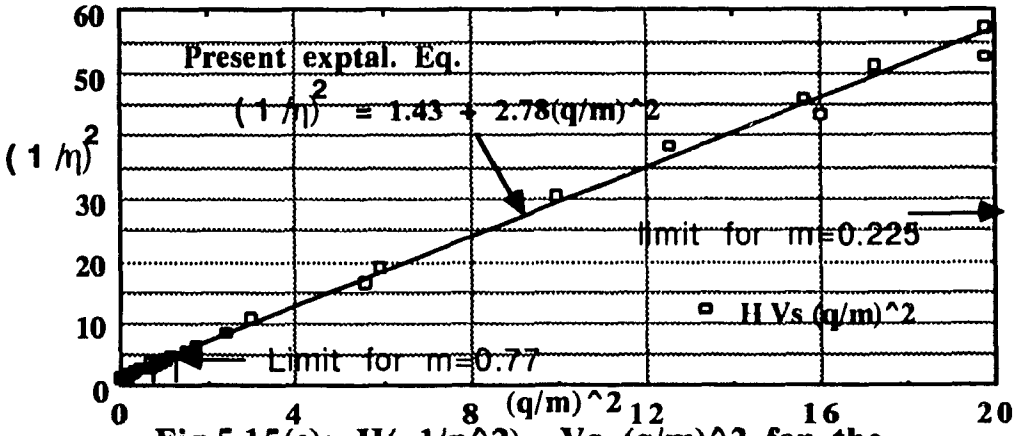

Fig.5.15(e): H(=1/n^2) Vs (q/m)^2 for the three laterals

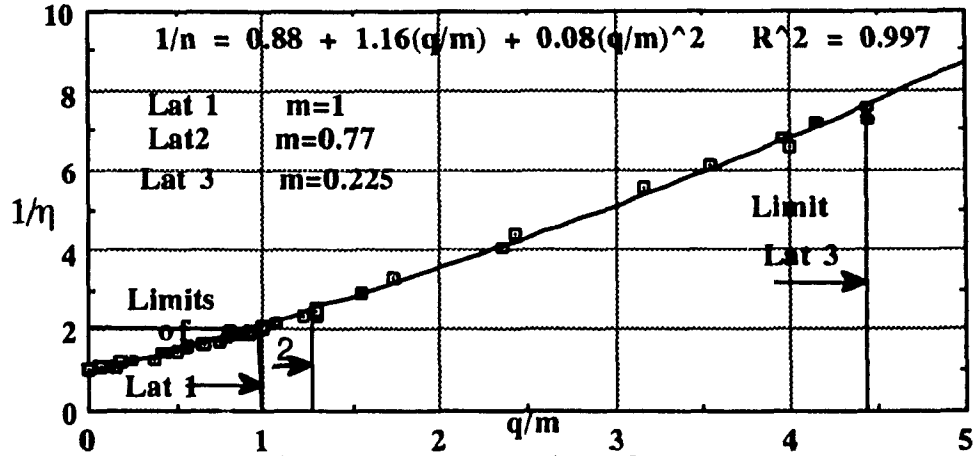

Fig.5.15(f): 1/n Vs (q/m) for the three laterals

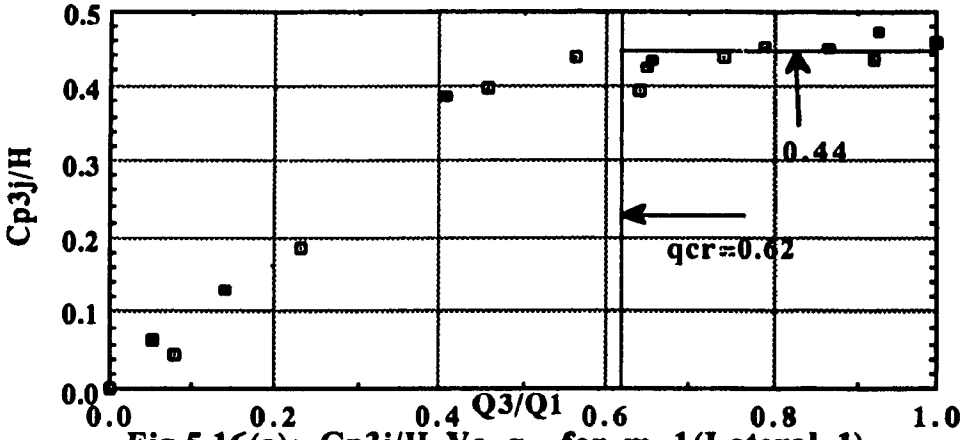

Fig.5.16(a): Cp3j/H Vs q for m=1(Lateral 1)

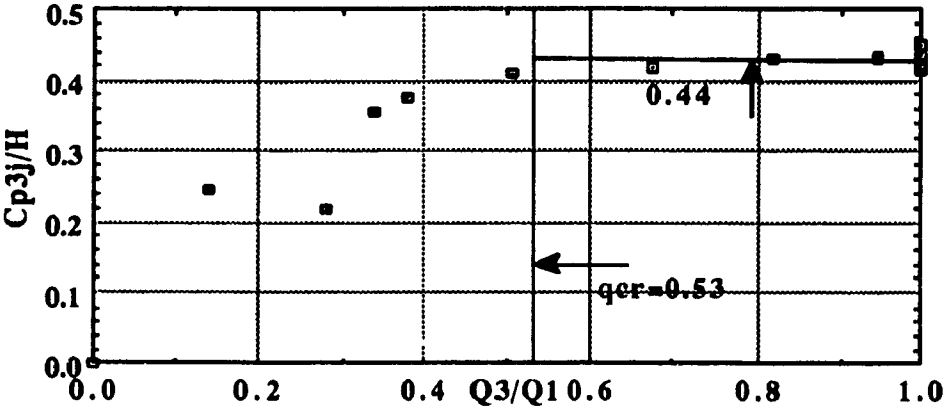

Fig.5.16(b):Cp3j/H vs q for m=0.77
(Lateral2)

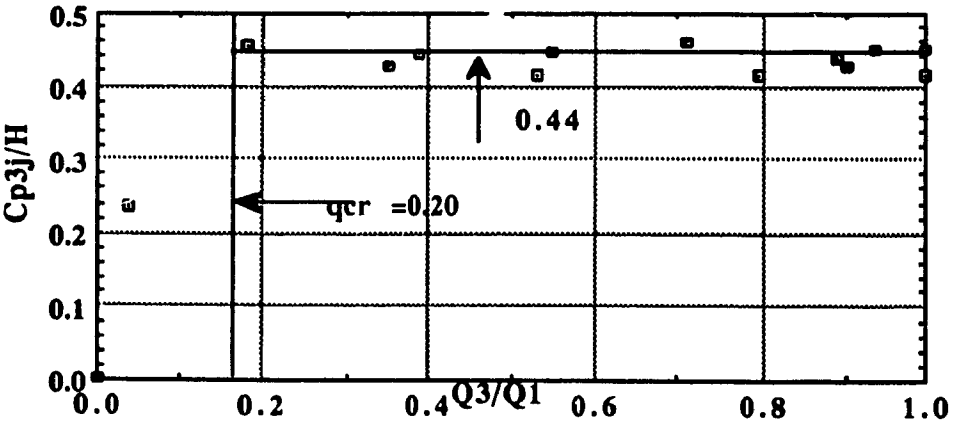

Fig.5.16(c): Cp3j/H Vs q for m=0.225
Lateral 3

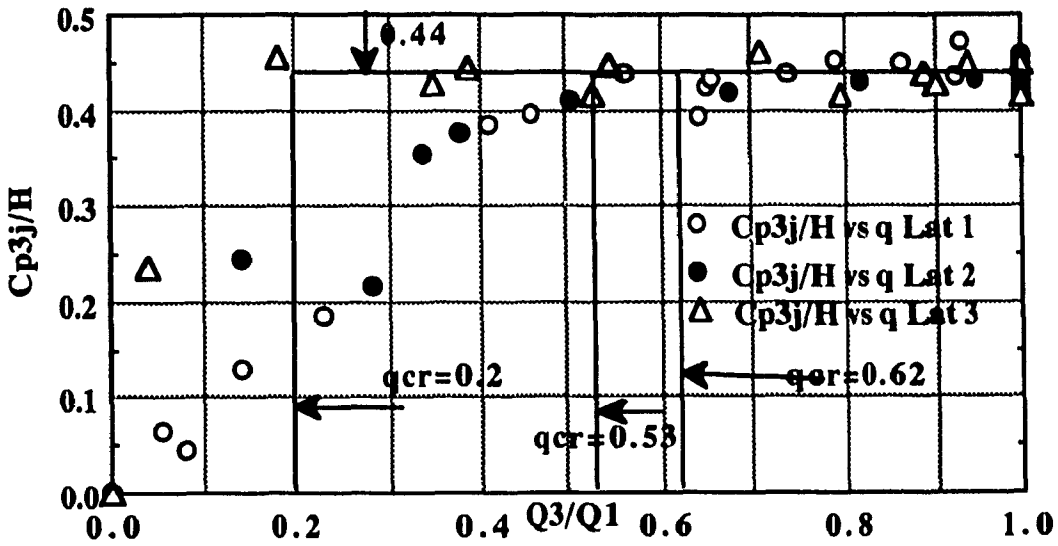

Fig.5.16(d):Cp3j/H Vs q forthe threelaterals

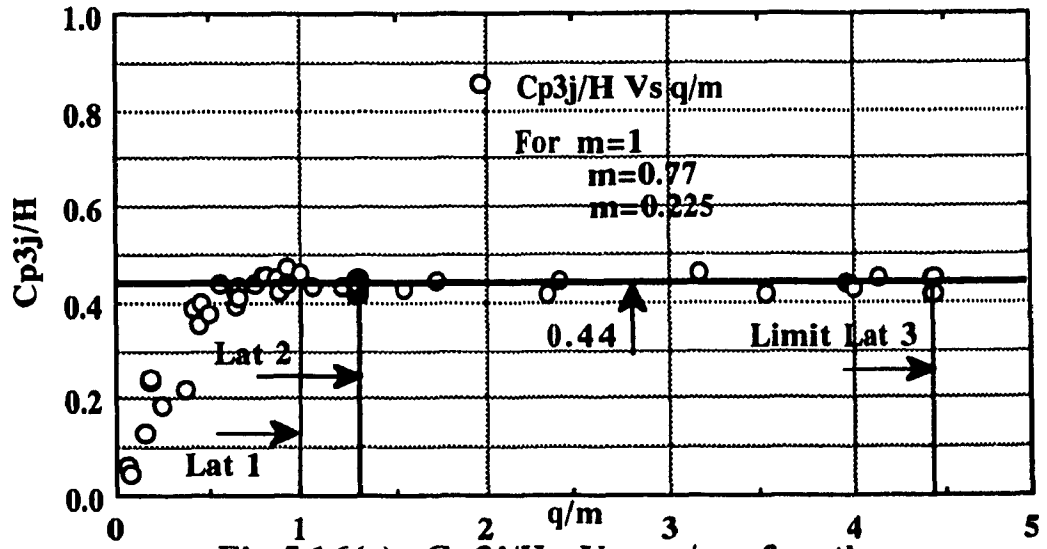

Fig.5.16(e): Cp3j/H Vs q/m for the three laterals

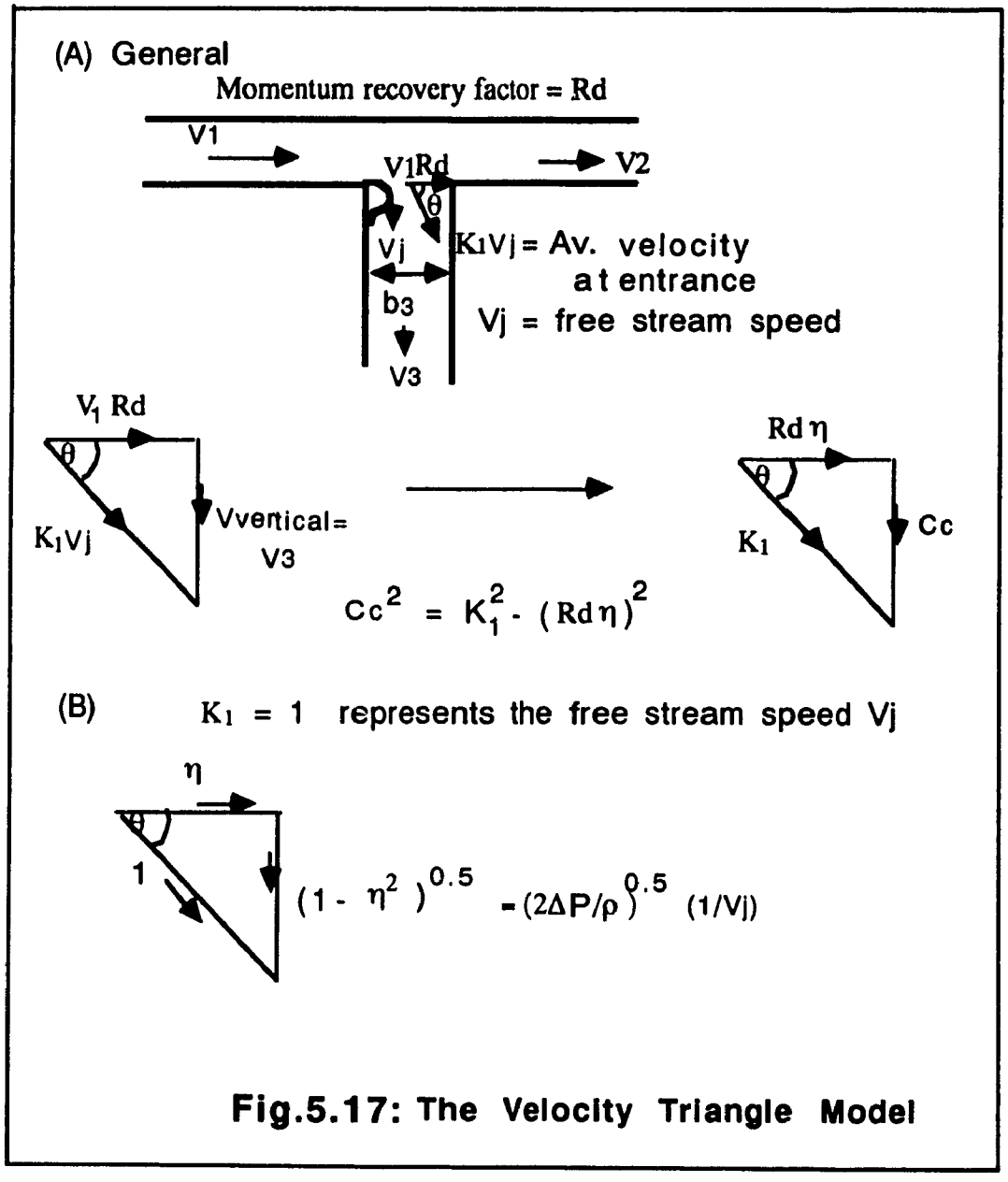

Fig.5.17: The Velocity Triangle Model

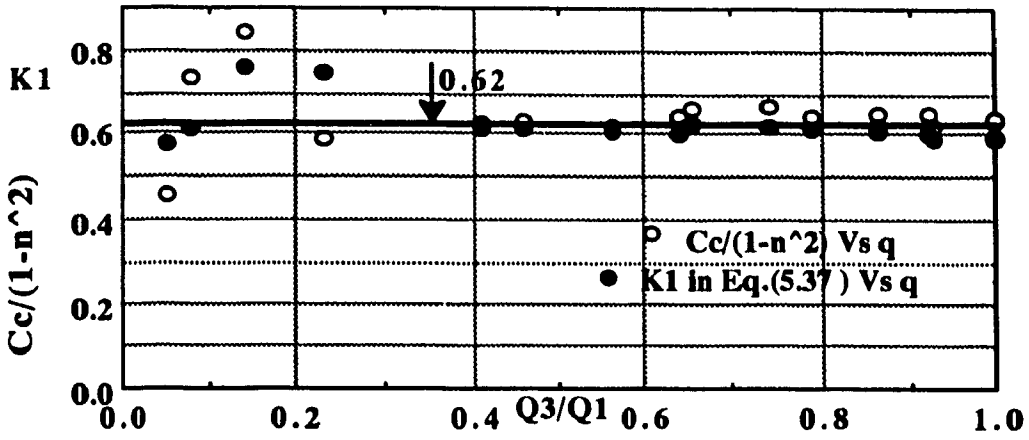

Fig. 5.18(a): Ca/(1-n^2) , K1 Vs q for m=1 (Lateral 1)

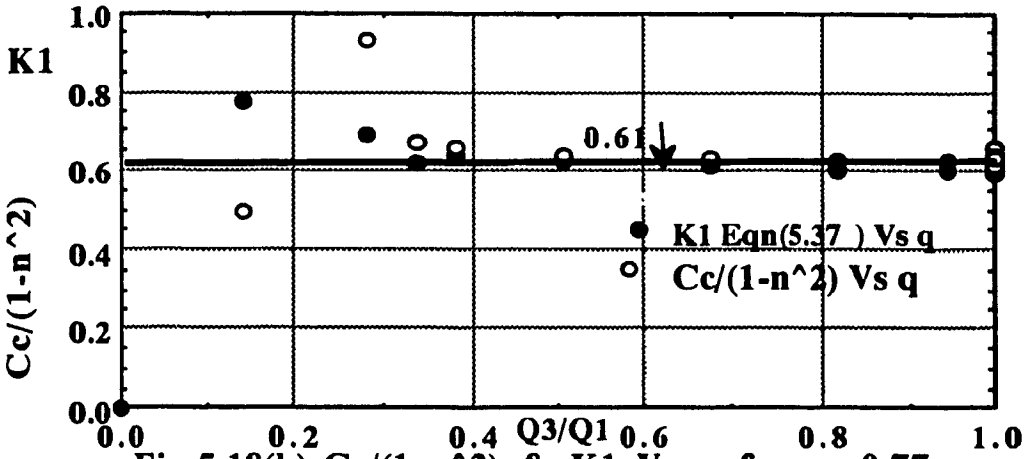

Fig.5.18(b):Ca/(1-n^2) & K1 Vs q for m=0.77 (Lateral 2)

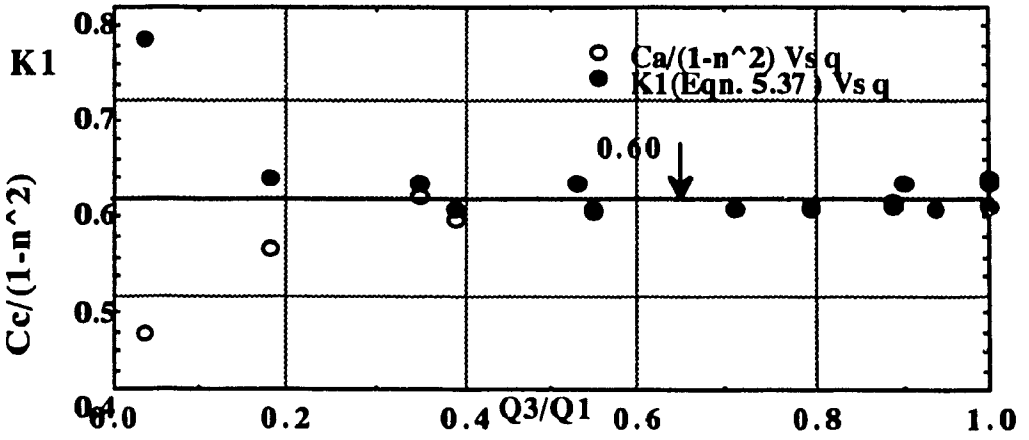

Fig.5.18(c): Cc/(1-n^2) & K1 Vs q for m=0.225 (Lateral 3)

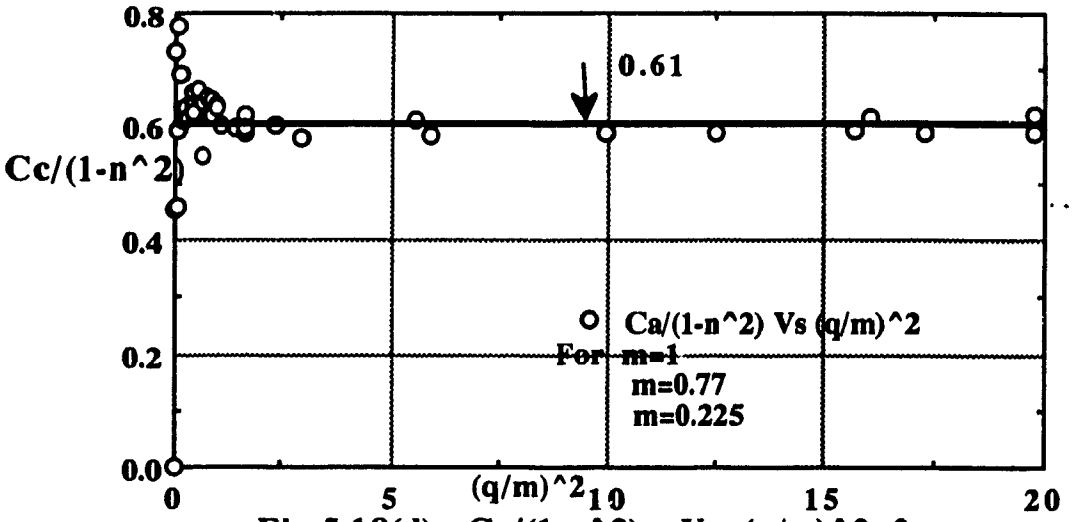

Fig.5.18(d): Cc/(1-n^2) Vs (q/m)^2 for the three Laterals.

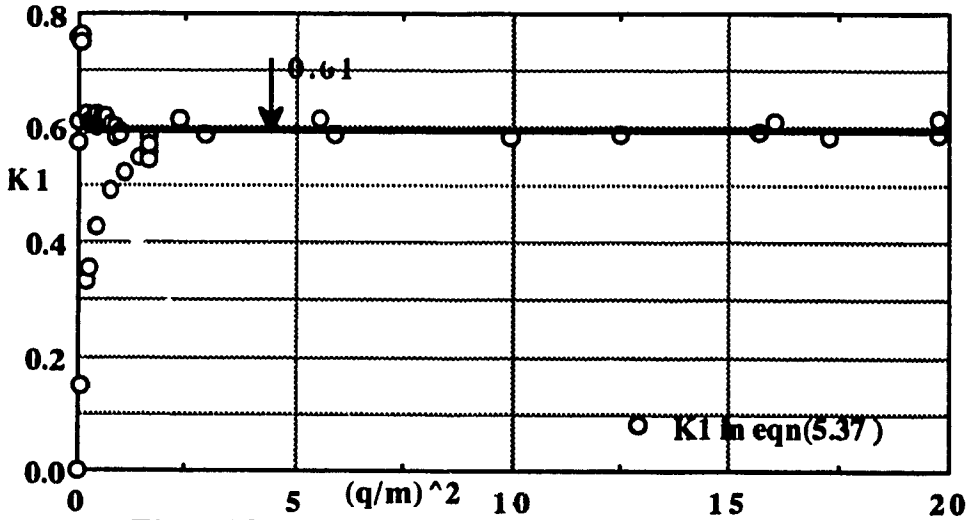

Fig.5.18(e): K1 (Eq.5.37) Vs (q/m)^2 for the three laterals

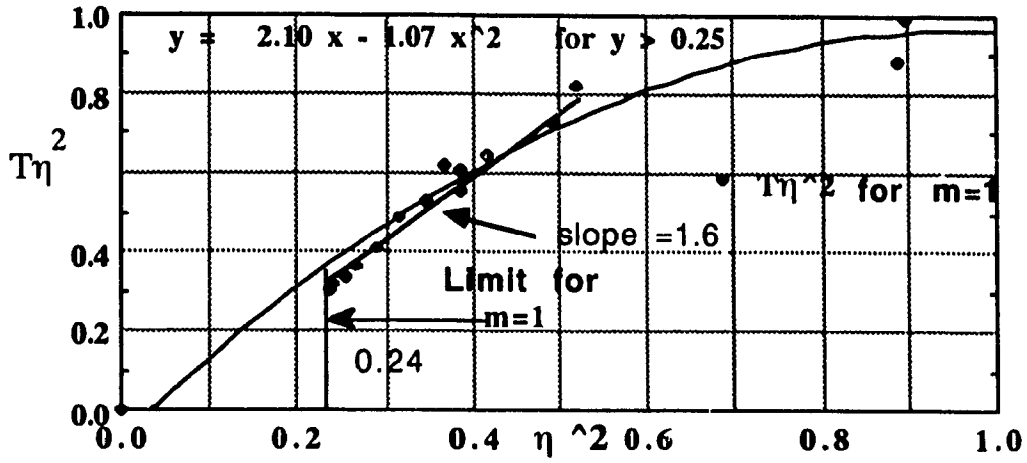

Fig.5.19(a):T η^2 Vs η^2 for m= 1

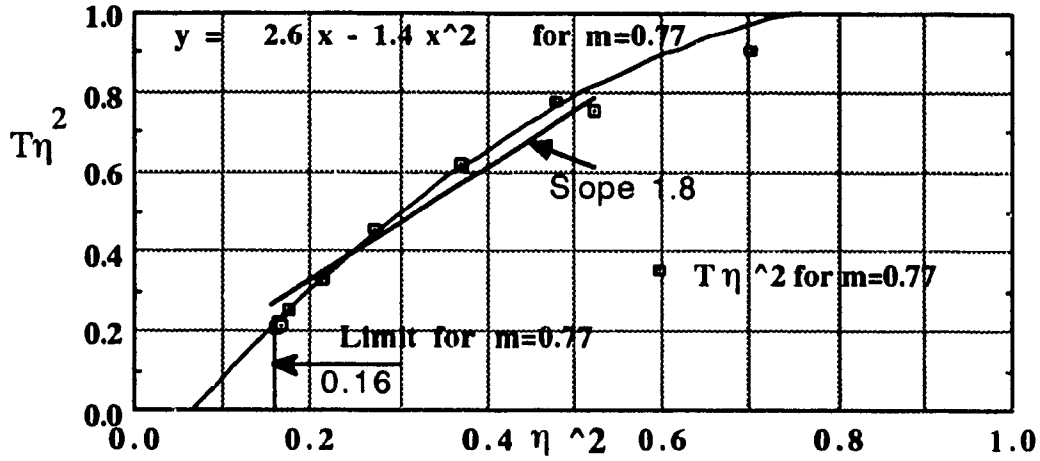

Fig.5.19(b): T η^2 Vs η ^2 for m=0.77

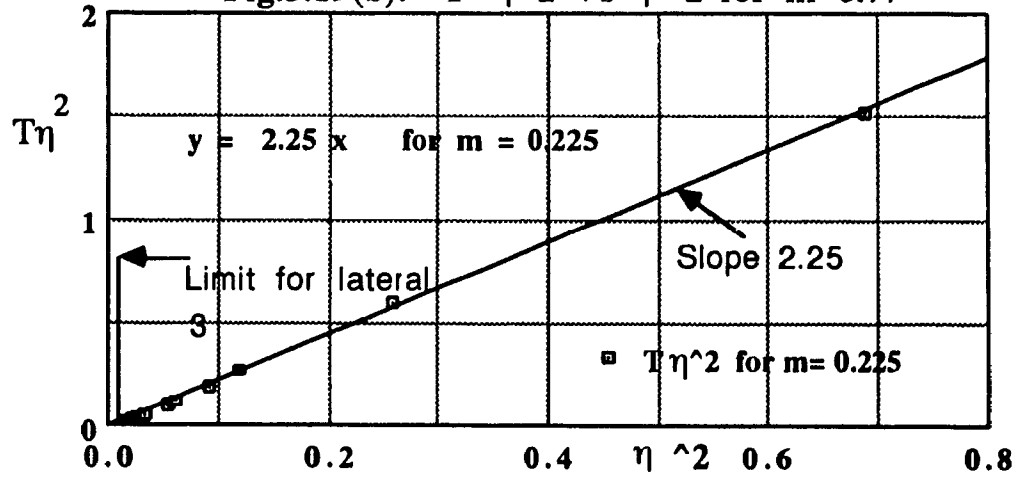

Fig.5.19(c): T η^2 Vs η ^2 for m=0.225

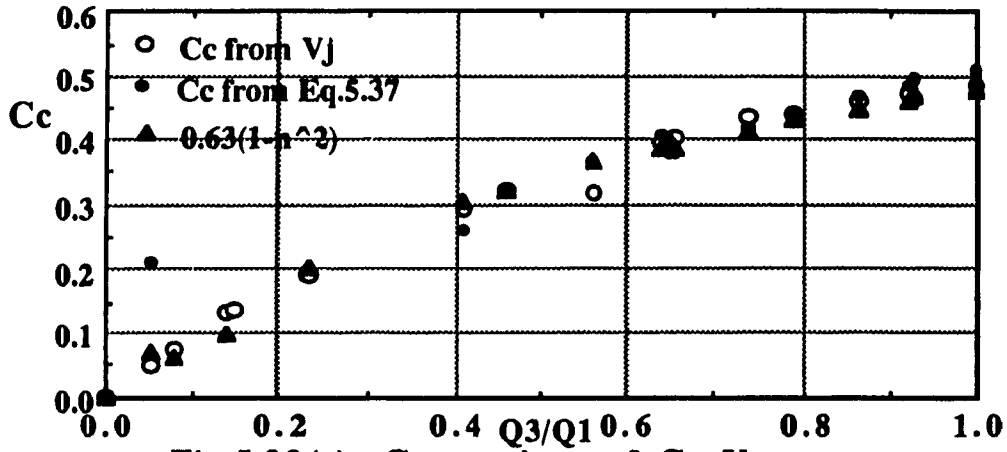

Fig.5.20(a): Comparison of Cc Vs by different formulas m=1

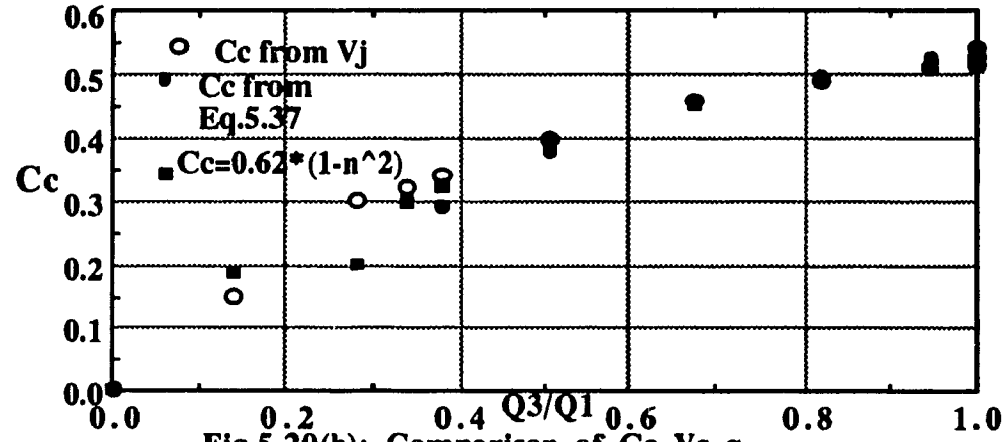

Fig.5.20(b): Comparison of Cc Vs q by different formulas, m=0.77

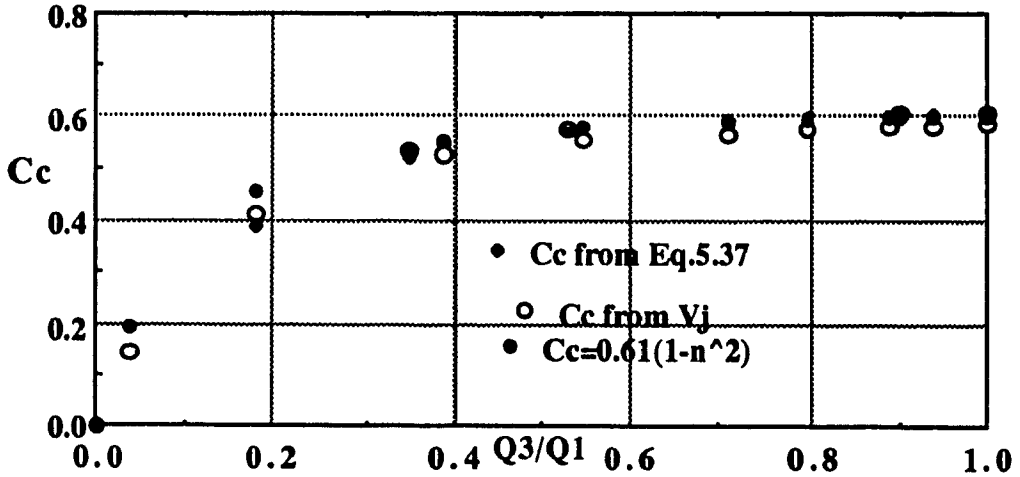

Fig.5.20(c): Comparison of Cc vs q by different formulas, m=0.225

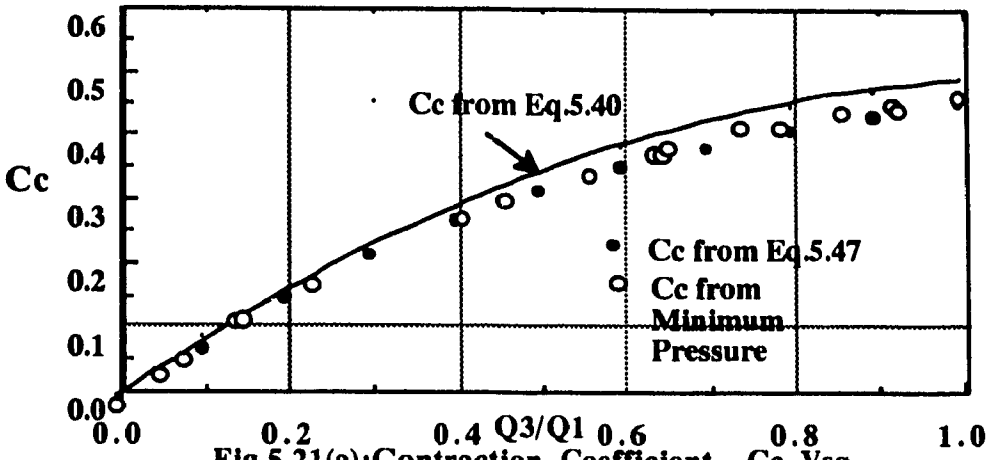

Fig.5.21(a):Contraction Coefficient Cc Vsq from Eqns. 5.47, 5.40 for m=1

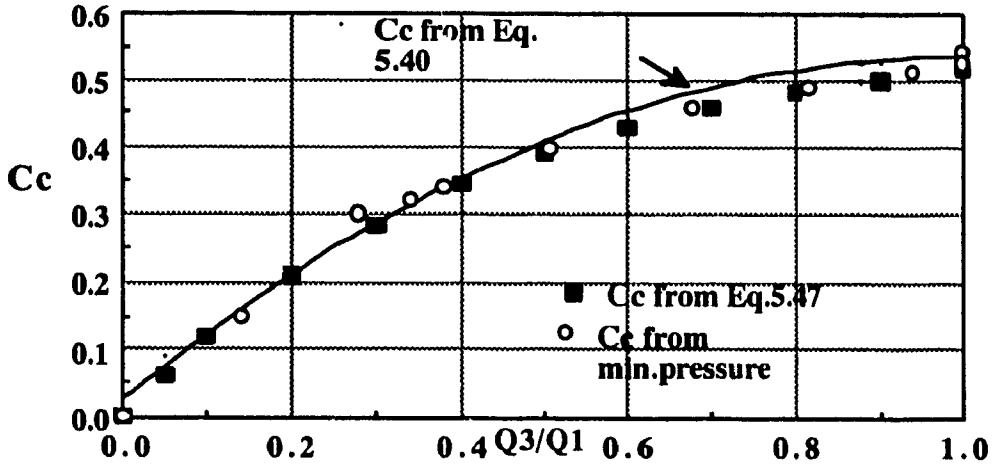

Fig.5.21(b):Contraction Coefficient Cc vsq from Eqns.5.47,5.40 for m=0.77

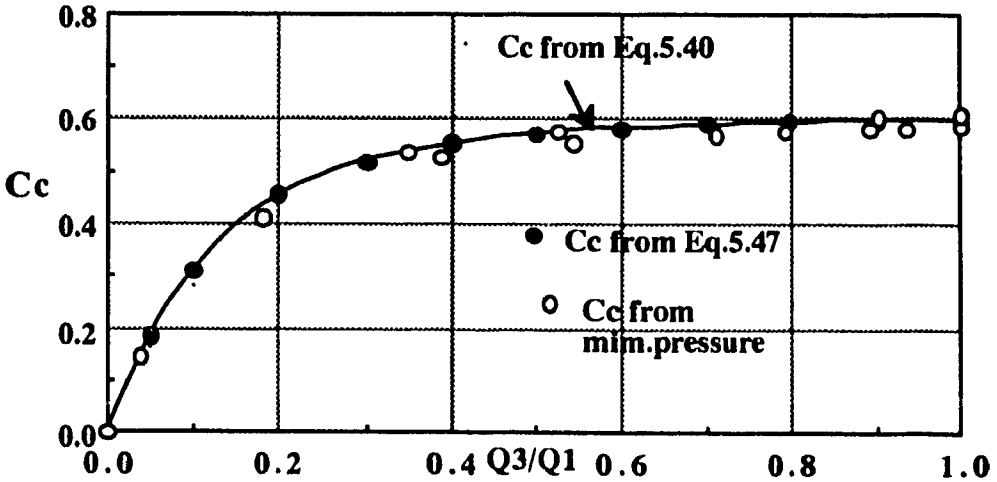

Fig.5.21(c):Contraction Coefficient Cc vs q from Eqn.5.47,5.40 ,m=0.225

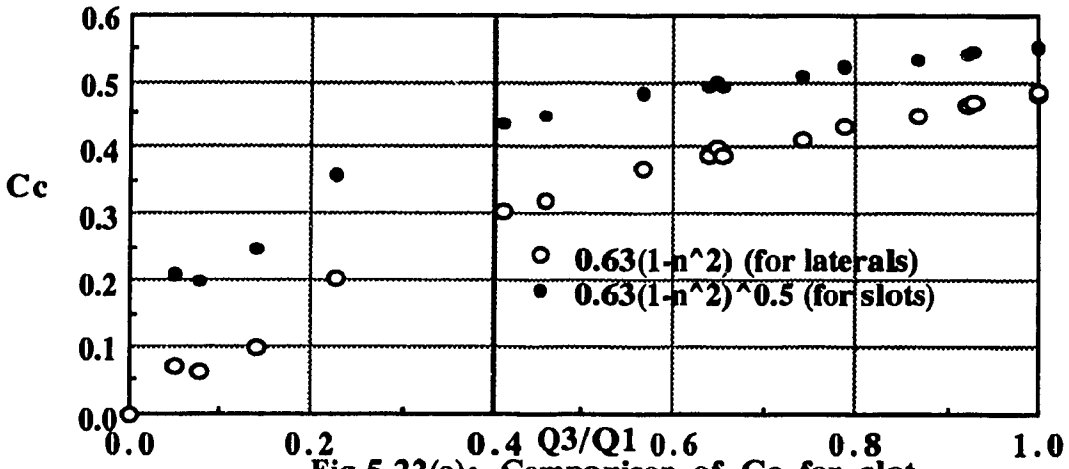

Fig.5.22(a): Comparison of Cc for slot and lateral m=1

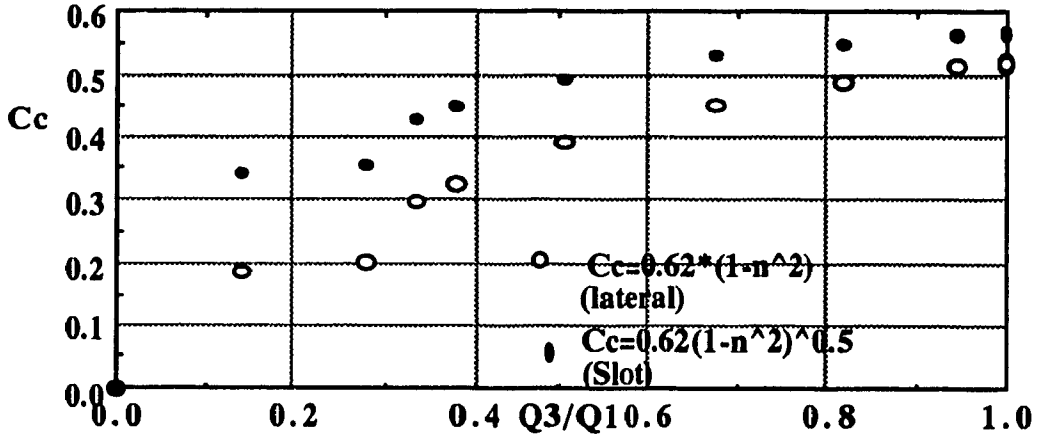

Fig.5.22(b): Comparison Of Cc Vsq for slot and lateral ,m=0.77

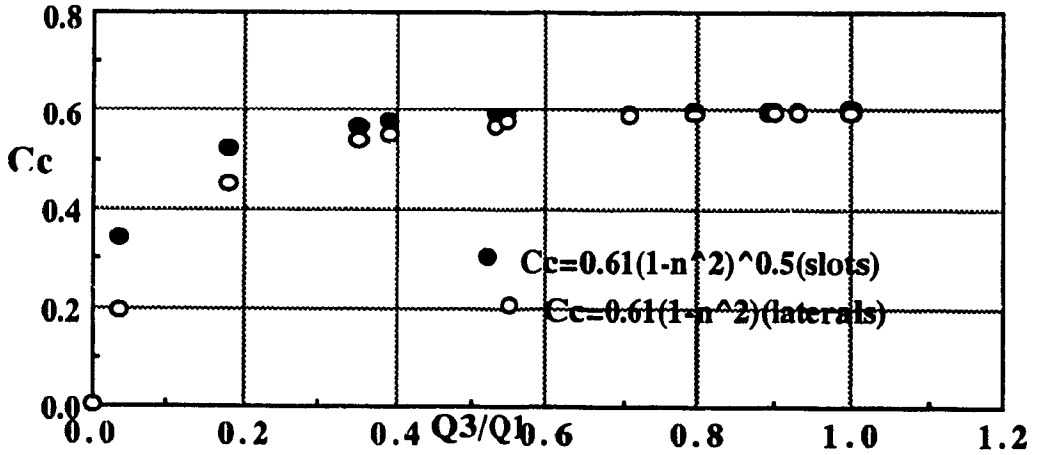

Fig.5.22(c): Comparison of Cc vs q for slot and for lateral, m=0.225

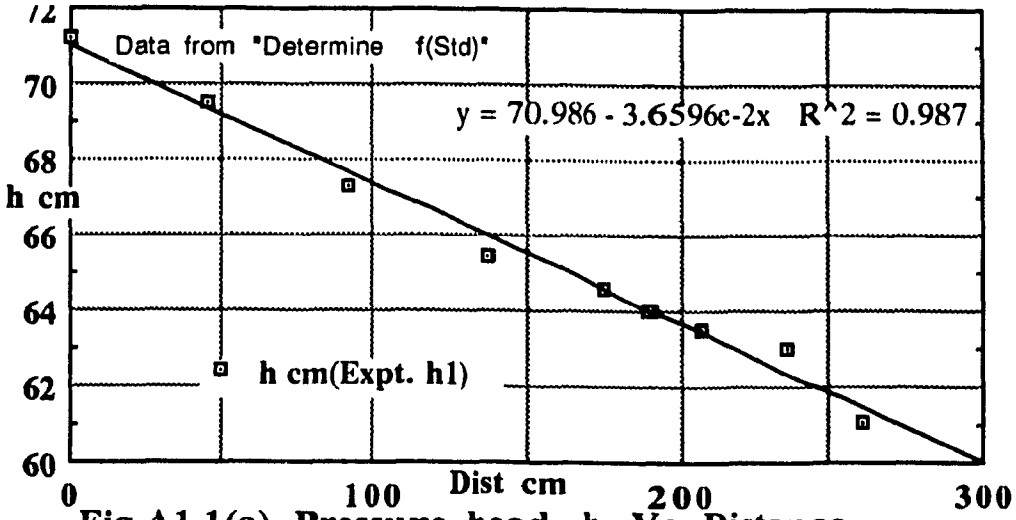

Fig.A1.1(a) Pressure head, h, Vs Distance for exnt. h1 (Aluminium duct).

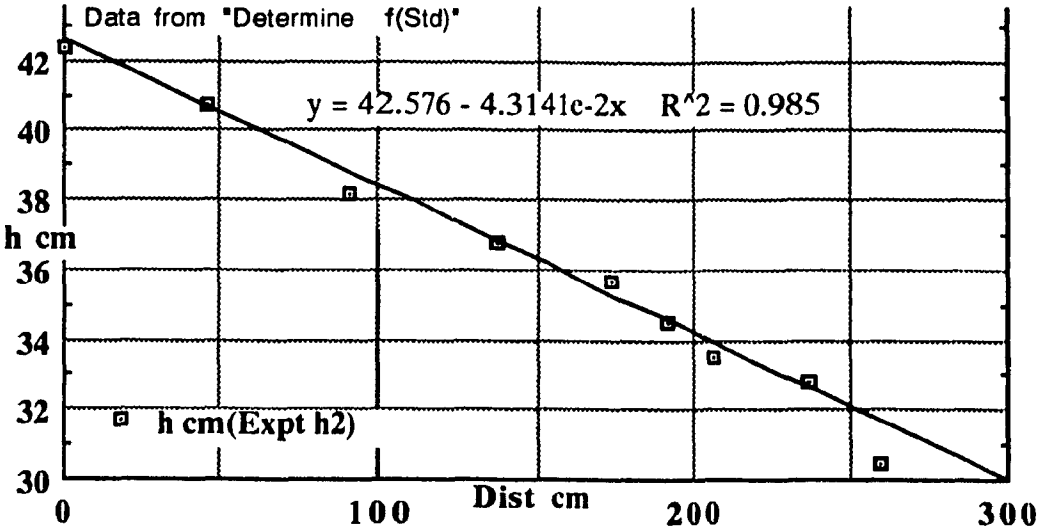

Fig.A1.1.(b): Pressure head,h, Vs Distance in expt.h2 (Aluminium duct)

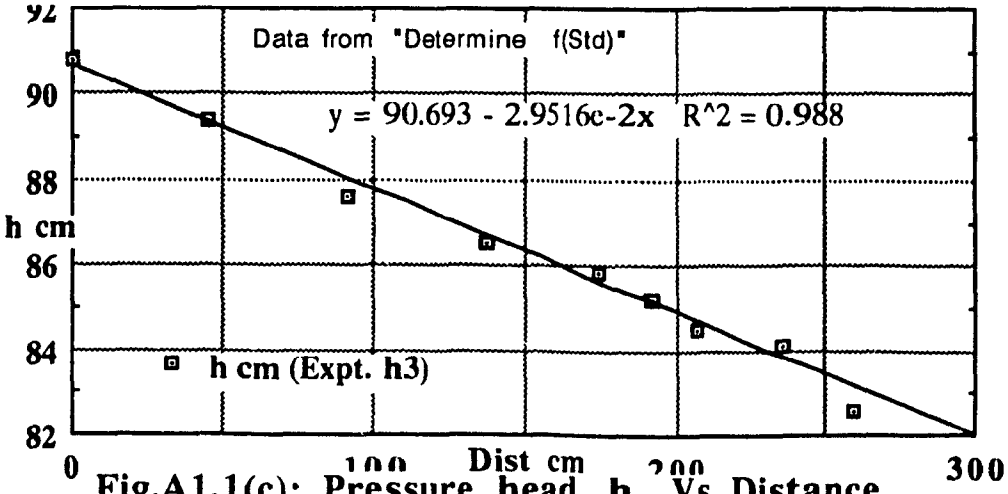

Fig.A1.1(c): Pressure head ,h, Vs Distance Exnt. h3 (Aluminium duct)

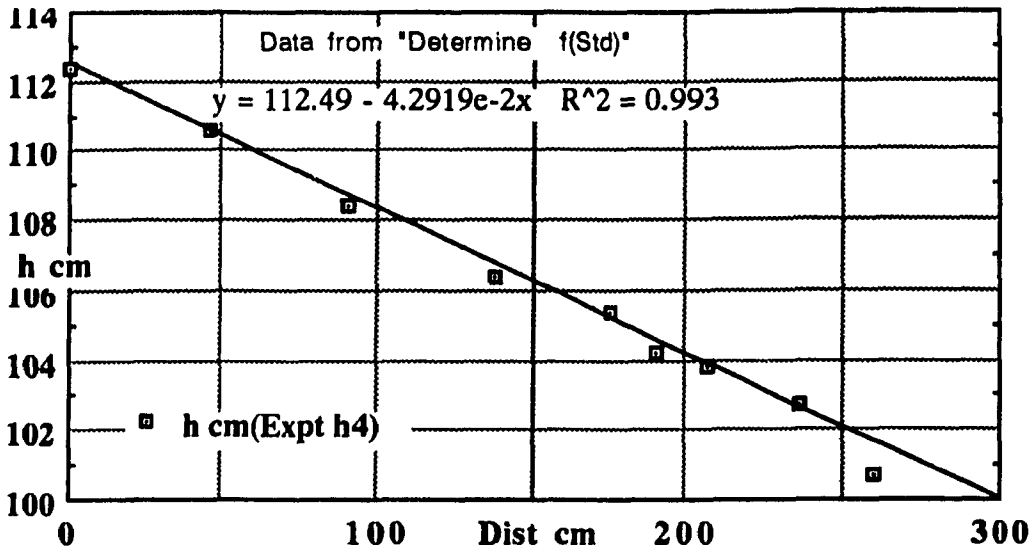

Fig.A1.1(d): Pressure head .h, Vs Distance in Expt. h4 (Aluminium duct)

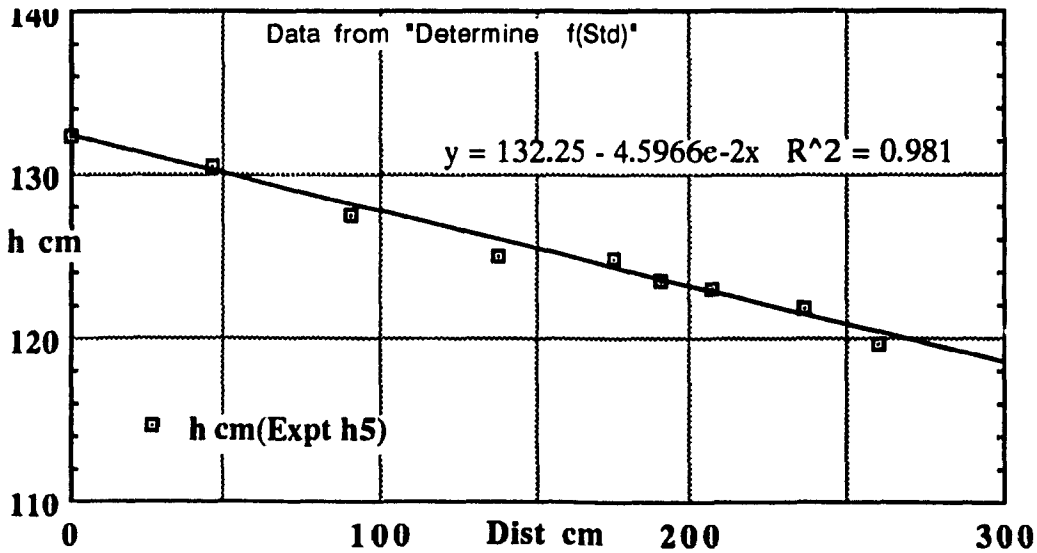

Fig.A1.1(e): Pressure head ,h, Vs Distance in expt. h5 (Aluminium duct)

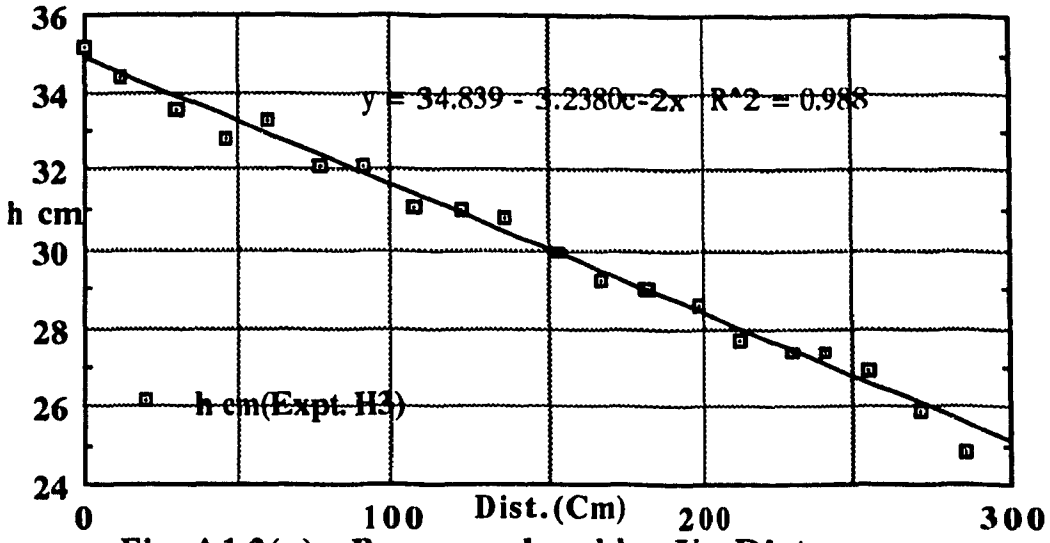

Fig:A1.2(a): Pressure head,h, Vs Distance for expt.H3 (Plexiglas)

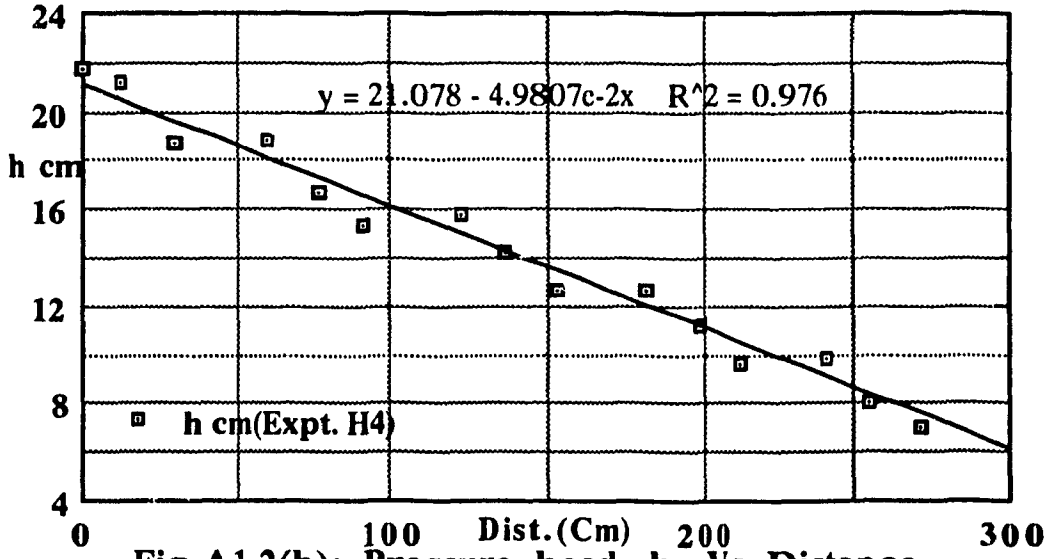

Fig.A1.2(b): Pressure head, h, Vs Distance for expt. H4(Plexiglas)

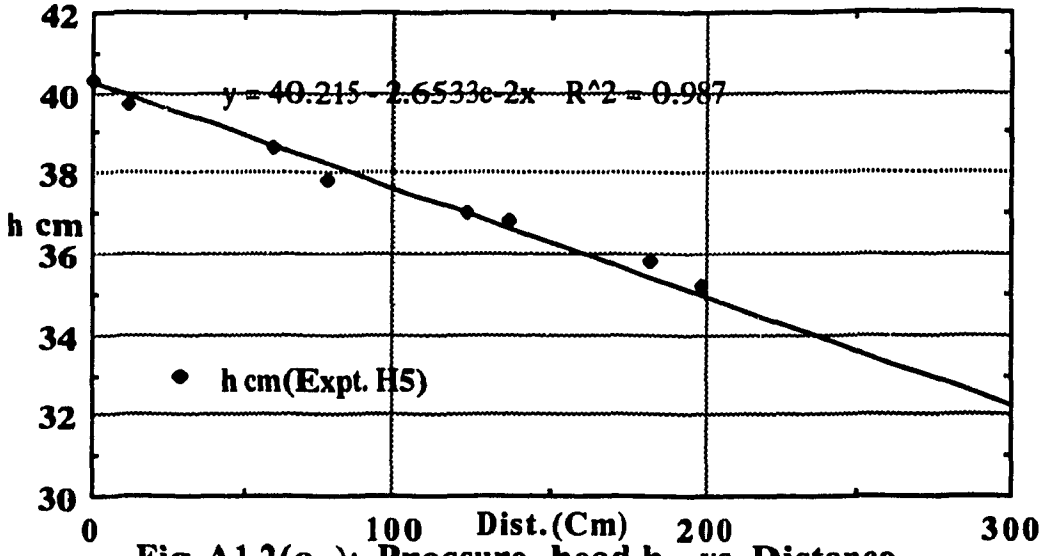

Fig.A1.2(c): Pressure head,h. vs Distance for expt.H5(Plexiglas)

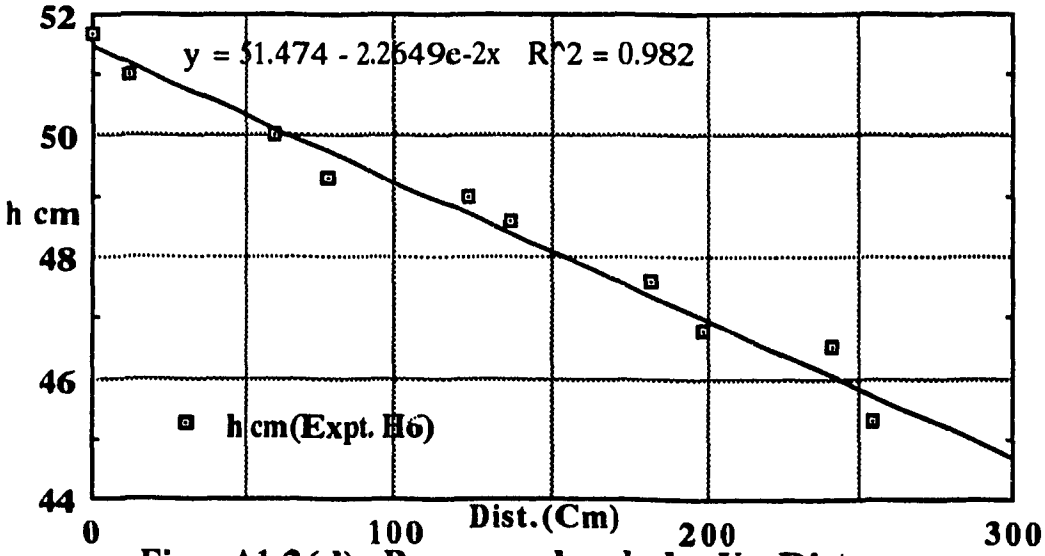

Fig: A1.2(d): Pressure head ,h, Vs Distance for expt.H6(Plexiglas)

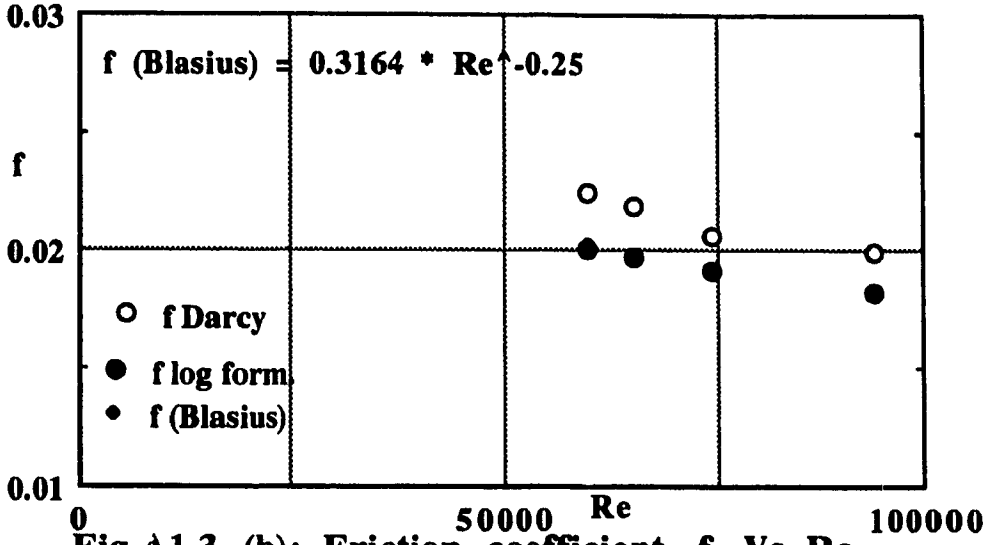

Fig.A1.3 (b): Friction coefficient ,f, Vs Re
Plexiglas conduit

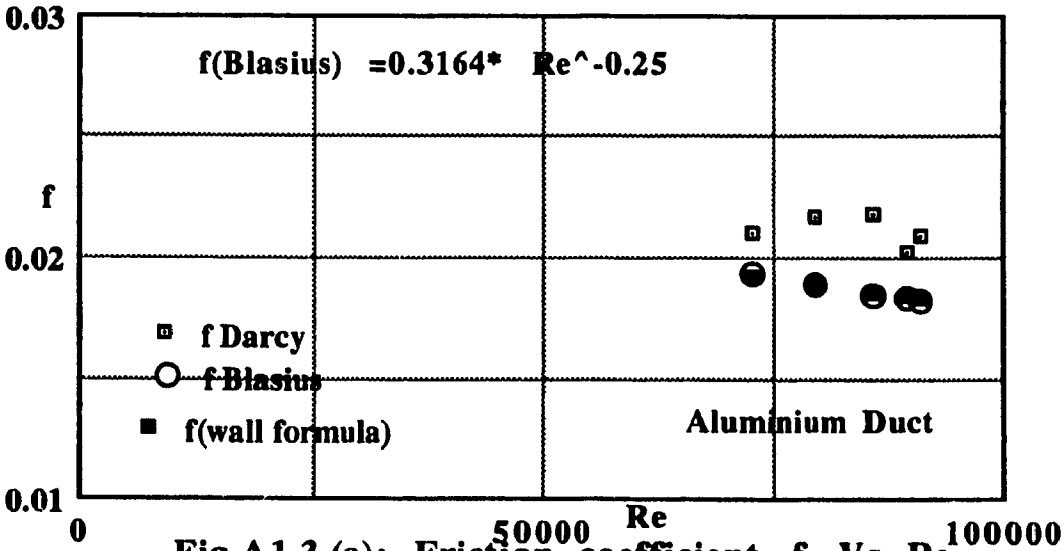

Fig.A1.3.(a): Friction coefficient ,f, Vs Re
Aluminium conduit

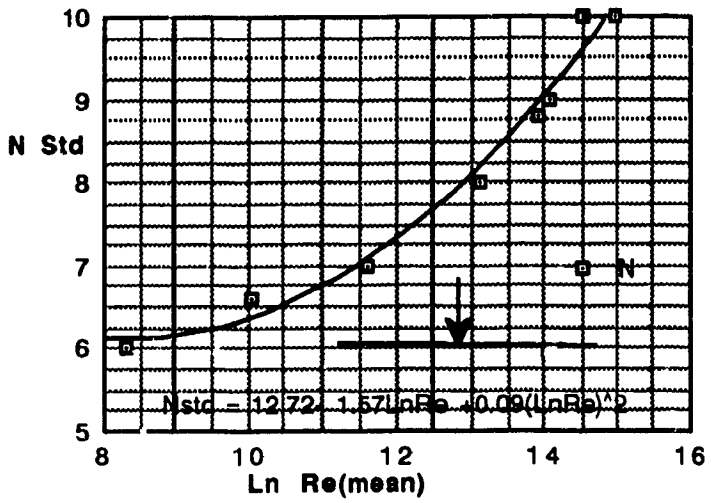

Fig. A1.4(a): N , V/Vmax Vs LOG (Re) From Sclichting

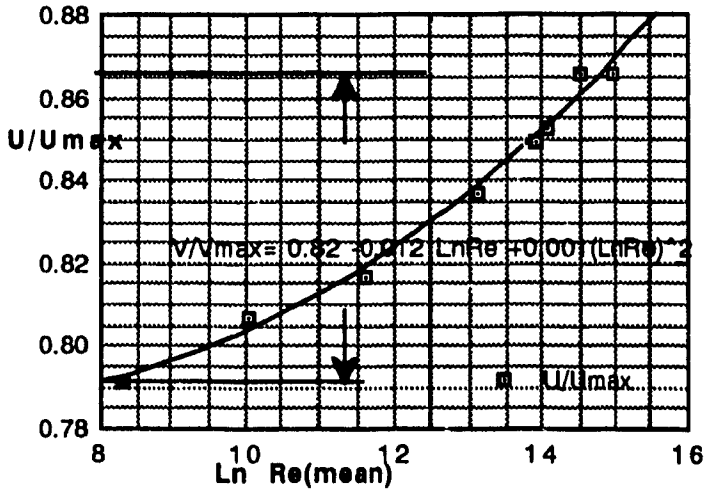

Fig.A1.4(b): V/Vmax vs ln(Re) from Schlichting,H.

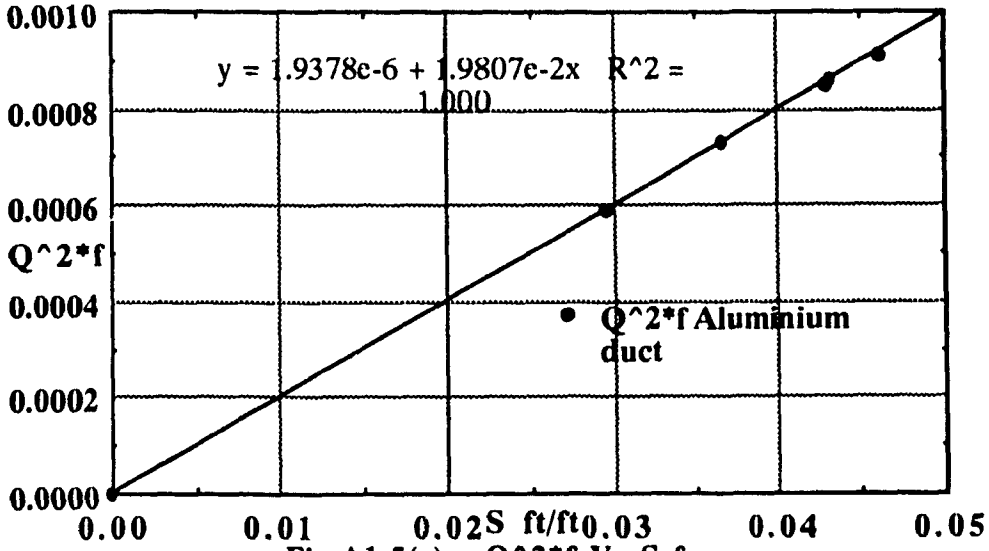

Fig.A1.5(a): Q^2*f Vs S for Aluminium duct (Expts h1-h5)

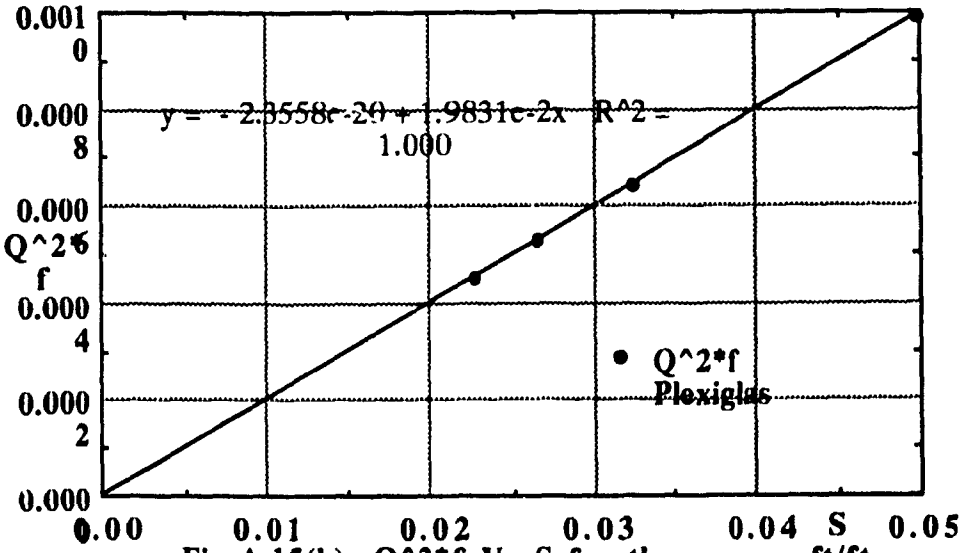

Fig:A.15(b): Q^2*f Vs S for the Plexiglas duct (Expts H1 to H5)

Fig.A1.6: Friction Coeffficient,f, Vs Re for Lateral 1

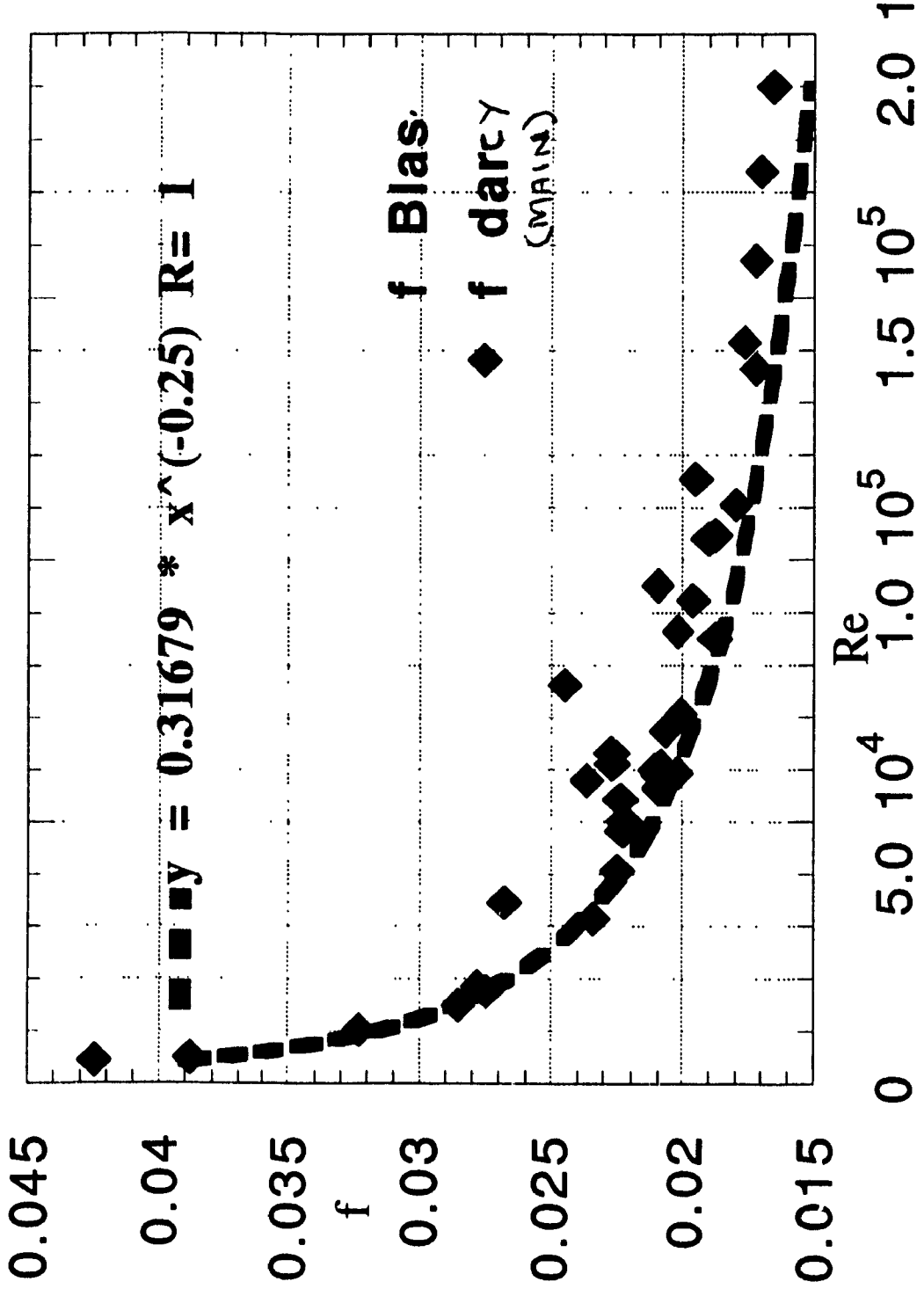

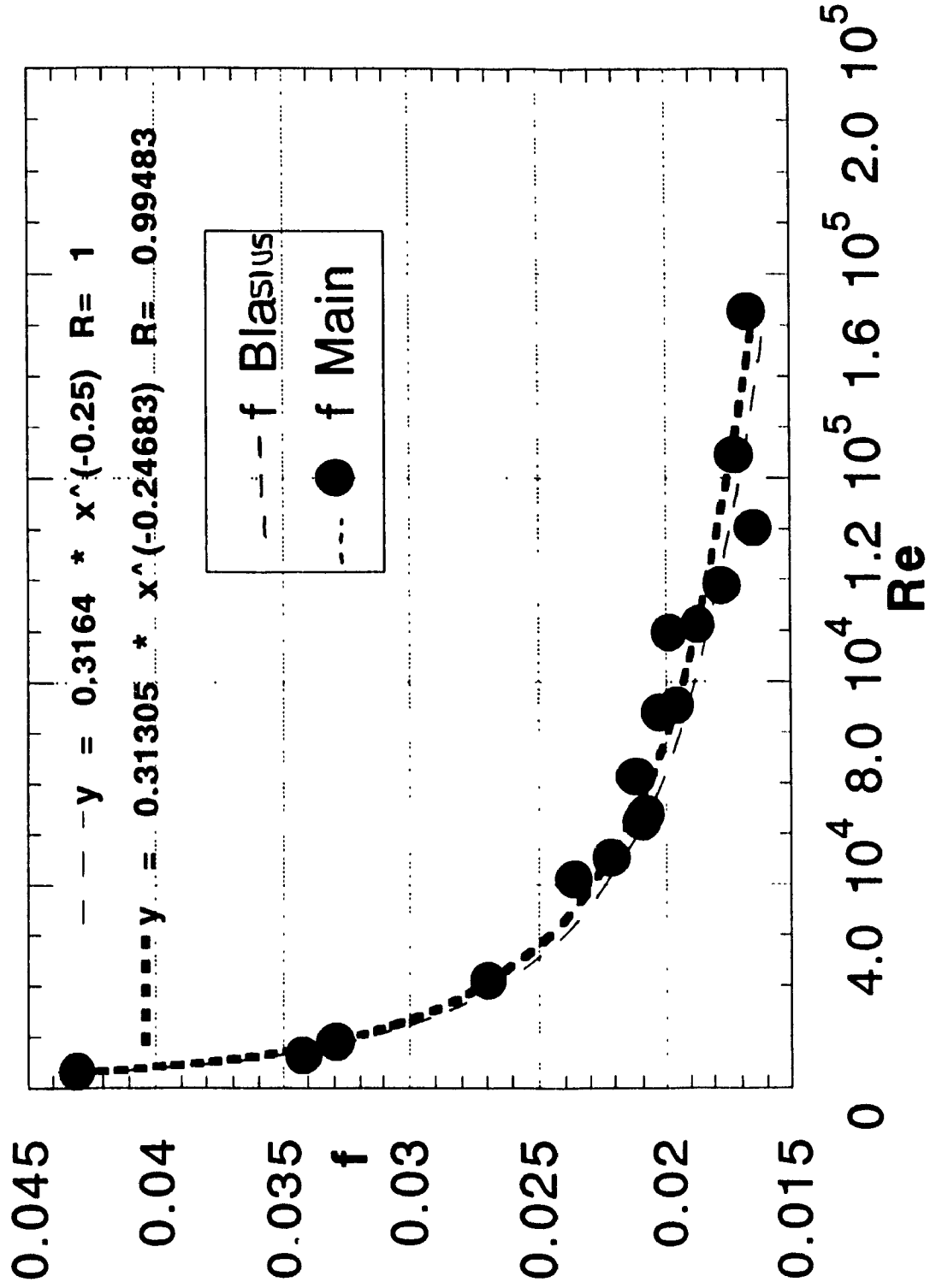
Fig.A1.7: Friction Coefficient,f. Vs Re for lateral 3
y = 0.3164 * x^(-0.25) R= 1
y = 0.31305 * x^(-0.24683) R= 0.99483
f Blasius
f Main
f
Re
0.045
0.04
0.035
0.03
0.025
0.02
0.015
0
4.0 10^4
8.0 10^4
1.2 10^5
1.6 10^5
2.0 10^5

Fig.A1.8 Friction coefficient , f, Vs Re for lateral 2

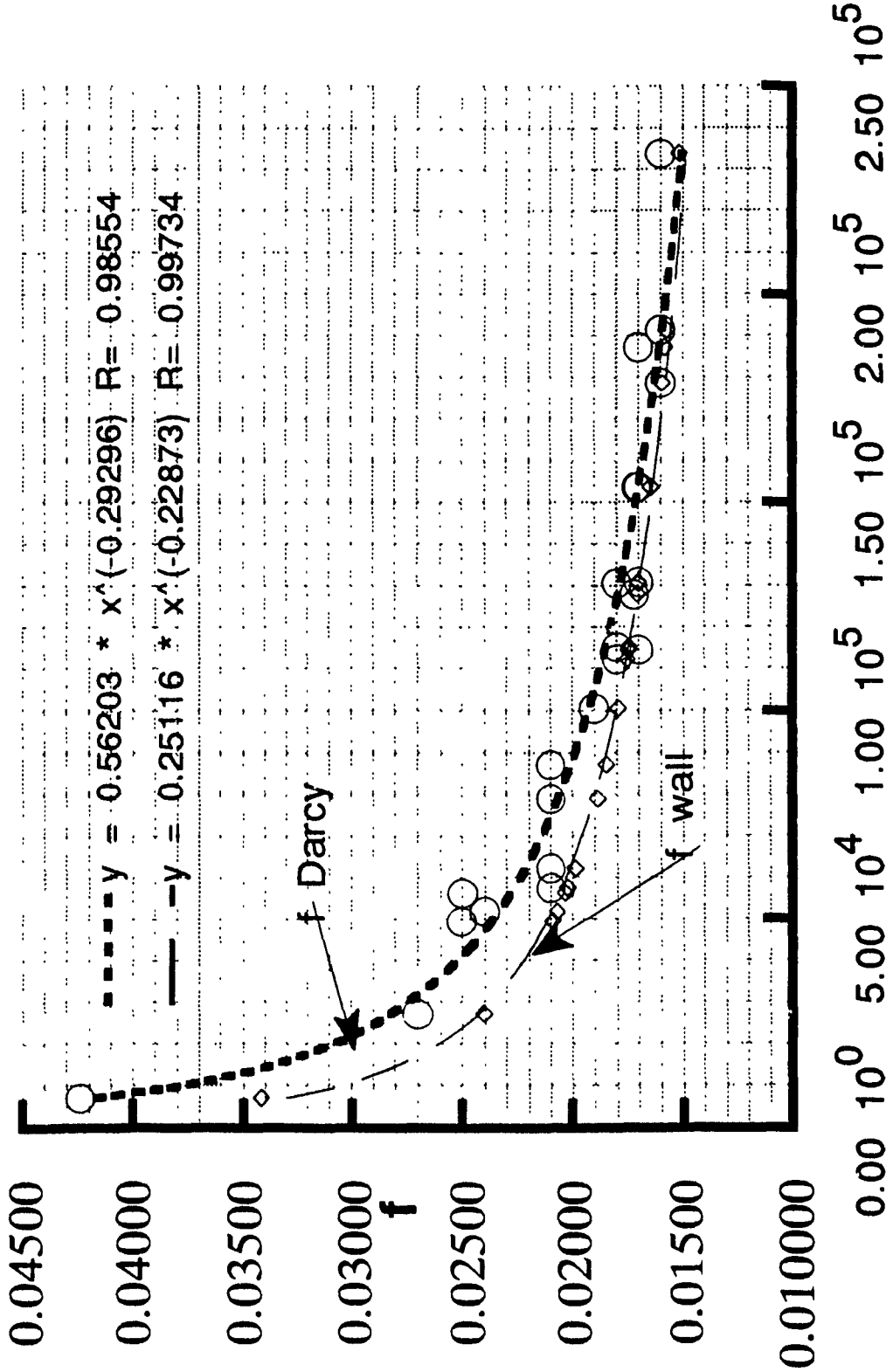

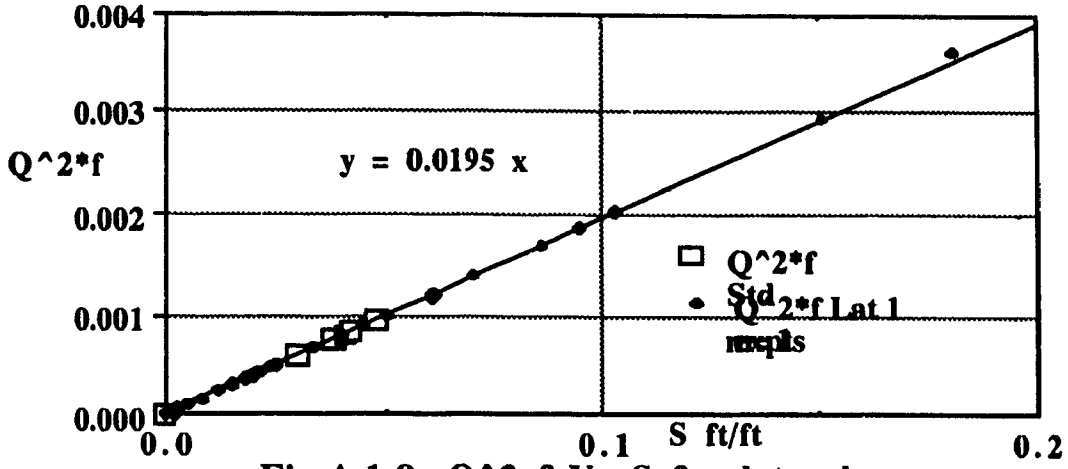

Fig.A.1.9: Q^2 f Vs S for lateral Expts.(m=1)

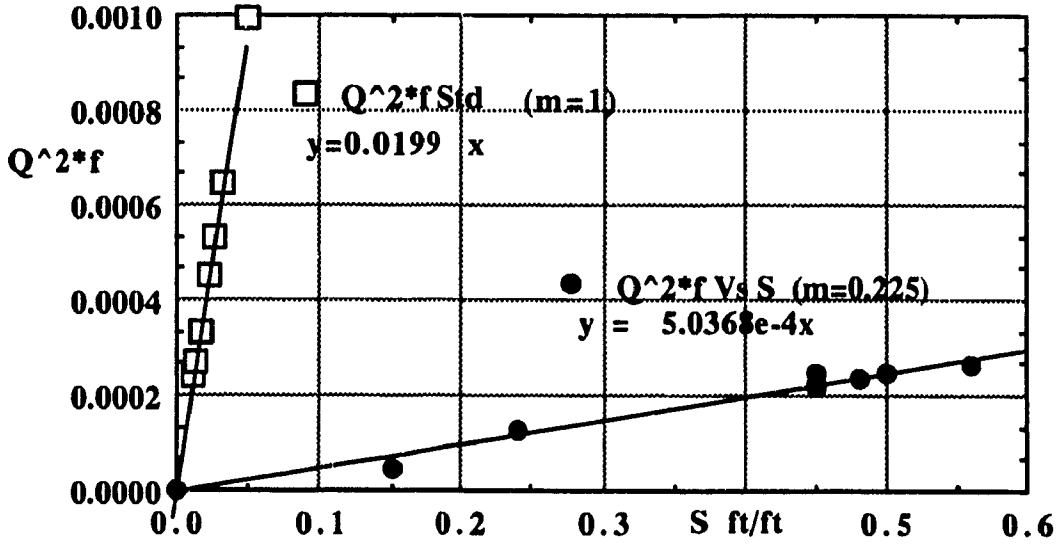

Fig.A1.10: Q^2f Vs S for m= 0.225 (Lateral 3)

APPENDIX VI

TABLES

Note: Some additional notations used in the tables are defined near the tabulations.

Table 2.1: Typical Studies Based On Free Streamline Theory.

INVESTIGATORS	REMARKS
(A) McNown [1951]. Free efflux and efflux with a barrier from a two dimensional conduit.	Obtained contraction coefficient Cc and angle α of the jet in terms of width ratios a/b, c/b and a group parameter V_2/V_1 and compared with the experimental results by Barton [1946] on circular conduits with main to lateral at 90^o and having diameter ratios of 1,1/2 and 1/4.
(B) Tsakonas [1957]. Slit at right angles from a straight constant cross section and a slit at the end of a divergence from a divergent inlet.	Discharge ratios were plotted against jet angle and Cc for different widths of slit (l) to width of the main at the junction (b). Experiments carried out agreed with the theory that for minimum losses to occur in the branch pipe it should be inclined to the main at the natural angle of the jet obtained from a slot in the main.
(C) Modi [1981]. Analysed combined junction flow for the two cases of non separated and separated flows.	Obtained stagnation points from the non separated flow condition and evaluated coordinates of the free streamline for differing stagnating conditions for flows with separation. Also evaluated V_3/V_1 ratios for the latter case.
(C) Ramamurthy [1979]. Efflux with barrier at an angle.	Cc plotted as a function of jet velocity ratio η and $\eta^2$with a group parameter β ($=V_2/V_1$). The results are also applicable to 90^o branching. The jet pressure corresponding to η is always atmospheric.

Table 2.2: Typical Studies On Pressure Recovery Factor.

INVESTIGATORS	REMARKS
(A) Bajura [1971] plotted static pressure regain coefficient in a practical range (0.1 to 0.5) of Q_3/Q_1 ratios of manifold flows for both single lateral and for laterals spaced at $4D_1$ in manifolds.The test results were those of McNown [1954].	His interpretation of the coefficient (γ_d) as zero when the flow leaves the manifold at right angles is not true and so is his $\gamma_{d=1}$ when there is no loss of axial momentum. He also studied multi laterals as a porous manifold with and without frictional effects.
(C) Shivarudrappa[1977] studied single orifices (diameters from 4mm to 14 mm) and muti orifices spaced at $3D_1$ to $16D_1$ in a G.I.main conduit of internal diameter 20 mm.	The single lateral results showed that Rd increases as the ratio Q_3/Q_1 increases to 0.5 and then decreases with further increase in Q3/Q1 to a value of about 0.7 at q=1.
(A) McNown[1954]. The Iowa experiments were carried out with 2 in.diameter brass main and two laterals of 1 in.and 1/2 in. To study the interference effects a second junction with 1 in. lateral at spacings of 4,8 and 14 conduit diameters were tested.	According to the report the results were not well defined but the variation of pressure coefficient was lesser than in single laterals by 15%, 10% and 5% for the spacings tested. It was also conluded that there was no interference effects if the spacing was $20D_1$.

Table 2.3: Major Experimental Studies In The Past

INVESTIGATORS	REMARKS
Vogel [1928], the Munich experiments. Studied sharp edged, rounded and conical entries with the aim of reducing losses at branching. He also studied rectangular Tee junctions.	Circular pipes with a 43mm main and branches varying from 15 to 43 mm were tested. The Raynolds no variation was from $5*10^3$ to $1*10^5$. Conclusion was that the loss coefficient was a function of Q3/Q1 but independant of total discharge Q1. The least loss was on the largest cone angles at the entry.
Thoma [1929] carried out tests on elbows,bends and tees.	The main pipe was 43 mm in diameter. The Reynolds no of the flow was 225,000. Produced design charts for hydraulic losses in rough and smooth pipes.
Petermann [1929]. Studied oblique angled branches Kinne [1931] partially repeated and corrected results of Vogel and Thoma	Same circular sizes as used by Vogel were tested. A saving in loss of 60% is achieved by a 45^0 branch compared to a 90^0. Kinne finalised the pressure and energy loss terms for Tees having branch to main ratio 1.
Gardel [1957]. Considered as one of the best in loss cofficients as the equations put forward encompassed branching angles, curvature of rounding and discharge coefficients.	The main pipe was 150 mm in diameter with branches ranging from 60 mm to 150 mm and inclined at 90^0, 45^0, and 135^0. Maximum Reynolds no tested was $4*10^5$. Two important results followed: (1) Whatever the shape of the Tee,there was no appreciable head loss in the main pipe till over 1/2 the flow was diverted. (2) When all the flow was diverted the main pipe acted as a total head tube measuring 0.65 of the main pipe velocity head

Table 5.1. List of Experiments Carried Out

LATERAL 1	LATERAL 2	LATERAL 3
Lat 1/21 h	Lat 2/18 v	Lat 3/2 v
Lat 1/20 h	Lat 2/10 v	Lat 3/3 v
Lat 1/19 h	Lat 2/9 v	Lat 3/4 v
Lat 1/18 h	Lat 2/11 v	Lat 3/5 v
Lat 1/12 v	Lat 2/12 v	Lat 3/6 v
Lat 1/8 v	Lat 2/13 v	Lat 3/9 v
Lat 1/10 v	Lat 2/14 v	Lat 3/7 v
Lat 1/7 v	Lat 2/15 v	Lat 3/10 v
Lat 1/14 v	Lat 2/19 v	Lat 3/8 v
Lat 1/5 v	Lat 2/8 v	Lat 3/101 v
Lat 1/15 v	Lat 2/6 v	Lat 3/100 h
Lat 1/9 v	Lat 2/5 v	Lat 3/103 h
Lat 1/11 v	Lat 2/7 v	Lat 3/102 h
Lat 1/6 v	Lat 2/4 v	Lat 3/ 104 h
Lat 1/100		
Lat 1/102		
Lat 1/103		
Lat 1/104		

Lat 1/18

Main No	Dist ft	P/γ +Z ft	US lat no	Dist ft	P/γ +Z ft	DS lat no	Dist ft	P/γ +Z ft
N 43	6.224		L 28A	-0.036	10.643	L 29A	-0.036	10.991
N 42	5.709		L 28B	0.036	10.374	L 29B	0.036	10.932
N 41	5.207		L 28C	0.074	10.351	L 29C	0.077	
N40	4.698		L 0	0.120	10.335	L30	0.120	10.580
N 39	4.357		L 1	0.163	10.325	L 31	0.161	10.650
N 38	4.108	10.988	L 11	0.204	10.351	L 32	0.205	10.600
N 37	3.845		L 2	0.247	10.384	L 33	0.246	10.590
N 36	3.517		L 3	0.289	10.328	L 34	0.288	10.520
N35	3.189	10.988	L 4	0.330	10.381	L 35	0.330	10.476
N 34	2.684	10.991	L 5	0.371	10.400	L 36	0.371	10.470
N 33	2.178		L 6	0.413		L 37	0.413	10.430
N 32	1.680	10.991	L 7	0.455	10.564	L 38	0.455	
N 31	1.171	10.974	L 8	0.497		L 39	0.498	10.531
N 30-1	0.942		L 9	0.538	10.531	L 40	0.538	
N 30	0.725	10.968	L 10	0.580		L 41	0.580	
N 29-1	0.449	11.024	L 11	0.622	10.548	L 42	0.621	10.581
N 29	0.285	11.047	L 12	0.663	10.581	L 43	0.663	
N29A	0 170	10.991	L 13	0.704		L 44	0.707	
C/L LATERAL	0.000		L 14	0.868	10.623	L 45	0.874	
N28A	-0.170	10.643	L 15	1.034	10.600	L 46	1.040	10.659
N 28	-0.285		L 16	1.201		L 47	1.207	
N 27-1	-0.449	10.807	L 17	1.368		L48	1.374	10.630
N 27	-0.696	10.814	L 18	1.534	10.620	L 49	1.540	
N 26	-0.951	10.853	L 19	1.790	10.597	L 50	1.791	
N 25	-1.444	10.860	L 20	2.044		L 51	2.044	
N 24	-1.952	10.866	N27-1	-0.300	10.807			
N 23	-2.457	10.879				N29-1	-0.299	11.024
N 22	-2.959	10.886				29T	-0.210	
N 21	-3.461							
N 20	-3.993							
N 19	-4.731							
N 18	-5.207							
N 17	-5.715							
N 16	-6.207							
N 15	-6.716							
N 14	-7.218							
N 13	-7.717							
N 12	-8.225							
N 11	-8.734							
N 10	-9.226							
N28T	-0.138							
N27T	-0.639							
N29T	0.360							

Table 5.2 (b): Manometric Heights Vs Distances Along the Walls

Lat 2/19

Main No	Dist ft	P/y+Z ft	US Lat no	Dist ft	P/y+Z ft	DS Lat	Dist ft	P/y+Z ft
17.	-5.446		Main 28A	-0.020	8.671	Main 29Y	-0.050	9.783
18	-4.970		28-B	0.036	6.070	Main 29x	-0.010	9.892
19	-4.429		L0	0.089	6.053	30-3	0.010	7.917
20.	-3.937	9.600	L1	0.151		30-2	0.030	8.533
21	-3.412	9.541	L2	0.194	6.053	30-1	0.089	7.818
22	-2.920	9.531	L3	0.233	6.155	31	0.151	7.257
23	-2.428	9.505	L4	0.276	6.398	32	0.194	6.939
24	-1.919	9.475	L5	0.318	6.742	33	0.233	6.939
25	-1.411	9.416	L6	0.358	7.100	34	0.276	
26	-0.909	9.426	L7	0.400	7.333	35	0.318	7.014
27.	-0.656	9.357	L8	0.443		36	0.358	
27-1	-0.427	9.347	L9	0.486	7.530	37	0.400	7.175
28	-0.246		L10	0.528		38	0.443	
28-1	-0.213		L11	0.568	7.644	39	0.486	7.388
28A	-0.134	8.671	L12	0.610	7.654	40	0.528	
303	0.114	7.917	L13	0.653		41	0.568	7.530
29-x	0.124	9.892	L14	0.696	7.674	42	0.610	
29-y	0.164	9.783	L15	0.735	7.661	43	0.653	7.612
29-A	0.229	9.800	L16	0.902	7.677	44	0.696	
29	0.328		L17	1.066		45	0.735	7.674
29-1	0.476	9.672	L18	1.234	7.694	46	0.902	7.684
30	0.722	9.741	L19	1.401	7.694	47	1.066	
31	1.493		L20	1.565		48	1.234	
32	1.985	9.836	L21	1.821		49	1.401	7.680
33	2.483	9.783	main27-1	-0.313	9.347	50	1.565	
34	2.985	9.803				51	1.821	
35	3.494	9.810				Main 29A	-0.115	9.800
36	3.986					main 29-1	-0.362	9.672
37	4.495	9.790						
38	4.987	9.760						
39	5.495	9.777						
40	5.987							

Table 5.3 (b): Manometric Heights Vs Distances Along the Walls

LAT 3/7v

	Main No	Dist ft	P/y+Z ft	US LAt N0	Dist ft	P/y+Z ft	DS lat No	Dist ft	P/Y+Z ft
1	17	-5.338		28B	0.036	3.556	L303	0.010	3.758
2	18	-4.846	10.787	L00	0.095	5.020	L302	0.039	6.521
3	19	-4.347		L0	0.157	6.581	L301	0.092	5.453
4	20	-3.838	10.771	L1	0.197	6.706	L30	0.157	6.217
5	21	-3.340	10.764	L2	0.240	6.677	L31	0.197	6.673
6	22	-2.815	10.755	L3	0.282	6.689	L32	0.240	6.653
7	23	-2.323	10.745	L4	0.322	6.690	L33	0.282	6.660
8	24	-1.827	10.738	L5	0.364	6.644	L34	0.322	
9	25	-1.329	10.700	L6	0.407		L35	0.364	6.627
10	26	-0.833	10.712	L7	0.449	6.627	L36	0.407	
11	27	-0.584	10.679	L8	0.489		L37	0.449	6.611
12	271	-0.335	10.663	L9	0.528	6.545	L38	0.489	
13	28	-0.171		L10	0.574		L39	0.528	6.570
14	281	-0.070	10.167	L11	0.617	6.480	L40	0.574	
15				L12	0.656		L41	0.617	6.578
16	2910	0.044	9.908	L13	0.696		L42	0.656	
17	2911	0.076	10.958	L14	0.738	6.414	L43	0.696	6.696
18	2912	0.158	10.810	L15	0.906		L44	0.738	
19	2913	0.244	10.810	L16	1.073	6.217	L45	0.906	6.348
20	290	0.303		L17	1.243		L46	1.073	6.250
21	29	0.394		L18	1.407	6.086	L47	1.243	
22	291	0.558	10.810	L19	1.571	5.912	L48	1.407	
23	30	0.820	10.860	L20	1.824		L49	1.572	
24	31	1.575		L21			L50	1.824	
25	32	2.100		Main			L51		
26	33	2.592	10.800	28A	-0.036	10.167	Main		
27	34	3.084	10.797	271	-0.300	10.663	2910	-0.010	9.908
28	35	3.576	10.778				2911	-0.043	10.958
29	36	4.068					2912	-0.125	10.810
30	37	4.560							
31	38	5.069	10.787						
32	39	5.577	10.787						
33	40	6.086	10.787						

Table 5.4 (b): Manometric Heights Vs Distances Along the Walls

Table 5.5 Representative Test Numbers and q ratios

LATERAL 1 (m=1)		LATERAL 2 (m=0.77)		LATERAL 3 (m=0.225)	
(a) Lat 1/20	q= 1	(a) Lat 2/4 v	q=1	(a) Lat 3/102h	q=1
(b) Lat 1/18 h	q=0.93	(b) Lat 2/19v	q=0.94	(b) Lat 3/7 v	q=0.89
(c) Lat 1/19 h	q=0.64	(c) Lat 2/13v	q=0.51	(c) Lat 3/5v	q=0.55
(d) Lat 1/6 v	q=0.41	(d) Lat 2/12v	q=0.38	(d) Lat 3/3v	q=0.35
(e) Lat 1/102	q=0.14	(e) Lat 2/10v	q=0.14	(e) Lat 3/2	q=0.18

Table 5.6(a):Main Parameters Lateral 1 Tests (m=1)

Description	Lat1/21h	Lat1/20h	Lat 1/19h	Lat 1/18h	Lat 1/12v
(1) V notch Readings					
Main 2 ft	0.515	0.000	0.316	0.179	0.517
Lateral ft	0.188	0.523	0.400	0.505	0.000
(2) DischargeQ cusec					
Q2 (Main)	0.132	0.000	0.040	0.010	0.134
Q3 (Lateral)	0.011	0.138	0.071	0.126	0.000
Q1 (Main)	0.144	0.138	0.111	0.136	0.134
q ratio =Q3/Q1	0.078	1.000	0.641	0.926	0.000
(3)Velocity in ft/sec					
V2 (main)	3.261	0.000	0.981	0.249	3.297
V3 (Lateral)	0.278	3.390	1.756	3.109	0.000
V1 (main)	3.559	3.411	2.753	3.379	3.297
(4) Reynolds no R					
R main 2	57769.000	0.000	17577.000	4360.000	56321.000
R Lateral	4919.000	60758.000	31462.000	54361.000	0.000
R main 1	63072.000	61129.000	49340.000	59081.000	56321.000
(5) N in power law					
N main 2	6.330		5.970	5.660	6.311
N lateral	5.880	6.350	6.110	6.300	
N main 1	6.360	6.350	6.260	6.340	6.311
(6)Velocitydeformity					
e main 2	0.249		0.265	0.269	0.250
e lateral	0.269	0.248	0.259	0.250	
e main 1	0.248	0.248	0.252	0.249	0.250
(7) Energy coeff.(a)					
a main 2	1.062		1.070	1.072	1.062
a lateral	1.072	1.062	1.067	1.063	
a main 1	1.062	1.062	1.064	1.062	1.062
(8)Momentum Coeff.B					
B Main 2	1.021		1.023	1.024	1.021
B Lateral	1.024	1.021	1.022	1.020	
B Main 1	1.021	1.021	1.021	1.021	1.021
(9) Friction Coeff f					
f(Darcy) Main 1	0.023	0.023	0.022	0.021	0.021
f(Darcy) Main 2	0.021		0.027	0.038	0.021
f(Darcy) Lateral	0.039	0.021	0.023	0.022	
(10) Pressure Coeff.					
In main Cp21	0.228	0.664	0.849	0.733	0.029
In lateral Cp13	0.000	1.218	0.425	1.015	0.029
(11) Total Energy ft					
P2+aV2^2/2g Main2	10.450	10.270	8.436	10.971	9.724
P3+aV3^2/2gLateral	10.231	10.119	8.321	10.819	9.535
P1+aV1^2/2gMain 1	10.439	10.342	8.445	11.028	9.721
(12)Energy Loss coeff					
E12 Main	-0.058	0.397	0.078	0.323	-0.016
E13 Lateral	1.055	1.231	1.055	1.177	1.092

Table 5.6(b):Main Parameters Lateral 1 Tests(m=1)

Description	Lat1/8v	Lat1/10v	Lat 1/7v	Lat 1/14v	Lat 1/5v
(1) V notch Readings					
Main 2 ft	0.323	0.295	0.448	0.000	0.527
Lateral ft	0.548	0.632	0.683	0.666	0.583
(2) DischargeQ cusec					
Q2 (Main)	0.042	0.034	0.093	0.000	0.140
Q3 (Lateral)	0.155	0.219	0.266	0.250	0.180
Q1 (Main)	0.197	0.253	0.360	0.250	0.320
q ratio =Q3/Q1	0.786	0.866	0.740	1.000	0.562
(3)Velocity in ft/sec					
V2 (main)	1.039	0.833	2.309	0.000	3.448
V3 (Lateral)	3.808	5.401	6.557	6.152	4.426
V1 (main)	4.877	6.273	8.921	6.190	7.923
(4) Reynolds no R					
R main 2	18410.000	14680.000	40687.000	0.000	59400.000
R Lateral	67478.000	95137.000	115525.000	104063.000	76260.000
R main 1	86415.000	110520.000	157168.000	104700.000	136491.000
(5) N in power law					
N main 2	5.980	5.900	6.200		6.340
N lateral	6.390	6.550	6.650	6.590	6.440
N main 1	6.500	6.630	6.820	6.590	6.740
(6)Velocitydeformity					
e main 2	0.265	0.267	0.255		0.249
e lateral	0.247	0.241	0.237	0.239	0.245
e main 1	0.243	0.238	0.231	0.239	0.234
(7) Energy coeff.(a)					
a main 2	1.070	1.072	1.065	1.000	1.060
a lateral	1.061	1.058	1.056	1.057	1.062
a main 1	1.059	1.056	1.053	1.057	1.054
(8)Momentum Coeff.B					
B Main 2	1.023	1.024	1.021	1.000	1.021
B Lateral	1.020	1.019	1.019	1.019	1.020
B Main 1	1.020	1.019	1.018	1.014	1.018
(9) Friction Coeff f					
f(Darcy) Main 1	0.019	0.018	0.017	0.019	0.017
f(Darcy) Main 2	0.028	0.029	0.022		0.020
f(Darcy) Lateral	0.021	0.019	0.020	0.017	0.025
(10) Pressure Coeff.					
In main Cp21	0.757	0.753	0.793	0.639	0.800
In lateral Cp13	0.677	0.851	0.558	1.227	0.297
(11) Total Energy ft					
P2+aV2^2/2g Main2	9.197	8.991	10.088	9.940	9.606
P3+aV3^2/2gLateral	8.888	8.453	9.035	9.451	8.653
P1+aV1^2/2gMain 1	9.291	9.131	10.321	10.189	9.658
(12)Energy Loss coeff					
E12 Main	0.252	0.285	0.189	0.419	0.053
E13 Lateral	1.089	1.123	1.041	1.240	1.031

Table 5.6(c):Main Parameters Lateral 1 Tests(m=1)

Description	Lat1/15v	Lat1/9v	Lat 1/11v	Lat 1/6v
(1) V notch Readings				
Main 2 ft	0.300	0.479	0.480	0.563
Lateral ft	0.816	0.624	0.412	0.528
(2) DischargeQ cusec				
Q2 (Main)	0.035	0.111	0.111	0.165
Q3 (Lateral)	0.413	0.213	0.077	0.141
Q1 (Main)	0.449	0.324	0.188	0.306
q ratio =Q3/Q1	0.920	0.656	0.407	0.410
(3)Velocity in ft/sec				
V2 (main)	0.870	2.744	2.744	4.072
V3 (Lateral)	10.173	5.243	1.889	3.469
V1 (main)	11.111	8.037	4.661	7.588
(4) Reynolds no R				
R main 2	14990.000	48346.000	50195.000	71747.000
R Lateral	175250.000	92379.000	34555.000	61123.000
R main 1	191400.000	141586.000	85269.000	133680.000
(5) N in power law				
N main 2	5.940	6.260	6.270	6.400
N lateral	6.880	6.540	6.140	6.350
N main 1	6.930	6.760	6.500	6.700
(6)Velocitydeformity				
e main 2	0.267	0.252	0.252	0.246
e lateral	0.229	0.241	0.258	0.249
e main 1	0.227	0.232	0.243	0.235
(7) Energy coeff.(a)				
a main 2	1.071	1.064	1.063	1.061
a lateral	1.052	1.058	1.066	1.062
a main 1	1.051	1.054	1.059	1.055
(8)Momentum Coeff.B				
B Main 2	1.024	1.021	1.021	1.020
B Lateral	1.017	1.019	1.022	1.021
B Main 1	1.017	1.018	1.019	1.018
(9) Friction Coeff f				
f(Darcy) Main 1	0.016	0.018	0.019	0.017
f(Darcy) Main 2	0.028	0.022	0.022	0.022
f(Darcy) Lateral	0.017	0.020	0.023	0.022
(10) Pressure Coeff.				
In main Cp21	0.715	0.797	0.711	0.772
In lateral Cp13	1.059	0.419	0.118	0.168
(11) Total Energy ft				
P2+aV2^2/2g Main2	10.613	10.074	9.794	3.553
P3+aV3^2/2gLateral	8.891	9.182	9.449	2.638
P1+aV1^2/2gMain 1	11.246	10.207	9.787	3.534
(12)Energy Loss coeff				
E12 Main	0.330	0.133	-0.021	-0.022
E13 Lateral	1.228	1.022	1.002	1.001

Table 5.6(d):Main Parameters Lateral 1 Tests(m=1)

Description	Lat1/100	Lat1/102	Lat 1/103	Lat 1/104
(1) V notch Readings				
Main 2 ft	0.650	0.637	0.619	0.416
Lateral ft	0.201	0.305	0.380	0.535
(2) DischargeQ cusec				
Q2 (Main)	0.238	0.224	0.209	0.078
Q3 (Lateral)	0.013	0.037	0.063	0.146
Q1 (Main)	0.249	0.261	0.271	0.224
q ratio =Q3/Q1	0.053	0.141	0.231	0.650
(3)Velocity in ft/sec				
V2 (main)	5.798	5.513	5.135	1.930
V3 (Lateral)	0.328	0.905	1.541	3.593
V1 (main)	6.164	6.458	6.718	5.557
(4) Reynolds no R				
R main 2	102127.000	97130.000	90470.000	34003.000
R Lateral	5778.000	15950.000	27145.000	63298.000
R main 1	108565.000	113770.000	118340.000	97869.000
(5) N in power law				
N main 2	6.600	6.550	6.530	6.140
N lateral	5.880	5.970	6.100	6.360
N main 1	6.630	6.630	6.650	6.550
(6)Velocitydeformity				
e main 2	0.239	0.241	0.241	0.258
e lateral	0.269	0.265	0.259	0.248
e main 1	0.238	0.238	0.237	0.241
(7) Energy coeff.(a)				
a main 2	1.057	1.057	1.058	1.066
a lateral	1.072	1.070	1.067	1.061
a main 1	1.056	1.056	1.056	1.058
(8)Momentum Coeff.B				
B Main 2	1.019	1.019	1.019	1.022
B Lateral	1.020	1.023	1.022	1.021
B Main 1	1.013	1.018	1.019	1.019
(9) Friction Coeff f				
f(Darcy) Main 1	0.017	0.016	0.018	0.019
f(Darcy) Main 2	0.018	0.018	0.023	0.025
f(Darcy) Lateral	0.045	0.029	0.025	0.019
(10) Pressure Coeff.				
In main Cp21	0.135	0.324	0.442	0.772
In lateral Cp13	-0.008	-0.031	0.142	0.500
(11) Total Energy ft				
P2+aV2^2/2g Main2	5.392	4.839	4.153	6.920
P3+aV3^2/2gLateral	4.747	4.164	3.349	6.463
P1+aV1^2/2gMain 1	5.363	4.814	4.153	6.997
(12)Energy Loss coeff				
E12 Main	-0.048	-0.038	-0.004	0.158
E13 Lateral	1.045	1.005	1.143	1.114

Table 5.7(a):Main Parameters Lateral 2 Tests (m=0.77)

Description	Lat 2/18v	Lat2/10v	Lat 2/9v	Lat 2/11v	Lat 2/12v
(1) V notch Readings					
Main 2 ft	0.588	0.672	0.510	0.639	0.665
Lateral ft	0.000	0.317	0.349	0.490	0.547
(2) DischargeQ cusec					
Q2 (Main)	0.184	0.256	0.130	0.226	0.250
Q3 (Lateral)	0.000	0.040	0.051	0.117	0.153
Q1 (Main)	0.184	0.296	0.181	0.343	0.403
q ratio =Q3/Q1	0.000	0.140	0.280	0.340	0.380
(3)Velocity in ft/sec					
V2 (main)	4.522	6.296	3.194	5.570	6.144
V3 (Lateral)	0.000	1.288	1.635	3.755	4.921
V1 (main)	4.551	7.331	4.480	8.511	9.992
(4) Reynolds no R					
R main 2	87801.000	112293.000	56275.000	100594.000	115218.000
R Lateral	0.000	21011.000	26350.000	62054.000	84407.000
R main 1	87614.000	130760.000	78917.000	153720.000	187348.000
(5) N in power law					
N main 2	6.500	6.620	6.300	6.600	6.620
N lateral	0.000	6.000	6.100	6.300	6.500
N main 1	6.500	6.700	6.400	6.800	6.930
(6)Velocitydeformity					
e main 2	0.243	0.238	0.251	0.239	0.238
e lateral	0.000	0.264	0.259	0.251	0.242
e main 1	0.243	0.235	0.247	0.231	0.227
(7) Energy coeff.(a)					
a main 2	1.059	1.057	1.063	1.057	1.057
a lateral		1.070	1.067	1.063	1.059
a main 1	1.059	1.055	1.061	1.053	1.051
(8)Momentum Coeff.B					
B Main 2	1.020	1.019	1.021	1.019	1.019
B Lateral		1.023	1.022	1.020	1.020
B Main 1	1.020	1.018	1.020	1.019	1.017
(9) Friction Coeff f					
f(Darcy) Main 1	0.019	0.017	0.021	0.017	0.017
f(Darcy) Main 2	0.019	0.018	0.021	0.019	0.018
f(Darcy) Lateral		0.027	0.033	0.023	0.018
(10) Pressure Coeff.					
In main Cp21	0.000	0.288	0.577	0.666	0.677
In lateral Cp13	0.000	0.024	0.096	0.178	0.245
(11) Total Energy ft					
P2+aV2^2/2g Main2	9.596	10.810	8.418	10.809	10.170
P3+aV3^2/2gLateral	9.260	9.928	8.084	9.583	10.130
P1+aV1^2/2gMain 1	9.600	10.800	8.400	10.735	8.518
(12)Energy Loss coeff					
E12 Main	0.013	-0.060	-0.057	-0.066	-0.025
E13 Lateral	1.059	1.046	1.015	1.024	1.040

Table 5.7(b):Main Parameters Lateral 2 Tests (m=0.77)

Description	Lat 2/13v	Lat2/14v	Lat 2/15v	Lat 2/19v	Lat 2/8v
(1) V notch Readings					
Main 2 ft	0.653	0.494	0.368	0.212	0.000
Lateral ft	0.660	0.666	0.681	0.675	0.855
(2) DischargeQ cusec					
Q2 (Main)	0.238	0.120	0.057	0.015	0.000
Q3 (Lateral)	0.245	0.250	0.264	0.258	0.465
Q1 (Main)	0.483	0.370	0.322	0.274	0.465
q ratio =Q3/Q1	0.507	0.676	0.820	0.940	1.000
(3)Velocity in ft/sec					
V2 (main)	5.868	2.947	1.414	0.374	0.000
V3 (Lateral)	7.841	8.006	8.472	8.272	14.875
V1 (main)	11.974	9.163	7.981	6.779	11.515
(4) Reynolds no R					
R main 2	114509.000	57517.000	27222.000	7196.000	0.000
R Lateral	139987.000	142929.000	149226.000	145696.000	226268.000
R main 1	233666.000	178815.000	153663.000	130528.000	191468.000
(5) N in power law					
N main 2	6.600	6.300	6.000	5.900	0.000
N lateral	5.900	6.700	6.700	6.700	7.000
N main 1	6.000	6.800	6.800	6.650	6.900
(6)Velocitydeformity					
e main 2	0.238	0.250	0.264	0.269	
e lateral	0.268	0.235	0.235	0.235	0.224
e main 1	0.263	0.231	0.231	0.237	0.227
(7) Energy coeff.(a)					
a main 2	1.057	1.062	1.069	1.072	
a lateral	1.072	1.055	1.055	1.055	1.050
a main 1	1.070	1.053	1.054	1.056	1.052
(8)Momentum Coeff.B					
B Main 2	1.019	1.021	1.023	1.024	
B Lateral	1.024	1.018	1.018	1.018	1.017
B Main 1	1.023	1.018	1.018	1.019	1.017
(9) Friction Coeff f					
f(Darcy) Main 1	0.016	0.016	0.017	0.018	0.016
f(Darcy) Main 2	0.017	0.021	0.027	0.005	
f(Darcy) Lateral	0.018	0.017	0.017	0.016	0.015
(10) Pressure Coeff.					
In main Cp21	0.764	0.767	0.728	0.658	0.583
In lateral Cp13	0.516	1.074	1.617	2.158	2.186
(11) Total Energy ft					
P2+aV2^2/2g Main2	10.815	10.243	9.303	9.812	15.300
P3+aV3^2/2gLateral	8.424	8.750	8.126	8.921	13.209
P1+aV1^2/2gMain 1	10.931	10.474	9.592	10.093	16.265
12)Energy Loss coeff					
E12 Main	0.052	0.177	0.292	0.394	0.469
E13 Lateral	1.126	1.322	1.482	1.643	1.485

Table 5.7(c):Main Parameters Lateral 2 Tests (m=0.77)

Description	Lat 2/6v	Lat2/5v	Lat 2/7v	Lat 2/4v
(1) V notch Readings				
Main 2 ft	0.000	0.000	0.000	0.000
Lateral ft	0.503	0.751	0.507	0.568
(2) Discharge Q cusec				
Q2 (Main)	0.000	0.000	0.000	0.000
Q3 (Lateral)	0.125	0.337	0.128	0.169
Q1 (Main)	0.125	0.337	0.128	0.169
q ratio =Q3/Q1	1.000	1.000	1.000	1.000
(3)Velocity in ft/sec				
V2 (main)	0.000	0.000	0.000	0.000
V3 (Lateral)	4.000	10.776	4.093	5.408
V1 (main)	3.098	8.342	3.168	4.186
(4) Reynolds no R				
R main 2	0.000	0.000	0.000	0.000
R Lateral	58380.000	151128.000	61220.000	73487.000
R main 1	49401.000	127885.000	51804.000	62185.000
(5) N in power law				
N main 2	0.000	0.000		
N lateral	6.300	6.800	6.300	6.400
N main 1	6.300	6.700	6.200	6.300
(6)Velocitydeformity				
e main 2				
e lateral	0.251	0.231	0.251	0.246
e main 1	0.251	0.235	0.254	0.251
(7) Energy coeff.(a)				
a main 2				
a lateral	1.063	1.053	1.063	1.061
a main 1	1.063	1.055	1.065	1.063
(8)Momentum Coeff.B				
B Main 2				
B Lateral	1.021	1.012	1.021	1.020
B Main 1	1.021	1.013	1.021	1.021
(9) Friction Coeff f				
f(Darcy) Main 1	0.022	0.017	0.018	0.021
f(Darcy) Main 2				
f(Darcy) Lateral	0.021	0.019	0.030	0.022
(10) Pressure Coeff.				
In main Cp21	0.671	0.648	0.641	0.625
In lateral Cp13	2.415	2.313	2.566	2.278
(11) Total Energy ft				
P2+aV2^2/2g Main2	8.300	12.600	8.860	10.240
P3+aV3^2/2gLateral	8.104	11.299	8.636	9.932
P1+aV1^2/2gMain 1	8.358	13.040	8.926	10.359
12)Energy Loss coeff				
E12 Main	0.392	0.407	0.423	0.438
E13 Lateral	1.705	1.611	1.857	1.571

Table 5.8(a):Main Parameters Lateral 3 Tests (m=0.225)

Description	Lat 3/2 V	Lat 3/3 v	Lat 3/4v	Lat 3/5v	Lat 3/6v
(1) V notch Readings					
Main 2 ft	0.607	0.622	0.554	0.434	0.330
Lateral ft	0.330	0.483	0.464	0.468	0.479
(2)Discharge Q cusec					
Q2 Main2	0.199	0.212	0.159	0.087	0.044
Q3 Lateral	0.044	0.113	0.102	0 104	0.111
Q1 Main1	0.243	0.325	0.261	0.191	0.155
q ratio =Q3/Q1	0.182	0.348	0.390	0.546	0.713
(3) Velocity in ft/sec					
V2 Main2	4.909	5.210	3.916	2.139	1.097
V3 Lateral	4.848	12.375	11.189	11.444	12.108
V1 Main1	6.038	8.045	6.474	4.743	3.848
(4) Reynolds no R					
R Main 2	89800.000	98976.000	75403.000	41173.000	21117.000
R Lateral	42850.000	113607.000	104099.000	106473.000	112643.000
R Main 1	110430.000	152837.000	124662.000	91336.000	74050.000
(5) N in power law					
N Main 2	6.520	6.600	6.400	6.200	6.000
N Lateral	6.200	6.640	6.600	6.600	6.630
N Main 1	6.620	6.800	6.900	6.500	6.400
(6)Velocitydeformity					
e main 2	0.242	0.239	0.247	0.255	0.264
e lateral	0.255	0.237	0.239	0.239	0.238
e main 1	0.238	0.231	0.228	0.242	0.247
(7) Energy coeff.(a)					
a Main 2	1.058	1.057	1.060	1.065	1.069
a Lateral	1.065	1.056	1.057	1.057	1.056
a Main 1	1.057	1.053	1.052	1.059	1.060
(8)Momentum Coeff.B					
B Main 2	1.019	1.019	1.020	1.022	1.023
B Lateral	1.022	1.018	1.019	1.019	1.019
B Main 1	1.019	1.018	1.017	1.020	1.020
(9) Friction Coeff f					
f(Darcy) Main 1	0.016	0.017	0.017	0.019	0.020
f (Darcy) Main 2	0.020	0.018	0.020	0.023	0.027
f(Darcy) Lateral	0.025	0.019	0.019	0.018	0.018
(10) Pressure Coeff.					
In Main Cp21	0.353	0.547	0.614	0.715	0.740
In Lateral Cp13	1.060	3.781	4.960	9.472	15.716
(11) Total Energy ft					
P2+aV2^2/2g Main 2	8.496	10.795	9.682	10.936	11.998
P3+aV3^2/2gLateral	7.689	8.512	7.855	9.450	10.605
P1+aV1^2/2g Main1	8.498	10.859	9.715	10.980	12.054
12)Energy Loss coeff					
E12 Main	0.003	0.063	0.049	0.127	0.233
E13 Lateral	1.430	2.346	2.857	4.379	6.307

Table 5.8(b):Main Parameters Lateral 3 Tests (m=0.225)

Description	Lat 3/9 V	Lat 3/7 v	Lat 3/10 v	Lat 3/8v	Lat 3/101 v
(1) V notch Readings					
Main 2 ft	0.234	0.204	0.155	0.000	0.201
Lateral ft	0.408	0.486	0.465	0.481	0.486
(2) DischargeQ cusec					
Q2 (Main)	0.019	0.014	0.007	0.000	0.013
Q3 (Lateral)	0.075	0.115	0.103	0.112	0.115
Q1 (Main)	0.094	0.129	0.110	0.112	0.128
q ratio =Q3/Q1	0.795	0.892	0.935	1.000	0.900
(3)Velocity in ft/sec					
V2 (main)	0.473	0.341	0.175	0.000	0.327
V3 (Lateral)	8.180	12.583	11.267	12.231	12.562
V1 (main)	2.329	3.193	2.728	2.770	3.174
(4) Reynolds no R					
R main 2	9105.000	6568.000	3371.000	0.000	5790.000
R Lateral	76102.000	117068.000	104826.000	115335.000	107550.000
R main 1	44835.000	61486.000	52531.000	54065.000	56241.000
(5) N in power law					
N main 2	5.800	5.900	5.900	0.000	6.000
N lateral	6.500	6.660	6.600	6.600	7.000
N main 1	6.200	6.350	6.300	6.300	6.600
(6)Velocitydeformity					
e main 2	0.273	0.269	0.269	0.000	0.264
e lateral	0.243	0.236	0.239	0.239	0.224
e main 1	0.255	0.249	0.251	0.251	0.239
(7) Energy coeff.(a)					
a main 2	1.075	1.072	1.072	1.000	1.069
a lateral	1.059	1.056	1.057	1.057	1.050
a main 1	1.065	1.062	1.062	1.063	1.057
(8)Momentum Coeff.B					
B Main 2	1.025	1.024	1.024	1.000	1.023
B Lateral	1.020	1.019	1.014	1.019	1.017
B Main 1	1.022	1.020	1.021	1.021	1.019
(9) Friction Coeff f					
f(Darcy) Main 1	0.022	0.021	0.021	0.021	0.021
f(Darcy) Main 2	0.032	0.031	0.043		0.039
f(Darcy) Lateral	0.017	0.020	0.018	0.017	0.018
(10) Pressure Coeff.					
In main Cp21	0.713	0.694	0.692	0.671	0.703
In lateral Cp13	20.307	24.626	26.990	30.540	23.583
(11) Total Energy ft					
P2+aV2^2/2g Main2	7.074	10.811	10.700	10.267	8.202
P3+aV3^2/2gLateral	6.400	9.396	9.584	8.955	6.974
P1+aV1^2/2gMain 1	7.100	10.868	10.743	10.267	8.255
(12)Energy Loss coeff					
E12 Main	0.308	0.355	0.366	0.392	0.343
E13 Lateral	8.307	9.396	10.027	11.003	8.189

Table 5.8(c):Main Parameters Lateral 3 Tests (m=0.225)

Description	Lat 3/100h	Lat 3/103h	Lat 3/102h	Lat 3/104 h
(1) V notch Readings				
Main 2 ft	0.457	0.581	0.000	0.645
Lateral ft	0.481	0.000	0.494	0.174
(2) DischargeQ cusec				
Q2 (Main)	0.099	0.178	0.000	0.231
Q3 (Lateral)	0.112	0.000	0.120	0.009
Q1 (Main)	0.211	0.178	0.120	0.241
q ratio =Q3/Q1	0.530	0.000	1.000	0.040
(3)Velocity in ft/sec				
V2 (main)	2.437	4.390	0.000	5.690
V3 (Lateral)	12.251	0.000	13.113	1.030
V1 (main)	5.227	4.390	2.970	5.959
(4) Reynolds no R				
R main 2	43169.000	77267.000	0.000	100825.000
R Lateral	104887.000	0.000	112262.000	8829.000
R main 1	92600.000	77267.000	52624.000	105581.000
(5) N in power law				
N main 2	6.000	6.400	0.000	6.600
N lateral	5.900	0.000	7.000	5.900
N main 1	6.600	6.400	6.700	6.600
(6)Velocitydeformity				
e main 2	0.263	0.247		0.239
e lateral	0.269	0.000	0.224	0.269
e main 1	0.239	0.247	0.235	0.239
(7) Energy coeff.(a)				
a main 2	1.070	1.069	1.000	1.057
a lateral	1.072		1.050	1.072
a main 1	1.057	1.061	1.055	1.057
8)Momentum Coeff.B				
B Main 2	1.023	1.020	1.000	1.019
B Lateral	1.024		1.011	1.024
B Main 1	1.019	1.020	1.013	1.014
(9) Friction Coeff f				
f(Darcy) Main 1	0.019	0.020	0.023	0.022
f(Darcy) Main 2	0.020	0.020		0.019
f(Darcy) Lateral	0.014		0.017	0.033
10) Pressure Coeff.				
In main Cp21	0.684	0.000	0.656	0.109
In lateral Cp13	8.628	-0.033	29.640	0.054
(11) Total Energy ft				
P2+aV2^2/2g Main2	8.142	7.787	8.997	5.721
'3+aV3^2/2gLateral	6.431	7.480	7.604	5.117
P1+aV1^2/2gMain 1	8.184	7.791	9.000	5.713
2)Energy Loss coeff				
E12 Main	0.141	0.013	0.398	-0.015
E13 Lateral	3.794	1.027	10.219	1.079

Table 5.9(a): Summary of More Parameters Lateral 1 (m=1)

Expt No	q	Cp21	E12(with a)	E13 (with a)	Rm	Rf	Ca	E13 from Ca
1/21h	0.078	0.229	-0.058	1.055	0.640	0.781	0.074	0.954
1/20h	1.000	0.664	0.397	1.231	0.692	0.704	0.484	1.123
1/19h	0.641	0.849	0.078	1.055	0.732	0.799	0.396	0.946
1/18h	0.926	0.733	0.323	1.177	0.704	0.796	0.464	1.133
1/12v	0.000	0.029	-0.016	1.092	0.000	0.000	0.000	0.000
1/8v	0.790	0.758	0.252	1.089	0.761	0.808	0.439	0.999
1/10v	0.866	0.753	0.285	1.123	0.725	0.750	0.463	0.999
1/7v	0.740	0.793	0.189	1.041	0.752	0.733	0.434	0.917
1/14v	1.000	0.639	0.419	1.240	0.704	0.760	0.486	1.105
1/5v	0.562	0.800	0.053	1.031	0.760	0.752	0.360	0.987
1/15v	0.921	0.715	0.330	1.228	0.714	0.759	0.473	1.039
1/9v	0.656	0.850	0.133	1.022	0.766	0.662	0.405	0.915
1/11v	0.150	0.387			0.595	0.463	0.136	
1/6v	0.408	0.711	-0.021	1.002	0.765	0.779	0.292	0.960
1/30	0.460	0.771	-0.022	1.001	0.740	0.733	0.321	0.935
1/100	0.054	0.169	-0.048	1.045	0.608	0.424	0.050	1.014
1/102	0.141	0.324	-0.038	1.005	0.811	0.770	0.133	0.895
1/103	0.231	0.442	-0.005	1.143	0.879	0.466	0.189	0.966
1/104	0.650	0.771	0.158	1.114	0.789	0.860	0.393	0.997

Table 5.9(b): Summary of More Parameters Lateral 1 (m=1)

Expt No	q	Cp13	Cp3j	n	n^2	H	Cp3j/H	1-n^2
1/21h	0.078	0.000	0.051	0.948	0.899	1.112	0.046	0.101
1/20h	1.000	1.218	1.937	0.487	0.237	4.219	0.459	0.763
1/19h	0.641	0.425	1.105	0.621	0.386	2.591	0.394	0.614
1/18h	0.926	1.015	1.861	0.504	0.254	3.937	0.473	0.746
1/12v	0.000	0.000	0.000	1.000	1.000	1.000	0.000	0.000
1/8v	0.790	0.677	1.435	0.562	0.315	3.171	0.453	0.685
1/10v	0.866	0.851	1.554	0.537	0.289	3.460	0.449	0.711
1/7v	0.740	0.558	1.254	0.591	0.349	2.865	0.438	0.651
1/14v	1.000	1.227	1.900	0.489	0.239	4.184	0.454	0.761
1/5v	0.562	0.297	1.057	0.644	0.415	2.410	0.439	0.585
1/15v	0.921	1.059	1.633	0.517	0.267	3.745	0.436	0.733
1/9v	0.656	0.419	1.117	0.621	0.386	2.589	0.431	0.614
1/11v	0.150							
1/6v	0.408	0.119	0.741	0.722	0.521	1.919	0.386	0.479
1/30	0.460	0.168	0.805	0.702	0.493	2.028	0.397	0.507
1/100	0.054	-0.005	0.072	0.943	0.890	1.124	0.064	0.110
1/102	0.141	-0.031	0.154	0.921	0.847	1.181	0.130	0.153
1/103	0.231	0.143	0.271	0.824	0.680	1.471	0.184	0.320
1/104	0.650	0.500	1.147	0.608	0.370	2.703	0.424	0.630
								0.000

Table 5.9(c): Summary of More Parameters Lateral 1 (m=1)

Expt no	q	E13 (no a)	E12(no a)	Ca/(1-n^2)	K1 Eqn(5.35)	Cd(free vortex
1/21h	0.078	0.994	-0.067	0.732	0.611	0.077
1/20h	1.000	1.230	0.336	0.634	0.590	0.530
1/19h	0.641	1.108	0.023	0.645	0.603	0.416
1/18h	0.926	1.169	0.261	0.621	0.584	0.525
1/12v	0.000	1.091	-0.017			0.000
1/8v	0.790	1.067	0.196	0.641	0.612	0.479
1/10v	0.866	1.109	0.230	0.651	0.605	0.494
1/7v	0.740	1.018	0.140	0.667	0.621	0.451
1/14v	1.000	1.239	0.361	0.638	0.595	0.533
1/5v	0.562	1.031	0.053	0.616	0.608	0.384
1/15v	0.921	1.221	0.279	0.646	0.600	0.508
1/9v	0.656	0.993	0.086	0.661	0.625	0.417
1/11v	0.150	1.059	-0.091			
1/6v	0.408	0.954	-0.021	0.611	0.625	0.310
1/30	0.460	0.959	-0.022	0.633	0.611	0.334
1/100	0.054	0.992	-0.054	0.454	0.576	0.051
1/102	0.141	0.949	-0.053	0.846	0.758	0.129
1/103	0.231	1.090	-0.027	0.592	0.749	0.190
1/104	0.650	1.082	0.108	0.624	0.620	0.413

Table 5.10(a): Summary of More Parameters Lateral 2 (m=0.77)

Expt No	q	Cp21	E12 (with a)	E13 (with a)	Rm	Rf	Cc	E13 from Cc
Lat 2/18V	0.000	0.000	0.013	1.058	0.000	0.000	0.000	0.000
Lat 2/10V	0.140	0.335	-0.060	1.046	0.694	0.590	0.147	1.038
Lat 2/9V	0.280	0.577	-0.057	1.015	0.756	0.514	0.300	0.724
Lat 2/11v	0.340	0.667	-0.066	1.024	0.731	0.785	0.320	0.883
Lat 2/12V	0.380	0.677	-0.025	1.040	0.774	0.851	0.341	0.904
2/13V	0.507	0.764	0.052	1.126	0.787	0.830	0.399	0.971
2/14V	0.676	0.767	0.177	1.322	0.786	0.855	0.457	1.081
2/15v	0.820	0.728	0.292	1.482	0.761	0.825	0.490	1.221
2/19V	0.940	0.658	0.394	1.643	0.731	0.820	0.513	1.346
Lat 2/8v	1.000	0.583	0.469	1.485	0.730	0.814	0.542	1.196
Lat 2/6V	1.000	0.670	0.392	1.705	0.690	0.787	0.529	1.322
lat 2/5v	1.000	0.648	0.407	1.611	0.700	0.806	0.528	1.330
Lat 2/7v	1.000	0.641	0.423	1.857	0.700	0.753	0.516	1.465
Lat 2/4V	1.000	0.625	0.438	1.571	0.713	0.738	0.525	1.369

Table 5.10(b) Summary of More Parameters Lateral 2 (m=0.77)

Expt No	q	Cp13	Cp3j	n	n^2	H	Cp3j/H	1-n^2
Lat 2/18V	0.000	0.000	0.000	1.000	1.000	1.000	0.000	0.000
Lat 2/10V	0.140	0.024	0.347	0.837	0.701	1.427	0.243	0.299
Lat 2/9V	0.280	0.096	0.321	0.823	0.677	1.477	0.217	0.323
Lat 2/11v	0.340	0.178	0.676	0.724	0.524	1.908	0.354	0.476
Lat 2/12V	0.380	0.245	0.787	0.693	0.480	2.083	0.378	0.520
2/13V	0.507	0.517	1.105	0.610	0.372	2.688	0.411	0.628
2/14V	0.676	1.074	1.534	0.522	0.273	3.663	0.419	0.727
2/15v	0.820	1.618	2.022	0.462	0.213	4.695	0.431	0.787
2/19V	0.945	2.158	2.452	0.420	0.176	5.682	0.432	0.824
Lat 2/8v	1.000	2.186	2.453	0.419	0.176	5.692	0.431	0.824
Lat 2/6V	1.000	2.415	2.482	0.409	0.168	5.963	0.416	0.832
lat 2/5v	1.000	2.313	2.609	0.409	0.167	5.988	0.436	0.833
Lat 2/7v	1.000	2.566	2.630	0.400	0.160	6.262	0.420	0.840
Lat 2/4V	1.000	2.278	2.719	0.406	0.165	6.061	0.449	0.835
					1.000			0.000
								0.000

Table 5.10(c): Summary of More Parameters Lateral 2 (m=0.77)

EXPT No	q	E13(no a)	E12 (no a)	Ca/(1-n^2)	K1 Eq.(5.35)	Cd(free vortex)	1/n^2	1+Cp13	H(1+Cp13)
Lat 2/18V	0.000	1.000	0.012		0.000	0.000	1.000	1.000	1.000
Lat 2/10V	0.140	0.993	-0.073	0.492	0.777	0.150	1.427	1.024	1.461
Lat 2/9V	0.280	0.963	-0.086	0.928	0.690		1.477	1.096	1.619
Lat 2/11v	0.340	0.983	-0.095	0.671	0.618	0.334	1.908	1.178	2.248
Lat 2/12V	0.380	1.003	-0.055	0.656	0.635	0.354	2.083	1.245	2.594
Lat 2/13V	0.507	1.087	-0.004	0.635	0.624	0.427	2.688	1.517	4.078
Lat 2/14V	0.676	1.310	0.130	0.628	0.614	0.489	3.663	2.074	7.597
Lat 2/15v	0.820	1.491	0.241	0.623	0.603	0.522	4.695	2.618	12.291
Lat 2/19V	0.945	1.669	0.338	0.622	0.598	0.549	5.682	3.158	17.943
Lat 2/8v	1.000	1.517	0.417	0.657	0.622	0.571	5.692	3.186	18.130
Lat 2/6V	1.000	1.747	0.329	0.636	0.600	0.560	5.963	3.415	20.364
lat 2/5v	1.000	1.644	0.352	0.634	0.601	0.545	5.988	3.313	19.838
Lat 2/7v	1.000	1.897	0.358	0.614	0.588	0.558	6.262	3.566	22.329
Lat 2/4V	1.000	1.609	0.375	0.628	0.599	0.584	6.061	3.278	19.867

Table 5.11(a): Summary of More Parameters Lateral 3 (m=0.225)

Expt No	q	Cp21	E12 (with a)	E13 (with a)	Rm	Rf	Cc (Min.Pres)	E13 from Cc
	0.000	0.000			0.000	0.000	0.000	0.000
Lat 3/2v	0.180	0.353	0.003	1.429	0.930	0.850	0.407	1.363
Lat 3/3v	0.350	0.547	0.062	2.346	0.910	0.735	0.533	1.857
Lat 3/4V	0.390	0.614	0.049	2.857	0.866	0.820	0.525	2.453
Lat 3/5v	0.546	0.715	0.127	4.379	0.836	0.712	0.554	3.764
Lat 3/6v	0.710	0.740	0.233	6.307	0.800	0.850	0.568	5.729
Lat 3/9v	0.796	0.710	0.308	8.307	0.790	0.800	0.574	6.777
Lat 3/7v	0.890	0.700	0.354	9.396	0.750	0.900	0.581	8.033
Lat 3/10v	0.935	0.692	0.366	10.027	0.720	0.898	0.580	9.100
Lat 3/8v	1.000	0.672	0.391	11.000	0.690	0.700	0.583	10.014
Lat 3/101h	0.900	0.703	0.342	8.189	0.737	0.836	0.602	6.829
Lat 3/100h	0.530	0.684	0.141	3.794	0.860	0.893	0.577	2.960
Lat 3/103h	0.000	0.000	0.013	1.020	0.000	0.000	0.000	1.000
Lat 3/102h	1.000	0.657	0.390	10.219	0.680	0.910	0.608	8.050
Lat 3/104	0.039	0.109	-0.016	1.079	0.906	0.775	0.143	1.068

Table 5.11(b): Summary of More Parameters Lateral 3 (m=0.225)

EXPT no	q	Cp13	Cp3j	n	n^2	1-n^2	H=(1/n^2)	Cp3j/H
	0.000	0.000	0.000	1.000	1.000	0.000	1.000	0.000
Lat 3/2v	0.180	1.059	1.766	0.507	0.257	0.743	3.891	0.454
Lat 3/3v	0.350	3.781	3.582	0.344	0.119	0.881	8.403	0.426
Lat 3/4V	0.390	4.961	4.839	0.304	0.092	0.908	10.870	0.445
Lat 3/5v	0.546	9.472	8.413	0.229	0.053	0.947	18.868	0.446
Lat 3/6v	0.710	15.716	13.930	0.180	0.033	0.967	30.303	0.460
Lat 3/9v	0.796	20.307	16.030	0.163	0.026	0.974	38.462	0.417
Lat 3/7v	0.890	24.626	20.206	0.147	0.022	0.978	46.083	0.438
Lat 3/10v	0.935	26.990	23.010	0.139	0.020	0.980	51.282	0.449
Lat 3/8v	1.000	30.541	25.840	0.132	0.017	0.983	57.471	0.450
Lat 3/101h	0.900	23.580	18.533	0.152	0.023	0.977	43.478	0.426
Lat 3/100h	0.530	8.628	6.837	0.246	0.061	0.939	16.393	0.417
Lat 3/103h	0.000	0.000	0.000	1.000	1.000	0.000	1.000	0.000
Lat 3/102h	1.000	29.640	21.900	0.138	0.019	0.981	52.632	0.416
Lat 3/104	0.039	0.054	0.344	0.829	0.687	0.313	1.456	0.236
						0.000		

Table 5.11(c): Summary of More Parameters Lateral 2 (m=0.77)

Expt No	q	E12(no a)	E13 (no a)	Cc/(1-n^2)	K1(Eq.5.35.)	Cd(free votex)	1+Cp13	H(1+Cp13)
	0.000	0.000				0.000	1.000	1.000
Lat 3/2v	0.180	-0.014	1.415	0.549	0.620	0.442	2.059	8.012
Lat 3/3v	0.350	0.033	2.415	0.602	0.616	0.581	4.781	40.176
Lat 3/4V	0.390	0.020	2.975	0.578	0.587	0.576	5.961	64.793
Lat 3/5v	0.546	0.080	4.651	0.585	0.588	0.614	10.472	197.585
Lat 3/6v	0.710	0.178	6.806	0.587	0.586	0.629	16.716	506.545
Lat 3/9v	0.796	0.246	8.968	0.590	0.588	0.642	21.307	819.500
Lat 3/7v	0.890	0.294	10.100	0.595	0.592	0.632	25.626	1180.922
Lat 3/10v	0.935	0.304	10.937	0.589	0.586	0.635	27.990	1435.385
Lat 3/8v	1.000	0.328	12.051	0.590	0.590	0.631	31.541	1812.701
Lat 3/101h	0.900	0.286	8.921	0.616	0.613	0.657	24.580	1068.696
Lat 3/100h	0.530	0.099	4.133	0.613	0.614	0.650	9.628	157.836
Lat 3/103h	0.000	0.012	0.967			0.000	1.000	1.000
Lat 3/102h	1.000	0.398	11.150	0.620	0.616	0.660	30.640	1612.632
Lat 3/104	0.039	-0.021	1.024	0.458	0.765	0.146	1.054	1.535

Table. 5.12: Observed Stagnation Points

LATERAL 1 (m=1)		LATERAL 2 (m=0.77)		LATERAL3 (m=0.225)	
q	Stagn Z/b	q	Stagn Z/b	q	Stagn Z/b
1	-0.233	1	-0.167	1	-0.3
0.93	-0.483	0.82	-0.033	0.55	-0.133
0.74	-0.133	0.38	0.033	0.35	-0.133
0.64	0.133	0.14	0.033	0.18	0.0
0.41	0.133			0.04	0.033
0.23	0.10				

Table 5.13: Critical Discharge Ratio q_{cr} (By potential flow theory)

Lateral No	width or area ratio	q_{cr}
1	1	0.618
2	0.77	0.528
3	0.225	0.202
Iowa expt.	0.25	0.390
Iowa expt	0.0625	0.055

Table 5.14: Summary of Cd by Free Vortex

Expt No	q	Cd	k	a	B
Lat 1/21h	0.078	0.077	0.807	1.002	1.001
Lat 1/20h	1.000	0.530	2.698	1.009	1.003
Lat 1/19h	0.641	0.416	4.014	1.002	1.001
Lat 1/18h	0.926	0.525	1.916	1.017	1.006
Lat 1/12v	0.000	0.000	0		
Lat 1/8v	0.790	0.479	2.539	1.008	1.003
Lat 1/10v	0.866	0.494	3.538	1.005	1.002
Lat 1/7v	0.740	0.451	5.903	1.001	1.000
Lat 1/14v	1.000	0.533	2.653	1.009	1.003
Lat 1/5v	0.562	0.384	2.849	1.004	1.001
Lat 1/15v	0.921	0.508	3.371	1.005	1.002
Lat 1/9v	0.656	0.417	7.012	1.001	1.000
Lat 1/11v	0.150				
Lat 1/6v	0.408	0.310	2.513	1.004	1.001
Lat 1/30	0.460	0.334	4.150	1.001	1.000
Lat 1/100	0.054	0.051	1.664	1.000	1.000
Lat 1/102	0.141	0.129	19.72	1.000	1.000
Lat 1/103	0.231	0.190	38.98	1.000	1.000
Lat 1/104	0.650	0.413	4.082	1.002	1.001
LATERAL 2					
Lat 2/18V	0.000	0.000	0		
Lat 2/10V	0.140	0.150	11.67	1.000	1.000
Lat 2/9V	0.280			1.000	1.000
Lat 2/11v	0.340	0.334	3.417	1.002	1.001
Lat 2/12V	0.380	0.354	4.399	1.002	1.000
Lat 2/13V	0.507	0.427	3.047	1.005	1.001
Lat 2/14V	0.676	0.489	3.33	1.005	1.002
Lat 2/15v	0.820	0.522	3.933	1.004	1.001
Lat 2/19V	0.945	0.549	3.743	1.005	1.002
Lat 2/8v	1.000	0.571	5.159	1.003	1.001
Lat 2/6V	1.000	0.560	4.679	1.003	1.001
Lat 2/5v	1.000	0.545	8.310	1.001	1.000
Lat 2/7v	1.000	0.558	3.329	1.007	1.002
Lat 2/4V	1.000	0.584	2.464	1.013	1.004
LATERAL 3					
	0.000	0.000			
Lat 3/2v	0.180	0.442	2.534	1.007	1.002
Lat 3/3v	0.350	0.581	2.953	1.009	1.003
Lat 3/4V	0.390	0.576	2.869	1.009	1.003
Lat 3/5v	0.546	0.614	2.735	1.012	1.004
Lat 3/6v	0.710	0.629	2.817	1.012	1.003
Lat 3/9v	0.796	0.642			
Lat 3/7v	0.890	0.632	3.487	1.007	1.002
Lat 3/10v	0.935	0.635	3.117	1.009	1.003
Lat 3/8v	1.000	0.631	3.623	1.007	1.002
Lat 3/101h	0.900	0.657	3.50	1.008	1.003
Lat 3/100h	0.530	0.650		1.018	1.006
Lat 3/103h	0.000	0.000		1.000	1.000
Lat 3/102h	1.000	0.660	3.615	1.007	1.002
Lat 3/104	0.039	0.146	3.834	1.003	1.001

Table A1.1: Straight Through Flow Tests(h1 to h5)-Aluminium Conduit

Table A1.1

Tap Nos	Dist cm	h cm(Expt h1)	h cm(Expt h2)	h cm (Expt h3)	h cm(Expt h4)	h cm(Expt h5)	Duct geometry
10	0.00	71.20	42.40	90.80	112.40	132.40	L=9.15cm
13	45.90	69.50	40.70	89.40	110.60	130.50	B=4.125cm
16	91.80	67.30	38.20	87.60	108.40	127.50	Ar=0.040627
19	137.70	65.40	36.60	86.50	106.40	125.00	ft^2
21	175.70	64.60	35.70	85.80	105.40	124.90	P=0.871 ft
22	191.20	64.00	34.50	85.20	104.20	123.50	other data
23	206.70	63.50	33.50	84.50	103.80	123.00	
25	237.20	63.00	32.80	84.10	102.70	121.90	T=70.5 F
26A	260.20	61.10	30.50	82.60	100.70	119.70	u=1.055e-5 ft^2/sec

Table A1.2: Straight Through Flow Tests (H3 to H5)- Plexi glas

Table A1.2

Dist (cm)	h cm(Expt H3)	h cm(Expt H4)	h cm(Expt H5)	h cm(Expt H6)	Duct geometry
0.00	35.20	21.70	40.30	51.70	L=9.15 cm
12.24	34.40	21.20	39.70	51.00	Ar=0.040627
30.48	33.60	18.70			ft^2
45.72	32.80				P=0.871 ft
60.96	33.30	18.80	38.60	50.00	
76.20	32.10	16.70	37.80	49.30	
91.44	32.10	15.30			
106.68	31.10				
121.92	31.00	15.80	37.00	49.00	
137.16	30.80	14.20	36.80	48.60	
152.40	29.90	12.70			
167.64	29.20				
182.88	29.00	12.70	35.80	47.60	
198.12	28.60	11.20	35.20	46.80	
213.36	27.70	9.60			
228.60	27.40				
240.03	27.40	9.80		46.50	
255.27	26.90	8.10		45.30	
270.51	25.90	7.00			
285.75	24.80				
300.99	25.50	7.00	31.80	44.50	

Table A1.3: Friction Coefficients- for the Two Types of Conduits

Table A1.3 f Darcy Aluminium duct

Expt,h1 to h5	Q cusecs	V ft/sec	V^2	V^2/12.01446	S fr.Fig.A1.1	f Darcy
EXPT h1	0.183	4.502	20.271	1.687	0.037	0.022
EXPT h2	0.206	5.059	25.596	2.130	0.043	0.020
EXPT h3	0.167	4.104	16.843	1.402	0.029	0.021
EXPT h4	0.198	4.869	23.710	1.973	0.043	0.022
EXPT h5	0.209	5.142	26.440	2.200	0.046	0.021

f DARCY. St. THro FLOW TESTS PLEXIGLAS

Expt No	Q cusec	V=Q/.040627	V*d	Re no	V^2 ft^2/se^2	V^2/12.01446	Slope S fr.gra.	f Darcy
EXPT H3	0.177	4.360	0.813	77109	19.013	1.583	0.0324	0.0205
EXPT H4	0.223	5.499	1.026	97236	30.234	2.516	0.0498	0.0198
EXPT H5	0.155	3.826	0.714	67650	14.635	1.218	0.0265	0.0218
EXPT H6	0.142	3.496	0.652	61818	12.220	1.017	0.0226	0.0223

Expts Nos	f Darcy	Re	Re/7	1.56Ln(Re/7)	f 1	f(wall formula)	Re^-0.25	f Blasius
Alum. EXPT h1	0.0217	79617.5680	11373.9383	14.5690	0.0047	0.0188	0.0595	0.0188
" EXPT h2	0.0202	89464.7641	12780.6806	14.7509	0.0046	0.0184	0.0578	0.0183
" EXPT h3	0.0210	72572.6908	10367.5273	14.4244	0.0048	0.0192	0.0609	0.0193
" EXPT h4	0.0217	86105.7341	12300.8192	14.6912	0.0046	0.0185	0.0584	0.0185
" EXPT h5	0.0209	90928.0140	12989.7163	14.7762	0.0046	0.0183	0.0576	0.0182
Plex. EXPT H3	0.0205	77108.9565	11015.5652	14.5190	0.0047	0.0190	0.0600	0.0190
" EXPT H4	0.0198	97236.0699	13890.8671	14.8808	0.0045	0.0181	0.0566	0.0179
" EXPT H5	0.0218	67650.4319	9664.3474	14.3149	0.0049	0.0195	0.0620	0.0196
" EXPT H6	0.0223	61817.7477	8831.1068	14.1742	0.0050	0.0199	0.0634	0.0201

Table A1.3(cotd)

Expt No	f (Darcy)	(f/2)	(f/2)^0.5	(k/d)	V ft/sec	Ut	(k/du)Ut=Sm.P
Alum. EXPT h1	0.022	0.011	0.104	0.000013	4.502	0.469	0.578
" EXPT h2	0.020	0.010	0.101	0.000013	5.059	0.509	0.627
" EXPT h3	0.021	0.011	0.103	0.000013	4.104	0.421	0.519
" EXPT h4	0.022	0.011	0.104	0.000013	4.869	0.508	0.626
" EXPT h5	0.021	0.010	0.102	0.000013	5.142	0.526	0.648
Plex. EXPT H3	0.020	0.010	0.101	0.000005	4.360	0.441	0.209
" EXPT H4	0.020	0.010	0.099	0.000005	5.499	0.547	0.259
" EXPT H5	0.022	0.011	0.104	0.000005	3.826	0.399	0.189
" EXPT H6	0.022	0.011	0.106	0.000005	3.496	0.369	0.175

Table A1.4: Energy and Momentum flux Coefficients-Wall Formula

Expt No	f Darcy	2.9297*f	f^3/2	1.5537*f^3/2	1+col 3	a (Eq.A1.6)	0.9766* f	b (Eq.A1.8)
EXPT h1	0.0217	0.0636	0.0032	0.0050	1.064	1.059	0.021	1.021
EXPT h2	0.0202	0.0593	0.0029	0.0045	1.059	1.055	0.020	1.020
EXPT h3	0.0210	0.0617	0.0031	0.0047	1.062	1.057	0.021	1.021
EXPT h4	0.0217	0.0637	0.0032	0.0050	1.064	1.059	0.021	1.021
EXPT h5	0.0209	0.0613	0.0030	0.0047	1.061	1.057	0.020	1.020
EXPT H3	0.0205	0.0599	0.0029	0.0045	1.060	1.055	0.020	1.020
EXPT H4	0.0198	0.0580	0.0028	0.0043	1.058	1.054	0.019	1.019
EXPT H5	0.0218	0.0638	0.0032	0.0050	1.064	1.059	0.021	1.021
EXPT H6	0.0223	0.0652	0.0033	0.0052	1.065	1.060	0.022	1.022

Table A1.5: Evaluation of N and ε in Power Law

Table A1.5

Expt no	f Darcy	Re	ln (Re)	(ln Re)^2	1.57 ln(Re)	0.09(ln Re)^2	12.72+col 7	col 8-col 6= N
EXPT h1	0.0217	79618	11.285	127.351	17.717	11.462	24.182	6.464
EXPT h2	0.0202	89465	11.402	129.996	17.901	11.700	24.420	6.519
EXPT h3	0.0210	72573	11.192	125.269	17.572	11.274	23.994	6.422
EXPT h4	0.0217	86106	11.363	129.125	17.840	11.621	24.341	6.501
EXPT h5	0.0209	90928	11.418	130.367	17.926	11.733	24.453	6.527
EXPT H3	0.0205	77109	11.253	126.629	17.667	11.397	24.117	6.449
EXPT H4	0.0198	97236	11.485	131.903	18.031	11.871	24.591	6.560
EXPT H5	0.0218	67650	11.122	123.701	17.462	11.133	23.853	6.391
EXPT H6	0.0223	61818	11.032	121.704	17.320	10.953	23.673	6.353

Table A.1.5

Expt no	N	2N	N^2	N+1	2N+1	(N+1)(2N+1)	col 7/2N^2	e=(Vmax/V)
EXPT h1	6.464	12.928	41.785	7.464	13.928	103.963	1.244	0.244
EXPT h2	6.519	13.038	42.500	7.519	14.038	105.557	1.242	0.242
EXPT h3	6.422	12.844	41.245	7.422	13.844	102.756	1.246	0.246
EXPT h4	6.501	13.002	42.261	7.501	14.002	105.025	1.243	0.243
EXPT h5	6.527	13.054	42.602	7.527	14.054	105.785	1.242	0.242
EXPT H3	6.449	12.899	41.596	7.449	13.899	103.540	1.245	0.245
EXPT H4	6.560	13.120	43.033	7.560	14.120	106.746	1.240	0.240
EXPT H5	6.391	12.783	40.850	7.391	13.783	101.874	1.247	0.247
EXPT H6	6.353	12.706	40.363	7.353	13.706	100.786	1.248	0.248

Table A1.6: Energy and Momentum Coefficients by the Power Law

Column 1	N	2N	N^2	N^4	N+1	(N+1)^2	(N+1)^3	2N+1
EXPT h1	6.464	12.928	41.785	1746.012	7.464	55.714	415.855	13.928
EXPT h2	6.519	13.038	42.500	1806.216	7.519	56.538	425.118	14.038
EXPT h3	6.422	12.844	41.245	1701.112	7.422	55.089	408.880	13.844
EXPT h4	6.501	13.002	42.261	1785.993	7.501	56.263	422.018	14.002
EXPT h5	6.527	13.054	42.602	1814.929	7.527	56.656	426.451	14.054
EXPT H3	6.449	12.899	41.596	1730.209	7.449	55.495	413.407	13.899
EXPT H4	6.560	13.120	43.033	1851.856	7.560	57.153	432.076	14.120
EXPT H5	6.391	12.783	40.850	1668.729	7.391	54.633	403.814	13.783
EXPT H6	6.353	12.706	40.363	1629.173	7.353	54.069	397.583	13.706

(2N+1)^2	(2N+1)^3	N+3	2N+3	col 12* col 13	(N+1)^3/col14	(2N+1)^3/N^4	col 15*col 16	a power
193.998	2702.063	9.464	15.928	150.748	2.759	1.548	4.269	1.067
197.075	2766.607	9.519	16.038	152.672	2.785	1.532	4.265	1.066
191.667	2653.510	9.422	15.844	149.289	2.739	1.560	4.272	1.068
196.047	2744.996	9.501	16.002	152.030	2.776	1.537	4.266	1.067
197.516	2775.898	9.527	16.054	152.947	2.788	1.529	4.265	1.066
193.181	2685.015	9.449	15.899	150.237	2.752	1.552	4.270	1.068
199.373	2815.129	9.560	16.120	154.106	2.804	1.520	4.262	1.066
189.966	2618.265	9.391	15.783	148.223	2.724	1.569	4.275	1.069
187.865	2574.947	9.353	15.706	146.905	2.706	1.581	4.278	1.069

N+2	(N+1)(N+2)	(N+1)^2/col20	(2N+1)^2/N^2	col 22*col 23	col23 /4=B
8.464	63.178	0.882	4.643	4.094	1.024
8.519	64.057	0.883	4.637	4.093	1.023
8.422	62.511	0.881	4.647	4.095	1.024
8.501	63.764	0.882	4.639	4.093	1.023
8.527	64.183	0.883	4.636	4.093	1.023
8.449	62.944	0.882	4.644	4.095	1.024
8.560	64.713	0.883	4.633	4.092	1.023
8.391	62.024	0.881	4.650	4.096	1.024
8.353	61.423	0.880	4.654	4.097	1.024

Table A1.7: Energy and Momentum Equations by Empirical Equations

expt No	N	e=(Vma/V)-1	e^2	a=1+e^2	e^2/3	B=1+(e^2)/3
EXPT h1	6.464	0.244	0.0595	1.060	0.020	1.020
EXPT h2	6.519	0.242	0.0585	1.058	0.019	1.019
EXPT h3	6.422	0.246	0.0604	1.060	0.020	1.020
EXPT h4	6.501	0.243	0.0588	1.059	0.020	1.020
EXPT h5	6.527	0.242	0.0583	1.058	0.019	1.019
EXPT H3	6.449	0.245	0.0598	1.060	0.020	1.020
EXPT H4	6.560	0.240	0.0577	1.058	0.019	1.019
EXPT H5	6.391	0.247	0.0610	1.061	0.020	1.020
EXPT H6	6.353	0.248	0.0617	1.062	0.021	1.021

Table A1.8: Summary of α,β Coefficients by the Three Methods

Expt No	a(log Eq.-A1.6)	B(log-Eq.A1.8)	a(powEq.A1.12	B(powEq.A113	a(empEq.A1.14	B(empEqA1.15l
EXPT h1	1.059	1.021	1.067	1.024	1.060	1.020
EXPT h2	1.055	1.020	1.066	1.023	1.058	1.019
EXPT h3	1.057	1.021	1.068	1.024	1.060	1.020
EXPT h4	1.059	1.021	1.067	1.023	1.059	1.020
EXPT h5	1.057	1.020	1.066	1.023	1.058	1.019
EXPT H3	1.055	1.020	1.068	1.024	1.060	1.020
EXPT H4	1.054	1.019	1.066	1.023	1.058	1.019
EXPT H5	1.059	1.021	1.069	1.024	1.061	1.020
EXPT H6	1.060	1.022	1.069	1.024	1.062	1.021

Table A1.9: Summary of friction coefficients and Reynold Nos. for all lateral flow tests.

Test No	Q cusecs	Re no	f Darcy	f Blasius	f wall
Lat 1/21h	0.011	4935	0.040	0.038	0.038
Main & Lateral	0.133	57956	0.023	0.020	0.020
both alum	0.144	63199		0.020	0.020
Lat 1/20h	0.138	60758	0.021	0.020	0.020
	0.000				
	0.138	61129	0.022	0.020	0.020
Lat 1/18h	0.126	54360	0.022	0.021	0.020
	0.010	4360	0.043	0.039	0.040
	0.136	59081	0.021	0.020	0.020
Lat 1/12v	0.000		0.000		
	0.134	56321	0.022	0.021	0.020
	0.134	56665	0.022	0.021	0.020
Lat 1/8v	0.155	67480	0.021	0.020	0.020
	0.042	18410		0.027	0.027
	0.197	86415		0.018	0.019
Lat 1/10v	0.220	95164	0.021	0.018	0.018
	0.034	14684		0.029	0.028
	0.253	110521	0.018	0.017	0.018
Lat 1/7v	0.266	115525		0.017	0.017
	0.094	40687		0.022	0.022
	0.360	157168	0.016	0.016	0.016
Lat 1/5v	0.180	76260		0.019	0.019
	0.140	59400	0.021	0.020	0.020
	0.320	136491	0.016	0.016	0.017
Lat 1/14v	0.250	104063	0.019	0.018	0.018
	0.000		0.000		
	0.250	104700	0.019	0.018	0.018
Lat 1/15v	0.413	173960	0.017	0.015	0.016
	0.035	14880	0.032	0.029	0.028
	0.449	189999	0.018	0.015	0.016
Lat 1/9v	0.213	92379	0.020	0.018	0.018
	0.111	48346	0.024	0.021	0.021
	0.325	141586	0.018	0.016	0.017
Lat 1/11v	0.023	10298	0.034	0.031	0.031
	0.133	60036	0.022	0.020	0.020
	0.156	70680	0.019	0.019	0.019
Lat 1/19v	0.071	31490	0.024	0.024	0.023
	0.040	17590	0.031	0.027	0.027
	0.111	49387	0.024	0.021	0.021
Lat 1/6v	0.077	34568	0.027	0.023	0.023
	0.111	50214	0.024	0.021	0.021
	0.188	85198	0.019	0.019	0.019
Lat 2/11v	0.226	100594	0.021	0.018	0.018
	0.344	153720	0.019	0.016	0.016
Lat 2/12v					
	0.250	115218	0.019	0.017	0.017
	0.403	187348	0.019	0.015	0.016
Lat 2/13v	0.238	114509	0.018	0.017	0.017
	0.483	233666	0.018	0.014	0.015

Table A1.9: Summary of friction coefficients and Reynold Nos. for all lateral flow tests.

Test No	Q cusecs	Re no	f Darcy	f Blasius	f wall
	0.184	87081	0.021	0.018	0.018
Lat 2/19v	0.015	7196	0.043	0.034	0.034
	0.274	130528	0.018	0.017	0.017
Lat 2/15v	0.057	27222	0.030	0.025	0.024
	0.322	153663	0.018	0.016	0.016
Lat 2/10v	0.256	112293	0.020	0.017	0.018
	0.296	130760	0.021	0.017	0.017
Lat 2/9v	0.130	56275		0.021	0.020
	0.181	78917		0.019	0.019
Lat 2/8v	0.000				
	0.464	191468	0.016	0.015	0.016
Lat 2/7v	0.000				
	0.128	51804		0.021	0.021
Lat 2/6v	0.000				
	0.125	49401	0.025	0.021	0.021
Lat 2/5v	0.000				
	0.337	127885	0.020	0.017	0.017
Lat 3/6v					
	0.045	21110	0.033	0.026	0.026
	0.155	74050	0.019	0.019	0.019
Lat 3/8v					
	0.000				
	0.112	54065	0.023	0.021	0.021
Lat 3/9v					
	0.019	9230	0.027	0.032	0.032
	0.094	45440		0.022	0.021
Lat 3/10v					
	0.007	3370		0.042	0.043
	0.110	52480	0.024	0.021	0.021
Lat 3/7v					
	0.014	6571	0.034	0.035	0.035
	0.129	61434		0.020	0.020
Lat 3/5v					
	0.087	41170		0.022	0.022
	0.192	91336	0.020	0.018	0.018
Lat 3/4v					
	0.159	75400		0.019	0.019
	0.261	124660	0.019	0.017	0.017
Lat 3/3V					
	0.212	98976	0.018	0.018	0.018
	0.325	152837	0.019	0.016	0.016
Lat 3/2v					
	0.199	89834	0.022	0.018	0.018
	0.244	110344	0.019	0.017	0.018